

# Integrative diagnosis, biological observations, and histopathology of the fig cyst nematode *Heterodera fici* Kirjanova (1954) associated with *Ficus carica* L. in southern Italy

Elena Fanelli<sup>1</sup>, Alessio Vovlas<sup>2</sup>, Simona Santoro<sup>3</sup>, Alberto Troccoli<sup>1</sup>,  
Giuseppe Lucarelli<sup>3</sup>, Nicola Trisciuzzi<sup>4</sup>, Francesca De Luca<sup>1</sup>

**1** Istituto per la Protezione Sostenibile delle Piante (IPSP), Consiglio Nazionale delle Ricerche (CNR), S.S. Bari, Via G. Amendola 122/D, 70126 Bari, Italy **2** A. P. S. Polycena, Via Donizetti 12, 70014 Conversano, Bari, Italy **3** Hortoservice, Via S. Pietro 2, Noicattaro, Bari, Italy **4** Centro Ricerca Sperimentazione e Formazione in Agricoltura (CRSFA), Locorotondo, Bari, Italy

Corresponding author: Francesca De Luca ([francesca.deluca@ipsp.cnr.it](mailto:francesca.deluca@ipsp.cnr.it))

Academic editor: S. Subbotin | Received 21 May 2018 | Accepted 15 July 2018 | Published 12 February 2019

<http://zoobank.org/7421B26E-679C-42EC-8464-C395CAB9A116>

**Citation:** Fanelli E, Vovlas A, Santoro S, Troccoli A, Lucarelli G, Trisciuzzi N, De Luca F (2019) Integrative diagnosis, biological observations, and histopathology of the fig cyst nematode *Heterodera fici* Kirjanova (1954) associated with *Ficus carica* L. in southern Italy. ZooKeys 824: 1–19. <https://doi.org/10.3897/zookeys.824.26820>

## Abstract

Morpho-biological notes and histopathology, based on LM and SEM observations, of the fig cyst nematode *Heterodera fici* isolated from *Ficus carica* roots, collected in home and public gardens of Apulia region, southern Italy, are described and illustrated. Seventy-five localities throughout the Apulia region were sampled and one-quarter of the sampled localities had fig roots infested with *H. fici*, with population densities ranging from 44 to 180 cysts/100 ml of soil. All attempts to detect *H. fici* on ornamental *Ficus* spp. as well as on imported bonsai in Italy were unsuccessful. Morphometric characters of the Italian population conform to those of the type and re-description populations reported for *H. fici*. Molecular analysis using ITS, D2–D3 expansion domains of the 28S rRNA, and the partial 18S rRNA sequences of *H. fici* newly obtained in this study matched well with the corresponding sequences of *H. fici* present in the GenBank database. Phylogenetic trees confirmed and supported the grouping of *H. fici* in the Humuli group. *Heterodera fici* completes its embryogenic development in 14–16 days at 25 °C. Post-invasion development and maturity in the roots of *F. carica* seedlings is completed in 64–68 days at 25–28 °C with juveniles and adults showing different parasitic habits, being endoparasitic and semi-endoparasitic respectively. The establishment of permanent feeding sites that consist of the formation of large syncytia causes anatomical

modification of vascular elements and general disorder in the root stelar structures. Syncytia structures associated with mature females showed different degrees of vacuolisation, numbers of syncytial cells, and contained nuclei and nucleoli which were constantly hypertrophied.

### Keywords

cyst-forming nematode, embryogenesis, histopathology, identification, phylogeny, SEM morphology

## Introduction

The fig cyst nematode *Heterodera fici* Kirjanova, 1954 was described from roots of rubber plants, *Ficus elastica* Roxb. ex Hornem from China by Kirjanova (1954) and 35 years later a re-description, based on observations of females, males, cysts, and juveniles collected in USA and Pakistan on *Ficus carica* Linnaeus, 1753 was given by Golden et al. (1988). Di Vito and Inserra (1982) demonstrated the pathogenicity of *H. fici* from *F. carica* seedlings in pots. However, the impact of the nematode on adult fig trees has never been ascertained. Therefore, *H. fici* is not considered a major pest and its narrow host range is limited to *Ficus* species only. Subbotin et al. (2010) summarised the known occurrence of the fig cyst nematode from Germany, Greece, Hungary, Italy, the Netherlands, Norway, Poland, Portugal, Russia, Spain, Yugoslavia, China, Georgia, Iran, Turkey, Uzbekistan, Australia, New Zealand, United States (California, Florida, Louisiana, Maryland, and Virginia), Brazil, Algeria, and South Africa. More recently, *H. fici* was also found for the first time on *F. carica* maintained in a nursery in Canada (Sun et al. 2017). *Heterodera fici* together with *H. vallicola* Eroshenko, Subbotin & Kazachenko, 2001 and *H. mediterranea* Vovlas, Inserra & Stone, 1981 are reported as parasites of woody plants. In particular, *H. fici* is a worldwide parasite of ornamental and cultivated *Ficus* species (*F. carica*, *F. elastica*, *F. rubiginosa* Desf. ex Vent., *F. benghalensis* Linnaeus, 1753, *F. lyrata* Warb., *F. australis* Wild., and *F. benjamina* Linnaeus, 1767) (Baldwin and Mundo-Ocampo 1991, Evans and Rowe 1998; Wohlfarter et al. 2011). Based on classical morphology and host data, *H. fici* has been variously placed with members of the Schachtii group (Mulvey and Golden 1983, Baldwin and Mundo-Ocampo 1991) or in the Avenae group (Stone 1975). Subbotin et al. (2001) and recently De Luca et al. (2013), placed *H. fici* within the Humuli group characterised by bifenestral vulva in most species of the group, few or absent bullae, very weak underbridge, and long vulval slit situated in a cleft between the thickened vulval lips.

Preliminary investigations indicated that *H. fici* was rather widespread in southern Italy and in particular in the Apulia region. The main objectives of the present research were to: (i) obtain additional information on distribution, morphology, and molecular details of *H. fici* from *F. carica*, (ii) establish the phylogenetic relationships among *Heterodera* species closely related to *H. fici*; (iii) obtain additional biological information (embryogenic and post-invasion development); and (iv) to provide morpho-biological details on the host-parasite relationships of this nematode species in fig-nematode-feeding sites and describe the *F. carica* host responses to the nematode parasitism.

## **Material and methods**

### **Nematode population**

In the framework of the project “Urban Phytonematology” and on the basis of occasional records of *H. fici* on edible figs (*Ficus carica*), an extensive survey, including more than 75 root and soil samples, was conducted in commercial orchards in several localities of the Apulia region and in private and public gardens of Bari city, southern Italy, in late May 2016. Twenty-five bonsai *Ficus* spp. from several import/export nurseries working with Asiatic *Ficus* plants, still in their original pots, were included in the present survey. The nematode population selected and used for the present study was collected at Bari University Campus (40°06'72"N, 16°52'54"E).

### **Nematode diagnosis**

For diagnosis and identification, cysts and eggs were collected directly from infested roots, whereas second-stage juveniles, mature cysts, and males were extracted from soil by the flotation method (Coolen 1979), and cysts by the routine sieving-decanting method (Fenwick 1940). Cysts recovered from infected root tissues were mounted in glycerine. For morphological and diagnostic studies, specimens were glycerine-infiltrated and preserved by conventional methods (Seinhorst 1966), and cysts were fixed and mounted in lactophenol. Glycerine-infiltrated specimens were used for studies on morphometric traits and illustrations with camera lucida and an AmScope microscope. All measurements are given in micrometres unless otherwise stated.

Terminal cone structures of mature cysts were prepared for scanning electron microscopy (SEM) observations. Specimens fixed in formaldehyde (4% solution) were dehydrated in an ethanol gradient, critical-point dried, sputter-coated with gold, and observed according to procedures described by Abolafia et al. (2002).

### **Molecular characterization**

Individual cysts were crushed with a sterile micro-spatula under a stereo-microscope and the second stage juveniles (J2) were collected. Genomic DNA was extracted from fifteen J2s as described by De Luca et al. (2013). The crude DNA isolated from each individual nematode was directly amplified. The ITS1-5.8S-ITS2 regions were amplified using the forward primer TW81 (5'-GTTTCCGTAGGTGAAC-CTGC-3') and the reverse primer AB28 (5'-ATATGCTTAAGTTCAGCGGGT-3') (Joyce et al. 1994); the D2A-D3B expansion segments of 28S rRNA gene was amplified using the primers D2A (5'-ACAAGTACCGTGGGGAAAGTTG-3') and the D3B (5'-TCGGAAGGAACCAGCTACTA-3') (Nunn 1992); the 18S rDNA was amplified using the 18SnF (5'-TGGATAACTGTGGTAATTCTAGAGC-3') and 18SnR (5'-TTACGACTTTTGCCCGGTTTC-3') (Kanzaki and Futai 2002). PCR

cycling conditions used for amplification were: an initial denaturation at 94 °C for 5 min, followed by 35 cycles of denaturation at 94 °C for 50s, annealing at 55 °C for 50s and extension at 72 °C for 1 min and a final step at 72 °C for 7 min. The size of the amplification products was determined by comparison with the molecular weight marker ladder 100 (Fermentas, St. Leon-Rot, Germany) following electrophoresis of 10 µl on a 1% agarose gel.

PCR products of the ITS containing region, the 18S rRNA gene and the D2-D3 expansion domains from three individual nematodes were purified using the protocol given by the manufacturer (High Pure PCR elution kit, Roche, Germany). Purified DNA fragments were cloned and sequenced, in both directions, at MWG-Eurofin in Germany.

### RFLP analysis

Ten µl of the ITS containing amplicons of *H. fici* from southern Italy were digested with the following restriction enzymes: *Alu* I (Roche), *Hae* III (Roche), *Pst* I (Roche) and *Rsa* I (Roche) (5 U of enzyme for each digestion) at 37 °C overnight. The digested DNA fragments were loaded onto 2.5% agarose gel and visualized by gel red staining gel. All gel images were stored digitally.

### Phylogenetic analysis

A BLAST (Basic Local Alignment Search Tool) search at NCBI (National Center for Biotechnology Information) was performed in order to confirm nematode origins and species (Altschul et al. 1997). The newly obtained sequences for ITS containing region, the D2-D3 expansion domains of 28S rRNA gene and 18S rRNA gene were aligned using MAFFT v.7 software (Kato and Standley 2013) with default parameters with the corresponding published gene sequences of *Heterodera* species. Sequence alignments were manually edited using BioEdit in order to improve the multi-alignment. Out-group taxa for each dataset were chosen according to the results of previously published data (De Luca et al. 2013). Phylogenetic trees, obtained for ITS dataset, the D2-D3 expansion domains and 18S rRNA gene were performed with the Maximum Likelihood (ML) method using MEGA version 6 software (Tamura et al. 2013). ML analysis under a general time reversible and a gamma-shaped distribution (GTR + G) model for ITS, 28S and 18 S datasets was carried out. Phylogenetic trees were bootstrapped 1000 times to assess the degree of support for the phylogenetic branching indicated by the optimal tree for each method. The newly obtained sequences were submitted to GenBank with the following accession numbers: LT996913 for the ITS region; LT996915 for the D2–D3 expansion domains; LT996914 for the 18S rRNA gene.

### **Embryogenic development**

The embryogenic development of *H. fici* was studied in Petri dishes, using single-celled eggs obtained (deposited) from newly formed cysts, washed in distilled water, placed in 2% water agar, and maintained in an incubator at  $26 \pm 2$  °C. Microscopic observations and micrographs were taken at six-hour intervals during the first week and daily for the second week.

### **Post-invasion development**

The duration of post-invasion development was determined on fig (*F. carica*) seedlings transplanted in pots containing 250 ml of pasteurised sand, and inoculated, five days later, by using 1250 juveniles per pot. Inoculated young plants were maintained in a glasshouse at 26–28 °C. Invasion and nematode development was studied by stereoscope observations in acid fuchsin stained roots at seven-day intervals (Fig. 4). The maximum developmental stage observed was that of young cysts containing more than 25 eggs.

### **Host-suitability test**

Host studies were made in a glasshouse at 26–28 °C using common Mediterranean fruit trees as possible hosts (almond, apple, orange, edible and wild fig, apricot, grapevine, loquat, walnut, and pistachio) and transplanted on naturally infested soil with estimated initial population 1500 juveniles + eggs per pot and exposed to the nematode for a three-month period. Plants were removed from pots, the roots washed free of adhering soil, and the nematode populations were recorded.

### **Histopathology**

The histological changes induced by *H. fici* were studied in nematode-infected fig roots. Infected and healthy root segments were fixed for 48 hours in formalin-acetic acid-ethanol (FAA) solution, dehydrated in tertiary butyl alcohol, and embedded in 56–58 °C melting-point paraffin. Embedded tissues were sectioned transversely and longitudinally in 10–12 µm thick with a rotary microtome, stained with safranin and fast-green, and mounted in dammar xylene for microscopic examinations (Johansen 1940).

## Results

### *Heterodera fici* Kirjanova, 1954

Figures 1–4

**Nematode population.** The fig cyst nematode *H. fici* was recovered in our survey in established commercial fig orchards (more than 30 years old) as well as in private and public gardens. High infection rates were observed ranging from 44 to 180 cycts/100 ml of soil, 12–36 cysts per g of roots; 1.2–1.6 eggs – J2 /ml of soil, thus suggesting that the nematode might be causing damage. Furthermore, *H. fici* was detected in one-quarter of the 75 localities sampled throughout the Apulia region. All sampling attempts to detect *H. fici* from ornamental *Ficus* spp. as well as from imported bonsai in Italy were unsuccessful.

**Description. Measurements.** See Table 1. *Nematode diagnosis.* Detailed morphometric observations of the Italian population based on second-stage juveniles, male body length and characteristic of tail, stylet length, adult female and cyst shape, and vulval cone features (Figs 1–4, Table 1) agree very well with most of the original morphometric data and the redescription.

Observing the morphology (Figs 1–4), as well the metric data of the Italian population (Table 1), together with molecular comparison, we conclude that our *H. fici* belongs to the Humuli group and is distinguished from similar species by a combination of morphological and morphometric characteristics; it differs from all other members of the Humuli group (*H. humuli* Filipjev, 1934, *H. ripae* Subbotin, Sturhan, Rumpenhorst & Moens, 2003, *H. vallicola* Eroshenko, Subbotin & Kazachenko, 2001, and *H. litoralis* Wouts & Sturhan, 1996 by ambifenestrate rather than bifenestrate cysts and a longer vulval slit (43–48 vs. <40  $\mu\text{m}$ ), and by the prominent nipples on the male tail tip, which are regularly annulated and obtusely rounded in all other members of the group.

**Females.** Body basically lemon-shaped. Neck elongate, protruding vulval cone prominent. Cyst cuticle with zigzag pattern. Vulval cone well developed. Egg sac present, but few eggs deposited. Cuticular striae, extending to vulval slit are present at fenestral area (Fig. 2H).

**Cysts.** Body light to dark brown, basically lemon-shaped, neck and vulval cone distinct. Neck protruding, curved laterally. Cuticle thin, without sub-crystalline layer. External wall pattern at mid-body with interlocking ridges, forming zigzag pattern. Terminus of vulval cone with strongly developed zigzag ridges surrounding vulval slit and fenestra. Fenestra ambi-fenestrate, vulval slit equal in length to bridge. Few but distinct bullae are present. Anus distinct, on a depressed area surrounded by continuous cuticle edge/margin (Figs 2F–J, 3F).

**Males.** Body slender, vermiform, slight ventral curvature. Cuticular annulation prominent. Lateral field areolated, with four incisures. Labial region slightly offset, hemispherical, with three or four annuli. Labial framework heavily sclerotised. Tail short, obtusely rounded, four prominent nipples on tail tip. Spicules arcuate, tapering distally. Gubernaculum slightly curved ventrally (Figs 2D, 3G).

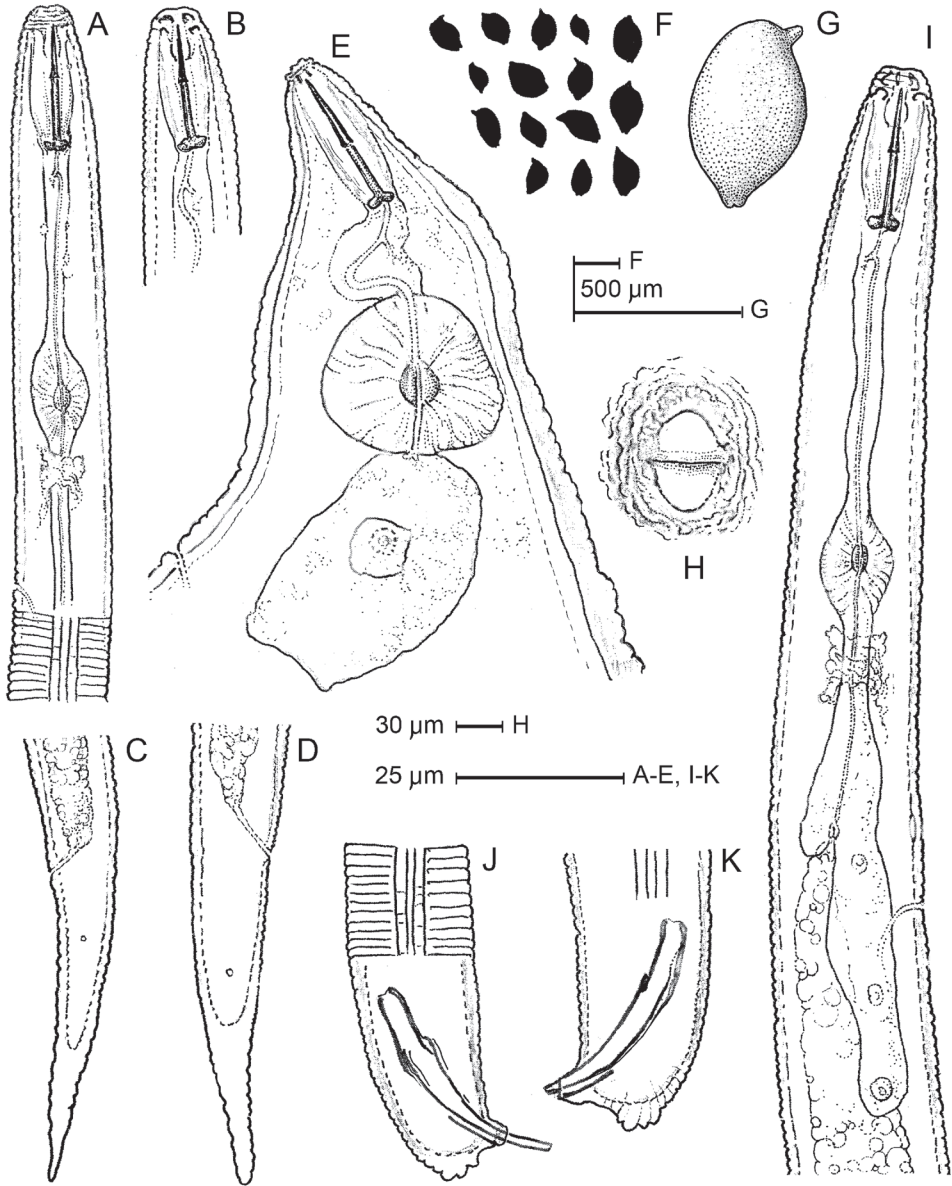


**Figure 1.** Line drawings of *Heterodera fici* from Italy. **A, B** Anterior body portions of second stage juvenile **C, D** Second stage juvenile tail **E** Female anterior region **F, G** Cyst shape **H** Fenestral structures **J, K** Male tail, showing spicules and cloacal tube **I** Male pharyngeal region.

**J2 (Second stage juveniles).** Body vermiform; tapering at both extremities, more marked posteriorly. Cuticular annulation prominent. Lateral field with four incisures. Labial region slightly offset, rounded, with three or four annuli. Labial framework moderately sclerotised. Stylet well developed, basal knobs rounded, directed slightly anteriorly. Median bulb ovoid. Pharyngeal lobe usually distinct, with three large nuclei

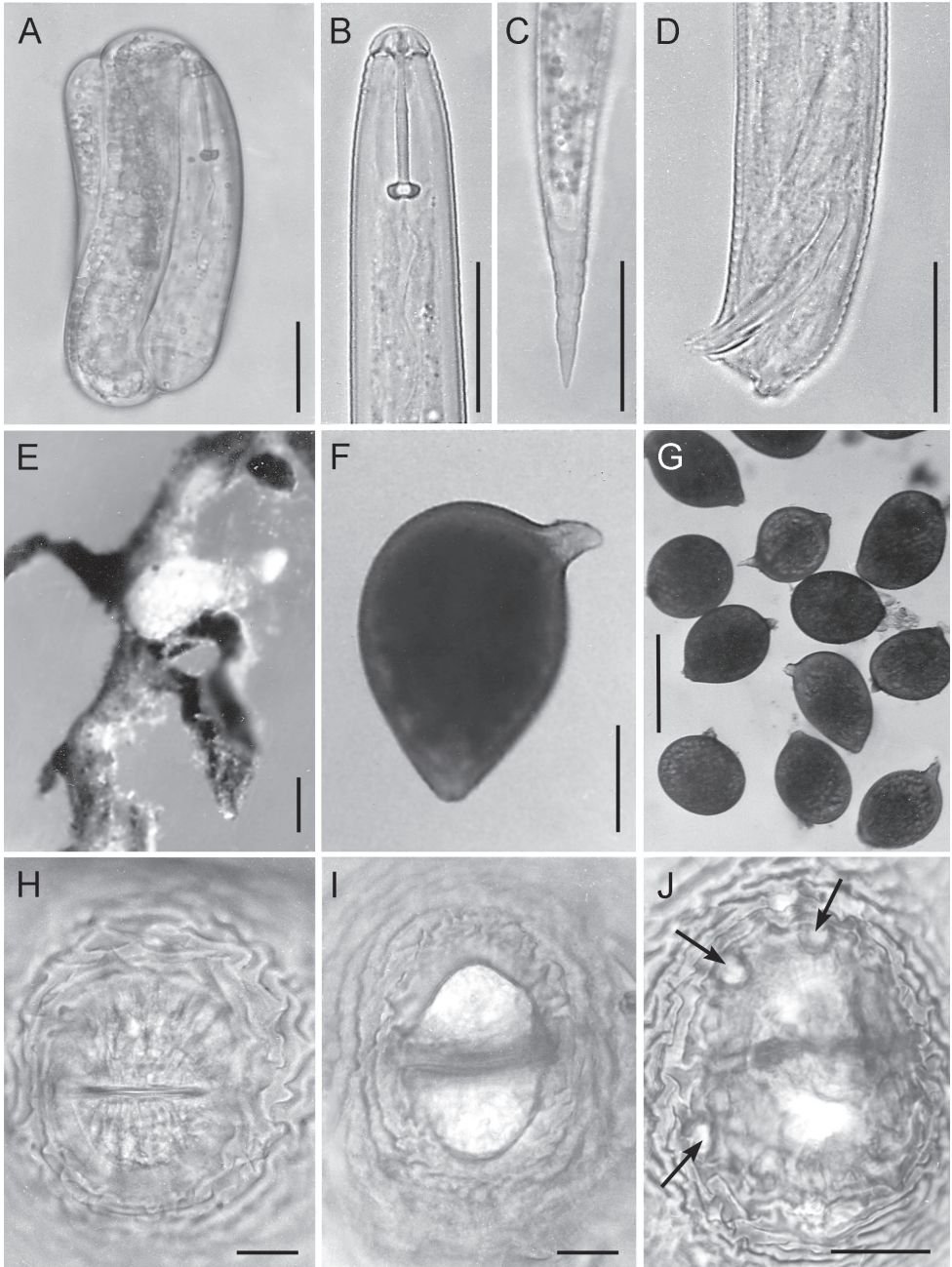


**Figure 2.** LM micrographs of *Heterodera fici* from Italy. **A** Embryonated egg with evident second stage juvenile stylet **B** Second stage juvenile anterior end **C** Second stage juvenile tail **D** Male tail with the characteristic tail tip **E** Females on *Ficus carica* roots **F** whole body of newly formed cyst **G** Females and cysts **H–J** Vulval cone structures, with clear illustration of vulval slit (in **H**), fenestral area (in **I**) and bullae (in **J**). Scale bars: 20  $\mu\text{m}$  (**A–D**, **H–J**); 200  $\mu\text{m}$  (**F**); 500  $\mu\text{m}$  (**E**, **G**).

**Table 1.** Morphometrics of an Italian population of *Heterodera fici* isolated from roots and soil around roots; specimens mounted in water agar temporary slides (Measurements are in  $\mu\text{m}$ ).

Character*	Females	Cysts	Males	juveniles
n	15	16	12	20
Body length (excl. neck) (L)	355–638	420–680	750–880	330–416
Max. body width (W)	230–422	280–550	25–26	17–20
L/W	1.2–1.5	1.1–1.5		
Neck length	75–126	–		
Fenestral length	–	46–72		
Fenestral width	–	28–46		
Vulva slit	–	35–44		
Bullae	–	Present, small		
Stylet length	23–28	–	27–31	20–22
Dorsal gland orifice (DGO)	4–5	–	5–6	4–5
Anterior end to centre of median bulb	60–65	–	80–106	64–76
Excretory pore from anterior end	132–138	–		
Head to end of pharyngeal gland lobe			200–275	136–156
Tail length			7.5–8.2	39–52
Hyaline tail portion			–	18–24
No of lines in lateral fields			4	4
Spicule length			26–32	–
Gubernaculum			7–8	–
a			30–38	17–22
b			2.5–4.5	2.4–3.2
c			102–128	8–9

\* All characters and indexes (a, b and c) are specified in Siddiqi (2000).

and overlapping anterior part of intestine. Tail long, tapering, terminus rounded. Anus distinct. Phasmid openings small but distinct, 11–14  $\mu\text{m}$ , posterior to anus and anterior to middle of tail. Hyaline tail region half of tail length (Fig. 2B, C).

**Embryogenesis.** Mean dimensions of single-celled and embryonated eggs were 40  $\times$  98  $\mu\text{m}$  (Fig. 2A). The first cleavage was equatorial and the two-blastomeres stage appeared after 14–18 hours. The second and third divisions were also transverse and the four-cell stage phase was obtained after three days. Forty-eight hours later, rapid cell division resulted in the formation of multicell eggs. The gastrula stage was observed during days 9–12. First and second-stage juveniles appeared in 11–13 and 14–16 days, respectively, and were coiled three or four times within the eggshell. The embryogenic development was basically the same as in *H. schachtii* Schmidt, 1871 and *H. mediterranea* (Mulvey and Golden 1983, Vovlas and Inserra 1983).

**Post-invasion development.** Post root-invasion development of *H. fici* on *Ficus carica* roots was completed in about 64–68 days at 26–28  $^{\circ}\text{C}$ . Invasion and nematode development stages were recorded by stereoscope observations on acid fuchsin-stained roots at seven-day intervals (Fig. 4). The maximum developmental phase observed was that of young cysts containing more than 25 eggs. The first period (24–26 days after inoculation) was utilized by the parasitic specimens for exploration, penetration, and se-

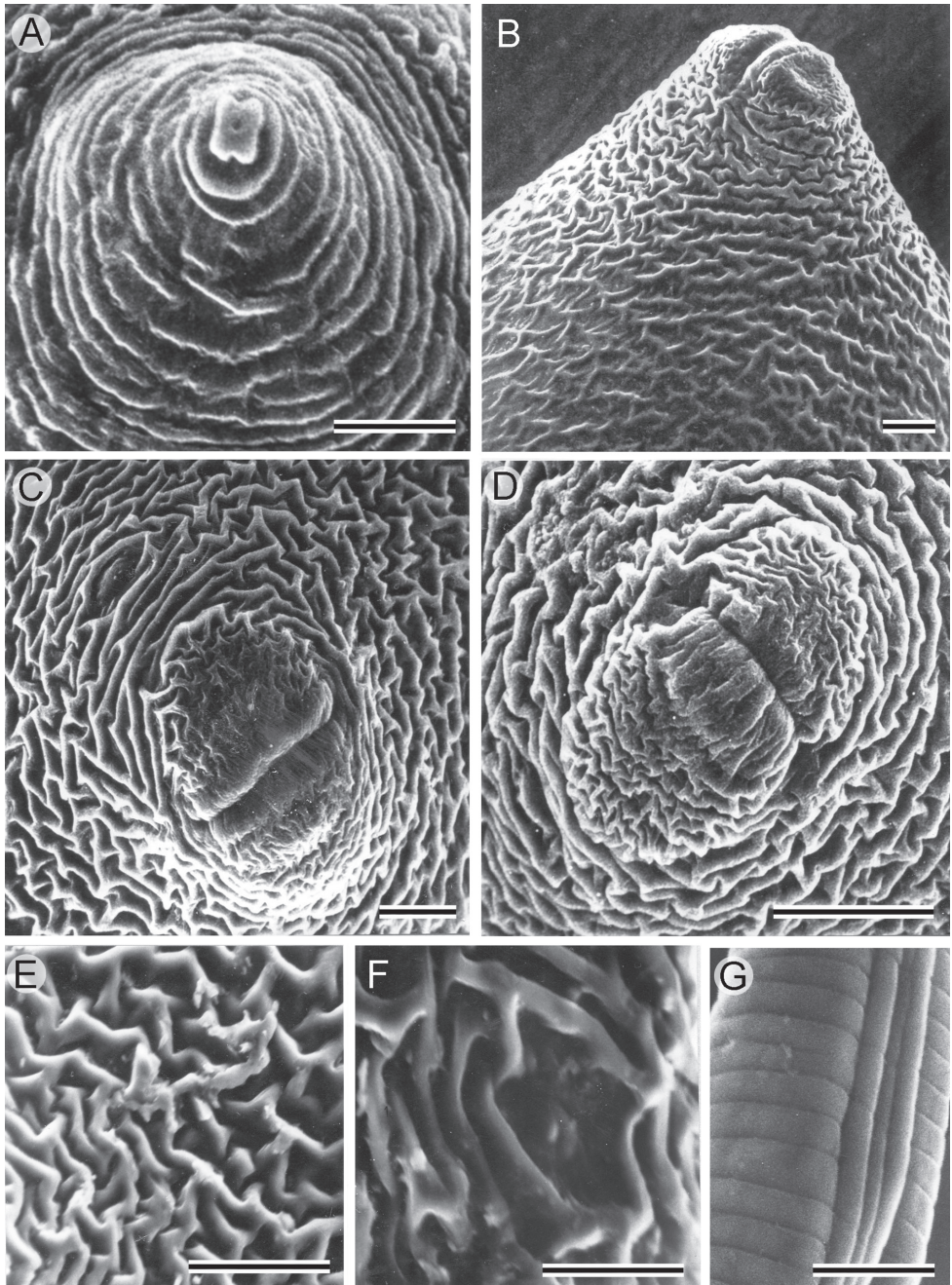


**Figure 3.** SEM photographs of the main cyst diagnostic characters of *Heterodera fici* from Italy. **A** Female anterior end **B** Lateral view of terminal cone **C, D** Fenestral area and anus **E** Maze-like cyst cuticular ornamentation **F** Cyst anal area **G** Male lateral fields. Scale bars: 10  $\mu\text{m}$  (**A, G**); 20  $\mu\text{m}$  (**B–F**).

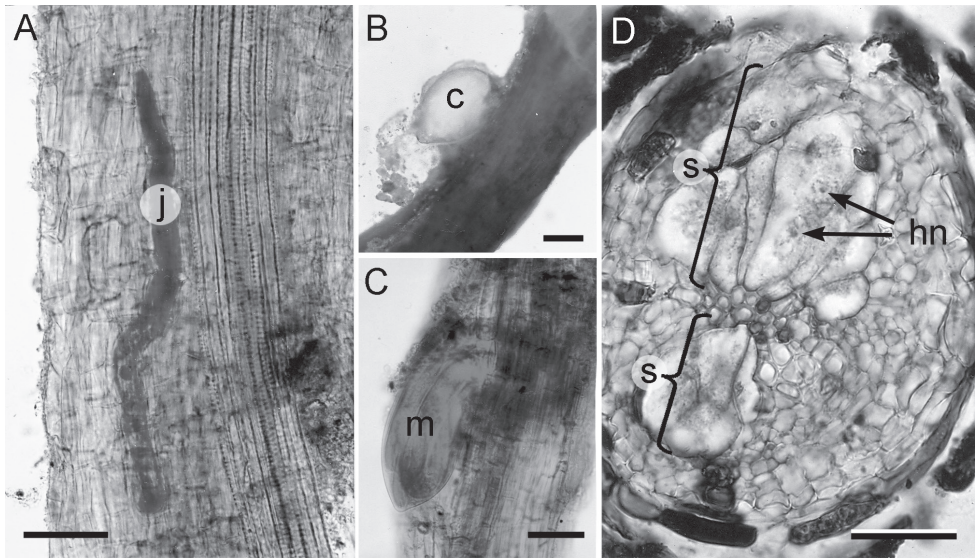


**Figure 4.** Post invasion development of *Heterodera fici* on *Ficus carica* roots. **A** Second stage juvenile within cortical layer, oriented in parallel position to the root axis **B** Newly formed cyst with gelatinous egg sac **C** Male inside 4<sup>th</sup> stage cuticle **D** Different sized syncytia (S) induced by female (the larger one), and by male. Abbreviations: j = juvenile; m = male; c = cyst; hn = hypertrophied nuclei. Scale bars: 50  $\mu\text{m}$  (**A**, **C**); 200  $\mu\text{m}$  (**B**); 100  $\mu\text{m}$  (**D**).

lection of the feeding site (Fig. 4A). The second stage juveniles stop penetration and start to feed on the initial feeding cells by using a sedentary endoparasitic feeding position. Observations at 50–56 days after inoculation revealed that the 3<sup>rd</sup> moult was completed and that sexual differentiation occurred. The swollen posterior portion of sexually mature nematodes (piriform females and 4<sup>th</sup> stage vermiform males still inside the cuticle) protrudes from the root. Fourth-stage females and males were observed one week later (Fig. 4C). Lemon-shaped mature females were observed eight weeks after invasion. The post infection period was concluded about 8 weeks later. No new cysts were observed.

**Histopathology.** *Heterodera fici* establishes permanent, fully-developed feeding sites on *F. carica* roots and reaches maturity in 64–68 days. Histological examination of sectioned healthy and nematode-infected (Fig. 4) fig roots showed that infection by *H. fici* can cause cellular alterations in the cortex, endodermis, pericycle, and vascular parenchyma tissues of fig roots. Observations of cross-sections of *H. fici* infected roots indicated that the nematode can induce the formation of both cortical and endodermal syncytia. In many cases, the nematode female only penetrated one to three layers of the cortical root cells without reaching the stele. In these roots, the nematode established a permanent feeding site in a cortical cell that was fused with adjacent cells forming the syncytium. Structurally, vascular syncytia varied in shape and expansion when induced by females or males. Those induced by females were larger and with more cytoplasmic

contents compared to those induced by males. All syncytial cells were hypertrophic with dense cytoplasm and large nuclei. In some cases, nematode females penetrated into the cortex with the anterior elongated body portion where they induced a permanent feeding site and continued to remain in a semi-endoparasitic position, probably because of the nature of root tissues (woody host).

**Host-suitability test.** The results presented in this paper as well as in the host-suitability test confirmed that *H. fici* has a narrow host range limited to *Ficus* species and for this reason it is not considered a major pest, as are other species of *Heterodera*.

**Molecular characterization.** The sequenced ITS, D2-D3 expansion domains of the 28S rRNA gene, and the 18S rRNA gene are 1035 bp, 780 bp, and 1627 bp long, respectively. BLAST search at NCBI revealed that the ITS, D2-D3 expansion domains of the 28S rRNA and the partial 18S rRNA sequences of *H. fici* from Italy, newly obtained in this study, matched well with the corresponding sequences of *H. fici* present in the database. The RFLP patterns of Italian *H. fici* were identical to those from Portugal, Greece, and another population from Potenza province, Basilicata, Italy (Madani et al. 2004) (Fig. 5). In particular, the ITS region of the Italian population of *H. fici* showed 99% similarity (1027/1029) with the corresponding region of *H. fici* deposited in GenBank, differing from 1 to 4 nucleotides; the next closest *Heterodera* species were *H. humuli* (coverage: 897/962), *H. vallicola* (coverage: 899/975), *H. ripae* (coverage: 894/972), and *H. litoralis* (coverage: 884/962) with 92–93% similarities. *Heterodera* species belonging to Schachtii group, instead, showed about 82% similarity with the Italian population of *H. fici*. The D2–D3 expansion domains of the Italian *H. fici*, obtained for the first time in this study, showed 95% similarity with the corresponding region of *H. latipons* Franklin, 1969 and *H. avenae* Wollenweber, 1924, while with *H. glycines* Ichinohe, 1952 and *H. schachtii* the similarity was 94%. The 18S rRNA gene of *H. fici* showed 99% similarity with the corresponding region of *H. avenae*, *H. hordecalis* Andersson, 1975, *H. schachtii*, and *H. glycines*, while its similarity with *H. elachista* Ohshima, 1974 was 98%.

Phylogenetic trees using the ML method are given in Figures 6–8. ITS, D2-D3, and 18S trees confirmed the separation of the genus *Heterodera* into different groups (Subbotin et al. 2010, De Luca et al. 2013). In particular, the Italian population of *H. fici* grouped within the Humuli group in all phylogenetic trees, closely related to the Schachtii group.

## Discussion

Our study reports the occurrence of *H. fici* in commercial fig trees in southern Italy showing no symptoms of retarded growth or yellowing of leaves related to nematode presence. The morphology (Fig. 1) and the morphometrics (Table 1) of cysts, females, males, and second stage juveniles recovered from the roots and the crushed cysts of Italian *H. fici* agree with the original species description and subsequent redescription (Kirjanova 1954, Golden et al. 1988) except for minor intraspecific differences. According to the morphological and molecular data, the Italian population of *H. fici*

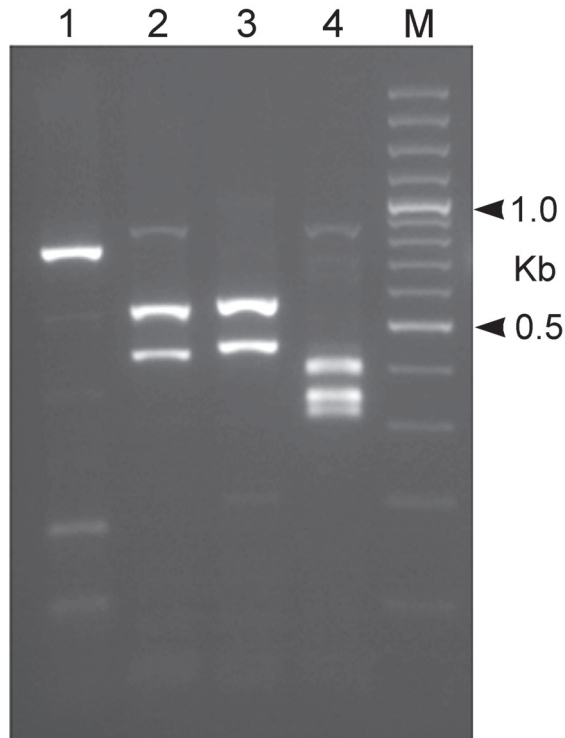


**Figure 5.** RFLP profiles of the ITS of *Heterodera fici* digested with four restriction enzymes. **M** 100 bp DNA ladder (Promega); **1** Alu I **2** Hae III **3** Rsa I **4** Pst I.

shows some diagnostic characters similar to *Heterodera* species belonging to the Humuli group differing, however, from the members of this group (*H. humuli*, *H. ripae*, *H. vallicola*, and *H. litoralis*) by having ambifenestrated rather than bifenestrated cysts, longer vulval slit, the shape and measurements of J2 tails, and four prominent nipples on the male tail tip. Furthermore, SEM observations of cysts and males showed greater details of various structures compared to the light microscopy (Fig. 3). Infection of Italian *H. fici* on Mediterranean fruit trees revealed no symptoms when compared to infected fig roots. The results obtained in the survey, as well as in the host suitability test, confirmed that *H. fici* has a narrow host range limited to *Ficus* spp. and for this reason it is not considered a major pest as are other *Heterodera* spp. Furthermore, these findings also confirmed that *H. fici* is the only species of Humuli group attacking woody host plants; all the other members parasitize herbaceous hosts.

ITS-RFLP patterns of *H. fici* from South Italy showed no heterogeneity or differences to the published RFLP patterns (Madani et al. 2004). The phylogenetic relationships of *H. fici* obtained in this study reported in Figs 6–8 strongly support the monophyly of the genus *Heterodera* using *Globodera pallida* Stone, 1973 and *G. rostochiensis* (Wollenweber, 1923) Skarbilovich, 1959 as outgroups. Figure 6 shows the phylogenetic tree based on the ITS region confirming that *H. fici* grouped with all populations of *H. fici* and clustered with high bootstrap support (99%) in the Humuli group. Close

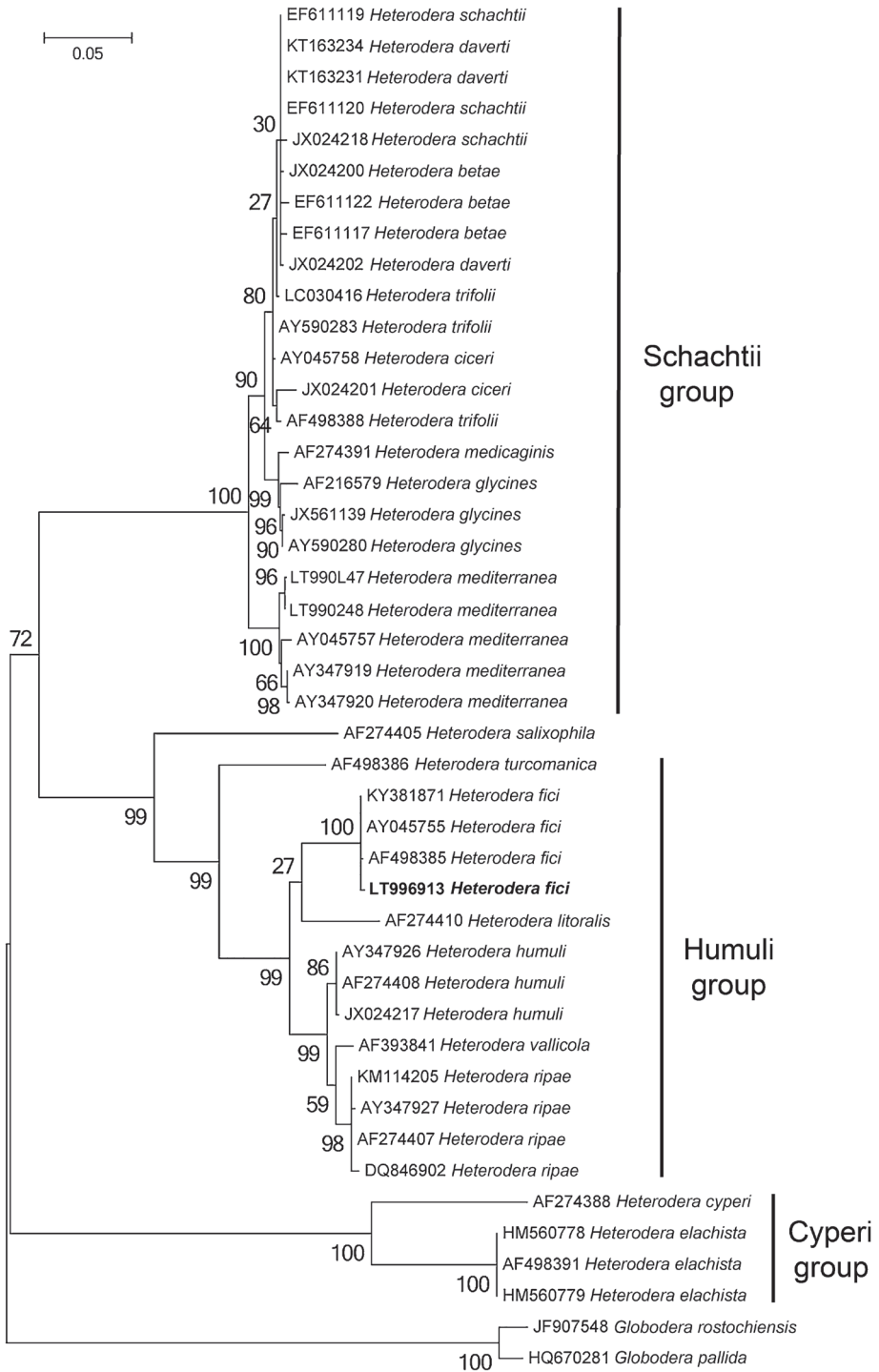


**Figure 6.** Phylogenetic trees of ITS containing region of *Heterodera fici* and the closest species. Sequences were analysed using the Maximum Likelihood method. Numbers at nodes indicate bootstrap values.

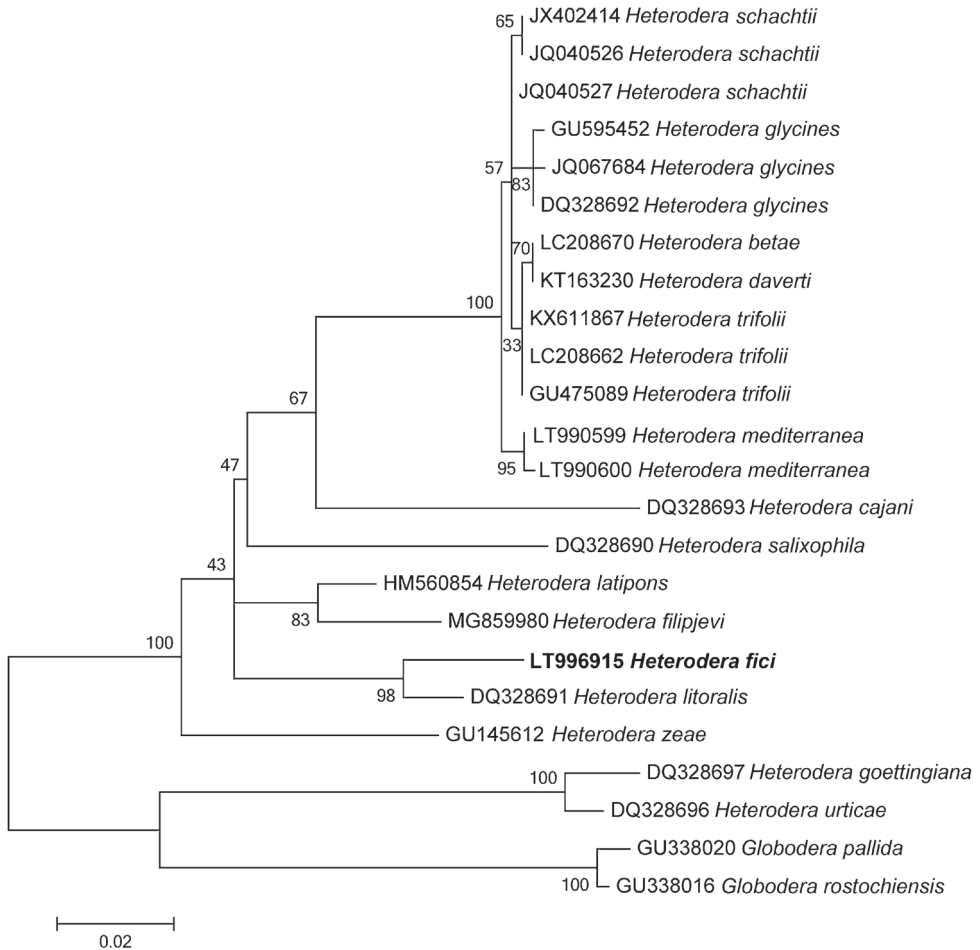


**Figure 7.** Phylogenetic trees of the D2–D3 expansion domains of the 28S rRNA gene of *Heterodera fici* and the closest species. Sequences were analysed using the Maximum Likelihood method. Numbers at nodes indicate bootstrap values.

relationships were revealed among the Humuli group, the species *H. salixophila* Kirjanova, 1969 and the Schachtii group, as already reported, confirming their coevolution with dicots (Subbotin et al. 2001). Furthermore, *H. fici* together with *H. vallicola* and *H. mediterranea* are the only *Heterodera* species known to attack woody plants belonging to different families, suggesting a host switch for these *Heterodera* species. The obtained phylograms are in agreement with the current morphological groupings of *Heterodera* species and coevolution with host plants.

In conclusion, our data confirm the occurrence of *H. fici* in two regions of southern Italy, Apulia and Basilicata, and on commercial fig orchards, approximately thirty years old, suggesting that this nematode despite its narrow host range is widespread all over the world and that it deserves attention. Maqbool et al. (1987) reported yellowing of fig trees in Pakistan but they were infested with both *Meloidogyne javanica* (Treub,

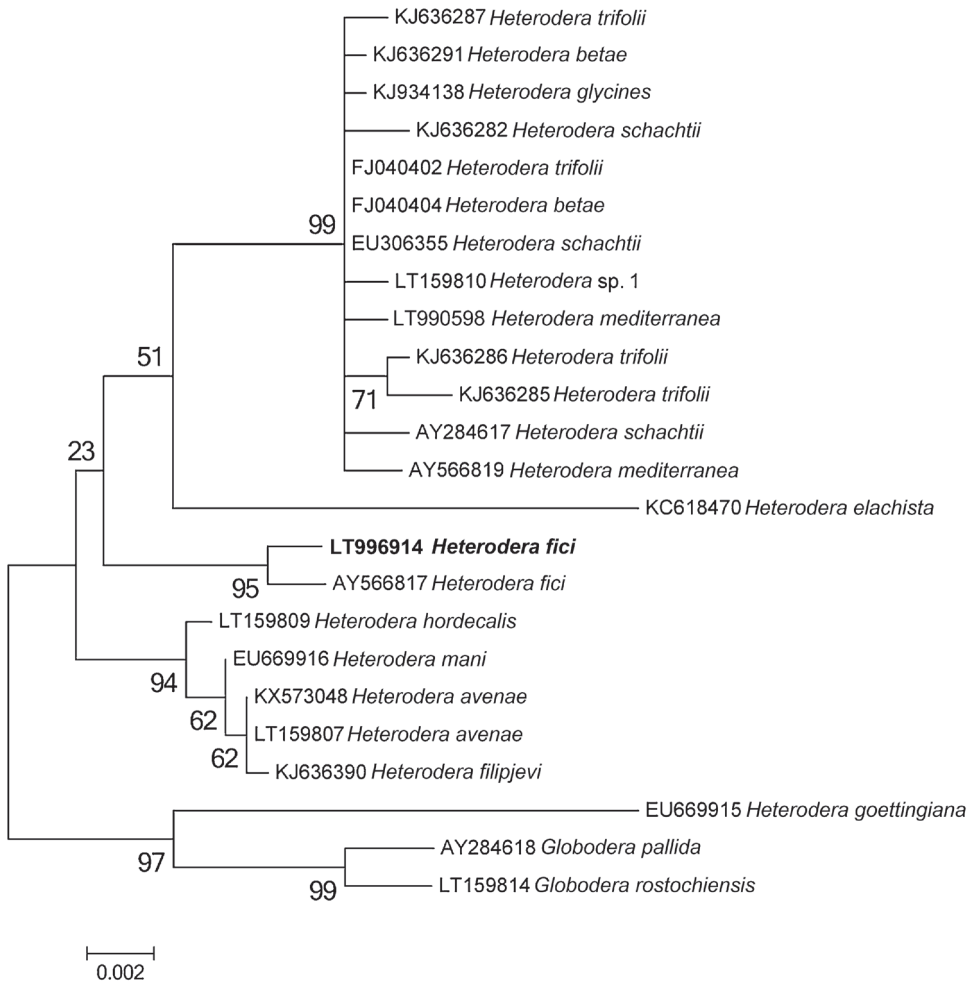


**Figure 8.** Phylogenetic trees of the 18S rRNA gene of *Heterodera fici* and the closest species. Sequences were analysed using the Maximum Likelihood method. Numbers at nodes indicate bootstrap values.

1885) Chitwood, 1949 and *H. fici* and, therefore, it was not possible to partition the observed damage between the two nematodes. However, during our survey *H. fici* was detected in rather large population densities both in soil and roots and appeared widespread (25% of the orchard infested). Therefore, although the impact of *H. fici* on fig yield still remains to be assessed, we believe that *H. fici* deserves attention to avoid its spread and subsequent yield loss.

## Acknowledgment

Authors acknowledge Nicola Vovlas for critical review of and suggestions to the manuscript before submission.

## References

- Abolafia J, Liébanas G, Peña-Santiago R (2002) Nematodes of the order Rhabditida from Andalucía Oriental Spain. The subgenus *Pseudacrobeles* Steiner, 1938, with description of a new species. *Journal of Nematode Morphology and Systematics* 4: 137–154.
- Altschul SF, Madden TL, Schaffer AA, Zhang J, Zhang Z, Miller W, Lipman DJ (1997) Gapped BLAST and PSI-BLAST: a new generation of protein database search programs. *Nucleic Acids Research* 25: 3389–3402. <https://doi.org/10.1093/nar/25.17.3389>
- Andersson S (1975) *Heterodra hordecalis* n. sp. (Nematoda: Heteroderidae) a cyst nematode of cereals and grass in southern Sweden. *Nematologica* 20: 445–454.
- Baldwin JG, Mundo-Ocampo M (1991) Heteroderinae, cyst and non-cyst-forming nematodes. In: Nickle WR (Ed.) *Manual of Agricultural Nematology*. Marcel Dekker, New York, 275–362.
- Chitwood BG (1949) Root-knot nematodes – Part 1. A revision of the genus *Meloidogyne* Goeldi, 1887. *Proceedings of the Helminthological Society of Washington* 16: 90–104.
- Coolen WA (1979) Methods for the extraction of *Meloidogyne* spp. and other nematode from roots and soil. In: Lamberti F, Taylor CE (Eds) *Root-knot Nematodes (Meloidogyne species) Systematics, Biology and Control*. Academic Press, London, 319–329.
- De Luca F, Vovlas N, Lucarelli G, Troccoli A, Radicci V, Fanelli E, Cantalapietra-Navarrete C, Palomares-Rius JE, Castillo P (2013) *Heterodera elachista* the Japanese cyst nematode parasitizing corn in Italy: integrative diagnosis and bionomics. *European Journal of Plant Pathology* 136: 857–872. <https://doi.org/10.1007/s10658-013-0212-9>
- Di Vito M (1976) Presenza di *Heterodera fici* in Basilicata. *Nematologia Mediterranea* 4: 107–108.
- Di Vito M, Inserra RN (1982) Effects of *Heterodera fici* on the growth of commercial fig seedlings in pots. *Journal of Nematology* 14: 416–418.
- Eroshenko AS, Subbotin SA, Kazachenko IP (2001) *Heterodera vallicola* sp. n. (Tylenchida: Heteroderidae) from elm trees, *Ulmus japonica* (Rehd.) Sarg. in the Primorsky territory, the Russian Far East, with rDNA identification of closely related species. *Russian Journal of Nematology* 9: 9–17.
- Evans K, Rowe JA (1998) Distribution and economic importance. In: Sharma SB (Ed.) *The cyst nematodes*. Kluwer Academic Publishers, Dordrecht, 1–30. [https://doi.org/10.1007/978-94-015-9018-1\\_1](https://doi.org/10.1007/978-94-015-9018-1_1)
- Fenwick DW (1940) Methods for the recovery and counting of cysts of *Heterodera schachtii* from soil. *Journal of Helminthology* 18: 155–172. <https://doi.org/10.1017/S0022149X00031485>
- Franklin MT (1969) *Heterodera latipons* n. sp., a cereal cyst nematode from the Mediterranean region. *Nematologica* 15: 535–542. <https://doi.org/10.1163/187529269X00867>
- Golden A M, Maqbool MA, Zarina F (1988) Redescription of *Heterodera fici* (Nematoda: Heteroderidae) with SEM observations. *Journal of Nematology* 20: 381–391.
- Greco N, Brandonisio A, De Marinis G (1982) Investigation on the biology of *Heterodera schachtii* in Italy. *Nematologia Mediterranea* 10: 201–214.
- Ichinohe M (1952) On the soybean nematode, *Heterodera glycines* n. sp., from Japan (trans.) *Oyo-Dobutsugaku-Zasshi* 17: 1–4.

- Johansen DA (1940) The plant microtechnique. McGraw Hill, New York, 523 pp.
- Joyce SA, Reid A, Driver F, Curran J (1994) Application of polymerase chain reaction (PCR) methods to the identification of entomopathogenic nematodes. In: Burnell AM, Ehlers RU, Masson JP (Eds) Cost 812 Biotechnology: genetics of entomopathogenic nematodes-bacterium complexes. Proceedings of symposium and workshop, St Patrick's College, Maynooth, County Kildare, Ireland. Luxembourg, European Commission, DGXII, 178–187.
- Kanzaki N, Futai K (2002) A PCR primer set for determination of phylogenetic relationships of *Bursaphelenchus* species within *xylophilus* group. *Nematology* 4: 35–41. <https://doi.org/10.1163/156854102760082186>
- Katoh K, Standley DM (2013) MAFFT multiple sequence alignment 542 software version 7: improvements in performance and usability. *Molecular Biology and Evolution* 30: 772–780. <https://doi.org/10.1093/molbev/mst010>
- Kirjanova ES (1954) Summaries and perspectives in the development of phytonematology in USSR. Zoological Institute of the Academy of Sciences, USSR, Trudy Prob. Tematicheskikh Soveshchaniy 3: 9–47.
- Kirjanova ES (1969) About the structure of the subcrystalline layer of the nematode genus *Heterodera* (Nematoda: Heteroderidae) with description of two new species. *Parazitologiya* 3: 81–91 [in Russian]
- Madani M, Vovlas N, Castillo P, Subbotin SA, Moens M (2004) Molecular characterization of cyst nematode species (*Heterodera* spp.) from the Mediterranean Basin using RFLPs and sequences of ITS-rDNA. *Journal of Phytopathology* 152: 229–234. <https://doi.org/10.1111/j.1439-0434.2004.00835.x>
- Maqbool MA, Qasim M, Zarina B (1987) New record of *Heterodera fici* Kirjanova, 1954 and *Meloidogyne javanica* (Treub, 1885) Chitwood, 1949 on *Ficus carica* L. *Pakistan Journal of Nematology* 5: 41–42.
- Mulvey RH (1972) Identification of *Heterodera* cysts by terminal and cone top structures. *Canadian Journal of Zoology* 50: 1277–1292. <https://doi.org/10.1139/z72-173>
- Mulvey R, Golden AM (1983) An illustrated key to the cyst-forming genera and species of Heteroderidae in the western hemisphere with species morphometrics and distribution. *Journal of Nematology* 15: 1–59.
- Nunn GB (1992) Nematode molecular evolution. Ph.D. thesis. University of Nottingham, UK.
- Ohshima Y (1974) *Heterodera elachista* n.sp., an upland rice cyst nematode from Japan. *Japanese Journal Nematology* 4: 51.
- Schmidt A (1871) Über den rüben-nematoden (*Heterodera schachtii* A. S.). *Z. Ver Ruben Zucker Industr. Zolliver* 21: 1–19.
- Seinhorst JW (1966) Killing nematodes for taxonomic study with hot f.a. 4:1. *Nematologica* 12: 178
- Seinhorst JW, den Ouden H (1966) An improvement of Bijloo's method for determining the eggs content of *Heterodera* cysts. *Nematologica* 12: 170–171. <https://doi.org/10.1163/187529266X00185>
- Siddiqi MR (2000) *Tylenchida Parasites of Plants and Insects* (2<sup>nd</sup> edn). CABI Publishing, Wallingford.
- Sigariova DD, Karplyk VG (2015) Parasitic nematodes in flowering and ornamental plants: effect of parasites on the plants and response of the plants to the presence of nematodes. *Vestnik Zoologii* 49: 427–432. <https://doi.org/10.1079/9780851992020.0000>

- Skarbilovich TS (1959) On the structure of the systematics of nematode order Tylenchida Thorne, 1949. *Acta Parasitologica Polonica* 7: 117–132.
- Stone AR (1973) *Heterodera pallida* n. sp. (Nematoda: Heteroderidae) a second species of potato cyst nematode. *Nematologica* 18: 591–606. <https://doi.org/10.1163/187529272X00179>
- Stone AR (1975) Head morphology of second-stage juveniles of some Heteroderidae (Nematoda: Tylenchoidea). *Nematologica* 21: 81–88. <https://doi.org/10.1163/187529275X00374>
- Subbotin SA, Mundo-Ocampo M, Baldwin JG (2010) Description and diagnosis of *Heterodera* species. *Systematics of Cyst Nematodes (Nematoda: Heteroderinae)*, vol. 8B. Koninklijke Brill NV, 35–449. <https://doi.org/10.1163/ej.9789004164345.i-512.14>
- Subbotin SA, Sturhan D, Rumpfenhorst HJ, Moens M (2003) Molecular and morphological characterisation of the *Heterodera avenae* species complex (Tylenchida: Heteroderidae) *Journal of Nematology* 5: 515–538. <https://doi.org/10.1163/156854103322683247>
- Subbotin SA, Vierstraete A, De Ley P, Rowe J, Waeyenberge L, Moens M, Vanfleteren JR (2001) Phylogenetic relationships within the cyst-forming nematodes (Nematoda, Heteroderidae) based on analysis of sequences from the ITS regions of ribosomal DNA. *Molecular Phylogenetics and Evolution* 21: 1–16. <https://doi.org/10.1006/mpev.2001.0998>
- Sun F, Henry N, Yu Q (2017) First report of the fig cyst nematode, *Heterodera fici* Kirjanova, on fig tree, *Ficus carica*, in Ontario, Canada. *Journal of Nematology* 49: 131–132. <https://doi.org/10.21307/jofnem-2017-056>
- Tamura K, Stecher G, Peterson D, Filipiński A, Kumar S (2013) MEGA6: Molecular Evolutionary Genetics Analysis Version 6.0. *Molecular Biology and Evolution* 30: 2725–2729. <https://doi.org/10.1093/molbev/mst197>
- Tanha Maafi Z, Sturhan D, Kheiri A, Geraert E, Subbotin S, Moens M (2004) Morphology of some cyst-forming nematodes from Iran. *Russian Journal of Nematology* 12: 59–77.
- Traub M (1885) Onderzoekingen over Sereh-Ziek Suikkeriet gedaan in s'Lands Plantentium te Buitenzorg. *Mededeelingen uit's Lands Plantentium, Batavia* 2: 1–39.
- Vovlas N, Inserra RN (1983) Biology of *Heterodera mediterranea*. *Journal of Nematology* 15: 571–576.
- Vovlas N, Inserra RN, Stone AR (1981) *Heterodera mediterranea* n. sp. (Nematoda: Heteroderidae) on *Pistacia lentiscus* in Southern Italy. *Nematologica* 27: 129–138. <https://doi.org/10.1163/187529281X00188>
- Wohlfarter M, Giliomee JH, Venter E, Storey S (2011) A survey of the arthropod pests and plant parasitic nematodes associated with commercial figs, *Ficus carica* (Moraceae), in South Africa. *African Entomology* 19: 165–172. <https://doi.org/10.4001/003.019.0118>
- Wollenweber HW (1923) Krankheiten und Beschädigungen der Kartoffel. *Arb. d. Forschungs Inst. Kartoffelbau, Berlin* 7: 1–56.
- Wollenweber HW (1924) Zur kenntnis der kartoffel-Heteroderen. *Illustrierte Landwirtschaftliche Zeitung* 44: 100–101.
- Wouts WM, Sturhan D (1996) *Heterodera litoralis* sp.n. (Nematoda: Heteroderidae) from austral glasswort, *Sarcocornia quinqueflora* in New Zealand. *Nematologica* 42: 62–10. <https://doi.org/10.1163/187529296X00067>



# *Coecobrya sirindhornae* sp. n., the most highly troglomorphic Collembola in Southeast Asia (Collembola, Entomobryidae)

Sopark Jantarit<sup>1</sup>, Chutamas Satasook<sup>2</sup>, Louis Deharveng<sup>3</sup>

**1** Excellence Center for Biodiversity of Peninsular Thailand, Faculty of Science, Prince of Songkla University, Hat Yai, Songkhla, 90110, Thailand **2** Princess Maha Chakri Sirindhorn Natural History Museum, Faculty of Science, Prince of Songkla University, Hat Yai, Songkhla, 90110, Thailand **3** Institut de Systématique, Evolution, Biodiversité (ISYEB) – UMR 7205 CNRS, MNHN, UPMC, EPHE, Muséum national d'Histoire naturelle, Sorbonne Universités, 45 rue Buffon, CP50, F-75005 Paris, France

Corresponding author: *Sopark Jantarit* ([fugthong\\_dajj@yahoo.com](mailto:fugthong_dajj@yahoo.com))

---

Academic editor: *W.M. Weiner* | Received 14 November 2018 | Accepted 14 January 2019 | Published 12 February 2019

---

<http://zoobank.org/6AD5E55D-1E0A-4D54-9BDB-63925159405B>

---

**Citation:** Jantarit S, Satasook C, Deharveng L (2019) *Coecobrya sirindhornae* sp. n., the most highly troglomorphic Collembola in Southeast Asia (Collembola, Entomobryidae). ZooKeys 824: 21–44. <https://doi.org/10.3897/zookeys.824.31635>

---

## Abstract

The most highly troglomorphic Collembola of Southeast Asia, *Coecobrya sirindhornae* sp. n., is described from a cave in Satun province, Thai Peninsula. It is characterised by its large size, extremely elongated antennae, relatively long legs and furca, reduced macrochaetotaxy, very long and slender claw, pointed tenent hair, four sublobal hairs on outer maxillary lobe, and the absence of eyes and pigmentation. A checklist of Thai *Coecobrya* species and a key to the troglomorphic species of Thailand are provided. Troglomorphy and conservation of cave habitats in the area are discussed.

## Keywords

new species, peninsular Thailand, subterranean environment, taxonomy, troglomorphy

## Introduction

The genus *Coecobrya* Yosii, 1956 is characterised by polymacrochaetotic chaetotaxy, absence or reduced eye number, absence of or weak pigmentation, four antennal segments, falcate mucro with a basal spine, and absence of body scales, labral papillae, and dental spines (Deharveng 1990, Chen and Christiansen 1993, Zhang et al. 2009).

So far, almost 60 species have been described worldwide (Bellinger et al. 1996–2019, Nilsai et al. 2017, Zhang et al. 2018). Among them, 30 species are cave dwellers. In Thailand, *Coecobrya* is widespread in both subterranean and epigeal habitats throughout the country, with many forms still undescribed (Deharveng 1990, Jantarit et al. 2016). To date, fourteen species are recorded in the country (see checklist) of which twelve are cave-restricted. With regard to cave species, two morphological types can be recognised. The first type has short antennae and appendages, short and rather swollen claw and small size (0.9–1.75 mm). Species of this type are usually associated with eutrophic habitat, especially bat guano, and are never troglomorphic (see Deharveng 1990, Zhang et al. 2018). The second type has long appendages (antennae, and to a lesser degree legs and furca), slender claws and larger body size (1.72–2.82 mm; see Nilsai et al. 2017). Its species are always linked to oligotrophic habitats in the dark zone of caves with wet and moist environment (Nilsai et al. 2017). Cave *Coecobrya* of both types have all very narrow ranges in Thailand (Deharveng 1990, Jantarit et al. 2016, Nilsai et al. 2017, Zhang et al. 2018).

Troglomorphic features in Collembola are large body size, elongated appendages (antennae, and to a lesser degree legs and furca), multiplication of antennal chaetae, elongated and slender claw complex, pointed tenent hair, blindness and depigmentation (Christiansen 2012, Deharveng and Bedos 2018, Lukić et al. 2018). Troglomorphic Collembola are increasingly reported from the tropics, but the degree of troglomorphy in the species described so far is less strong than in temperate regions. Species which exhibit significant morphological adaptation to cave life in Southeast Asia include a single Neanuridae (*Coecoloba plumleyi* Deharveng, 1983), all others being Entomobryoidea of various genera: *Coecobrya*, *Cyphoderopsis* Carpenter, 1917, *Lepidonella* Yosii, 1960, *Pseudosinella* Schäffer, 1897, *Sinella* Brook, 1882, and *Troglopedetes* Absolon, 1907 (Deharveng 1987, Deharveng and Gers 1993, Deharveng and Bedos 2000, 2012, Jantarit et al. 2013, 2016, Nilsai et al. 2017, Deharveng et al. 2018). All are narrow range species. But in a broad regional context, data on their distribution are lacking throughout most karsts of the region (Deharveng and Bedos in press, Lukić in press).

In the present study, we describe an extremely troglomorphic new species of Collembola discovered in a cave in Satun province, Thailand. We discuss its level of troglomorphy, by far the highest for Collembola of continental Southeast Asia. A key to Thai troglomorphic species is provided.

## Materials and methods

We sampled at least 130 caves throughout Thailand to date. Collembola were collected by an aspirator or extracted on Berlese funnel from organic debris. The highly troglomorphic *Coecobrya* was found in a single cave, located in Satun province. Specimens were stored in 95% ethanol and were mounted on slides in Marc Andre II medium after clearing in Nesbitt solution. Morphological characters were examined using Leica DM1000 LED microscope with phase-contrast. Drawings were made using a drawing tube, and figures were

improved with Illustrator CC (Adobe Inc). Specimens were brought alive to the laboratory, where photos were taken using a Leica M80 with Leica MC170 HD, and enhanced by LAS V4.12 software. Scanning Electron Micrographs were taken by Apreo SEM/FEI from the Scientific Equipment Center, Prince of Songkla University (Thailand).

### Abbreviations used in the description:

Morphological structures:

<b>Ant.</b>	antennal segment,	<b>mes</b>	mesochaeta(e),
<b>Abd.</b>	abdominal segment,	<b>mic</b>	microchaeta(e),
<b>psp</b>	pseudopore(s),	<b>ms</b>	S-microchaeta(e)/
<b>Th.</b>	thoracic segment,		microsensillum(a),
<b>Gr.</b>	group,	<b>tric</b>	trichobothrium(ia),
<b>tita</b>	tibiotarsus,	<b>s</b>	ordinary S-chaeta(e)/sens
<b>mac</b>	macrochaeta(e),		

Institutions:

<b>BDCM</b>	Biology department, Chiang Mai University, Chiang Mai, Thailand;
<b>BPBM</b>	Bishop Museum, Honolulu, Hawaii;
<b>LEITT</b>	Laboratoire d'Ecologie des Invertébrés Terrestres, Université Paul Sabatier, Toulouse, France (= Laboratoire de Zoologie, Université Paul Sabatier, Toulouse, France);
<b>MNHN</b>	Museum national d'Histoire naturelle, Paris, France;
<b>NHM-PSU</b>	Princess Maha Chakri Sirindhorn Natural History Museum, Prince of Songkla University, Songkhla, Thailand;
<b>NJAU</b>	Department of Entomology, College of Plant Protection, Nanjing Agricultural University, China.

### Terminology

Dorsal body chaetotaxy follows Szeptycki (1979) and Zhang et al. (2011). We use the notation of Zhang et al. (2016) for clypeal chaetotaxy, Fjellberg (1999) for labial palp. Dorsal chaetotaxy of head follows Jordana and Baquero (2005). Ventral chaetotaxy of head follows Chen and Christiansen (1993). Labial chaetae notation follows Gisin (1967), with the upper-case letter for ciliated and lower-case letter for smooth chaetae. The number of dorsal macrochaetae is given from Th. II–Abd. IV. Symbols representing chaetal types used in the figures are as follows: large circle = macrochaeta; small circle = mesochaeta; cross = trichobothrium; and circle with a slash = pseudopore. Chaeta-to-chaeta homologies proposed here are indicative for several parts of the body where chaetae are known to be more or less variable in number or position.

## Taxonomy

**Class Collembola Lubbock, 1873**

**Order Entomobryomorpha Börner, 1913**

**Family Entomobryidae Tömösváry, 1882**

**Subfamily Entomobryinae Schäffer, 1896**

**Genus *Coecobrya* Yosii, 1956**

***Coecobrya sirindhornae* sp. n.**

<http://zoobank.org/E4EADDEEB-F274-4CAE-9ABB-40FF14934965>

Figs 1–7

**Type material. *Holotype*:** male on slide, Thailand: Satun province: Manang district, Tham Rusri, altitude 58 m, nine specimens (one male, one female and three subadults in slides, three in ethanol), dark zone of cave, by aspirator, S Jantarit and A Nilsai leg. (sample # THA\_SJ\_STN09), 30/04/2016 (A Nilsai), six specimens (three subadults in slides, three in ethanol); 03/05/2016 (S Jantarit and A Nilsai), five specimens in ethanol; 25/07/2017 (S Jantarit and A Nilsai), three specimens in ethanol; 17/03/2018 (S Jantarit and A Nilsai), three specimens in ethanol. Holotype and 13 paratypes in slides deposited in NHM-PSU. Two paratypes in alcohol in MNHN. Three paratypes on slides and three in alcohol in NJAU. Tham = cave (in Thai).

**Description. *Habitus*** (Fig. 1A–D, G). Medium size Entomobryidae. Body length up to 2.6 mm (holotype 2.1 mm). No scales. Eyes absent. Colour: pale yellow to whitish in alcohol, without pigments. Four antennal segments (sometimes Ant. III and IV fused together). Body slender with very long antennae and moderately elongate legs and furca. Body not bent nor humped at level of Th. II. Th. II slightly longer than Th. III; Abd. IV 3–4 times as long as Abd. III.

***Pseudopores*** (Figs 2B, 3D–E, 3H, 4A–C, 5E–G, 6F). Pseudopores present as round flat disks, smaller than mac sockets (Figs 3H, 4A–C), except for the coxae and manubrium where psp are as large as mac sockets, present on various parts of the body: antennae, head, tergites, coxae and manubrium. On antennae, psp located ventro-apically between the tip of antennal segments and the chaetae of the apical row, or just below apical row of chaetae (two on Ant. I, 2–3 on Ant. II, and 4–7 on Ant. III) (Figs 2B, 3D–E). On head, 1–(2) psp located externally on each peri-antennal area (Fig. 4A). On tergites, 1+1 psp close to the axis from Th. II to Abd. IV (Fig. 4B, C). Coxae I, II, and III with 2– (3), 2– (3), and 1–2 psp respectively, located close to longitudinal rows of chaetae (Fig. 5E–G). On manubrium, 2+2 dorso-apical ones (Fig. 6F).

***Mouthparts and ventral head chaetotaxy*** (Figs 2E–J, 3F, 3K). Clypeal area with three long, smooth prefrontal and 6–10 ciliated and two long smooth facial chaetae (Fig. 2E), sometimes asymmetric arrangement. Distal border of the apical non-granulated area of the labrum with a relatively narrow median U-form intrusion into the granulated area dorsally; apical edge not adorned with spines (Figs 2F, 3F). Ventro-distal complex of labrum well differentiated, asymmetrical, with 1+1 distal combs of 13–21 minute teeth

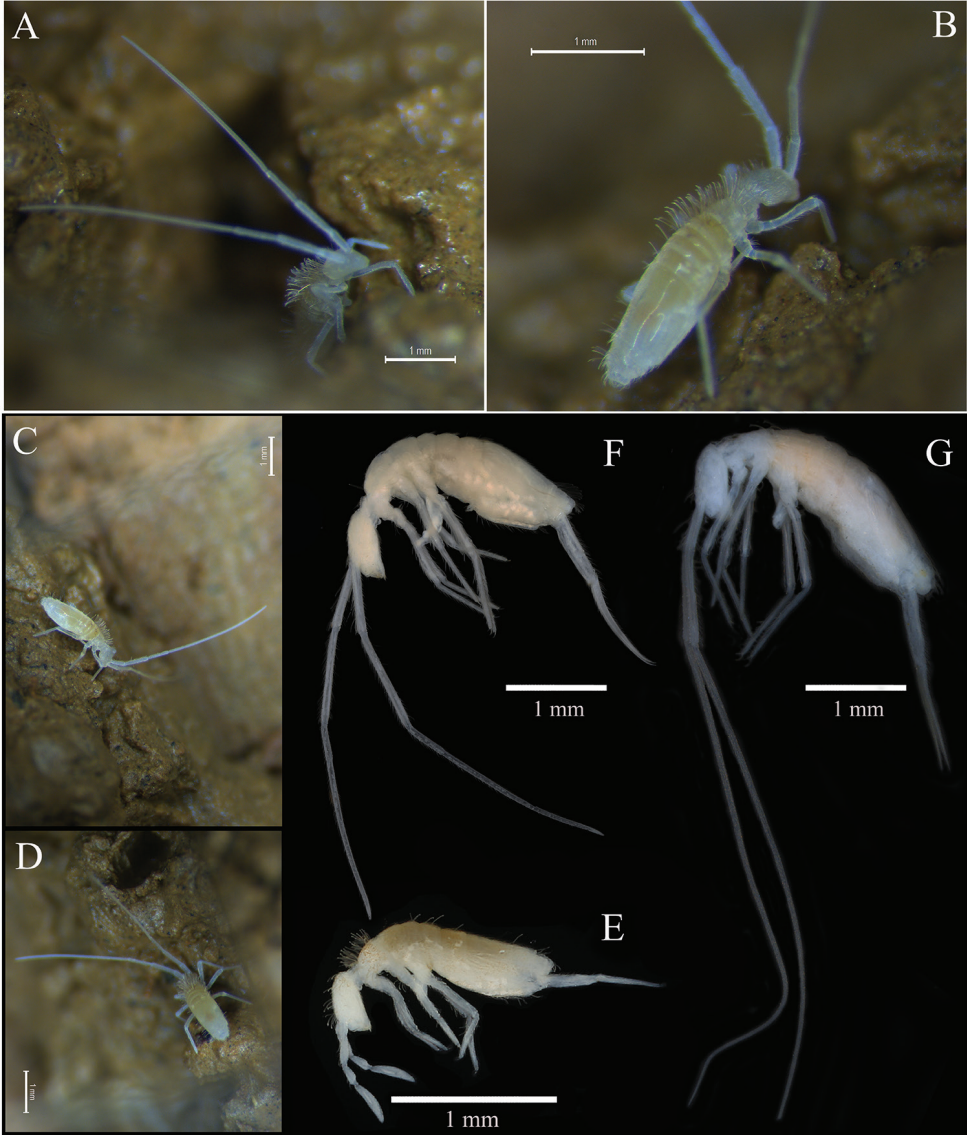


**Figure 1.** *Coecobrya sirindhornae* sp. n. **A–D** Habitus **E–F** Two morphological types of cave *Coecobrya* in Thailand **E** *Coecobrya phanthuratensis* Zhang & Jantarit, 2018; normal form with short antennae, appendages and small size **F** *Coecobrya polychaeta* Zhang & Nilsai, 2017; troglomorphic form with long antennae and appendages with large body size and **G** *Coecobrya sirindhornae* sp. n., highly troglomorphic characters with extremely long antennae and appendages and also large body size.

on the left side and 10–11 strong and larger teeth on the right side, and an axial pair of long sinuous tubules, round apically (Fig. 2J). Prelabral and labral chaetae 4/5, 5, 4, all thin and smooth; three median chaetae of the first and second rows longer and slightly larger than those of the distal and proximal rows (35–45 vs, 30  $\mu$ m)(Figs 2F, 3F). Maxillary



**Figure 2.** *Coecobrya sirindhornae* sp. n. continued. **A** Distal part of Ant. II dorsally of left antenna **B** Ant. III organ of left side **C** Distal part of Ant. IV with subapical organite **D** Ratio of antennal length **E** Clypeal chaetae **F** Prelabral and labral chaetae **G** Labial palp **H** Outer maxillary lobe **I** Mandibles **J** Ventro-distal complex of labrum **K** Chaetae of labial basis and ventral chaetotaxy of head.

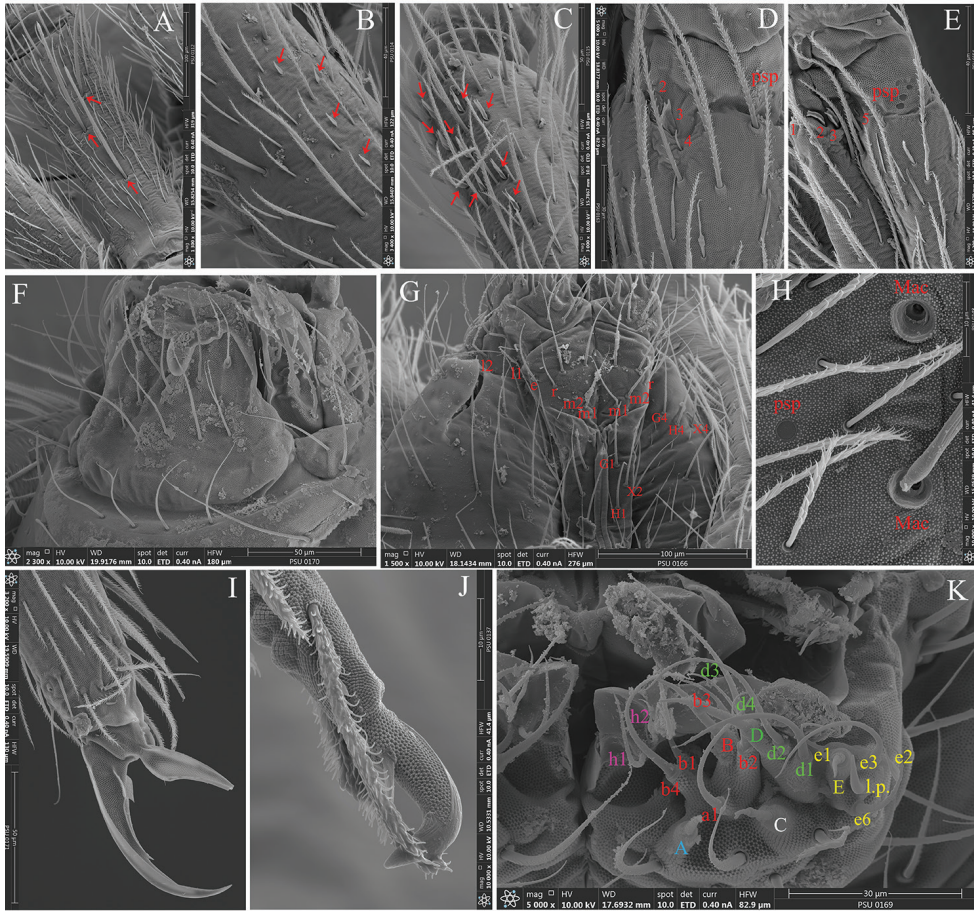


**Figure 3.** *Coecobrya sirindhornae* sp. n. continued with SEM. **A** Ant. I dorsally with three mac (arrows) **B** Ant. I latero-dorsally with a row of spear-like chaetae (arrows) **C** Distal part of Ant. II dorsally with a group of paddle-like chaetae (arrows) **D–E** Ant. III organ of right side **F** Labral chaetae and maxillary outer lobe **G** Ventral chaetotaxy of head **H** Pseudopore and mac on Th. III **I** Claw III morphology **J** Mucro **K** Labial palp with its notation after Fjellberg (1999).

outer lobe with one papillate chaeta, one basal chaeta, and four sublobal hairs of which the upper one is three times shorter than the others (Figs 2H, 3F). Labium and ventral head (Figs 2G, K, 3G, K). Labial palp strongly modified for the genus, with 0, 5, 0, 4, 4 guards for papillae A–E, like that described by Fjellberg (1999) for Entomobryidae or by Xu and Zhang (2015) for *Coecobrya*. Lateral process of labial palp subcylindrical, as thick as normal chaetae, with tip slightly beyond apex of labial papilla (Figs 2G, 3K). Five smooth and acuminate proximal chaetae. Chaetae of labial basis all smooth ( $m_1, m_2, r, l_1, l_2$ ); chaetae  $m_2$  slightly larger and longer than  $m_1$ , chaetae  $m_1$ ,  $e$  and  $l_1$  subequal,  $r$  thin and shortest, and  $l_2$  longest (Figs 2K, 3G). One short and smooth chaeta present in one individual between  $m_2$  and  $r$ , other two chaetae of the submentum smooth and acuminate, of similar size. Postlabial chaetae  $X_2, X_3, X_4$  smooth, long and acuminate,  $X_1$  absent; 2–5 smooth

and minute chaetae between  $H_2$  and  $H_3$ . On each side of linea ventralis, 7–9 smooth and 3–7 ciliate chaetae, the anterior 6 always long, smooth and acuminate, the posterior ones either smooth or ciliated (Figs 2K, 3G). Mandible apex strong, asymmetrical (left with four teeth, right with five teeth); molar plate with three strong pointed basal tooth, and 3–(5) smaller inner distal teeth, identical in both mandibles (Fig. 2I). Maxilla capitulum with a three-toothed claw and several stout ciliated lamellae; lamella 2 large and broad, lamella 3 well developed; several other lamellae present.

*Antennae* (Figs 1A–D, 1G, 2A–D, 3A–E). Antennae extremely long, approximately 8.0–12.3 times as long as cephalic diagonal and 2.0–2.2 times longer than (head + body). Antennal segment ratio as I : II : III : IV = 1 : 1.3–1.9 : 1.6–2.0 : 8.1–11.3 (N = 5). Antennal segments not subdivided nor annulated. At least three specimens with asymmetrical antennae, one with four segments and the other one slightly shortened with three segments; two specimens with three antennal segments of both sides. Antennal chaetal types not analysed in detail. Ant. I dorsally with three mac (Fig. 3A) and a row of 2–4 spear-like chaetae latero-dorsally (Fig. 3B). Ant. I ventrally with many smooth spiny mic of various sizes in its basal part, many subcylindrical, hyaline sens in its middle to apical part, and many long smooth straight chaetae. Ant. II dorsally with 10–12 paddle-like chaetae (sensu Nilsai et al. 2017) in its distal part (Figs 2A, 3C). Ant. III organ with five sens; sens one and four subequal, hyaline; sens five acuminate, dark and shorter; sens two and three swollen resting in shallow groove (Figs 2B, 3D–E), not clearly seen in most specimens. Ant. IV very long, not subdivided, without apical bulb (Fig. 2C–D). Subapical organite not distinctly knobbed, swollen, slightly enlarged apically, inserted dorsally at 35–45  $\mu\text{m}$  from the tip (Fig. 2C).

*Dorsal head chaetotaxy* (Fig. 4A). Dorsal cephalic chaetotaxy with one antennal (An), without median (M) and five sutural (S) mac; Gr. II with only one mac;  $A_0$  as mes; 7+7 scale-like structures (2–3  $\mu\text{m}$ ) present below sutural mac, probably inside the integument; a pair of short cephalic trichobothria, external and close to the middle of the head (Fig. 4A).

*Tergites* (Fig. 4B–D). Th. II with three (m1, m2, m2i) medio-medial, two (m4, m4p) medio-sublateral and 15–18 posterior mac; 1+1 ms and 1+1 sens antero-laterally. Th. III with 32–35 mac; a1a as mac. 2+2 sens laterally. Abd. I with six (a3, m2–4, m2i, m4p) mac. 1+1 ms and 1+1 sens laterally. Abd. II with two (m3, m3e) central and one (m5) lateral mac. 2+2 tric without modified chaetae, 1+1 sens laterally and 1+1 mic near internal tric. Abd. III with one (m3) central and three (am6, pm6, p6) lateral mac. 3+3 tric not surrounded by modified chaetae, 1+1 sens laterally, 1+1 mic near m3, ms not seen (Fig. 4B). Abd. IV with six central mac (I, M, A5–6, A5p, B6) and eight (D3, E2–4, E2p, F1–3) lateral mac, 2+2 tric and approx. 5–7 long S-like chaetae anteriorly, without modified chaetae (Fig. 4C). Abd. V with 13–15 mac and 2+2 sens (Fig. 4D). Abd. VI not analysed. S-chaetae formula from Th. II to Abd. V: 2+ms, 2/1+ms, 2, 2+ms, 1+  $\approx$ 5–7, 2; as sens not seen and ps on Abd. IV 1/4 as long as S-like chaetae (Fig. 4C).

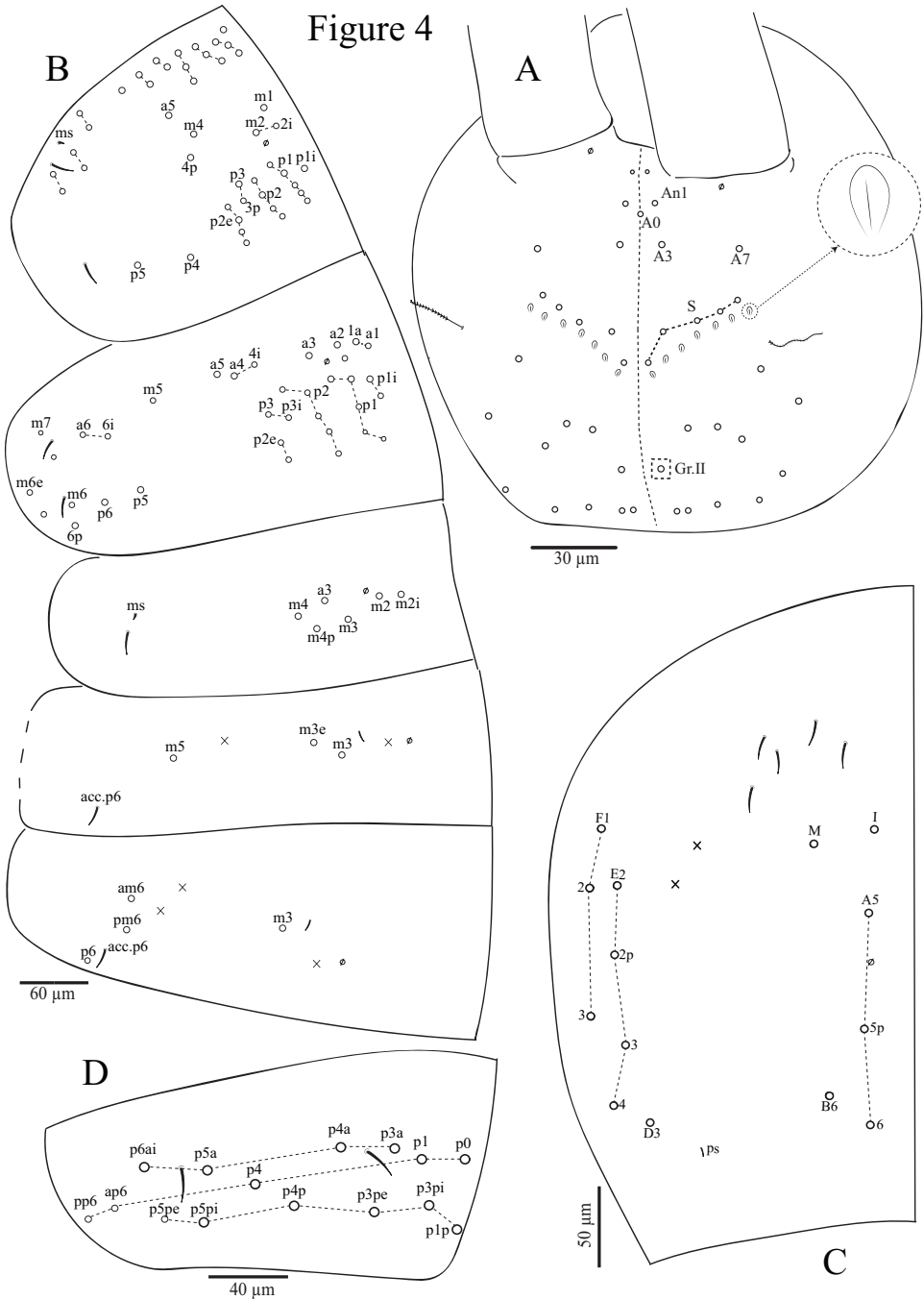


Figure 4. *Coecobrya sirindhornae* sp. n. continued. **A** Chaetotaxy of dorsal head **B** Chaetotaxy of dorsal Th. II-Abd. III **C** Chaetotaxy of dorsal Abd. IV **D** Chaetotaxy of dorsal Abd. IV.

*Legs* (Figs 3I, 5A–G) long; tita of leg III slightly longer than tita of legs I and II. Legs devoid of scales, covered with ordinary ciliated chaetae of various lengths, mic not seen. Coxa of leg I with three proximal psp and two chaetae posteriorly; coxa of leg II with 8–10 chaetae (5–6 mac) in anterior row, 3–4 chaetae (mac) in posterior row and 2–3 proximal psp in between; coxa of leg III with 13+15 chaetae (6–7 mac) in anterior row, and one proximal psp posteriorly. Trochanteral organ with 12–18 smooth, straight, unequal spine-like chaetae (Fig. 5D). The distal whorl of tita with 10–12 subequal ciliated mes, irregularly arranged, and a thin, acuminate, smooth dorso-apical tenent hair. Tenent hair of tita I longer (50–65  $\mu\text{m}$ ) than that of tita II and III (30–40  $\mu\text{m}$ ) (Fig. 5A–C). Tita I–III with one smooth, thin and long chaetae close to tenent hair (25–40  $\mu\text{m}$ , N = 5) (Figs 3I, 5A–C). Ventro-distal smooth chaeta of tita III thick, erected, pointed, rather short (35–40  $\mu\text{m}$ , N = 5). Pretarsal mic minute (2.5–3.0  $\mu\text{m}$ ). Claw slender and elongated; claw I and II subequal (60–98  $\mu\text{m}$  long, 7–12  $\mu\text{m}$  wide at basis), claw III slightly longer (80–100  $\mu\text{m}$  long, 15–17  $\mu\text{m}$  wide at basis) (N = 5). All claw with one strong inner tooth at 50–55% and a pair of basal inner teeth at approx. 22–25% of inner edge from basis. Unguiculus approx. 3/5 as long as inner edge of claw, slightly swollen baso-internally, pointed apically, devoid of inner tooth, not truncated, with 2–3 minute outer teeth, often inconspicuous, at 1/3 of its length (Figs 3I, 5A–C).

*Ventral tube* (Fig. 6A–D). Ventral tube four times longer than wide. Lateral flaps with 7–8+7–8 smooth chaetae (sometimes with 5+5 ciliated and 3+3 smooth) (Fig. 6C–D). Anteriorly with 10+10 large chaetae, 3+3 ciliated and 7+7 smooth, two of them larger (Fig. 6B); posteriorly with 20–30 mes, all serrated, arranged roughly asymmetrically, with 1+1 smooth, straight, distal mac close together (Fig. 6A).

*Furcal complex* (Figs 3J, 6E–I). Tenaculum with four large teeth of decreasing size from the basal to the distal one of each ramus, on a prominent, irregular body, with a postero-basal strong serrated chaeta bent distally (Fig. 6E). Mucrodens 1.25–1.60 times longer than manubrium. Furcula without smooth chaetae. Manubrium with a dense cover of ciliated chaetae both dorsally and ventrally. Manubrial plaque with two pseudopores and three ciliate chaetae (Fig. 6F). Distal part of manubrium ventrally with 8–10 ciliate chaetae on each side, four of them mac (Fig. 6G). Inside the manubrium, two thin, straight longitudinal structure running on  $\frac{3}{4}$  of manubrium length from its apex like in *Lepidonella doveri* (Carpenter, 1933) (after Deharveng et al. 2018) (Fig. 6H). Dens without spines, annulated and covered with ciliated chaetae on both sides. Distal smooth part of dens slightly shorter than mucro. Mucro strong and falcate, basal spine long, nearly reaching the tip of the mucronal tooth (Figs 3J, 6I).

*Genital plate* (Fig. 6J). Male genital plate with 3+3 genital mic, acuminate circum-genital mes not clearly seen, without modified chaetae. Spermathecal duct elongated and annulated (Fig. 6J). Female genital plate not clearly seen.

**Ecology.** *Coecobrya sirindhornae* sp. n. is restricted to the dark zone of the cave where it has been found, in the oligotrophic environment of a small chamber, on muddy ground and wet rock walls. The chamber is connected to a narrow steep hole. Small puddles are present in the chamber and water is dripping from the ceiling. Muddy ground surface is flooded during rainy season. Some individuals were found feeding

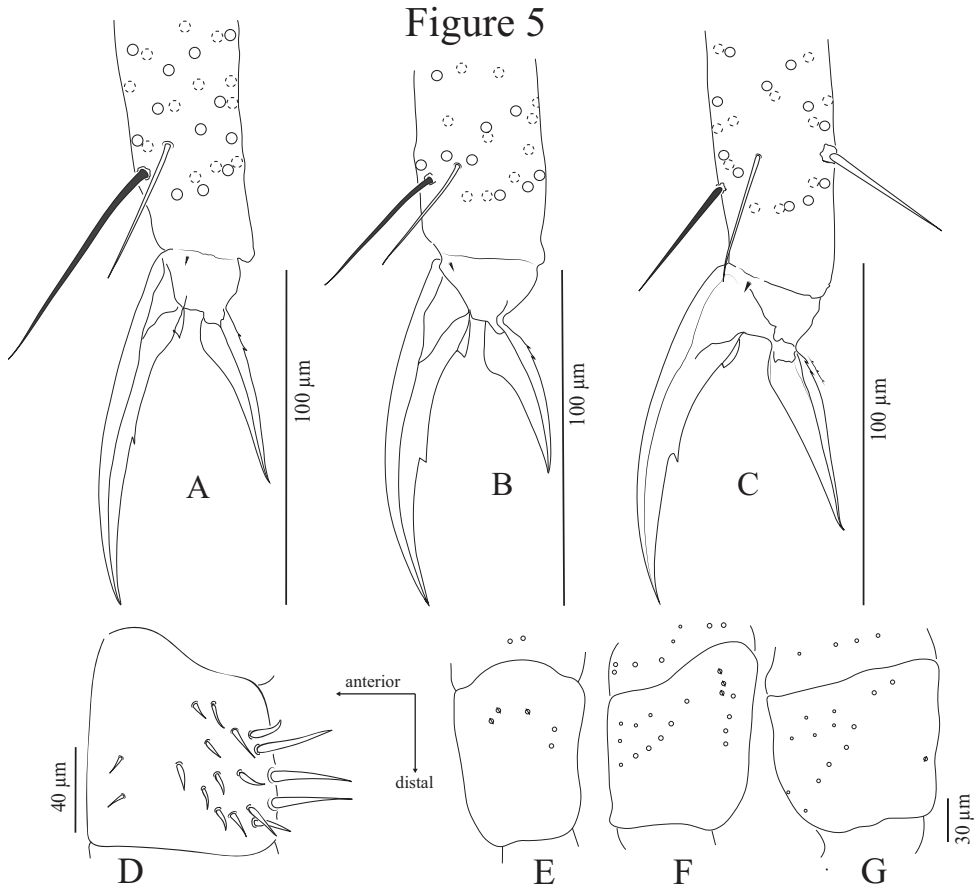


**Figure 5.** *Coecobrya sirindhornae* sp. n. continued. **A** Distal part of tita I and claw complex **B** Distal part of tita II and claw complex **C** Distal part of tita III and claw complex **D** Trochanteral organ **E** Pseudopores and chaetae sockets of coxae I–III (left to right).

on a cricket corpse. They were quick jumping and moved rapidly. The species is found only in that chamber where humidity is at saturation, and temperature is constant (23–24 degrees Celsius). The population seems rather limited (only 26 specimens were collected from five attempts, each time one hour collecting by 2 people). Small (young) individuals were less numerous and not collected.

**Etymology.** This species is named to honour Her Royal Highness Princess Maha Chakri Sirindhorn, who is passionately interested in natural history and plays an important role in promoting the conservation of biodiversity and the environment of Thailand.

**Remarks.** *Coecobrya sirindhornae* sp. n. differs at first from all other species of the genus by its highly troglomorphic characters. Diagnostic morphological characters of the new species and related troglomorphic *Coecobrya* are listed in Table 1. *Coecobrya sirindhornae* sp. n. is well characterised by the combination of large body size, extreme-

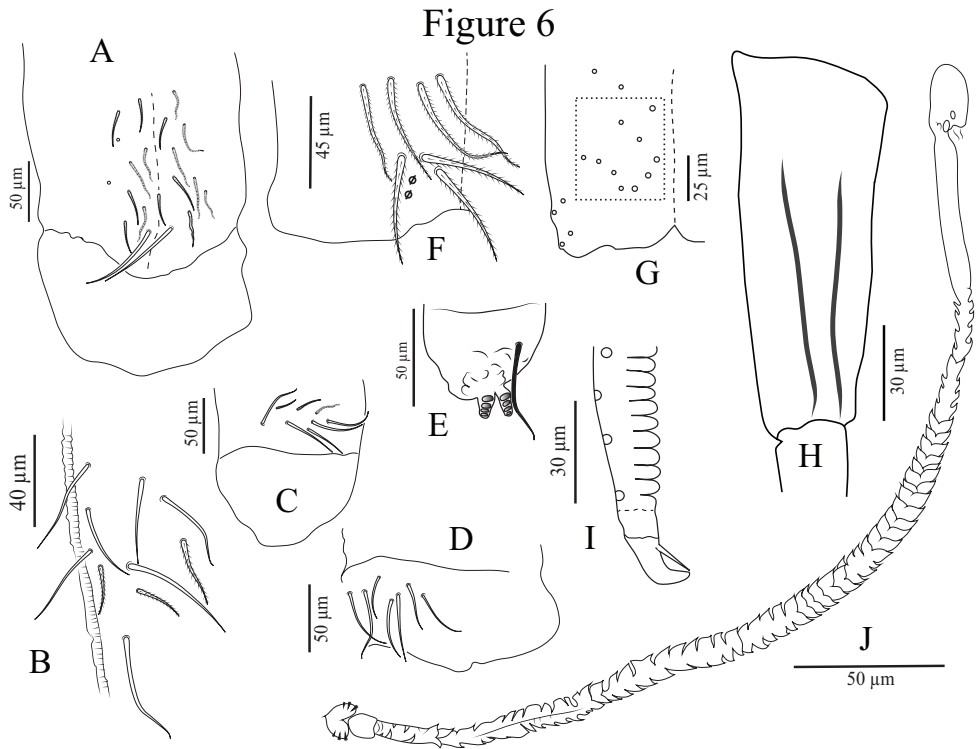


**Figure 6.** *Coecobrya sirindhornae* sp. n. continued. **A** Posterior side of ventral tube **B** Anterior side of ventral tube **C, D** Lateral flap **E** Tenaculum **F** Manubrium plaque **G** Distal part of manubrium ventrally **H** Manubrium with two thin, straight longitudinal structures inside **I** Mucro **J** Spermathecal duct.

ly long antennae, all labial chaetae smooth, elongated lateral process of labial palp and four sublobal hairs on maxillary outer lobe, very elongated and slender claw, presence of 2–3 minute teeth on outer edge on unguiculus, less chaetae on ventral tube and both sides of distal part of manubrium, and reduced dorsal chaetotaxy of both head and tergites. Head is without M row and with internal scale-like structures below the sutural mac. We have been unable to detect the third pair of sens on Abd. V, but we do not consider this absence as diagnostic as it would be a very unusual feature for a *Coecobrya*, and it is often difficult to observe or fallen down. Antennae of the new species are the longest known in the genus, longer than *C. nupa* Christiansen & Bellinger, 1992 from Hawaii, previously the species with the longest antennae; and *C. polychaeta* Zhang & Nilsai, 2017 and *C. chumphonensis* Zhang & Nilsai, 2017 (both in Nilsai et al. 2017) from Thai peninsula (Table 1). According to the three troglomorphic species of Thailand, *C. polychaeta* comes near to *C. sirindhornae* sp. n. in body length, colour, clypeus chaetae, elongated lateral process of labial palp and number of sublobal hairs on maxillary outer lobe, but can be clearly differentiated from it by the characters listed in Table 1. The other two taxa from Thailand are not close to the new species. *Coecobrya nupa*, the first report of highly troglomorphic species in the genus, differs

**Table 1.** Comparison of troglomorphic *Coecobrya*: *C. chumphonensis* Zhang & Nilsai, 2017, *C. cavicta* Nilsai & Zhang, 2017, *C. polychaeta* Zhang & Nilsai, 2017, *C. sirindhornae* sp. n., and *C. nupa* Christian- sen & Bellinger, 1992. Key: c = ciliated chaetae, s = smooth chaetae, ? = not given in literature description. Characters indicated in parentheses are rarely observed.

Characters	<i>C. chumphonensis</i>	<i>C. cavicta</i>	<i>C. polychaeta</i>	<i>C. sirindhornae</i> sp. n.	<i>C. nupa</i>
Body length	up to 2.82 mm	1.72 mm	up to 2.58 mm	up to 2.6 mm	2.0 mm
Ant. /head	3.70–4.48	2.67	5.91–7.12	8.0–12.3	6.5
Long smooth straight chaetae on antennae	absent	present	absent	present	?
Number of paddle-like chaetae on Ant. II	2–4	?	1	10–12	?
Clypeus					
prefrontal	3s	?	3s	3s	?
facial	8s	?	2s7–10c	2s7–10c	?
Dorsal head					
An	2	4	4	1	?
A0	mac	mac	mic	mes	?
M	4	3	3	0	?
Gr. II	6(7)	4	3	1	?
Sublobal hairs on maxillary outer lobe	3	3	4	4	3
Lateral process of labial palp	short	short	long	long	short
Labial chaetae	mRel <sub>1</sub> <sub>2</sub>	mrel <sub>1</sub> <sub>2</sub>	M <sub>1</sub> m <sub>1</sub> rel <sub>1</sub> <sub>2</sub>	m <sub>1</sub> m <sub>1</sub> rel <sub>1</sub> <sub>2</sub>	M <sub>1</sub> m <sub>1</sub> rel <sub>1</sub> <sub>2</sub>
Postlabial chaeta X	minute	minute	normal	normal	?
Chaetae along cephalic groove	4s5–7c	3–4s7–8c	6–7s5–10c	7–9s3–7c	?
Chaetotaxy of Th. II					
medio-medial mac	4–6	3	7(6)	3	2
medio-sublateral mac	3	4	3	2	?
Posterior mac Th. II	25–32	30–31	29–40	15–18	?
Mac on Th. III	32–35	35	35–43	32–35	15?
Mac on Abd. I	6–7	6–7	8–9	6	4
Central mac Abd. II	3	3	4(3)	2	2
Chaetotaxy of Abd. III					
central mac	2	1	1	1	1
lateral mac	3	3	3	3	2?
ms	not seen	not seen	present	not seen	?
Chaetotaxy of Abd. IV					
central mac	7	7–9	6	6	4
lateral mac	10–12	11	9	8	?
Tenent hair	usually pointed	pointed	pointed	pointed	pointed
Ungual inner teeth	3	2	3	3	3
Unguiculus outer edge	serrate	serrate	serrate	2–3 teeth	?
Ventral tube					
anterior face	9–12	?	12	10	?
posterior face	13	?	20–31	20–30	7
lateral flap	7(10)	?	9–12	7–8s(5c)	6
Smooth chaetae trochanteral organ	12–22	15–16	15–25	12–18	16
Chaetae on manubrial plaque	4–7	4	4–10	3	5
Chaetae on ventro-distal part of manubrium	11–15c	13c	15–25c	8–10c	?
Mucronal spine	nearly reaching mucronal apex	nearly reaching mucronal apex	nearly reaching mucronal apex	nearly reaching mucronal apex	beyond mucronal apex
Locality	Chumphon, Thailand	Satun, Thailand	Satun, Thailand	Satun, Thailand	Maui, Hawaii

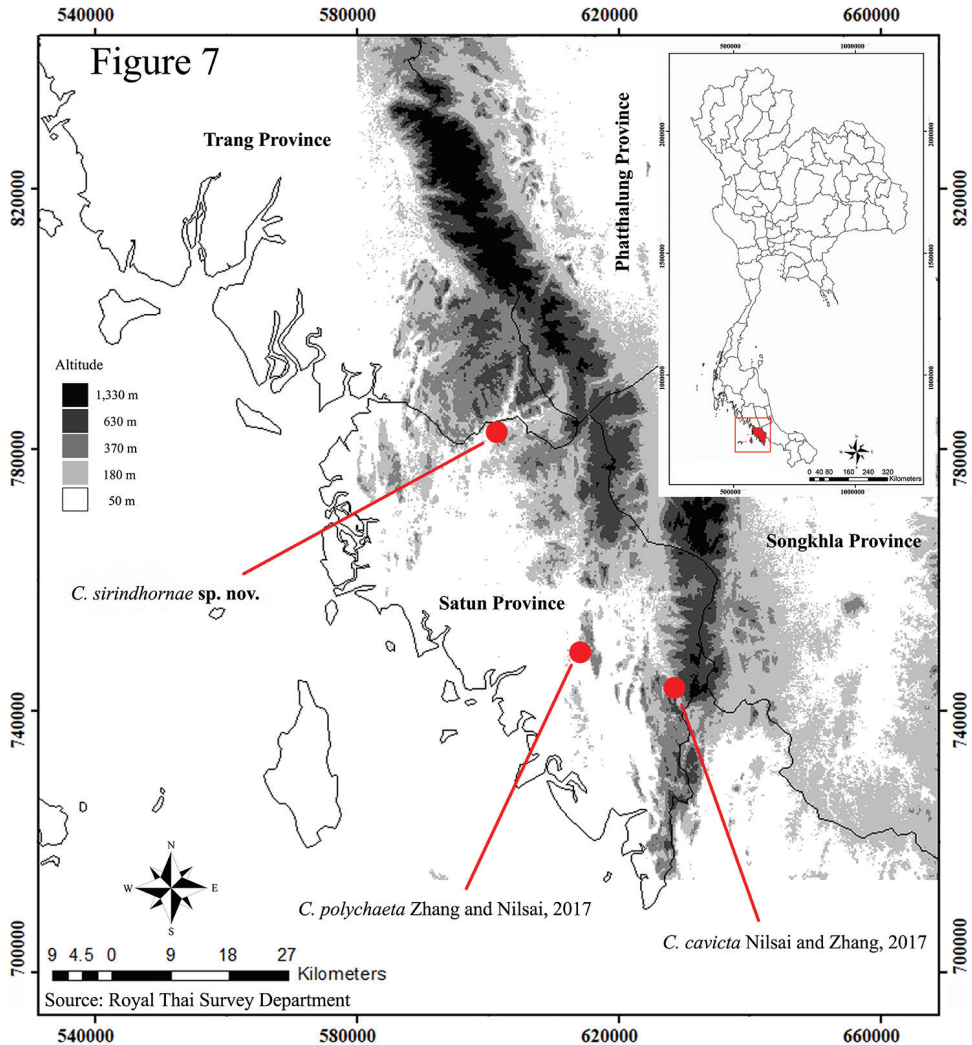


**Figure 7.** Distribution of three troglomorphic *Coecobrya* species in Satun caves, all located in lowland areas.

from the new species mainly in shorter antennae length, labial basis chaetotaxy, claw morphology and mucronal spine exceeding the tip of the apical tooth (Table 1). The distribution map of *C. sirindhornae* sp. n. and the other two troglomorphic *Coecobrya* discovered in Satun province is shown in Figure 7.

### Checklist of Thai species of *Coecobrya*

Jantarit et al. (2016) listed only three species of genus *Coecobrya* and erroneously did not include *C. lanna* Zhang, Deharveng & Chen, 2009 in the checklist of Collembola of Thailand. Recently, ten newly discovered species were described by Nilsai et

al. (2017) and Zhang et al. (2018). *Coecobrya* species are listed here by including the valid names, author(s) and year of publication, source(s), type deposition, altitude, coordinates (if available), ecological data, and distribution. Records are updated to 10/01/2019.

***Coecobrya cf. hoefti* (Schäffer, 1896)**

**Sources.** Yosii 1961, Takeda 1981, Deharveng 1986, Deharveng et al. 1989, Rojanavongse et al. unpublished report, Jantarit et al. 2016.

**Altitude.** > 2,000 m a.s.l. in Doi Inthanon, Chiang Mai province (Yosii 1961); 800 m a.s.l. in Chaiyaphum province (Takeda 1981) (given as Khon Kaen province in Jantarit et al. 2016; Khon Kaen experimental farm is actually located in Chaiyaphum).

**Habitat.** No ecological data in Chiang Mai province; soil sample in mixed dry deciduous forest and deforested area in Chaiyaphum province.

**Distribution.** Doi Inthanon, Chiang Mai province, northern Thailand and Khon San district, Chaiyaphum province, northeastern Thailand.

**Distribution outside Thailand.** Europe.

***Coecobrya guanophila* Deharveng, 1990**

**Sources.** Deharveng 1990, Bedos 1994, Deharveng and Bedos 2001, Rojanavongse et al. unpublished report, Jantarit et al. 2016.

**Type deposition.** BDCM, BPBM, LEITT, MNHN.

**Altitude.** 458 m a.s.l.

**Coordinates.** 19°23.6386'N; 98°55.6864'E

**Habitat.** Dark zone of cave (Tham Chiang Dao) on bat guano.

**Distribution.** Chiang Dao district, Chiang Mai province, northern Thailand (only known from the type locality).

***Coecobrya similis* Deharveng, 1990**

**Sources.** Deharveng 1990, Bedos 1994, Rojanavongse et al. unpublished report, Jantarit et al. 2016.

**Type deposition:** BDCM, BPBM, LEITT, MNHN.

**Altitude.** 500 m a.s.l.

**Coordinates.** around Tham Chiang Dao (19°23.6386'N; 98°55.6864'E)

**Habitat.** Near the entrance of Tham Chiang Dao, litter and soil.

**Distribution.** Chiang Dao district, Chiang Mai province, northern Thailand (only known from the type locality).

***Coecobrya lanna* Zhang, Deharveng & Chen, 2009**

**Sources.** Zhang et al. 2009, Cipola and Bellini 2016, Nilsai et al. 2017.

**Type deposition.** MNHM and NJAU.

**Altitude.** 1,720 m a.s.l.

**Coordinates.** 19°23.5213'N; 98°52.4899'E

**Habitat.** Forest litter at Doi Chiang Dao.

**Distribution.** Chiang Dao district, Chiang Mai province, northern Thailand (only known from the type locality).

***Coecobrya cavicta* Nilsai & Zhang, 2017**

**Source.** Nilsai et al. 2017.

**Type deposition.** NHM-PSU.

**Altitude.** 115 m a.s.l.

**Coordinates.** 6°43.5816'N; 100°9.7494'E

**Habitat.** Dark zone of cave (Tham Ton Din) in wet and humid environment, near a stream bank, without bat guano.

**Distribution.** Khuan Don district, Satun province, southern Thailand (only known from the type locality).

***Coecobrya chumphonensis* Zhang & Nilsai, 2017**

**Source.** Nilsai et al. 2017.

**Type deposition.** NHM-PSU and NJAU.

**Altitude.** 70 m a.s.l.

**Coordinates.** 10°26.7841'N; 99°2.1018'E

**Habitat.** Dark zone of cave (Tham Chang Puak) on wet ground and rocks near a puddle; wet and humid environment, in an oligotrophic habitat without bat guano.

**Distribution.** Mueang district, Chumphon province, southern Thailand (only known from the type locality).

***Coecobrya polychaeta* Zhang & Nilsai, 2017**

**Source.** Nilsai et al. 2017.

**Type deposition.** NHM-PSU and NJAU.

**Altitude.** 23 m a.s.l.

**Coordinates.** 6°46.5246'N; 100°2.4966'E

**Habitat.** Dark zone of cave (Tham Phraya Bangsa) in a small chamber of muddy ground, wet and humid environment, in an oligotrophic habitat without bat guano.

**Distribution.** Mueang district, Satun province, southern Thailand (only known from the type locality).

***Coecobrya* cf. *polychaeta* Zhang & Nilsai, 2017**

**Source.** Nilsai et al. 2017.

**Altitude.** 115 m a.s.l.

**Coordinates.** 6°43.5816'N; 100°9.7494'E

**Habitat.** Dark zone of cave (Tham Ton Din) along a stream bank, on stalagmites, muddy and clay substrate, gravels and rocks in wet and humid environment, without bat guano.

**Distribution.** Khuan Don district, Satun province, southern Thailand (only known from this cave).

***Coecobrya donyoo* Zhang & Jantarit, 2018**

**Source.** Zhang et al. 2018.

**Type deposition.** NHM-PSU and NJAU.

**Altitude.** 65 m a.s.l.

**Coordinates.** 9°54.238'N; 99°2.685'E

**Habitat.** Dark zone of cave (Tham Don Yoa) on bat guano.

**Distribution.** Lang Suan district, Chumphon province, southern Thailand (only known from the type locality).

***Coecobrya khaopaela* Zhang & Jantarit, 2018**

**Source.** Zhang et al. 2018.

**Type deposition.** NHM-PSU and NJAU.

**Altitude.** 300 m a.s.l.

**Coordinates.** 9°33.5599'N; 98°58.9364'E

**Habitat.** Dark zone of cave (Tham Khao Paela) on bat guano.

**Distribution.** Tha Chana district, Surat Thani province, southern Thailand (only known from the type locality).

***Coecobrya kbromwanaramica* Zhang, 2018**

**Source.** Zhang et al. 2018.

**Type deposition.** NHM-PSU and NJAU.

**Altitude.** 77 m a.s.l.

**Coordinates.** 8°46.194'N; 99°22.106'E

**Habitat.** Twilight to dark zone of a rather dry cave (Tham Khromwanaram) on bat guano.

**Distribution.** Ban Na San district, Surat Thani province, southern Thailand (only known from the type locality).

***Coecobrya phanthuratensis* Zhang & Jantarit, 2018**

**Source.** Zhang et al. 2018.

**Type deposition.** NHM-PSU and NJAU.

**Altitude.** 82 m a.s.l.

**Coordinates.** 8°54.028'N; 98°31.498'E

**Habitat.** Twilight to dark zone of cave (Tham Phanthurat) on bat guano.

**Distribution.** Phanom district, Surat Thani province, southern Thailand (only known from the type locality).

***Coecobrya promdami* Zhang & Jantarit, 2018**

**Source.** Zhang et al. 2018.

**Type deposition.** NHM-PSU and NJAU.

**Altitude.** 78 m a.s.l.

**Coordinates.** 9°12.293'N; 99°46.47'E

**Habitat.** Dark zone of humid cave (Tham Khao Wang Thong) on bat guano.

**Distribution.** Khanom district, Nakhon Si Thammarat province, southern Thailand (only known from the type locality).

***Coecobrya ranongica* Nilsai & Zhang, 2018**

**Source.** Zhang et al. 2018.

**Type deposition.** NHM-PSU and NJAU.

**Altitude.** 52 m a.s.l.

**Coordinates.** 10°19.5745'N; 98°45.9012'E

**Habitat.** Twilight to dark zone of cave (Tham Phra Khayang) on bat guano.

**Distribution.** Kra Buri district, Ranong province, southern Thailand (only known from the type locality).

***Coecobrya specusincola* Zhang & Nilsai, 2018.**

**Source.** Zhang et al. 2018.

**Type deposition.** NHM-PSU and NJAU.

**Altitude.** 160 m a.s.l.

**Coordinates.** 8°59.996'N; 99°46.692'E

**Habitat.** Dark zone of cave (Tham Khao Phab Pha) on scattered bat guano.

**Distribution.** Sichon district, Nakhon Si Thammarat province, southern Thailand (only known from the type locality).

**Key to the troglomorphic *Coecobrya* of Thailand**

This key includes *C. sirindhornae* sp. n. and all other species of Thailand which have long antennae (more than 2.5 times as long as the cephalic diagonal). All are cave restricted.

- 1            Outer maxillary lobe with 3 sublobal hairs; a single chaeta m on labium .... **2**
- Outer maxillary lobe with 4 sublobal hairs; two chaetae m on labium; claw with unpaired inner tooth..... **3**

- 2 Labial chaetae as mrel112; claw without unpaired inner tooth ..... *C. cavicta* Nilsai & Zhang, 2017
- Labial chaetae as mRel112, claw with unpaired inner tooth ..... *C. chumphonensis* Zhang & Nilsai, 2017
- 3 Labial chaetae as M1m2rel112; antennae 5–7 times as long as cephalic diagonal; tita without a dorso-distal smooth chaeta in addition to the tenent hair; claw moderately slender ..... 4
- Labial chaetae as m1m2rel112, ; antennae >8 times as long as cephalic diagonal; tita with a dorso-distal smooth chaeta in addition to the tenent hair; claw very slender ..... *C. sirindhornae* sp. n.
- 4 Postlabial chaeta X4 ciliate; mac a1 present on Abd. I ..... *C. polychaeta* Zhang & Nilsai, 2017
- Postlabial chaeta X4 smooth; mac a1 absent on Abd. I ..... *C. cf. polychaeta* Zhang & Nilsai, 2017

## Discussion

*Coecobrya* is, among Collembola, one of the genera that exhibit most frequently morphological modifications considered to be linked to subterranean environments (Christiansen and Bellinger 1992, Deharveng 1990, Jordana 2012, Nilsai et al. 2017). As illustrated on Fig. 1E–G, its cave species show various degrees of troglomorphy. A first type corresponds to forms of small size, with short antennae and short appendages, resembling epigeal species of the genus (Fig. 1E). In Thai caves they are mostly linked to guano deposits (Deharveng 1990). A second type displays troglomorphic characters, i.e., long antennae and large body size (Fig. 1F). *Coecobrya sirindhornae* sp. n. described here belongs to this second type. Its troglomorphy is stronger than that of all other species of the genus, expressed as extremely long antennae, slender claw, and large body size (Fig. 1G). Like other described troglomorphic *Coecobrya* of Thailand (Nilsai et al. 2017), *C. sirindhornae* sp. n. is linked to oligotrophic habitat in the dark zone of the cave where it has been discovered, living in an atmosphere permanently wet and moist. All these species are very rare and narrow-range endemics in the country.

The first highly troglomorphic *Coecobrya*, *C. nupa*, was described by Christiansen and Bellinger in 1992 from Hawaii. Later on, Nilsai et al. (2017) described two long-antennae species, *C. chumphonensis* and *C. polychaeta* from Thailand. The antennae of *C. sirindhornae* sp. n. are distinctly longer. They are even longer than those of the most troglomorphic tropical Collembola, i.e., an undescribed Paronellidae from Laos (figured in Culver and Pipan 2009 where it is mistakenly cited from Cambodia) and an undescribed *Cyphoderopsis* from Sumatra (Deharveng and Bedos 2000), both with antennae approx. two times longer than (body + head). The elongation of antennae in *C. sirindhornae* sp. n. is only similar to that of *Verhoeffiella longicornis* recently redescribed by Lukić et al. (2018) from the Dinarides in Europe, i.e., under temperate climate. The presence of such highly troglomorphic *Coecobrya* in Satun province is unexpected and raises evolutionary questions relative to the climatic drivers of colonisation, diversifica-

tion and adaptation. Following the discovery of a rich troglobitic fauna in the lava tube fauna of Hawaii, Howarth (1973) was the first to challenge the view that cave adapted species were absent or exceptional in the tropics and proposed a bioclimatic model to account for this (Howarth 1980). This presence of true troglobites under tropical climate was later confirmed by Deharveng (1987) for Collembola. However, it was till recently admitted that tropical cave species rarely reach levels of troglomorphy as marked as some temperate species (Deharveng and Bedos 2000). The present discovery is a new compelling evidence that morphological modifications linked to cave life are often as strong in the lowland tropics than in temperate regions.

As Thailand is under tropical climate, cave temperature in the dark zone of lowland Thai peninsula is warm. It ranges from 23 to 30 degree Celsius (an average of 25–26 degree Celsius for the caves studied so far) while humidity is approx. 70–93% (unpublished observations). The new highly troglomorphic species described here is restricted to a single small chamber (0.8 × 3–4 m) without organic resources, where humidity is very high (> 90%), but temperature is only 23–24 degree Celsius, a value very low in caves of the region. The karst where the cave is developed is a small outcrop of low elevation, that cannot account for the low temperature observed. The other troglomorphic species of southern Thailand were also often collected in relatively low temperature microhabitats. These rough ecological data suggest that highly troglomorphic Collembola may require a specific environment in tropical caves, not only oligotrophic habitats. This remains to be investigated in more detail.

Three of the four most troglomorphic *Coecobrya* known in Thailand (*C. sirindhornae* sp. n., *C. polychaeta*, and *C. cavicta*) are limited to Satun caves. The fourth one is *C. chumphonensis*, from the province of Chumphon, 380 km to the north. The karst of Satun highlights the region's most complete Palaeozoic geological history and outstanding features of karst landscape that have developed during long geological periods (Department of Mineral Resources 2014). The limestone outcrop where the cave is developed is Ordovician of the Thung Song Group (480–445 million years ago), one of the oldest thick sequence of carbonate rock in Thailand (Wongwanich et al. 1990). The last emergence of the limestones above sea level in the region, i.e., the oldest possible date of cave colonisation, is in Jurassic after the continental collision in the Late Triassic (Department of Mineral Resources 2014). This may have allowed Collembola to early colonise caves and to evolve in this habitat over millions of years. Molecular analyses like those initiated these last years (Nilsai et al. 2017, Zhang et al. 2018) will be useful to understand the origin and regional diversification of the *Coecobrya* lineage.

This exceptional richness in troglomorphic species of the karst of Satun highlights that the country's first UNESCO Global Geopark (Satun Geopark) is also a spot of major biological importance. Regarding *C. sirindhornae* sp. n. itself, its area of occurrence is extremely reduced to a small chamber in a small cave of a small isolated hill. The hill is approx. 110 × 250 m and distant of approximately 400 m from the closest neighbouring limestone hill, which is approx. 500 × 2500 m. The cave is occupied by a temple and surrounded by agricultural lands. Two caves of the same small hill were surveyed but did not provide any specimen of the new species. All this makes *C. sirindhornae* sp. n.

highly vulnerable in the face of growing anthropic disturbance which are spreading over Thailand karsts, especially in lowland. The survey of neighbouring hill caves is on the way to better evaluate the fine distribution and vulnerability of this remarkable species. In a broader context, this discovery underlines a need higher than expected for rapid evaluation and assessment of the cave fauna of the numerous karstic outcrops spread on the plain of southern Thailand, and of the current threats affecting these karsts.

## Acknowledgements

We would like to thank Areeruk Nilsai and Katthaleeya Surakhamhaeng for their kind assistance in the fieldwork and improving some figures. Anne Bedos is thanked for her review of the initial draft, and Mark Judson for style improvement of part of the manuscript. This work was supported by Prince of Songkla University (PSU-15443: SCI580885S) and the Thailand Research Fund (TRG-5880189 and MRG-6080287) for the first author.

## References

- Absolon K (1907) Zwei neue Collembolen-Gattungen. Wiener Entomologische Zeitung 26: 335–343.
- Bedos A (1994) Les Collemboles édaphiques du massif du Doi Inthanon (Thaïlande): biodiversité et écologie en forêt tropicale. PhD Thesis, University of Toulouse, Toulouse.
- Bellinger PF, Christiansen KA, Janssens F (1996–2019) Checklist of the Collembola of the World. <http://www.collembola.org> [10 January 2019]
- Börner C (1913) Die Familien der Collembolen. Zoologischer Anzeiger 41: 315–322.
- Brook G (1882) On a new genus of Collembola (*Sinella*) allied to *Degeeria* Nicolet. Journal of the Linnean Society of London Zoology 16: 541–545. <https://doi.org/10.1111/j.1096-3642.1882.tb02398.x>
- Carpenter GH (1917) Zoological results of the Abor Expedition 1911–12: Collembola. Records of the Indian Museum, Calcutta 8: 561–568.
- Chen JX, Christiansen K (1993) The genus *Sinella* with special reference to *Sinella s. s.* (Collembola: Entomobryidae) of China. Oriental Insects 27: 1–54. <https://doi.org/10.1080/0305316.1993.10432236>
- Christiansen K (2012) Morphological adaptations. In: Culver DC, White WB (Eds) Encyclopedia of Caves. 2<sup>nd</sup> ed. Academic Press, Amsterdam, Netherlands, 517–528. <https://doi.org/10.1016/B978-0-12-383832-2.00075-X>
- Christiansen K, Bellinger P (1992) Insects of Hawaii. Vol 15, Collembola. University of Hawaii Press, Honolulu, 455 pp.
- Cipola NG, Bellini BC (2016) A new cave species of *Coecobrya* Yosii (Collembola, Entomobryidae, Entomobryinae) from South Africa, with an identification key to the genus. Zootaxa 4200(3): 351–366. <https://doi.org/10.11646/zootaxa.4200.3.1>

- Culver DC, Pipan T (2009) The biology of cave and other subterranean habitats. Oxford University Press, New York, 254 pp.
- Deharveng L (1986) 26-Collemboles. In: Association Pyrénéenne de Spéléologie (Ed) Expédition Thaï-Maros 85, Rapport Spéléologique et Scientifique. Association Pyrénéenne de Spéléologie, Toulouse, 191–198.
- Deharveng L (1987) Cave Collembola of South-East Asia. The Korean Journal of Systematic Zoology 3: 165–174.
- Deharveng L (1990) Fauna of Thai caves. II. New Entomobryoidea Collembola from Chiang Dao cave, Thailand. Occasional Papers of the Bernice P. Bishop Museum 30: 279–287.
- Deharveng L, Bedos A (2000) The cave fauna of Southeast Asia: ecology, origin, evolution. In: Wilkens H, Culver DC, Humphreys WF (Eds) Ecosystem of the World 30. Subterranean Ecosystems. Amsterdam, Elsevier, 603–632.
- Deharveng L, Bedos A (2001) Thaïlande. In: Juberthie C, Decu V (Eds) Encyclopaedia Biospeologica. Tome III. Société de Biospéologie, Moulis, 1991–2006.
- Deharveng L, Bedos A (2012) Diversity Patterns in the Tropics. In: William BW, Culver DC (Eds) Encyclopedia of Caves. Academic Press, Chennai, 238–250. <https://doi.org/10.1016/B978-0-12-383832-2.00032-3>
- Deharveng L, Bedos A (2018) Diversity of Terrestrial Invertebrates in Subterranean Habitats. In: Moldovan OT, Kovác L, Halse S (Eds) Cave Ecology, Ecological Studies 235. Springer Nature Switzerland AG, 107–172. [https://doi.org/10.1007/978-3-319-98852-8\\_7](https://doi.org/10.1007/978-3-319-98852-8_7)
- Deharveng L, Bedos A (in press) Diversity Patterns in the Tropics. In: White WB, Culver DC (Eds) Encyclopedia of Caves. Academic Press, Elsevier.
- Deharveng L, Bedos A, Leksawasdi P (1989) Diversity in tropical forest soils: the Collembola of Doi Inthanon (Thailand). In: Dallai R (Ed.) Third International Seminar on Apterygota. University of Siena, Siena, 317–328.
- Deharveng L, Gers C (1993) Ten new species of *Troglopedetes* Absolon, 1907 from caves of Thailand (Collembola, Paronellidae). Bijdragen tot de Dierkunde 63(2): 103–113.
- Deharveng L, Jantarit S, Bedos A (2018) Revisiting *Lepidonella* Yosii (Collembola: Paronellidae): character overview, checklist of world species and reassessment of *Pseudoparonella doveri* Carpenter. Annales de la Société entomologique de France (NS) 54(5): 1–20. <https://doi.org/10.1080/00379271.2018.1507687>
- Department of Mineral Resources (2014) Geology of Thailand. Department of Mineral Resources, Ministry of Natural Resources and Environment, Bangkok, 508 pp.
- Fjellberg A (1999) The labial palp in Collembola. Zoologischer Anzeiger 237: 309–330.
- Gisin H (1967) Espèces nouvelles et lignées évolutives de *Pseudosinella* endogées (Collembola). Memórias e Estudos do Museu Zoológico da Universidade de Coimbra 301: 1–21.
- Howarth FG (1973) The cavernicolous fauna of Hawaiian lava tubes, 1. Introduction. Pacific Insects 15(1): 139–151.
- Howarth FG (1980) The zoogeography of specialized cave animals: a bioclimatic model. Evolution 34(2): 394–406. <https://doi.org/10.1111/j.1558-5646.1980.tb04827.x>
- Jantarit S, Bedos A, Deharveng L (2016) An annotated checklist of the Collembola fauna of Thailand. Zootaxa 4169(2): 301–360. <https://doi.org/10.11646/zootaxa.4169.2.4>

- Jantarit S, Satasook C, Deharveng L (2013) The genus *Cyphoderopsis* (Collembola: Paronellidae) in Thailand and a faunal transition at the Isthmus of Kra in Troglopedetinae. *Zootaxa* 3721: 49–70. <https://doi.org/10.11646/zootaxa.3721.1.2>
- Jordana R (2012) Synopses on Palaearctic Collembola : Capbryinae and Entomobryini. Senckenberg Museum of Natural History (Görlitz) 7(1): 1–390.
- Jordana R, Baquero E (2005) A proposal of characters for taxonomic identification of *Entomobrya* species (Collembola, Entomobryomorpha), with description of a new species. *Abhandlungen und Berichte des Naturkundemuseums, Görlitz* 76: 117–134.
- Lubbock J (1873) Monograph of the Collembola and Thysanura. Ray Society, London, 276 pp.
- Lukić M (in press) Collembola. In: White WB, Culver DC (Eds) *Encyclopedia of Caves*. Academic Press, Elsevier.
- Lukić M, Delić T, Zagmajster M, Deharveng L (2018) Setting a morphological framework for the genus *Verhoeffiella* (Collembola, Entomobryidae) for describing new troglomorphic species from the Dinaric karst (Western Balkans). *Invertebrate Systematics* 32(5): 1118–1170. <https://doi.org/10.1071/IS17088>
- Nilsai A, Jantarit S, Satasook C, Zhang F (2017) Three new species of *Coecobrya* (Collembola: Entomobryidae) from caves in the Thai Peninsula. *Zootaxa* 4286(2): 187–202. <https://doi.org/10.11646/zootaxa.4286.2.3>
- Rojanavongse V, Hormchan P, Wiwatwitaya D, Lee B-H, Kim JT, Park K-H (not dated) Study on diversity of Collembola (Insecta) in Thailand. Research report to the National Research Council of Thailand, 81 pp. [in Thai, unpublished report]
- Schäffer C (1896) Die Collembolen der Umgebung von Hamburg und benachbarter Gebiete. *Mitteilungen aus dem Naturhistorischen Museum Hamburg* 13: 149–216.
- Schäffer C (1897) Apterygoten. *Hamburger Magalhaensische Sammelreise Apterygoten* 8: 1–48.
- Szeptycki A (1979) Morpho-systematic studies of Collembola. IV. Chaetotaxy of the Entomobryidae and its phylogenetical significance. *Polska Akademia Nauk, Zakład Zoologii Systematycznej i Doświadczalnej, Państwowe Wydawnictwo Naukowe, Warszawa and Kraków*, 218 pp.
- Takeda H (1981) Effects of shifting cultivation on the soil mesofauna with special reference to collembolan populations in North-East Thailand. *Memoirs of the College of Agriculture, Kyoto University* 118: 45–60.
- Tömösváry Ö (1882) Adatok hazánk Thysanura-faunájához. *A Magyar Tudományos Akadémia Matematikai és Természettudományi Közleményei* 18: 119–132.
- Wongwanich T, Burrett CF, Tansathein W, Chaodumrong P (1990) Lower to Mid Palaeozoic stratigraphy of mainland Satun province, southern Thailand. *Journal of Southeast Asian Earth Science* 4(1): 1–9. [https://doi.org/10.1016/0743-9547\(90\)90020-E](https://doi.org/10.1016/0743-9547(90)90020-E)
- Xu G-L, Zhang F (2015) Two new species of *Coecobrya* (Collembola, Entomobryidae) from China, with an updated key to the Chinese species of the genus. *Zookeys* 498: 17–28. <https://doi.org/10.3897/zookeys.498.9491>
- Yosii R (1956) Höhlencollembolen Japans II. *Japanese Journal of Zoology* 11: 609–627.
- Yosii R (1960) On some Collembola of New Caledonia, New Britain and Solomon Islands. *Bulletin of the Osaka Museum of Natural History* 12: 9–38.

- Yosii R (1961) On some Collembola from Thailand. *Nature and Life in Southeast Asia* 1: 171–198.
- Zhang F, Bedos A, Deharveng L (2016) Cave-dwelling *Coecobrya* from southern China with a survey of clypeal chaetae in Entomobryoidea (Collembola). *European Journal of Taxonomy* 226: 1–21. <https://doi.org/10.5852/ejt.2016.226>
- Zhang F, Deharveng L, Chen J-X (2009) New species and rediagnosis of *Coecobrya* (Collembola: Entomobryidae), with a key to the species of the genus. *Journal of Natural History* 43(41): 2597–2615. <https://doi.org/10.1080/00222930903243970>
- Zhang F, Jantarit S, Nilsai A, Stevens MI, Ding Y, Satasook C (2018) Species delimitation in the morphologically conserved *Coecobrya* (Collembola: Entomobryidae): a case study integrating morphology and molecular traits to advance current taxonomy. *Zoologica Scripta* 47(3): 342–356. <https://doi.org/10.1111/zsc.12279>
- Zhang F, Yu D, Xu G (2011) Transformational homology of the tergal setae during postembryonic development in the *Sinella-Coecobrya* group (Collembola: Entomobryidae). *Contributions to Zoology* 80(4): 213–230.

# *Cheleion watanabei* sp. n., a new species of Stereomerini (Coleoptera, Scarabaeidae, Aphodiinae), and description of the male of *C. jendeki*

Showtaro Kakizoe<sup>1,2</sup>, Munetoshi Maruyama<sup>3</sup>, Kimio Masumoto<sup>4</sup>

**1** Entomological Laboratory, Graduate School of Bioresource and Bioenvironmental Sciences, Kyushu University, Motoooka 744, Nishi-ku, Fukuoka, 819-0395, Japan **2** Japan Society for the Promotion of Science (DC1), Tokyo, Japan **3** The Kyushu University Museum, Hakozaki 6-10-1, Higashi-ku, Fukuoka, 812-8581, Japan **4** Kamezawa 3-chôme 14-13-1001, Sumida-ku, Tokyo, 130-0014, Japan

Corresponding author: Showtaro Kakizoe ([showtarok@gmail.com](mailto:showtarok@gmail.com))

---

Academic editor: A. Frolov | Received 14 November 2018 | Accepted 18 January 2019 | Published 12 February 2019

---

<http://zoobank.org/5CFE1A60-EC42-4B85-86F4-479FFA96123F>

---

**Citation:** Kakizoe S, Maruyama M, Masumoto K (2019) *Cheleion watanabei* sp. n., a new species of Stereomerini (Coleoptera, Scarabaeidae, Aphodiinae), and description of the male of *C. jendeki*. ZooKeys 824: 45–52. <https://doi.org/10.3897/zookeys.824.31627>

---

## Abstract

*Cheleion watanabei* sp. n. is described from Pahang, Peninsular Malaysia and represents the third species of the genus *Cheleion* Vårdal & Forshage, 2010 (Coleoptera, Scarabaeidae, Aphodiinae, Stereomerini). A description of the previously unknown male of *C. jendeki* Král & Hájek, 2015, and a key to the species of the genus *Cheleion* are also provided.

## Keywords

Aphodiines, new species, Oriental region, Peninsular Malaysia, Southeast Asia, taxonomy

## Introduction

The aphodiine tribe Stereomerini was established by Howden and Storey (1992) based on the genus *Stereomera* Arrow, 1905, from Singapore. Currently, 9 genera and 22 species from the Oriental and Australian regions are recognized in Stereomerini (Howden and Storey 1992, 2000; Bordat and Howden 1995; Storey and Howden 1996; Maruyama 2009; Vårdal and Forshage 2010; Maruyama and Nomura 2011; Král and Hájek 2015).

The Oriental species are known to be extremely rare; all of them are known from single or a few specimens collected so far. Therefore, the males are rare and consequently most entomologists have avoided dissection of the genitalia; male genitalia of Stereomerini have been described only for two Australian species (Howden and Storey 1992; Storey and Howden 1996). Recently we examined two Stereomerini specimens from Peninsular Malaysia: one was found to be a female of an undescribed species belonging to the genus *Cheleion* and the other was identified as a male of *Cheleion jendeki* Král & Hájek, 2015. The description of the new species and the previously unknown male of *C. jendeki* as well as a key to the species of *Cheleion* are provided herein.

## Materials and methods

All specimens were dried and mounted on paper cards for morphological observation; dissected genitalia were mounted in Euparal on a small glass plate (10×5 mm), and subsequently glued onto a paper card (6×5 mm) and pinned under the specimen (Maruyama 2004). Specimen photographs were taken with an Olympus OM-D E-M1 Mark II with a Canon MP-E 65 mm 1–5× macro lens and KIPON EF-MFT AF adapter for Figures 1–6, with a Canon EOS 7D Mark II with a Mitutoyo M Plan Apo 20× and a Raynox DCR-150 for Figures 8–11, and subsequently stacked using CombineZP software. Images were edited using Adobe Photoshop CS6. Terminology of the species description follows Howden and Storey (1992), Vårdal and Forshage (2010) and Král and Hájek (2015).

## Taxonomy

### *Cheleion watanabei* Kakizoe, Maruyama & Masumoto, sp. n.

<http://zoobank.org/9186941F-6E3F-4EB8-829D-78AB1D4C594F>

Figs 1–4, 9, 11

**Type material.** Holotype, female, deposited in the National Museum of Nature and Science, Tsukuba, Japan: “PENINSULAR MALAYSIA, Pahang, Cameron Highlands, Tanah Rata, 8–12. III. 2006, T. Watanabe leg., by FIT [= flight interception trap]”.

**Distribution.** (Fig. 12) Peninsular Malaysia, Pahang, Cameron Highlands, Tanah Rata.

**Etymology.** Dedicated to Mr Takashi Watanabe, the collector of the type specimen.

**Diagnosis.** This new species is easily distinguished from all known congeners by the following character states: 1) larger body size (total body length ca. 2.5 mm); 2) anterior ridges of the two distinct pronotal depressions short; 3) pads bearing lanceolate scale on the elytra slightly developed; 4) elytral posterior margin strongly depressed; and 5) elytral ridges indistinct.

**Description. Holotype female.** Large species (2.51 mm). Body (Figs 1–4) slightly convex dorsally, dorsal surface more or less covered with appressed lanceolate scales, general color uniformly matte brown. **Head** (Figs 1–4) wide, subrectangular in dor-



**Figures 1–4.** Habitus of *Cheleion watanabei* sp. n. (♀ holotype) **1** dorsal view (anterior ridge of pronotal depression arrowed) **2** ventral view **3** dorsolateral view **4** anterodorsal view.

sal view, with densely appressed lanceolate scales. Clypeus impunctate, shiny, apically pointed and reflexed under head. Frons flat with five anteriorly divergent furrows, second and fourth furrows strongly curved medially. Genal tip slightly obtusely angular in dorsal view. Eyes large, visible ventrally, less visible dorsally. Occiput with numerous small, longitudinal punctures. Antennae long, amber colored, with long setae; club lamellae long. Maxillary palpi as long as head, amber colored, with securiform ultimate palpomeres. **Prothorax** (Figs 1–4) large and transverse, anterior edge slightly bisinuate,

side edges weakly rounded in dorsal view. Base of pronotum with a median protrusion, wider than base of elytra. Pronotal disc with seven furrows medially, concave at middle of hourglass pattern, with tufts of dense trichomes, with densely appressed lanceolate scales; mid furrow shallower than lateral furrows. Lateral furrows large, flat. Subtriangular depressions delineated by more furrows sparsely appressed lanceolate scales medially. Anteromedial disc distinctly high, tuberculate; promedial disc and posterolateral sides slightly low, less tuberculate than anteromedial disc. Prosternum fairly elevated and expanded anteriorly and posteriorly, rugose; anterior part grooved longitudinally and sinuate apically, posterior part hastate; prosternal spine apically pointed. **Scutellum** (Figs 1, 3, 4, 9) triangular, notably small. **Elytra** (Figs 1–4, 9, 11) approximately as wide as pronotum and only slightly longer than pronotum and head combined; feebly tapered posteriorly, fairly rounded apically; posterior margin strongly depressed. Each elytron with three indistinct ridges; intervals (between ridges) flat, rugose, with densely appressed lanceolate scales. Epipleura broadly inflexed; posterior two-thirds of lateral edge slightly recurved to allow free movement of metalegs. Macropterous. **Mesoven-trite** (Fig. 2) strongly narrow with alutaceous and punctured surface. **Metaventr-rite** (Fig. 2) flat, alutaceous, subtriangular, tapering, widest anteriorly, grooved along mid-line, with coarse, macrosetigerous punctures. **Legs** (Figs 1–4) short with broad femora and tibiae. Femora shiny, covered with coarse, macrosetigerous punctures. Protibiae flattened; each with two teeth on outer edge, sparsely macrosetose outward. Protarsi pentamerous, amber colored, long, sparsely macrosetose medially, inserted well before protibial apex. Proclaws normal, symmetrical. Meso- and metatibiae with concave, sparsely macrosetose apex; each with five inconspicuous terminal spurs; dorsal sides shiny, glabrous; ventrolateral sides with densely appressed lanceolate scales. Meso- and metatarsi tetramerous, short, compacted-complanate, sparsely macrosetose medially. Meso- and metaclaws slightly weak, symmetrical. **Abdomen** (Fig. 2) with five visible ventrites apparently fused, covered with coarse, dense, macrosetigerous punctures. Pygidium exposed, strongly punctate proximally, less strongly apically.

**Male.** Unknown.

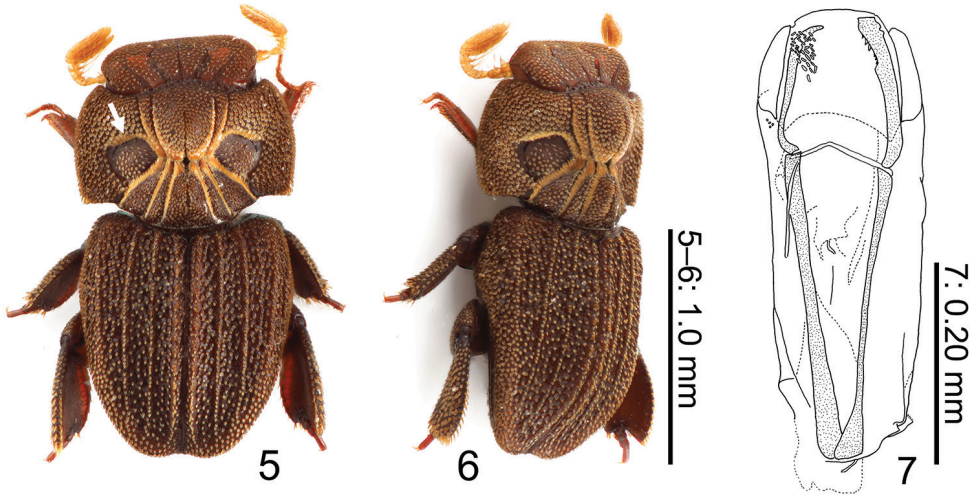
**Measurements.** Body length 2.51 mm; maximum width of head 0.79 mm; median dorsal length of pronotum 0.74 mm, maximum width 1.16 mm; sutural length of elytra 1.15 mm, maximum length 1.26 mm, maximum width 1.22 mm.

### ***Cheleion jendeki* Král & Hájek, 2015**

Figs 5–8, 10

*Cheleion jendeki* Král & Hájek, 2015: 88 (original description based on a female).

**Material examined.** PENINSULAR MALAYSIA, Pahang, near the gate of Taman Negeri Endau Rompin, alt. 30 m, 8–23. III. 2015, S. Kakizoe, K. Hoshino, S. Kakinuma & H. Osaki leg., by FIT, 1 ex. male.



**Figures 5–7.** Habitus of *Cheleion jendeki* (♂) **5** dorsal view (anterior ridge of pronotal depression arrowed) **6** dorsolateral view **7** Aedeagus in dorsal view.



**Figures 8–11.** Comparison of scale between *Cheleion jendeki* and *C. watanabei* sp. n. **8, 10** *C. jendeki* (♂) **9, 11** *C. watanabei* sp. n. (♀ holotype) **8, 9** base of right elytron **10, 11** posterior part of right elytron.



**Figure 12.** Distribution map of *Cheleion* species: black star *C. watanabei* sp. n., black circle *C. malayanum*, black triangle *C. jendeki*.

**Additional description based on male. Legs** (Figs 5, 6). Protarsi pentamerous, amber colored, long, sparsely macrosetose medially, inserted well before protibial apex. **Aedeagus** (Fig. 7). Symmetrical. Phallobase elongate, cylindrical. Parameres short, almost a quarter length of basal piece. Phallus a little longer than parameres, rounded apically. Struts long, almost two-thirds length of tegmen.

**Sexual dimorphism.** No sexual dimorphism detected.

**Measurements.** Body length 1.80 mm; maximum width of head 0.67 mm; median dorsal length of pronotum 0.61 mm, maximum width 0.94 mm; sutural length of elytra 0.92 mm, maximum length 0.96 mm, maximum width 0.92 mm.

**Remarks.** No males were known for the genus *Cheleion* so far, therefore a description of the male of *C. jendeki* is provided here. Furthermore, Král and Hájek (2015) reported that the tarsal formula for *C. jendeki* was 4-4-4, but it is actually 5-4-4. Therefore, the tarsal formula of *C. malayanum* given by Vårdal and Forshage (2010) is probably also inaccurate.

### Key to the species of the genus *Cheleion*

- 1 Large (2.5 mm); anterior ridges of two distinct pronotal depressions short (Fig. 1, arrowed); elytral ridges indistinct, each pad bearing slightly-devel-

- oped lanceolate scales, densely appressed on elytra; elytral posterior margin strongly depressed ..... ***C. watanabei* sp. n.**
- Small (1.8–1.9 mm); anterior ridges of distinct pronotal depressions long (Fig. 5, arrowed); elytral ridges distinct, each pad bearing well-developed lanceolate scales, moderately appressed on elytra, elytral posterior margin not or feebly depressed ..... **2**
- 2 1<sup>st</sup> and 5<sup>th</sup> divergent furrows on head weakly s-shaped; distinct pronotal depressions small, subtriangular; prosternal spine apically pointed; elytral ridges broad, most pads bearing lanceolate scale confluent to subconfluent ..... ***C. malayanum* Vårdal & Forshage, 2010**
- 1<sup>st</sup> and 5<sup>th</sup> divergent furrows on head straight; distinct pronotal depressions large, subrectangular; prosternal spine apically not pointed; elytral ridges narrow, most pads bearing lanceolate scale separated ..... ***C. jendeki* Král & Hájek, 2015**

## Acknowledgements

We wish to express our cordial thanks to Mr Takashi Watanabe (Kanagawa Pref., Japan) for kindly providing the material, Dr Andrey Frolov (Universidade Federal de Mato Grosso), Dr Marco Dellacasa (Museo di Storia Naturale e del Territorio dell'Università di Pisa) and Dr David Král (Charles University) for critically reading the manuscript, Mr Konosuke Hoshino (Nagaoka Municipal Science Museum), Mr Shunsuke Kakinuma (Tokyo University of Agriculture and Technology), Ms Haruka Osaki (Kyushu University) for their kind assistance in the field survey and to Dr Rosli Hashim (University of Malaya) for his kind support in the field survey by SK, Mr Hoshino, Mr Kakinuma and Ms Osaki. This work was partially supported by a Grant-in-Aid for JSPS Fellow (17J07016) to SK from the Japan Society for the Promotion of Science, Japan.

## References

- Arrow GJ (1905) LXX – On some Oriental aphodiid Coleoptera of the *Rhyparus* group, with description of a new genus. The Annals and Magazine of Natural History, including Zoology, Botany and Geology 15 (ser. VII) (90): 534–540.
- Bordat P, Howden HF (1995) Trois nouveaux genres, trois nouvelles espèces de Stereomerinae de Bornéo (Coleoptera, Aphodiidae). Bulletin de la Société Entomologique de France 100(1): 11–20.
- Howden HF, Storey RI (1992) Phylogeny of the Rhyparini and the new tribe Stereomerini, with descriptions of new genera and species (Coleoptera; Scarabaeidae; Aphodiinae). Canadian Journal of Zoology 70: 1810–1823. <https://doi.org/10.1139/z92-248>
- Howden HF, Storey RI (2000) New Stereomerini and Rhyparini from Australia, Borneo and Fiji (Coleoptera: Scarabaeidae: Aphodiinae). Memoirs of the Queensland Museum 46(1): 175–182.

- Král D, Hájek J (2015) A second species of *Cheleion* from Johor, Malaysia (Coleoptera, Scarabaeidae, Aphodiinae, Stereomerini). *ZooKeys* 532: 87–97. <https://doi.org/10.3897/zookeys.532.6116>
- Maruyama M (2004) A permanent slide pinned under a specimen. *Elytra* 32(2): 276. [http://coleoptera.sakura.ne.jp/Elytra/Elytra32\(2\)2004.pdf](http://coleoptera.sakura.ne.jp/Elytra/Elytra32(2)2004.pdf) [June 25, 2018]
- Maruyama M (2009) *Rhinocerotopsis nakasei* (Coleoptera, Scarabaeidae, Aphodiinae), a new genus and species of Stereomerini from Peninsular Malaysia. *Esakia* 49: 103–106. <http://hdl.handle.net/2324/16151> [June 25, 2018]
- Maruyama M, Nomura S (2011) Taxonomy of the genus *Stereomera* Arrow, 1905 (Coleoptera, Scarabaeidae, Aphodiinae), with description of a new species from Peninsular Malaysia. *Special Publication of the Japanese Society of Scarabaeoidology* 1: 171–175.
- Storey RI, Howden HF (1996) Revision of *Australoxenella* Howden & Storey in Australia (Coleoptera: Scarabaeidae: Aphodiinae). *Memoirs of the Queensland Museum* 39(2): 365–380.
- Vårdal H, Forshage M (2010) A new genus and species and a revised phylogeny of Stereomerini (Coleoptera, Scarabaeidae, Aphodiinae), with notes on assumedly termitophilic aphodines. In: Ratcliffe B, Krell F-T (Eds) *Current advances in Scarabaeoidea research*. *ZooKeys* 34: 55–76. <https://doi.org/10.3897/zookeys.34.264>

# A new species of puddle frog from an unexplored mountain in southwestern Ethiopia (Anura, Phrynobatrachidae, *Phrynobatrachus*)

Sandra Goutte<sup>1\*</sup>, Jacobo Reyes-Velasco<sup>1\*</sup>, Stephane Boissinot<sup>1</sup>

<sup>1</sup> *New York University Abu Dhabi, Saadiyat Island, Abu Dhabi, UAE*

Corresponding author: *Sandra Goutte* ([sg5533@nyu.edu](mailto:sg5533@nyu.edu))

---

Academic editor: *A. Crottini* | Received 12 November 2018 | Accepted 2 December 2018 | Published 12 February 2019

---

<http://zoobank.org/BDDAF7D8-F5E5-406D-A485-E4D062271833>

---

**Citation:** Goutte S, Reyes-Velasco J, Boissinot S (2019) A new species of puddle frog from an unexplored mountain in southwestern Ethiopia (Anura, Phrynobatrachidae, *Phrynobatrachus*). ZooKeys 824: 53–70. <https://doi.org/10.3897/zookeys.824.31570>

---

## Abstract

A new species of *Phrynobatrachus* is described from the unexplored and isolated Bibita Mountain, southwestern Ethiopia, based on morphological characters and sequences of the mitochondrial rRNA16s. The new species can be distinguished from all its congeners by a small size (SVL = 16.8 ± 0.1 mm for males, 20.3 ± 0.9 mm for females), a slender body with long legs and elongated fingers and toes, a golden coloration, a completely hidden tympanum, and a marked canthus rostralis. The phylogenetic hypothesis based on 16s sequences places the new species as sister to the species group that includes *P. natalensis*, although it is morphologically more similar to other dwarf *Phrynobatrachus* species, such as the Ethiopian *P. minutus*.

## Keywords

Bibita Mountain, Ethiopia, morphology, phylogenetic relationships, *Phrynobatrachus bibita* sp. n., taxonomy

## Introduction

The highlands of Ethiopia are known for their high degree of diversity and endemism (Williams et al. 2004). Approximately half of all species of anurans (frogs and toads) of Ethiopia are endemic, including five endemic genera (Largen and Spawls 2010, Gower et

---

\* These authors contributed equally.

al. 2013). Despite a recent increase in studies on the diversity of the Ethiopian fauna, the southwestern part of the country remains poorly studied, in part due to the difficulty in accessing the region. A small number of collections of amphibians have been obtained in this area, most of them from the vicinity of the towns of Bonga and Mizan Teferi (Figure 1A). Recent sampling campaigns conducted in the forests of the southwest revealed the existence of multiple undescribed taxa (Reyes-Velasco et al. 2018a, b). Additionally, the area harbors some of the last remaining forests in Ethiopia, giving it great potential for undiscovered diversity and making it of particular interest for taxonomists and conservationists.

While conducting fieldwork in the southwestern part of the country, we came across an undescribed species member of the genus *Phrynobatrachus*. This genus is one of the most species rich genera of African anurans, with 91 described and multiple undescribed taxa (Zimkus and Schick 2010, Frost 2018). This genus is widespread across sub-Saharan Africa. At least five species of *Phrynobatrachus* are found in Ethiopia: *P. bullans* Cruetsinger, Pickersgill, Channing, and Moyer, 2004, *P. inexpectatus* Largen, 2001, *P. minutus* (Boulenger, 1895), *P. natalensis* (Smith, 1849), as well as *P. sp. n.* “Oromia” (Zimkus 2008, Largen and Spawls 2010, Zimkus et al. 2010, Frost 2018). The new species described here has multiple morphological characters that differentiate it from all other members of the genus, which is also supported by molecular evidence. Here, we describe the species as new to science.

## Materials and methods

### Taxonomic sampling

The mountain of Bibita in southwestern Ethiopia (6.8034N, 35.0602E), an isolated plateau located between the Gambela and the Southern Nations, Nationalities, and Peoples’ Regions, in the Bench Maji Zone, was explored (Figure 1). This mountain is approximately 50 km southwest of Mizan Teferi and ~18 km east from the border with South Sudan. Bibita Mountain is separated from the rest of the Ethiopian highlands by the lowlands formed by the tributaries of the Akobo River, including the Gilo River. This mountain is also sometimes referred to as Gurra Farda (Hundera and Deboch 2008), which translates to “donkey’s ears” in Oromo. On 16 and 17 June 2018, ten specimens of an undescribed species of *Phrynobatrachus* (two males, eight females) were collected, as well as multiple egg clutches from a pond in Bibita Mountain (6.82293N, 35.0938E; 1972 m a. s. l.). We photographed the specimens in situ, and took live photographs in captivity. We then euthanized them using a ventral application of 20% benzocaine gel (Chen and Comb 1999). After euthanasia, we took additional photographs of dorsal and ventral views of each specimen. We collected liver tissue samples from all specimens and egg clutches and stored them in RNAlater (ThermoFisher Scientific), and then fixed all specimens in 10% formalin for 48 hours and stored them in 70% Ethanol. All specimens are deposited at the Herpetology Collection of the Addis Ababa University, Addis Ababa, Ethiopia.

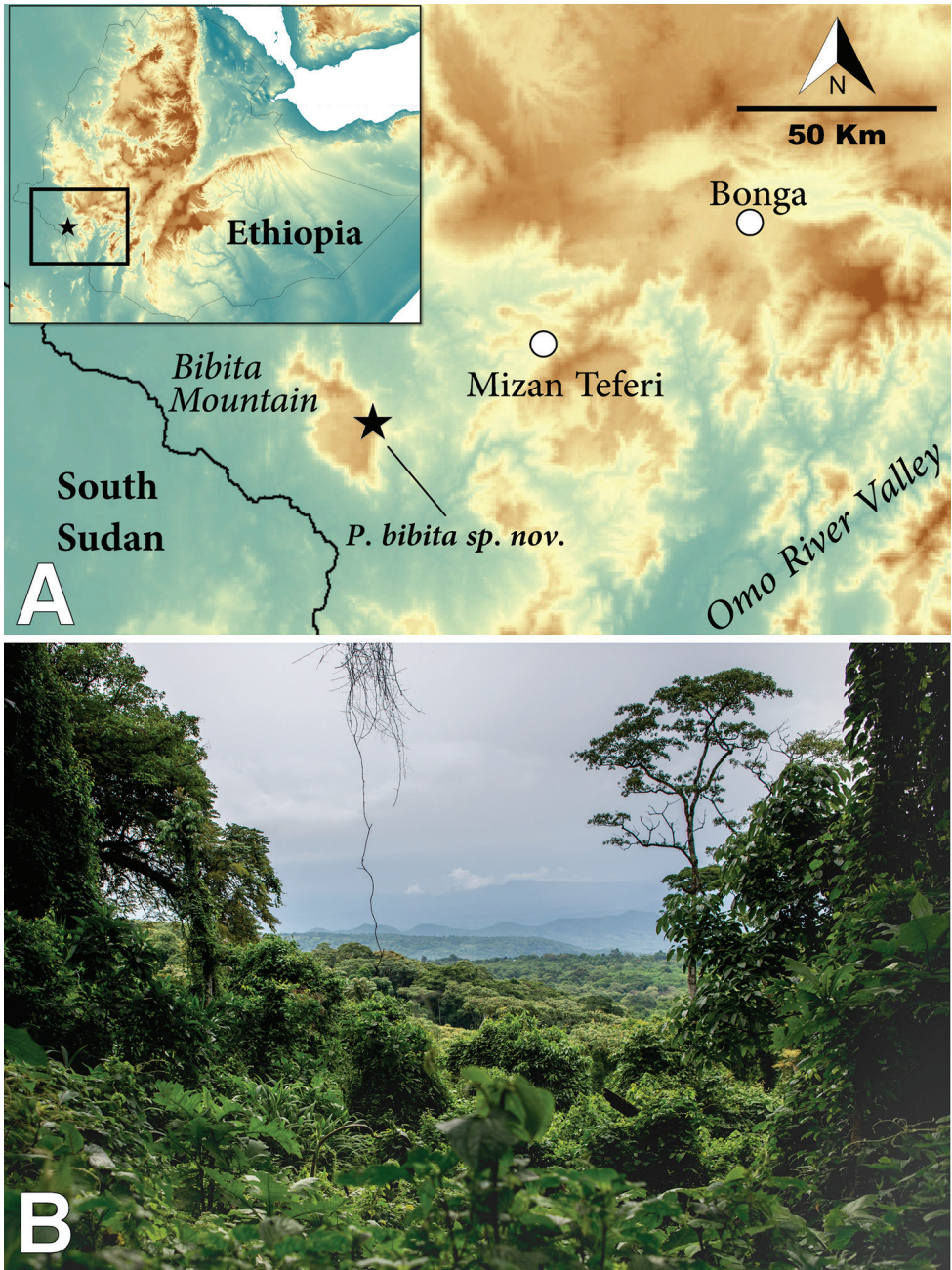


**Figure 1.** Type locality of *Phrynobatrachus bibita* sp. n. **A** Map of Ethiopia showing the location of Bibita Mountain **B** View from Bibita Mountain looking east, at an elevation of approximately 1900 m.

## Recordings of advertisement calls

A single calling male was recorded during the night of 17 June 2018 using a Sony Handycam camcorder. The soundtrack of the video was extracted using Adobe Premiere Pro and analyzed using Praat (Boersma and Weenink 2013). We analyzed two call bouts and fourteen notes produced by a single individual for dominant frequency, note duration, and interval inter-notes. We compared these calls to the advertisement calls of *Phrynobatrachus minutus* (recorded between Bonga and Jimma; 7.5350N, 36.5606E, 2216 m a. s. l.; SB233) and *P. natalensis* (east of Kibre Mengist; 5.8679N, 39.0490E, 1665 m a. s. l.; specimen not collected) which we recorded using a Marantz PMD661 MKII solid-state recorder and Sennheiser ME66 microphone. Unfortunately, calls for the other three *Phrynobatrachus* that occur in Ethiopia (*P. bullans*, *P. inexpectatus*, and *P. sp. n.* “Oromia” of Zimkus and Schick 2010) were not available for comparison.

## Morphological measurements

For each specimen of the type series, we used an SPI dial caliper (model #31-415-3, precision: 0.1 mm) to take the following measurements as defined in Watters et al. (2016):

<b>SVL</b>	snout vent length,	<b>UEW</b>	pper eyelid width,
<b>HL</b>	head length,	<b>FLL</b>	forearm length,
<b>HW</b>	head width,	<b>HAL</b>	hand length,
<b>SL</b>	snout length,	<b>FinDW</b>	third finger disk width,
<b>NS</b>	nostril-snout distance,	<b>THL</b>	thigh length,
<b>ED</b>	eye diameter,	<b>TL</b>	tibiofibula length,
<b>EN</b>	eye-nostril distance,	<b>FL</b>	foot length,
<b>IOD</b>	interorbital distance,	<b>Toe4DW</b>	toe IV disk width,
<b>IND</b>	inter-narinal distance,	<b>MTL</b>	metatarsal tubercle length.
<b>ED</b>	eye diameter,		

## DNA extraction, PCR amplification, and phylogenetic analyses

We extracted DNA from the liver tissue samples stored in RNAlater with the use of standard potassium acetate protocol, or with the use of a DNeasy Blood & Tissue Kit (Qiagen). We also extracted DNA from eggs collected on leaves where females and the amplected pair of the new species were found, to ensure that these belonged to the new species. We then measured DNA concentration for each one of the samples using a broad range kit in a Qubit fluorometer (Life Technologies). We amplified a fraction of the 16s rRNA mitochondrial gene with the use of the primers LX12SN1a (forward) and LX16S1Ra (reverse) of Zhang et al. (2013). We performed Polymerase Chain Reaction (PCR) in total volumes of 48 µl with the use of regular Taq (Invitrogen), with the following conditions: initial denaturation at 94 °C (two minutes), followed

by 35 cycles consisting of a denaturation step at 94 °C (30 seconds), annealing step at 48 °C (30 seconds), and extension step at 72 °C (one minute). The final extension step consisted of one minute at 72 °C. We shipped the unpurified PCR products for sequencing at BGI Tech Solutions (Hong Kong).

We used the program Geneious v 9.1.6 (Biomatters Ltd., Auckland, NZ) to manually trim and edit the raw chromatograms. We included additional sequences of *Phrynobatrachus* from GenBank in order to infer the phylogenetic positions of the new material. We deposited all new sequences in GenBank (Suppl. material 1: Table S1). We aligned all sequences in MAFFT (Katoh et al. 2017) version 7, with the Q-INS-I option, which resulted in a final alignment of 589 bp. We then selected the best-fit model of nucleotide substitution in PartitionFinder v.1.1.1 (Lanfear et al. 2012). The model selected was the K2P + I + gamma. We performed Bayesian inference of phylogeny (BI) in MrBayes v 3.2.2 (Ronquist et al. 2012) in the CIPRES science gateway server (Miller et al. 2010). The Bayesian analysis consisted of four runs of  $10^7$  generations each, with four chains (one cold and three heated), sampling every 1,000 generations. We used Tracer v1.6 (Drummond and Rambaut 2007) to confirm that independent runs had converged, based on the overlap in likelihood and parameter estimates among runs, as well as effective sample size (ESS) and Potential Scale Reduction Factor value estimates (PSRF). PSRF indicated that individual runs had converged by  $10^5$  generations, so we discarded the first 25% of the runs as burn-in. We then annotated posterior probability values on the resulting topology in the program TreeAnnotator v 1.8.3 (Rambaut 2014).

## Systematic account

### *Phrynobatrachus bibita* Goutte, Reyes-Velasco & Boissinot, sp. n.

<http://zoobank.org/3B046650-2B48-4740-9ED9-A29A4EC10A72>

Common name (English): Bibita Mountain dwarf puddle frog

**Material. Holotype.** A male (SB440; Figure 2), collected on 17 June 2018, at night, in Bibita Mountain, southwestern Ethiopia (6.8229N, 35.0938E, datum = WGS84; 1972 m a.s.l.). The specimen was collected while in amplexus (female paratopotype SB439), on vegetation, in overgrown pond in primary forest. **Paratopotypes.** Nine specimens: eight females collected in the same pond as the holotype on 16 June 2018 (SB418-SB420, SB424-SB427) and on 17 June 2018 (SB439); another male (SB421) collected at night in the water (probably calling), at same locality as the holotype on 16 June 2018.

**Diagnosis.** Small species (SVL =  $16.8 \pm 0.1$  mm for males,  $20.3 \pm 0.9$  mm for females) attributed to the genus *Phrynobatrachus* by the presence of tarsal and outer metatarsal tubercles (Suppl. material 2: Figure S1A). Body slender, with long legs (tibia length/SVL = 0.6 in both sexes) rather long snout for the genus and very elongated fingers (hand length/SVL = 0.3 in both sexes) and toes (foot length/SVL = 0.6 in both sexes) in comparison to its congeners. Webbing absent between fingers and minimal between toes. Tympanum not visible. Canthus rostralis marked and concave from

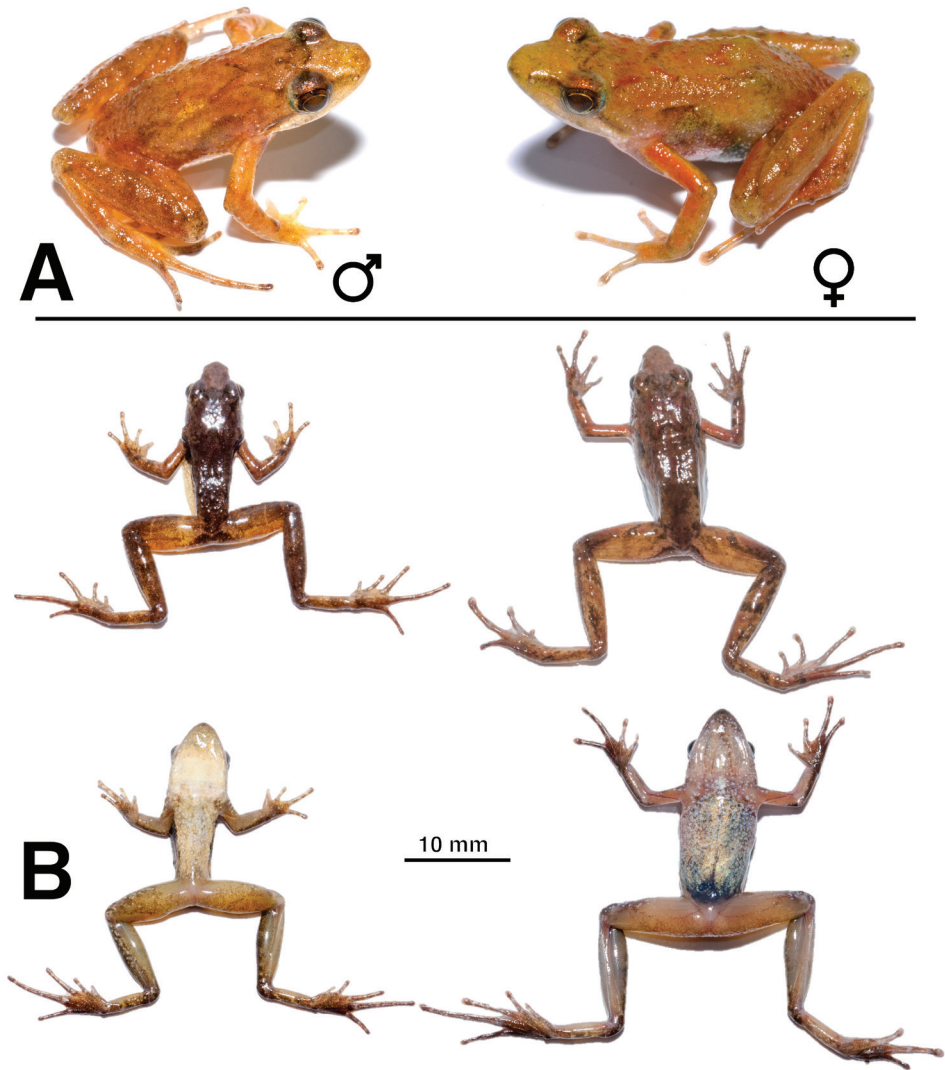


**Figure 2.** *Phrynobatrachus bibita* sp. n. **A** Live pictures of *P. bibita* sp. n. Male holotype (left; SB440) and female paratopotype (right; SB424) **B** Ventral and dorsal views of the same individuals, with male on the left and female on the right. Scale bar: 10 mm.

nostril to eye. Snout pointed. Nostrils not visible from above. Eyelid spine absent. Throat of adult males white with light grey freckles on the anterior third, without any spinulae. Femoral glands hardly distinguishable but present in adult males. Two ridges in the scapular region and two short, oblique ridges behind the eyes. These four ridges may be all disjointed, the two scapular ridges may be jointed to form a chevron shape, or the ridges may be jointed laterally in an hourglass shape.

**Comparisons.** This species can easily be distinguished from other Ethiopian *Phrynobatrachus*: the body is slenderer, the hind limbs, fingers and toes are longer than all four other described Ethiopian *Phrynobatrachus*, *P. bullans*, *P. natalensis*, *P. minutus*, and *P. inexpectatus*. Additionally, the tips of fingers and toes are more enlarged than in any of these species, particularly in females. It is similar in size as *P. minutus*, slightly larger than *P. inexpectatus* and much smaller than *P. bullans* and *P. natalensis*. It can be further distinguished from *P. natalensis* by a more marked canthus rostralis and a completely hidden tympanum. Adult males of *P. bibita* sp. n. can be distinguished from *P. bullans*, *P. natalensis*, *P. minutus*, and *P. inexpectatus* by the white coloration of their throat (Largen 2001, Cruetsinger et al. 2004). The new species is also distinct from the three junior synonyms of *P. natalensis* described from Ethiopia: *Arthroleptis bottegi* Boulenger, 1895, described from Auta, Bale province, possesses a distinct tympanum, a rounded snout, and is much larger than *P. bibita* (SVL of female holotype = 31 mm vs.  $20.3 \pm 0.9$  mm in female *P. bibita*). *Phrynobatrachus sciangallarum* Scortecci, 1943, described from a presumably adult male from Murle, Gemu-Gofa province, differs from *P. bibita* by the presence of a considerably darkened throat and the lack of femoral glands. Additionally, it has more extensive foot webbing than *P. bibita* (Largen 2001). *Arthroleptis-Phrynobatrachus zavattarii* Scortecci, 1943, described from Caschei, Gemu-Gofa province, only differs from *P. sciangallarum* by the extent of the foot webbing, and all measurements of the type specimens fall within the range of *P. natalensis* (Largen 2001). Blackburn (2014) provided color photographs of the holotypes of these last two junior synonyms of *P. natalensis*. Based on those photographs, it appears that *P. bibita* has a slenderer head and more elongated fingers than these individuals. Finally, the type localities for these three junior synonyms of *P. natalensis* are in the southern part of the country, an area that is dry and at low elevation, in contrast with the habitat occupied by *P. bibita* sp. n.

Among Eastern African *Phrynobatrachus*, *P. bibita* sp. n. can be distinguished from *P. acridoides* (Cope, 1867), *P. auritus* Boulenger, 1900, *P. dendrobates* (Boulenger, 1919), *P. graueri* (Nieden, 1911), *P. keniensis* Barbour & Loveridge, 1928, *P. krefftii* Boulenger, 1909, *P. perpalmatum* Boulenger, 1898, *P. petropedetoides* Ahl, 1924, and *P. versicolor* Ahl, 1924, by a completely hidden tympanum (Cope 1867, Boulenger 1882, 1909, Razzetti and Msuya 2002, Pickersgill 2007). This species can further be distinguished from *P. auritus* Boulenger, 1900, *P. dendrobates*, *P. graueri*, *P. kinagopenensis* Angel, 1924, *P. krefftii*, *P. mababiensis* FritzSimons, 1932, *P. parvulus* (Boulenger, 1905), *P. rouxi* (Nieden, 1912), *P. scheffleri* (Nieden, 1911), and *P. ukigensis* Grandison & Howell, 1983, by the white and light grey coloration of adult males' throat (Boulenger 1909, Angel 1924, FritzSimons 1932). The new species differs from *P. bullans*, *P. kakamikro* Schick, Zimkus, Channing, Köhler, & Lötters, 2010, and *P. perpalmatum* by the presence of femoral glands in adult males (Cruetsinger et al. 2004, Pickersgill 2007, Schick et al. 2010). The new species is also larger than *P. pallidus*, *P. parvulus*, *P. scheffleri*, and *P. ungujae* Pickersgill, 2007 (Boulenger 1905, Pickersgill 2007, Schick et al. 2010), and possesses longer legs than *P. kakamikro* and *P. pallidus* Pickersgill, 2007, as well as longer feet than *P. pallidus* and *P. ungujae* (Pickersgill 2007, Schick et al. 2010). Finally, *P. bibita* sp. n. can be distinguished from *P. acridoides*, *P. bullans*, *P. mababiensis*,

*P. natalensis*, *P. pallidus*, *P. ungujae*, and *P. versicolor* Ahl, 1924, by the absence of dark bars on the lower jaw (Cope 1867, Boulenger 1882, Fritzsims 1932, Cruetsinger et al. 2004, Pickersgill 2007).

**Description of the holotype.** Adult male (Figure 2; Table 1), body slender, head longer than wide ( $HW/HL = 0.96$ ), the snout is pointed and the canthus rostralis is marked and concave from nostril to eye. Tympanum not visible. Pupil horizontal. Eyelid spine absent. Maxillary teeth present, vomerine teeth absent. Tongue elongate, free for two thirds of its length, tip divided in two short lobes. Legs and feet long for the genus ( $TL/SVL = 0.6$ ;  $FL/SVL = 0.6$ ). Tarsal tubercle and outer metatarsal tubercle present, but inner metatarsal tubercle not distinguishable. Subarticular tubercles absent on the hands and small and barely distinguishable on the feet. Palmar tubercle absent. Fingers and toes elongated and their tips slightly swollen but not forming discs. First fingers shorter and swollen but nuptial pads absent. Fingers free of webbing. No webbing between toe I and II, and minimal webbing between the other toes. Finger formula:  $I < II < IV < III$ . Toe formula:  $I < II < V < III < IV$ . Skin of dorsum and dorsal side of limbs covered by small pointy asperities. Femoral glands hardly visible but present (Suppl. material 2: Figure S1B). Chevron-shaped gland in scapular region extending from above the shoulder girdle to approx. mid-body. Two rows of small warts form faint ridges between the eye and the scapular region but do not reach the chevron-shaped gland. The skin of the throat is not thin and loose as in many other *Phrynobatrachus* species and gular folds and spinulae are absent.

**Coloration of holotype in life.** The body is golden (Figure 2A); a dark chevron is present in the scapular region underlining two short back ridges. A faint dark triangle is present between the eyes and a faint dark bar is present between the eye and the shoulder. The upper eyelids are darker than the rest of the head. Loreal region faintly darker than the rest of the head. Upper and lower jaws lack any blotching. The flanks and the sides of the head present numerous small white spots, extending to the upper lip below the eye. Iris dark gold with a golden ring around the iris interrupted by a black dot at the bottom of the iris. The thighs and legs are faintly and irregularly banded. The back of the thighs is yellowish with irregular coverage of melanophores. A dark triangle is present in the vent region. Ventral region is white molted with light grey. The throat is white, with the anterior third light grey with white freckles. Ventral side of the thighs and legs shows irregular melanophores and white spots.

**Coloration of holotype in preservative.** After euthanasia, the individual's coloration darkened notably (Figure 2B). In preservative, the dorsum presents a grey coloration.

**Variation.** Morphometric variations of the type series are summarized in Table 1. Inner metatarsal tubercles are not visible in all individuals. Subarticular tubercles are more pronounced in some individuals. Webbing of the feet presents small variation, ranging from minimal to no webbing for toes I and II, and webbed to the first phalange for toes III to V. The dorsal and leg skin is mostly smooth with small warts more pronounced in some individuals. The two ridges in the scapular region and two oblique ridges behind the eyes were visible in all examined specimens. In four specimens, they formed a chevron in the scapular region, in three specimens the ridges jointed laterally, forming an hourglass, and in two specimens all four ridges were disjointed.

**Table 1.** Morphometric measurements of *Phrynobatrachus bibita* sp. n.

Specimen	SB 440	SB 421	SB 418	SB 419	SB 420	SB 424	SB 425	SB 426	SB 427	SB 439	Males (n = 2)	Females (n = 8)
Sex	♂	♂	♀	♀	♀	♀	♀	♀	♀	♀		
SVL	16.8	16.7	19.3	19.2	21.5	20.6	20.9	20.3	21.0	19.4	16.6 ± 0.1	20.3 ± 0.9
HW	5.5	5.7	5.9	6.2	6.8	6.2	6.5	6.5	7.3	5.9	5.6 ± 0.1	6.4 ± 0.5
HL	5.7	5.8	6.6	6.7	7.1	7.4	6.9	6.6	6.8	6.7	5.6 ± 0.1	6.9 ± 0.3
SL	2.4	2.7	2.8	3.0	3.3	3.3	3.2	3.1	3.0	2.8	2.6 ± 0.2	3.1 ± 0.2
NS	1.4	1.1	1.5	1.6	1.6	1.8	1.6	1.7	1.7	1.7	1.3 ± 0.2	1.7 ± 0.1
IND	2.0	1.8	2.1	2.2	2.4	2.3	2.3	2.4	2.1	2.2	1.9 ± 0.1	2.3 ± 0.1
EN	1.2	1.6	1.5	1.5	1.6	1.4	1.5	1.2	1.3	1.2	1.4 ± 0.3	1.4 ± 0.2
IOD	2.0	2.0	1.8	2.2	2.2	2.5	2.0	2.4	1.9	2.1	2.0 ± 0.0	2.1 ± 0.2
ED	2.5	1.8	2.0	2.3	2.0	2.3	2.3	2.1	2.1	2.2	2.2 ± 0.5	2.2 ± 0.1
UEW	1.8	1.3	1.4	1.8	1.5	1.9	1.6	1.5	1.5	1.8	1.6 ± 0.4	1.6 ± 0.2
FLL	3.2	3.7	3.5	4.1	3.8	4.6	4.0	3.9	4.0	3.6	3.5 ± 0.4	3.9 ± 0.3
HAL	5.1	5.0	5.4	5.5	6.0	7.5	6.5	5.8	6.5	6.1	5.1 ± 0.1	6.2 ± 0.7
FinDW	0.6	0.3	0.6	0.7	0.7	0.8	0.7	0.7	0.6	0.8	0.5 ± 0.2	0.7 ± 0.1
THL	8.0	8.0	8.9	9.1	9.6	9.7	9.6	9.6	9.1	9.4	8.0 ± 0.0	9.4 ± 0.3
TL	9.5	9.6	10.6	10.8	11.5	11.6	11.2	11.4	11.2	10.7	9.6 ± 0.1	11.1 ± 0.4
FL	10.5	9.5	12.7	11.7	11.3	12.2	11.5	11.5	11.0	11.4	10 ± 0.7	11.7 ± 0.5
Toe4DW	0.3	0.4	1.0	0.6	0.7	0.6	0.6	0.9	0.6	0.6	0.4 ± 0.1	0.7 ± 0.2
MTL	NA	0.6	NA	NA	0.7	0.4	1.1	NA	NA	0.7	-	-
TL/SVL	0.57	0.57	0.55	0.56	0.53	0.56	0.54	0.56	0.53	0.55	0.6 ± 0.0	0.6 ± 0.0
HW/HL	0.96	0.98	0.89	0.93	0.96	0.84	0.94	0.98	1.07	0.88	1.0 ± 0.0	0.9 ± 0.1
EN/IND	0.60	0.89	0.71	0.68	0.67	0.61	0.65	0.50	0.62	0.55	0.7 ± 0.1	0.6 ± 0.1
HW/SVL	0.33	0.34	0.31	0.32	0.32	0.30	0.31	0.32	0.35	0.30	0.3 ± 0.0	0.3 ± 0.0
FL/TL	1.11	0.99	1.20	1.08	0.98	1.05	1.03	1.01	0.98	1.07	1.1 ± 0.1	1.1 ± 0.1
FL/SVL	0.63	0.57	0.66	0.61	0.53	0.59	0.55	0.57	0.52	0.59	0.6 ± 0.0	0.6 ± 0.0
HL/SVL	0.34	0.35	0.34	0.35	0.33	0.36	0.33	0.33	0.32	0.35	0.3 ± 0.0	0.3 ± 0.0

Measurements for the male holotype and the paratopotypes, and average values ± standard deviations for males and females are given in millimeters. Abbreviations: SVL = snout vent length, HL = head length, HW = head width, SL = snout length, NS = nostril-snout distance, ED = eye diameter, EN = eye-nostril distance, IOD = interorbital distance, IND = inter-narial distance, ED = eye diameter, UEW = upper eyelid width, FLL = forearm length, HAL = hand length, FinDW = third finger disk width, THL = thigh length, TL = tibiofibula length, FL = foot length, Toe4DW = Toe IV disk width, MTL = metatarsal tubercle length.

Males and females differ in size and in proportions (Figure 2). Finger and toe tips are enlarged in females and fingertips are slightly enlarged in males. Males' first finger is short and swollen but no distinct nuptial pad is visible. Adult males present femoral glands, which are lacking in females. Bicolor eggs are visible through the skin of gravid females.

Coloration of the body varies from golden to light brown, with few large light green blotches in some individuals. Most specimens present a dark chevron in the scapular region underlining two short back ridges that are either jointed or disjointed with two oblique ridges between the back of the eye and the shoulders. A more or less pronounced dark stripe is present between the nostril and the eye, and between the eye and the arm. A more or less distinctive dark bar is present between the eyes and some individuals present a lighter or green snout. The flanks and the sides of the head present numerous small white spots, extending to the upper lip in some individuals. The thighs and legs of some individuals are very faintly and irregularly banded. The back of the thighs is cream with small light grey spots. Vocal sac in adult males is white with

the frontal third of the throat light grey with white freckles, while in females the throat and the ventral skin is light grey or yellowish molted with white. Some individuals have a thin light line on the backside of the thigh from the vent to the tarsal tubercle. A dark triangle is generally present in the back of the thigh, around the vent.

**Etymology.** The specific name refers to Bibita Mountain, the type and only known locality for the species. It is an invariable noun used in apposition.

**Habitat, distribution, and natural history.** All individuals were collected in a single large overgrown forest pond (Figure 3A), at night. The surrounding forest consisted of large trees with overhanging epiphytes and dense undergrowth. All females and the amplexed pair were found on vegetation ca. 30 cm above water (Figure 3B). A single male was found in the water, presumably while calling. All collected females were gravid, and bicolor eggs were visible through the skin. Females seemed to aggregate in specific areas of the pond, were numerous egg clutches were found on leaves overhanging the water (Figure 3B). Laying eggs on vegetation overhanging the water is unusual in *Phrynobatrachus*, most species laying their eggs directly in the water (Zimkus et al. 2012). We thus confirmed that these eggs belonged to *Phrynobatrachus bibita* sp. n. by sequencing their mitochondrial rRNA 16s. Various forms of terrestrial egg deposition have been described in the genus *Phrynobatrachus* (Zimkus et al. 2012): most similarly to *P. bibita*, *P. sandersoni* (Parker, 1935) lays its eggs on vegetation up to 2 m above small puddles, small streams or water-saturated soil (Amiet 1981) and *P. krefftii* lays its eggs above the water, on rocks or vegetation (Harper and Vonesh 2010). *Phrynobatrachus guineensis* Guibé & Lamotte, 1961 lays its eggs on the bark of trees above water-filled tree holes (Rödel 1998) and *P. dendrobates* lays its eggs in tree holes or above streams (Zimkus et al. 2012). Finally, *P. phyllophilus* Rödel & Ernst, 2002, *P. tokba* (Chabanaud, 1921), and *P. villiersi* Guibé, 1969 lay their eggs on the leaf litter or the forest floor (Rödel and Ernst 2002a, 2002b; Zimkus et al. 2012). *Phrynobatrachus bibita* sp. n. thus adds to the diversity of reproductive modes in the genus.

Five egg clutches were photographed and contained approximately 30 eggs each (range 22 to 33). All observed clutches were found between 20 – 40 cm above water on vegetation, and up to two clutches were found on a single leaf. When laid, the eggs are bicolor, heavily pigmented, and encased in a thin gelatinous layer; as the egg develops, the pigmentation is more evenly distributed at its surface, with dark brown freckle, and the gelatinous layer becomes much thicker. It is possible that female *P. bibita* sp. n. are guarding their egg clutches in a similar manner as *P. sandersoni* females, which attend their eggs at night by standing over them or staying in the close proximity (Amiet 1981). Additional behavioral observations are necessary to determine whether females *P. bibita* sp. n. truly display such parental care. Other frog species were found in the same pond or nearby, including *Afrixalus enseticola* Largen, 1974, *Leptopelis vannutellii* (Boulenger, 1898), *Paracassina obscura* (Boulenger, 1895), and *Ptychadena* cf. *erlangeri* (Ahl, 1924).

The forest in Bibita Mountain appears to be well preserved, as there are no settlements inside the forest, and a footpath is the only way to cross the forest. People from the surrounded villages harvest wild honey from the forest, but this is the only

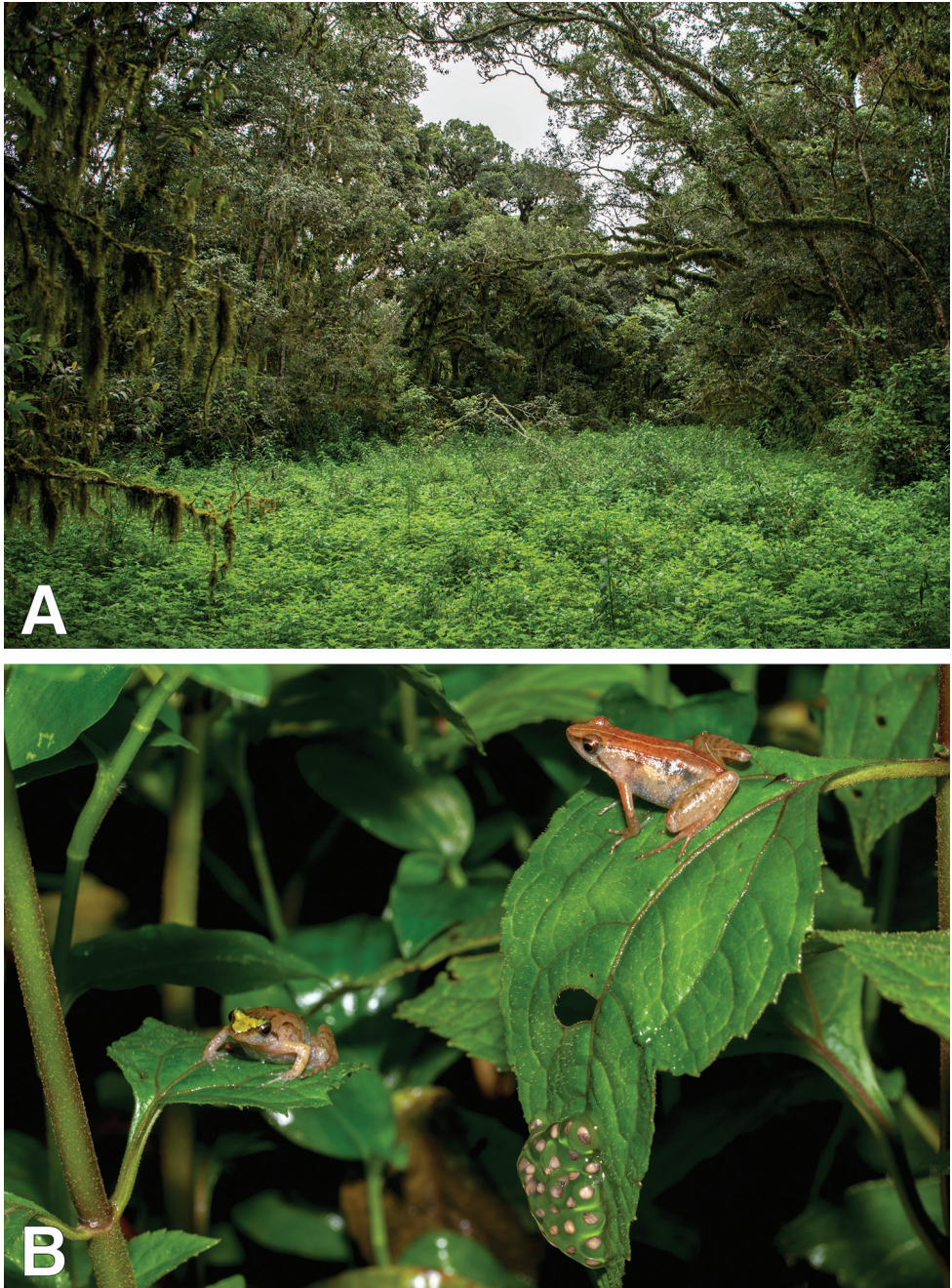


**Figure 3.** Habitat of *Phrynobatrachus bibita* sp. n. **A** Type locality of *P. bibita* sp. n. Overgrown pond in primary forest **B** Two females *P. bibita* sp. n. *in situ*, next to a clutch of eggs, in vegetation at ca. 30 cm above the water. Multiple females and egg clutches were found in similar circumstances.

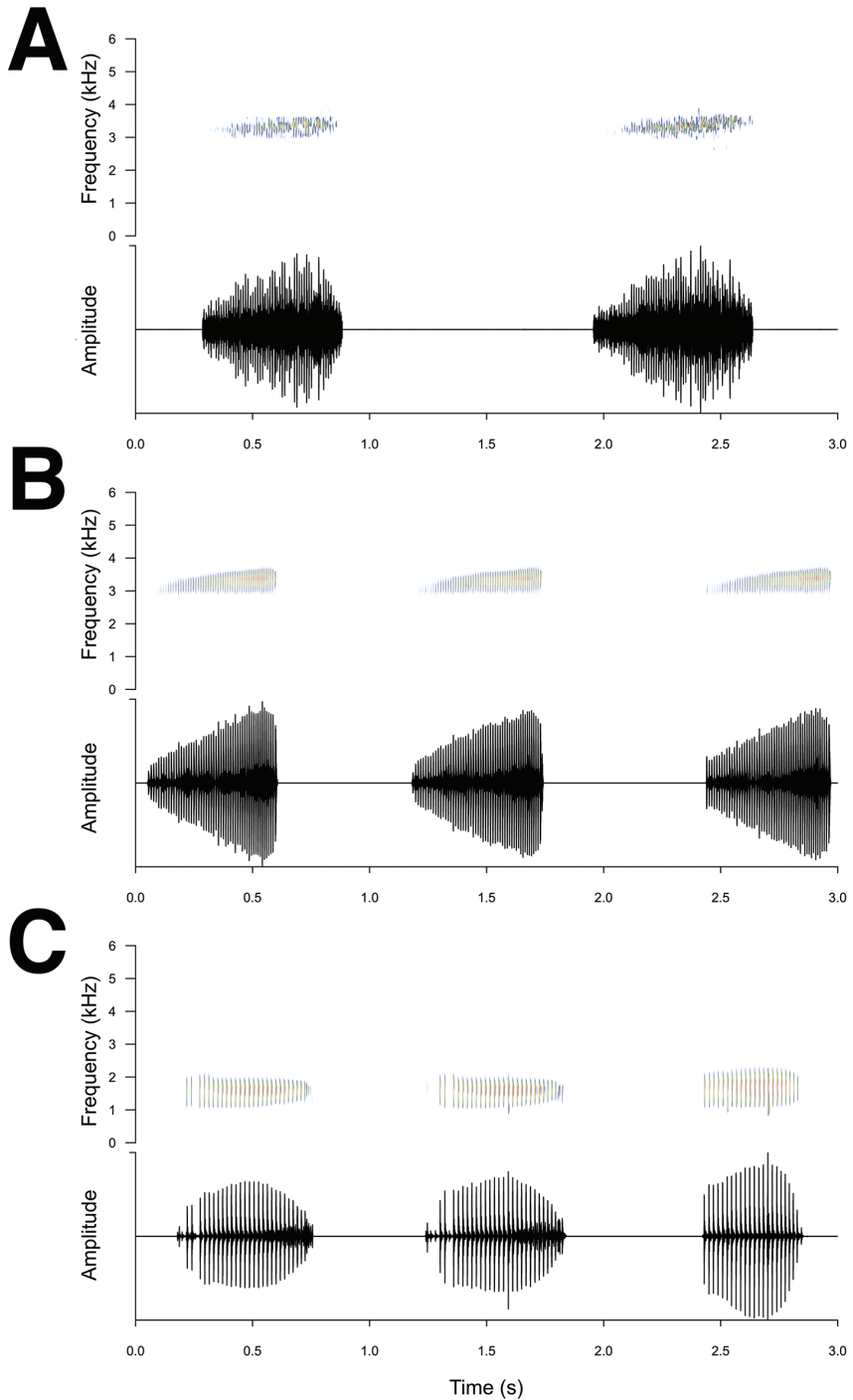


**Figure 4.** Advertisement call of *Phrynobatrachus bibita* sp. n. Spectrograms (upper panels) and sonograms (lower panels; relative amplitude) of Ethiopian *Phrynobatrachus* advertisement calls. **A** *Phrynobatrachus bibita* sp. n. (specimen not collected) **B** *P. minutus* (SB233) **C** *P. natalensis* (specimen not collected).

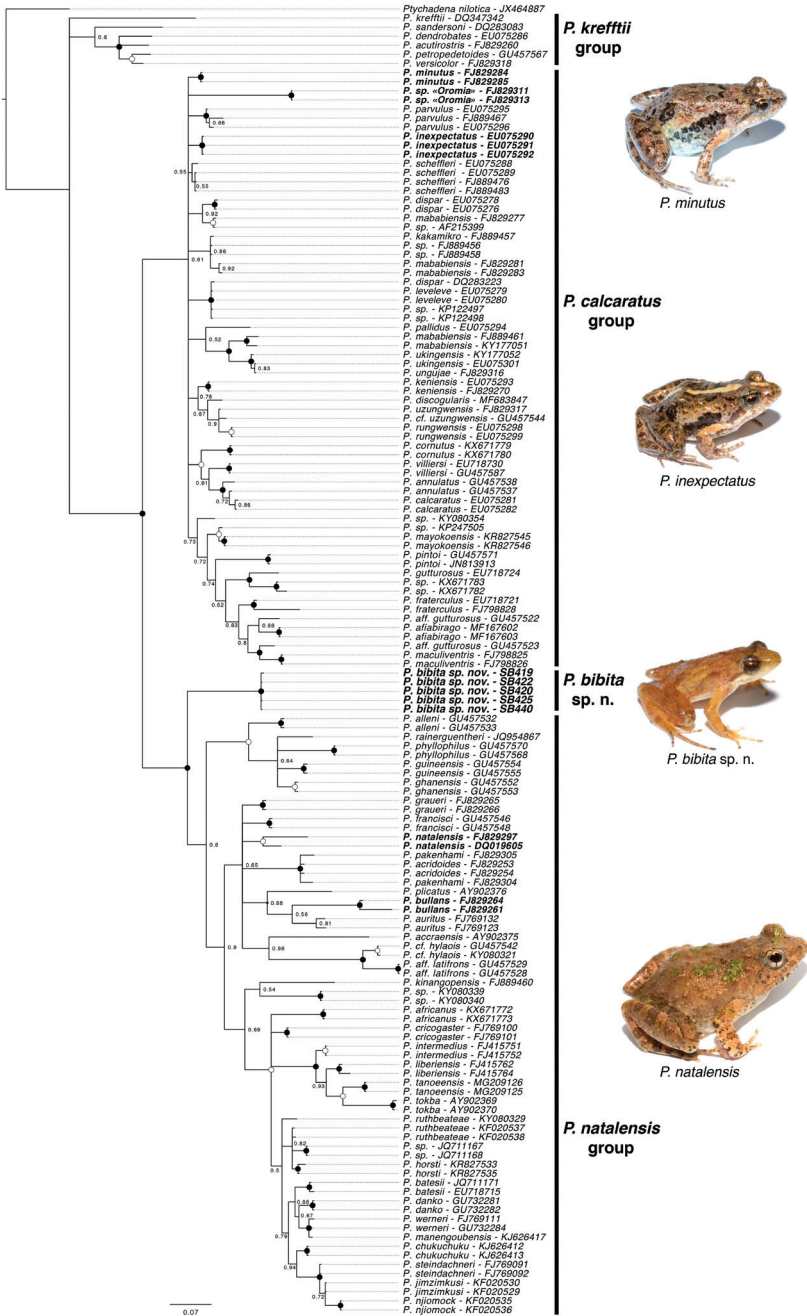


**Figure 5.** Phylogenetic placement of *Phrynobatrachus bibita* sp. n. Bayesian phylogenetic inference of the genus *Phrynobatrachus* based on the mitochondrial rRNA 16S. Nodes with a posterior support of 1 are marked with a black circle and nodes with high posterior support (>0.95) are marked with a white circle. Individuals of *Phrynobatrachus* species known to occur in Ethiopia are shown in boldface. Photos of Ethiopian representatives are displayed, from top to bottom: *Phrynobatrachus minutus* (SB175; Kibre Mengist), *P. inexpectatus* (SB143; Magnete, Harena forest), *P. bibita* sp. n. (SB440; male holotype), *P. natalensis* (SB454; Mizan Teferi).

noticeable human activity there. Based on satellite imagery, no human disturbance is apparent at the higher elevations of the mountain; however, most areas below 1900 m have been transformed into agricultural land.

**Call.** The advertisement call is composed of a series of pulsed notes with a slight upward frequency modulation within each note (Figure 4A). It is similar to that of *Phrynobatrachus minutus* (Figure 4B) in spectral structure, note length, and dominant frequency. The vocalization of *P. bibita* sp. n. can be distinguished from that of *P. natalensis* (Figure 4C) by its higher dominant frequency, indicative of its smaller body size. Dominant frequency:  $3318 \pm 94$  Hz. Note duration =  $630 \pm 80$  ms. Interval inter-notes =  $1085 \pm 630$  ms. The mediocre quality of our recording prevents us from analyzing the advertisement call of *P. bibita* sp. n. in further details, and a more complete description of their vocalization will be needed in the future, in particular to distinguish it from other species of dwarf *Phrynobatrachus*.

**Estimates of evolutionary relationships.** The goal of our phylogenetic analysis was to test the phylogenetic position of the new species, not to obtain a phylogeny of the genus, which has been previously done elsewhere (Zimkus et al. 2010). Our phylogenetic estimates recovered three main lineages in the genus *Phrynobatrachus* (Figure 5); however, several of the nodes have low support. We briefly describe the resulting topology below.

We recovered a basal group of *Phrynobatrachus*, which included the species *P. acutirostris* Nieden, 1912, *P. krefftii*, *P. dendrobates*, *P. petropedetoides* Ahl, 1924, and *P. sandersoni*. This clade is consistent with the “Clade A” of Zimkus et al. (2010), however this clade received low support (posterior probability (pp) < 0.5). All remaining species in the genus were grouped into two major clades, which received strong support (pp = 1). The first one of these two groups is similar to the “Clade B” of Zimkus et al. (2010), which includes the Ethiopian species *P. minutus*, *P. inexpectatus*, and *P. sp. n. “Oromia”* of Zimkus and Schick (2010), while the second group is consistent with the “Clade C” of Zimkus et al. (2010), and includes the Ethiopian species *P. natalensis*. *Phrynobatrachus bibita* sp. n. was not closely related to any of the other Ethiopian species, and instead basal to the last group (“Clade C” of Zimkus et al. (2010)), however with high support (pp = 1). Our analysis grouped the egg clutch collected (SB422) with the adults *P. bibita* sp. n. (holotype SB440 and paratopotypes SB419, SB420, SB425), ensuring that it belonged to the new species. We did not include samples of three junior synonyms of *P. natalensis* from Ethiopia (see *Comparisons*), however, samples referable to these junior synonyms have previously been included on a phylogeny of members of the *P. natalensis* group (Lara 2016), and they are well nested within *P. natalensis*, we can thus conclude that they do not represent *P. bibita*.

## Discussion

Most of the natural vegetation of the Ethiopian highlands has been transformed for agriculture or into grazing fields for cattle (Williams et al. 2004). However, in the southwestern end of the country, a few areas still conserve their original vegetation, and

several of these areas remain largely unexplored. Bibita Mountain is one of such areas, and to our knowledge, no vertebrate collections has ever been obtained there. The only published account on the flora or fauna of Bibita Mountain comes from a study on plant composition and structure (Hundera and Deboch 2008). The discovery of a distinctly new species of *Phrynobatrachus* after only two days of survey calls out for further exploration of the biological diversity in this area. Our previous research showed that the amphibian fauna of Ethiopia is underestimated by the current taxonomy, and we believe that further research on Bibita Mountain, as well as in other nearby areas might greatly increase the number of species of amphibians in Ethiopia.

The phylogenetic relationships of many members of the genus *Phrynobatrachus* remains unresolved. Zimkus et al. (2010) recovered three main clades of *Phrynobatrachus* in their analysis, which they designated as groups 'A', 'B' and 'C'. Our results show that *P. bibita* sp. n. is not related to other currently described species of Ethiopian *Phrynobatrachus*, and instead, it appears to be sister to all the members of the *P. natalensis* group (Figure 5). Interestingly, the morphology of *P. bibita* sp. n., including long limbs, elongated fingers and toes, enlarged toe tips and pointed snout, is most similar to the more distantly related species *P. sandersoni*, *P. dendrobates*, and *P. krefftii*. In addition, *P. bibita* sp. n. shares with these species a rare behavior for the genus consisting of laying eggs on vegetation above the water (Amiet 1981, Harper and Vonesh 2010, Zimkus et al. 2012). Finally, *P. bibita* sp. n. might display parental care, as observed in *P. sandersoni* and *P. dendrobates* (Amiet 1981, Zimkus et al. 2012) and unknown from any other species of the genus. Whether *P. bibita* sp. n. retained ancestral morphological and behavioral characters shared with the *P. krefftii* species group, or whether it is a case of convergence remains to be investigated. Additional work is necessary to better understand the evolutionary history of this diverse genus.

## Acknowledgments

We would like to thank the Ethiopian Wildlife Conservation Authority for providing us with collecting permits. We are very grateful for all the people from the town of Bibita for their hospitality, especially Abatyhun, Keysi, and Coma. Fieldwork in Ethiopia would not have been possible if not for the invaluable assistance of Megersa Kelbessa and Samuel Woldeyes of Rock Hewn Tours. This research was supported by New York University Abu Dhabi Research Funds AD180 (to SB). We are grateful to the two reviewers for their useful comments on our manuscript.

## References

- Amiet J-L (1981) Ecologie, éthologie et développement de *Phrynodon sandersoni* Parker, 1939 (Amphibia, Anura, Ranidae). *Amphibia-Reptilia* 2: 1–13. <https://doi.org/10.1163/156853881X00249>

- Angel F (1924) Description de deux Batraciens nouveaux, d'Afrique Orientale anglaise, appartenant au genre *Phrynobatrachus* (Mission Alluaud et Jeannel, 1911–1912). Bulletin du Muséum national d'Histoire naturelle 30: 130–132.
- Boersma P, Weenink D (2013) Praat: doing phonetics by computer. <http://www.praat.org>
- Boulenger GA (1882) Catalogue of the Batrachia Salientia. Ecaudata in the collection of the British Museum. 2d ed., British Museum (Natural History), London, 588 pp.
- Boulenger GA (1905) A list of the batrachians and reptiles collected by Dr. W. J. Ansorge in Angola with descriptions of new species. Annals and Magazine of Natural History; Zoology, Botany, and Geology 16: 105–115. <https://doi.org/10.1080/03745480509443656>
- Boulenger GA (1909) Descriptions of three new frogs discovered by Dr. P. Krefft in Usambara, German East Africa. Annals and Magazine of Natural History 4: 496–497. <https://doi.org/10.1080/00222930908692705>
- Chen MH, Comb CA (1999) An alternative anesthesia for amphibians: ventral application of benzocaine. Herpetological Reviews 30: 34.
- Cope ED (1867) On the families of raniform Anura. Journal of the Academy of Natural Sciences of Philadelphia 6: 189–206.
- Crutsinger G, Pickersgill M, Channing A, Moyer D (2004) A new species of *Phrynobatrachus* (Anura: Ranidae) from Tanzania. African Zoology 39: 19–23.
- Drummond AJ, Rambaut A (2007) BEAST: Bayesian evolutionary analysis by sampling trees. BMC Evolutionary Biology 7: 214. <https://doi.org/10.1186/1471-2148-7-214>
- FritzSimons V (1932) Preliminary description of new forms of South African Reptilia and Amphibia, from the Vernay-Lang Kalahari Expedition, 1930. Annals of the Transvaal Museum 15: 35–40.
- Frost DR (2018) Amphibian species of the World: an online reference. Version 6.0. <http://research.amnh.org/herpetology/amphibia/index.html> [accessed: January 11, 2018]
- Gower DJ, Aberra RK, Schwaller S, Largen MJ, Collen B, Spawls S, Menegon M, Zimkus BM, Sá R de, Mengistu AA, Gebresenbet F, Moore RD, Saber SA, Loader SP (2013) Long-term data for endemic frog genera reveal potential conservation crisis in the Bale Mountains, Ethiopia. Oryx 47: 59–69. <https://doi.org/10.1017/S0030605311001426>
- Harper E, Vonesh JR (2010) Field Guide to the Amphibians of the East Usambara Mountains. Camerapix Publishers International, Nairobi.
- Hundera K, Deboch B (2008) Woody species composition and structure of the Gurra Farda forest, Snnpr, south western Ethiopia. Ethiopian Journal of Education and Sciences 3. <https://doi.org/10.4314/ejesc.v3i2.42006>
- Katoh K, Rozewicki J, Yamada KD (2017) MAFFT online service: multiple sequence alignment, interactive sequence choice and visualization. Briefings in Bioinformatics. <https://doi.org/10.1093/bib/bbx108>
- Lanfear R, Calcott B, Ho SYW, Guindon S (2012) PartitionFinder: Combined Selection of Partitioning Schemes and Substitution Models for Phylogenetic Analyses. Molecular Biology and Evolution 29: 1695–1701. <https://doi.org/10.1093/molbev/mss020>
- Lara JA (2016) Phylogeography of the Natal puddle frog *Phrynobatrachus natalensis* (Anura: Phrynobatrachidae) in sub-Saharan Africa. Master thesis. Department of Biological Sciences, University of Texas at El Paso.

- Largen M, Spawls S (2010) Amphibians and reptiles of Ethiopia and Eritrea. Edition Chimaira/Serpent's Tale NHBD, Frankfurt am Main, 687 pp.
- Largen MJ (2001) The status of the genus *Phrynobatrachus* Günther 1862 in Ethiopia and Eritrea, including description of a new species (Amphibia, Anura, Ranidae). *Tropical Zoology* 14: 287–306. <https://doi.org/10.1080/03946975.2001.10531158>
- Miller MA, Pfeiffer W, Schwartz T (2010) Creating the CIPRES science gateway for inference of large phylogenetic trees. 2010 Gateway Computing Environments Workshop (GCE), 1–8. <https://doi.org/10.1109/GCE.2010.5676129>
- Pickersgill M (2007) Frog search results of expeditions to southern and eastern Africa. Serpent's Tale NHBD / Edition Chimaira, Frankfurt am Main, 575 pp.
- Rambaut A (2014) TreeAnnotator v1.8.2. <http://beast.bio.ed.ac.uk/TreeAnnotator> [accessed: Sep 10, 2018]
- Razzetti E, Msuya CA (2002) Field guide to the amphibians and reptiles of Arusha national park (Tanzania). Pubblinova Edizioni Negri and Istituto OIKOS, city, 83 pp.
- Reyes-Velasco J, Manthey JD, Bourgeois Y, Freilich X, Boissinot S (2018a) Revisiting the phylogeography, demography and taxonomy of the frog genus *Ptychadena* in the Ethiopian highlands with the use of genome-wide SNP data. *PLOS ONE* 13: e0190440. <https://doi.org/10.1371/journal.pone.0190440>
- Reyes-Velasco J, Manthey JD, Freilich X, Boissinot S (2018b) Diversification of African tree frogs (genus *Leptopelis*) in the highlands of Ethiopia. *Molecular Ecology* 27: 2256–2270. <https://doi.org/10.1111/mec.14573>
- Rödel MO (1998) A reproductive mode so far unknown in African ranids: *Phrynobatrachus guineensis* Guibé & Lamotte, 1961 breeds in tree holes. *Herpetozoa* 11(1/2):19–26.
- Rödel MO, Ernst R (2002a) A new reproductive mode for the genus *Phrynobatrachus*: *Phrynobatrachus alticola* has nonfeeding, nonhatching tadpoles. *Journal of Herpetology* 36(1):121–125. [https://doi.org/10.1670/0022-1511\(2002\)036\[0121:ANRMFT\]2.0.CO;2](https://doi.org/10.1670/0022-1511(2002)036[0121:ANRMFT]2.0.CO;2)
- Rödel MO, Ernst R (2002b) A new *Phrynobatrachus* from the upper Guinean rain forest, West Africa, including a description of a new reproductive mode for the genus. *Journal of Herpetology* 36(4):561–571. [https://doi.org/10.1670/0022-1511\(2002\)036\[0561:ANPFTU\]2.0.CO;2](https://doi.org/10.1670/0022-1511(2002)036[0561:ANPFTU]2.0.CO;2)
- Ronquist F, Teslenko M, Mark P van der, Ayres DL, Darling A, Höhna S, Larget B, Liu L, Suchard MA, Huelsenbeck JP (2012) MrBayes 3.2: efficient Bayesian phylogenetic inference and model choice across a large model space. *Systematic Biology*: sys029. <https://doi.org/10.1093/sysbio/sys029>
- Schick S, Zimkus BM, Channing A, Köhler J, Lötters S (2010) Systematics of “Little Brown Frogs” from East Africa: recognition of *Phrynobatrachus scheffleri* and description of a new species from the Kakamega Forest, Kenya (Amphibia: Phrynobatrachidae). *Salamandra* 46: 24–36.
- Watters JL, Cummings ST, Flanagan RL, Siler CD (2016) Review of morphometric measurements used in anuran species descriptions and recommendations for a standardized approach. *Zootaxa* 4072: 477–495. <https://doi.org/10.11646/zootaxa.4072.4.6>
- Williams SD, Vivero JL, Spawls S, Anteneh S, Ensermu K (2004) The Ethiopian Highlands. In: Mittermeier RA, Robles-Gil P, Hoffman M, Pilgrim JD, Brooks TM, Mittermeier CG, Fonseca G (Eds) *Hotspots Revisited: Earth's Biologically Richest and Most Endangered Ecoregions*. Mexico City, Mexico, 262–273.

- Zhang P, Liang D, Mao R-L, Hillis DM, Wake DB, Cannatella DC (2013) Efficient Sequencing of Anuran mtDNAs and a Mitogenomic Exploration of the Phylogeny and Evolution of Frogs. *Molecular Biology and Evolution* 30: 1899–1915. <https://doi.org/10.1093/molbev/mst091>
- Zimkus BM (2008) *Phrynobatrachus bullans*: geographic distribution (Tanzania, Kenya, and Ethiopia). *Herpetological Review* 39: 235.
- Zimkus BM, Lawson L, Loader SP, Hanken J (2012) Terrestrialization, miniaturization and rates of diversification in African puddle frogs (Anura: Phrynobatrachidae). *PLoS ONE* 7: e35118. <https://doi.org/10.1371/journal.pone.0035118>
- Zimkus BM, Rödel M-O, Hillers A (2010) Complex patterns of continental speciation: molecular phylogenetics and biogeography of sub-Saharan puddle frogs (*Phrynobatrachus*). *Molecular Phylogenetics and Evolution* 55: 883–900. <https://doi.org/10.1016/j.ympev.2009.12.012>
- Zimkus BM, Schick S (2010) Light at the end of the tunnel: insights into the molecular systematics of East African puddle frogs (Anura: Phrynobatrachidae). *Systematics and Biodiversity* 8: 39–47. <https://doi.org/10.1080/14772000903543004>

## Supplementary material 1

### Table S1. GenBank accession numbers

Authors: Sandra Goutte, Jacobo Reyes-Velasco, Stephane Boissinot

Data type: molecular data

Copyright notice: This dataset is made available under the Open Database License (<http://opendatacommons.org/licenses/odbl/1.0/>). The Open Database License (ODbL) is a license agreement intended to allow users to freely share, modify, and use this Dataset while maintaining this same freedom for others, provided that the original source and author(s) are credited.

Link: <https://doi.org/10.3897/zookeys.824.31570.suppl1>

## Supplementary material 2

### Photographs of some morphological details of *Phrynobatrachus bibita* sp. n.

Authors: Sandra Goutte, Jacobo Reyes-Velasco, Stephane Boissinot

Data type: multimedia

Explanation note: A – Right foot of female paratopotype SB424, showing the tarsal tubercle (a), inner metatarsal tubercle (b) and outer metatarsal tubercle (c). B – Left hind limb of male holotype SB440, showing the femoral gland.

Copyright notice: This dataset is made available under the Open Database License (<http://opendatacommons.org/licenses/odbl/1.0/>). The Open Database License (ODbL) is a license agreement intended to allow users to freely share, modify, and use this Dataset while maintaining this same freedom for others, provided that the original source and author(s) are credited.

Link: <https://doi.org/10.3897/zookeys.824.31570.suppl2>

# A new species of *Pelodiscus* from northeastern Indochina (Testudines, Trionychidae)

Balázs Farkas<sup>1</sup>, Thomas Ziegler<sup>2,3</sup>, Cuong The Pham<sup>4</sup>, An Vinh Ong<sup>5</sup>, Uwe Fritz<sup>6</sup>

**1** 21 Bercsényi St., 2464 Gyúró, Hungary **2** Cologne Zoo, 173 Riebler St., 50735 Cologne, Germany **3** Institute of Zoology, Cologne University, 47b Zülpicher St., 50674 Cologne, Germany **4** Institute of Ecology and Biological Resources, Vietnam Academy of Science and Technology, 18 Hoang Quoc Viet St., Cau Giay, Hanoi, Vietnam **5** Department of Zoology, Vinh University, 182 Le Duan St., Vinh City, Nghe An Province, Vietnam **6** Museum of Zoology, Senckenberg Dresden, A. B. Meyer Building, 01109 Dresden, Germany

Corresponding author: Uwe Fritz ([uwe.fritz@senckenberg.de](mailto:uwe.fritz@senckenberg.de))

Academic editor: J. Penner | Received 5 November 2018 | Accepted 16 January 2019 | Published 13 February 2019

<http://zoobank.org/5ED5756E-F13D-4759-9F88-7DAF82100180>

**Citation:** Farkas B, Ziegler T, Pham CT, Ong AV, Fritz U (2019) A new species of *Pelodiscus* from northeastern Indochina (Testudines, Trionychidae). ZooKeys 824: 71–86. <https://doi.org/10.3897/zookeys.824.31376>

## Abstract

A new, critically endangered species of softshell turtle, *Pelodiscus variegatus* **sp. n.** is described from north-central Vietnam and Hainan Island, China, distinguished by a unique set of genetic and morphological traits from all other congeners (*P. axenaria*, *P. maackii*, *P. parviformis*, *P. sinensis*, and unnamed genetic lineages). Morphologically, *P. variegatus* is characterized, among others, by its strong ventral ornamentation in all age classes.

## Keywords

China, genetics, morphology, softshell turtles, Vietnam

## Introduction

“Chinese softshell turtles” were considered for decades to represent the morphologically highly variable and geographically widespread species *Pelodiscus sinensis* (Wiegmann, 1834), distributed from the Russian Far East through the Korean Peninsula, eastern and central China to Vietnam (e.g., Pope 1935; Wermuth and Mertens 1961, 1977; Pritchard 1979; Meylan 1987; Ernst and Barbour 1989). Another species, *P. maackii*

(Brandt, 1857), from the northernmost part of the distributional range, was resurrected from the synonymy of *P. sinensis* by Chkhikvadze (1987) employing osteological features. On the basis of morphological characters, two additional species from central China were described in the 1990s, *P. axenaria* (Zhou, Zhang & Fang, 1991) and *P. parviformis* Tang, 1997. However, the validity of the latter three species was repeatedly questioned or rejected (Ernst et al. 2000; TTWG 2007). Using three mitochondrial DNA (mtDNA) fragments and one nuclear locus, Fritz et al. (2010) confirmed that *Pelodiscus* represents a species complex. These authors tentatively recognized *P. axenaria* and *P. maackii* and highlighted that the assignment of scientific names was difficult because the identity of the oldest available name, *Trionyx sinensis* Wiegmann, 1834, remained unclear. Stuckas and Fritz (2011) designated a lectotype for this species and succeeded in sequencing approximately 1500 base pairs of mtDNA of this 180-year-old type specimen. This allowed the conclusive recognition of four genetically distinct species, *P. axenaria*, *P. maackii*, *P. parviformis*, and *P. sinensis*. Yang et al. (2011) arrived at the same judgment with respect to *P. parviformis* after evaluating molecular and morphological data but emphasized the near-impossibility of distinguishing *P. axenaria* from *P. parviformis* by external characters alone. Finally, based on comprehensive sampling, Gong et al. (2018) examined the diversity of *Pelodiscus* using mtDNA and five nuclear loci. These authors showed that the diversity of *Pelodiscus* is still underestimated and provided evidence that two genetically and morphologically distinct *Pelodiscus* species occur syntopically in northern Vietnam. One of these species was found widely distributed and occurring also in China, whereas the other seemed to be confined to northern and central Vietnam. Mitochondrial DNA of the two species was only moderately divergent, albeit representing distinct lineages. In contrast, the studied nuclear loci revealed discrete gene pools, suggestive of ancient mitochondrial capture. In the present study, we describe this as yet unnamed taxon with introgressed mitochondria.

## Taxonomy

### *Pelodiscus variegatus* sp. n.

<http://zoobank.org/95F21749-6C4A-439F-BBC0-A44B6F82F1AA>

Figs 1–4, Tables 1–4

**Holotype.** Institute of Ecology and Biological Resources, Hanoi: IEBR 4480, adult female preserved in alcohol, Thai Thinh village, Kinh Mon District, Hai Duong Province, Vietnam, leg. Cuong The Pham, 20 June 2009 (Fig. 1).

**Paratypes** (all preserved in alcohol). American Museum of Natural History, New York: AMNH 30125, hatchling, Nodda (= Nada, Danzhou), Hainan Province, China, leg. Clifford H Pope, December 1922–July 1923; Hungarian Natural History Museum, Budapest: HNHM 2018.111.1, adult male, same data as for the holotype; HNHM 2018.112.1, female, Song Rac Lake, Cam Xuyen District, Cam Lac Commune, Ha Tinh Province, Vietnam (18.1665N, 106.0957E), leg. An Vinh Ong, Quang Xuan Hoang



**Figure 1.** Dorsal and ventral aspects of the holotype of *Pelodiscus variegatus* sp. n. (IEBR 4480, adult female, 134.2 mm PL). Photographs Balázs Buzás.

**Table 1.** Selection of diagnostic sites of the 12S rRNA gene for *Pelodiscus* species (84 wild-caught individuals from Gong et al. 2018). Positions refer to the 400-bp-long reference alignment in the Supporting Information. G, H, and I are genetic lineages that represent putatively distinct taxa (Gong et al. 2018).

	<i>n</i>	13	14	20	34	96	222	223	224	225	234	327	330	384	385
<i>P. variegatus</i> sp. n.	4	T	T	T	T	C	T	T	T	T	A	C	T	G	C
<i>P. axenaria</i>	5	.	.	A	C	T	C	.	C	A	C	T	C	C	T
G	1	.	.	.	.	T	.	.	.	.	.	.	.	.	.
H	1	.	.	.	.	T	.	.	.	.	.	.	.	.	.
I	6	.	.	.	C	T	C	.	C	A	C	.	.	C	.
<i>P. maackii</i>	10	.	.	C	.	T	.	G	.	.	.	.	.	.	.
<i>P. parviformis</i>	8	C	C	C	C	T	.	G	.	.	.	.	.	.	.
<i>P. sinensis</i>	49	.	.	.	.	T	.	.	.	.	.	.	.	A/.	.

and Trung Van Vo, 20 October 2018; Museum of Zoology, Senckenberg Dresden: MTD 42534, adult female, through local trade (Nha Trang), Khanh Hoa Province, Vietnam, leg. Edgar Lehr, February 2000; MTD 42834, female, through local trade (from lowland forest northwest of Ky Thuong village; Ziegler 2002), Ha Tinh Province, Vietnam, leg.



**Figure 2.** Two paratypes of *Pelodiscus variegatus* sp. n. in life. **A, C** MTD 44045, female, 75.2 mm PL **B, D** MTD 42834, female, 86.6 mm PL. Photographs Thomas Ziegler.

**Table 2.** Selection of diagnostic sites of the *cyt b* gene for *Pelodiscus* species (94 wild-caught individuals from Gong et al. 2018). Positions refer to the 1168-bp-long reference alignment in the Supporting Information. G, H, and I are genetic lineages that represent putatively distinct taxa (Gong et al. 2018).

	<i>n</i>	130	132	147	148	195	204	285	288	315	477	520	730	741	1081
<i>P. variegatus</i> sp. n.	4	A	A	C	C	G	T	T	C	C	T	T	A	T	T
<i>P. axenaria</i>	10	C	C	T	T	A	C	.	T	.	.	C	G	C	C
G	1	C	C	.	.	.	C	C	.	T	.	C	G	C	C
H	1	C	C	.	.	.	C	C	.	T	.	C	G	C	C
I	6	C	C	.	T	A	C	.	T	.	.	C	G	C	C
<i>P. maackii</i>	11	C	C	.	.	A	C	C	.	.	.	C	G	C	C
<i>P. parviformis</i>	10	C	C	.	.	A	C	C	.	T	C	C	G	C	C
<i>P. sinensis</i>	51	C	.	.	.	.	C	C	.	T	.	C*	G*	C	C

\*Among 51 sequences of *P. sinensis*, only the holotype had the same character state as *P. variegatus*.

Thomas Ziegler, 12 August 1997 (field number TZ 584); MTD 44045, female, through local trade (allegedly captured in a sandy stream in Phong Nha–Ke Bang Reserve; Ziegler et al. 2004), Quang Binh Province, Vietnam, leg. Thomas Ziegler, August/September 2001 (field number TZ V8); Natural History Museum Vienna: NMW 30221:1–6, six hatchlings, Phuc Son, Tan Yen District, Bac Giang Province, Vietnam, leg. Hans Fruhstorfer, 1903; Zoological Collection, Vinh University, Vinh, Nghe An Province: AQT001-HTVN2018, female, Song Rac Lake, Cam Xuyen District, Cam Lac

Commune, Ha Tinh Province, Vietnam (18.1665N, 106.0957E), leg. An Vinh Ong, Quang Xuan Hoang and Trung Van Vo, 20 October 2018; Zoological Research Museum Alexander Koenig, Bonn: ZFMK 101820, female, through local trade (surroundings of the area named “Chin Xai” by local people; Ziegler 2002), Ha Tinh Province, Vietnam, leg. Thomas Ziegler, 23 August 1997 (field number TZ 679).

**Additional specimens** (all preserved in alcohol). American Museum of Natural History, New York: AMNH 28345, adult female, Nodda (= Nada, Danzhou), Hainan Province, China, leg. Clifford H Pope, December 1922–July 1923; Field Museum, Chicago: FMNH 6626 and 6627, females, Nodda (= Nada), Hainan Province, China, leg. Clifford H Pope, 1923; Museum of Vertebrate Zoology, Berkeley: MVZ 23946, male, Kachek (= Jiayi, Qionghai), Hainan Province, China, 20 m a.s.l. (23.36667N, 116.65E), leg. J Linsley Gressitt, 8 August 1935; Natural History Museum Vienna: NMW 30219:1, female, River of Mount Wuchi (= Wanquan He, Wuzhi Shan), Hainan Province, China, don. Franz Steindachner, 1906; NMW 30232:3, adult male, Kaukong River (to be identified with Gaogong He according to Zhao and Adler 1993), Hainan Province, China, don. Franz Steindachner, 1906; Naturalis Leiden: RMNH 4752 and 4753, juveniles, “Annam” (= possibly Phuc Son, Tan Yen District, Bac Giang Province, Vietnam, the declared origin of all of Fruhstorfer’s specimens in other collections), leg. Hans Fruhstorfer, 1903; Zoological Research Museum Alexander Koenig, Bonn: ZFMK 44212 and 44213, adult males, near Hanoi, Vietnam, leg. Ivan Reháč, March 1984; ZFMK 44214, adult female, near Hanoi, Vietnam, leg. Ivan Reháč, March 1984; ZFMK 59199 and 59200, females, Red River (Song Hong), Hanoi, Vietnam, leg. Václav Laňka, June 1985; Natural History Museum Berlin: ZMB 29614, 49775 and 49776, juveniles, Phuc Son, Tan Yen District, Bac Giang Province, Vietnam, leg. Hans Fruhstorfer.

**Diagnosis.** In the 12S rRNA gene, *Pelodiscus variegatus* differs from all other species and genetic lineages of *Pelodiscus* by the presence of cytosine (C) instead of thymine (T) at position 96 of the reference alignment (Suppl. material 1). In the *cyt b* gene, *P. variegatus* differs from all other species and genetic lineages of *Pelodiscus* by the presence of adenine (A) instead of cytosine (C) in position 130 and by the presence of thymine (T) instead of cytosine (C) in positions 204, 741, and 1081 of the reference alignment (Suppl. material 2). In the mtDNA fragment corresponding to the partial ND4 gene plus adjacent DNA coding for tRNAs, *P. variegatus* differs from all other species and genetic lineages of *Pelodiscus* by the presence of adenine (A) instead of guanine (G) in position 94 of the reference alignment (Suppl. material 3). These and further species-specific differences are shown in Tables 1–3.

In addition to the genetic distinctiveness of *P. variegatus*, the strong ventral ornamentation clearly sets apart adult individuals from *P. maackii*, which has a uniform yellowish white or straw yellow plastron devoid of any markings in adults; from *P. sinensis*, which may retain faint remnants of its juvenile pattern on its snow white to reddish white plastron but the round to oval spots are usually isolated and proportionally much smaller; from *P. axenaria*, which has a yellowish white plastron with just a single large black central figure enclosed by the hypo- and xiphiplastra throughout its life (Zhou et

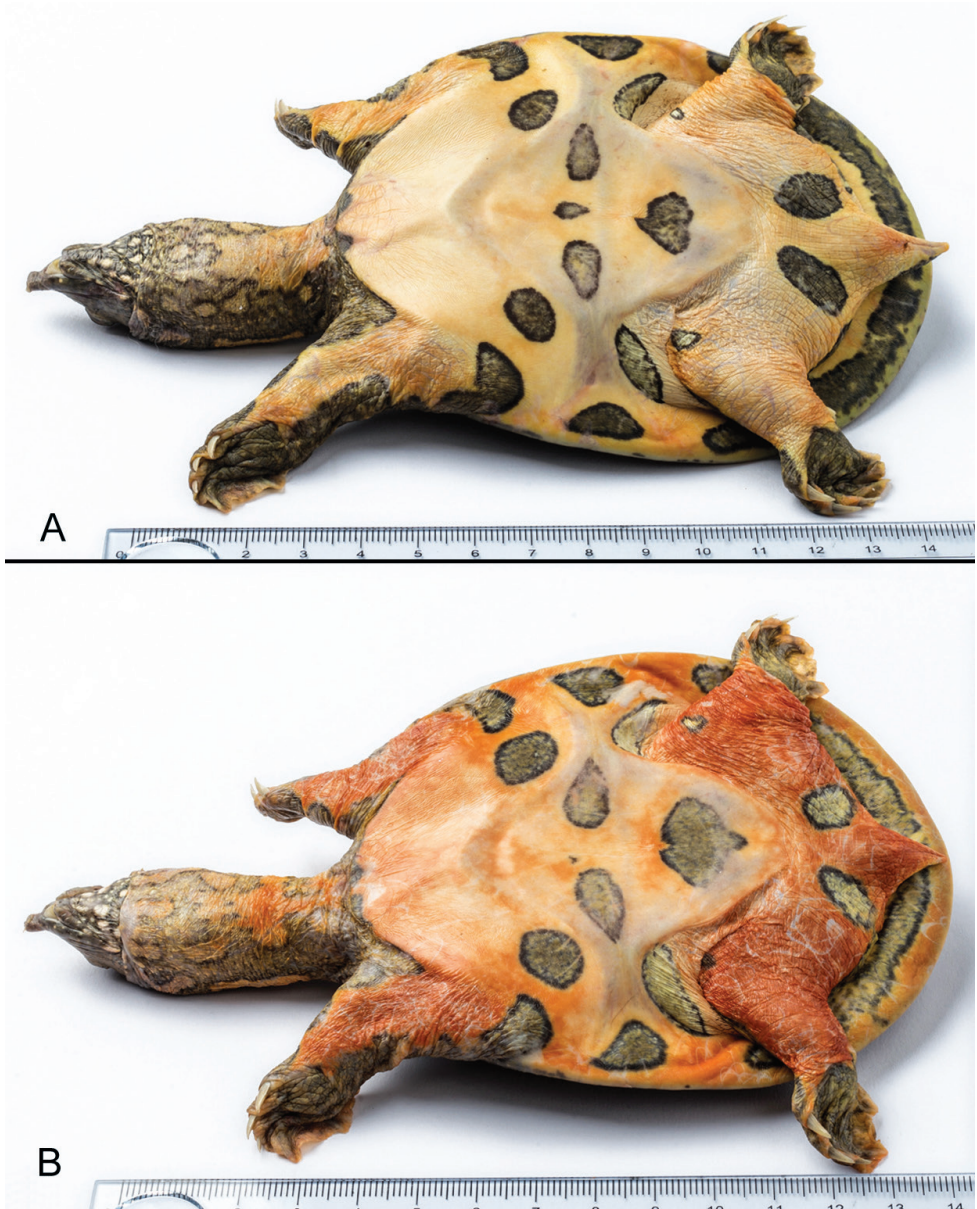


**Figure 3.** Plastral views of two freshly dead paratypes of *Pelodiscus variegatus* sp. n. **A** HNHM 2018.112.1, female, 77.4 mm PL **B** AQT001-HTVN2018, female, 77.3 mm PL. Photographs An Vinh Ong.

al. 1991); and from *P. parviformis*, which has an unmarked yellowish white plastron at all ages. According to the specimens investigated and data available to us, *P. variegatus* also reaches a much smaller maximum size (23 cm CL; AMNH 28345) than *P. maackii* (at least 35 cm CL; Brandt 1857) but grows bigger than *P. parviformis* (16 cm CL; NMW 30232:6); *P. sinensis* (23 cm CL; ZMB 9784) and *P. axenaria* (20 cm CL; Gong

**Table 3.** Selection of diagnostic sites of the mtDNA fragment comprising the partial ND4 gene and adjacent DNA coding for tRNAs for *Pelodiscus* species (91 wild-caught individuals from Gong et al. 2018). Positions refer to the 838-bp-long reference alignment in the Supporting Information. G, H, and I are genetic lineages that represent putatively distinct taxa (Gong et al. 2018).

	<i>n</i>	10	18	31	64	94	148	151	211	262	263	301	305	508
<i>P. variegatus</i> sp. n.	4	C	T	C	A	G	A	G	G	C	C	C	T	A
<i>P. axenaria</i>	10	.	.	T	G	A	C	A	A	T	T	T	C	G
G	1	.	.	.	.	A	.	.	A	.	.	.	.	G
H	1	.	.	.	.	A	.	.	A	.	.	.	.	G
I	6	T	C	T	.	A	C	A	A	T	.	.	A	G
<i>P. maackii</i>	10	.	.	.	.	A	.	.	A	.	.	.	.	G
<i>P. parviformis</i>	9	.	.	.	.	A	G	A	A	.	.	.	.	G**
<i>P. sinensis</i>	50	.	.	.	.	A	G*	.	A/.	.	.	.	.	G**

\*Among 50 *P. sinensis*, only one individual had the same character state as *P. variegatus*.

\*\*Among nine *P. parviformis* and 50 *P. sinensis*, two and one individuals, respectively, had the same character state as *P. variegatus*.

et al. 2018) attain dimensions resembling *P. variegatus*. The diagnostic morphological features of adults of these five *Pelodiscus* species are summarized in Table 4.

**Description of the holotype.** Carapace length (CL) 171.0 mm, carapace width (CW) 148.0 mm, plastron length (PL) 134.2 mm, head width (HW) 32.2 mm, eye diameter 9.8 mm, interorbital distance 5.4 mm, snout length (SL) 13.3 mm. Carapace oval, slightly domed but with a medial keel, widest at level of the posterior buttress spurs of the hypoplastra. Marginal ridge low, central tubercle indistinct. Dorsal surface roughened by longitudinal ridging and smaller protuberances spread over the leathery margin. The yellowish gray carapace is adorned with an extremely complex greenish black pattern consisting of reticulations and stellate spots enclosed by incomplete rings of the same color, finely dotted with siskin green on either side of the vertebral keel, with those above the pelvis being more pronounced but with additional ones towards the perimeter of the bony disk. The ridging of the carapace is enhanced by the siskin green color of the vertebral keel and the longitudinal rows of tubercles.

Ventral surfaces yellowish white with distinct greenish gray blotches extending onto the plastron. Two dark patches below the neck along the anterior carapace margin, one oval mark between the epiplastra, one on both sides behind the armpits and continuing towards but not reaching the hypoplastra, as well as on the hyo- and hypoplastra and the xiphiplastra, the latter meeting along the midline but not contacting those covering the hyo- and hypoplastra. Additional blotches at the insertion of the hindlimbs and some vague, bruise-like markings on the bridge and the underside of the leathery margin.

Head, extended to posterior level of eyes, terminating in flexible snout. Jaws closed, each covered by fleshy lips except anteriorly where the horny beaks are exposed. Top of head with fine, greenish black specks and streaks. Pre-, sub- and postocular stripes thick (approx. 2 mm wide), locally interrupted and yellowish black in color with thin siskin green outlines. Chin with a contrasting yellowish white pattern on yellowish

**Table 4.** Diagnostic morphological features of adults of *Pelodiscus* species.

	<i>P. axenaria</i>	<i>P. maackii</i>	<i>P. parviformis</i>	<i>P. sinensis</i>	<i>P. variegatus</i> sp. n.
Maximum carapace length (in cm)	20	more than 35	16	23	23
Prevalent carapace color	yellowish brown	olive brown to dark brown	yellowish brown	olive green to olive gray	yellowish brown
Carapace pattern	blurred dark mottling with indistinct stellate spots and ill-defined half oval blotches around perimeter of leathery margin	fine dark-edged yellowish to orange spots, background sometimes dark-mottled	dark marbling with indistinct stellate spots and ill-defined half oval blotches around perimeter of leathery margin	none or small, irregular black blotches and vermiculations or small, faint stellate spots	complex dark marbling, large, irregularly disposed black stellate spots and half oval blotches around perimeter of leathery margin
Prevalent plastron color	yellowish white	white to straw yellow	yellowish white	snow white to pinkish white	pinkish white to pale reddish orange
Plastral pattern	a single dark gray central figure enclosed by hypo- and xiphiplastra, underside of leathery margin of carapace unmarked	no pattern, underside of leathery margin of carapace unmarked	no pattern, underside of leathery margin of carapace unmarked	no pattern or relatively small, faint round to oval dark markings, underside of leathery margin of carapace unmarked	distinct, large dark blotches, underside of leathery margin of carapace pigmented
Head and neck pattern	numerous fine dark brown to black markings, pre- and postocular stripes thin and discontinuous	fine dark-edged yellowish to orange spots, pre- and postocular stripes thick, edged in yellowish white	numerous fine dark brown to black markings, pre- and postocular stripes thin and discontinuous	a few scattered dark and light markings, pre- and postocular stripes of medium thickness, sometimes accentuated with white	numerous fine dark brown to black markings edged in yellowish white, pre- and postocular stripes thick
Throat pattern	minuscule, indistinct yellowish white spots	large light, dark-edged markings	minuscule, barely discernible black spots	small whitish spots or large light, dark-edged markings	large light, dark-edged markings
Carapace tuberculation	dorsal tubercles in longitudinal series more or less discrete, central tubercle in front of marginal ridge of carapace small	tubercles restricted to leathery margin, central tubercle in front of marginal ridge of carapace distinct	dorsal tubercles in longitudinal series more or less discrete, central tubercle in front of marginal ridge of carapace small	dorsal tubercles in longitudinal series more or less discrete, central tubercle in front of marginal ridge of carapace small	dorsal tubercles more or less fused with one another in longitudinal series, central tubercle in front of marginal ridge of carapace indistinct
Medial keel	high	low, carapace flat or longitudinally depressed in middle	high	low, carapace evenly arched or longitudinally depressed in middle	high

gray ground, which gradually fades towards the throat and gets almost indiscernible at the base of the neck.

Fore- and hindfeet well-webbed, having five digits each, with claws on the first three digits only. Each forelimb with four antibranchial scales, three of them free-edged. These are wide, the upper one stretching across nearly the whole width of the forelimb (approx. 16 mm long) and the lower two overlapping each other (approx. 20 mm together). Each hindlimb with two horny scales, one smooth on the posterodorsal surface while the other, which is free-edged, is located on the posteroventral surface.

Tail short, barely extending beyond the rear margin of the carapace.

Undersurface of soft parts of body yellowish white embellished with large yellowish gray markings, encroaching on soles and palms, and on either side of the tail.

**Variations.** There is considerable, in part also age-dependent, variation in pattern intensity among *Pelodiscus variegatus*. For instance, our male paratype (HNHM 2018.111.1; 109.7 mm PL; Fig. 4A) has somewhat smaller but much more conspicuous stellate spots on its carapace and very large dark (greenish black) markings on its undersurfaces. Those on the hyo-, hypo- and xiphiplastra are fused into a single mushroom-shaped figure, while the “bruises” on the bridge and the ventral surface of the leathery margin also manifest themselves as true blotches.

In one of our female paratypes (MTD 44045; 75.2 mm PL; Fig. 2A, C) the dark blotches on either side of the tail are connected with those at the insertion of the hindlimbs, the leathery margin and the bridge, whereas the ones in front of the entoplastron are fused with those in the armpits, extend towards the central patch between the epiplastra and actually reach the marks on the anterior edge of the plastron, at the base of the neck.

In a battered, presumably very old male examined by us (ZFMK 44212; 116.4 mm PL; Fig. 4B) comparable in size to our male paratype, the ventral ornamentation has lost definition but is still perceptible.

Hatchlings (Fig. 4C, D) have similar markings to adults but the overall effect is even more striking. The parts colored yellowish white in preservative are orpiment to reddish orange in life (Farkas and McCormack 2010) and fade remarkably slowly as age advances (Figs 2–3). In some individuals the light blotches framed with black on the sides of the neck intermingle to form wide bands on a yellowish gray (in life yellowish brown) ground (Fig. 2A). The subocular stripes are occasionally reduced to short streaks and vary between two and three in number. Although the dark longitudinal striation on the nape of juveniles dissolves in adults, a central spot typically remains discernible just in front of the marginal ridge.

Our modest sample size does not allow us to draw definite conclusions about ontogenetic variation and it is presently unknown at what CL sexual maturity is reached in this species. Individuals are sexually clearly dimorphic, with males having much longer and thicker tails, at a PL of 98.8 mm (ZFMK 44213) but a slight variation in TL can be noticed even among hatchlings (NMW 30221:1–6). Anyhow, smaller (younger) specimens appear to possess proportionally wider heads and rounder shells than larger (older) ones. PL/HW 3.50–4.44, mean 3.925; CL/CW 1.02–1.23, mean 1.149; HW/SL 1.98–2.60, mean 2.213, CL/PL 1.18–1.43, mean 1.283.

**Distribution.** The exact range is unknown but includes lowland areas in the provinces Bac Giang, Ha Tinh (Fig. 5), Hai Duong (own data), “Hai Hung” (a former administrative unit encompassing present-day Hai Duong and Hung Yen; Rudolphi and Weser 1998), Ninh Binh (Rudolphi and Weser 1998; Nguyen et al. 2009; Farkas and McCormack 2010), Phu Tho (Nguyen et al. 2009), Quang Binh (own data), Quang Nam (Farkas and McCormack 2010), Tuyen Quang (Rudolphi and Weser 1998) and Yen Bai (Nguyen et al. 2009) of Vietnam as well as the lower reaches of the Gaogong

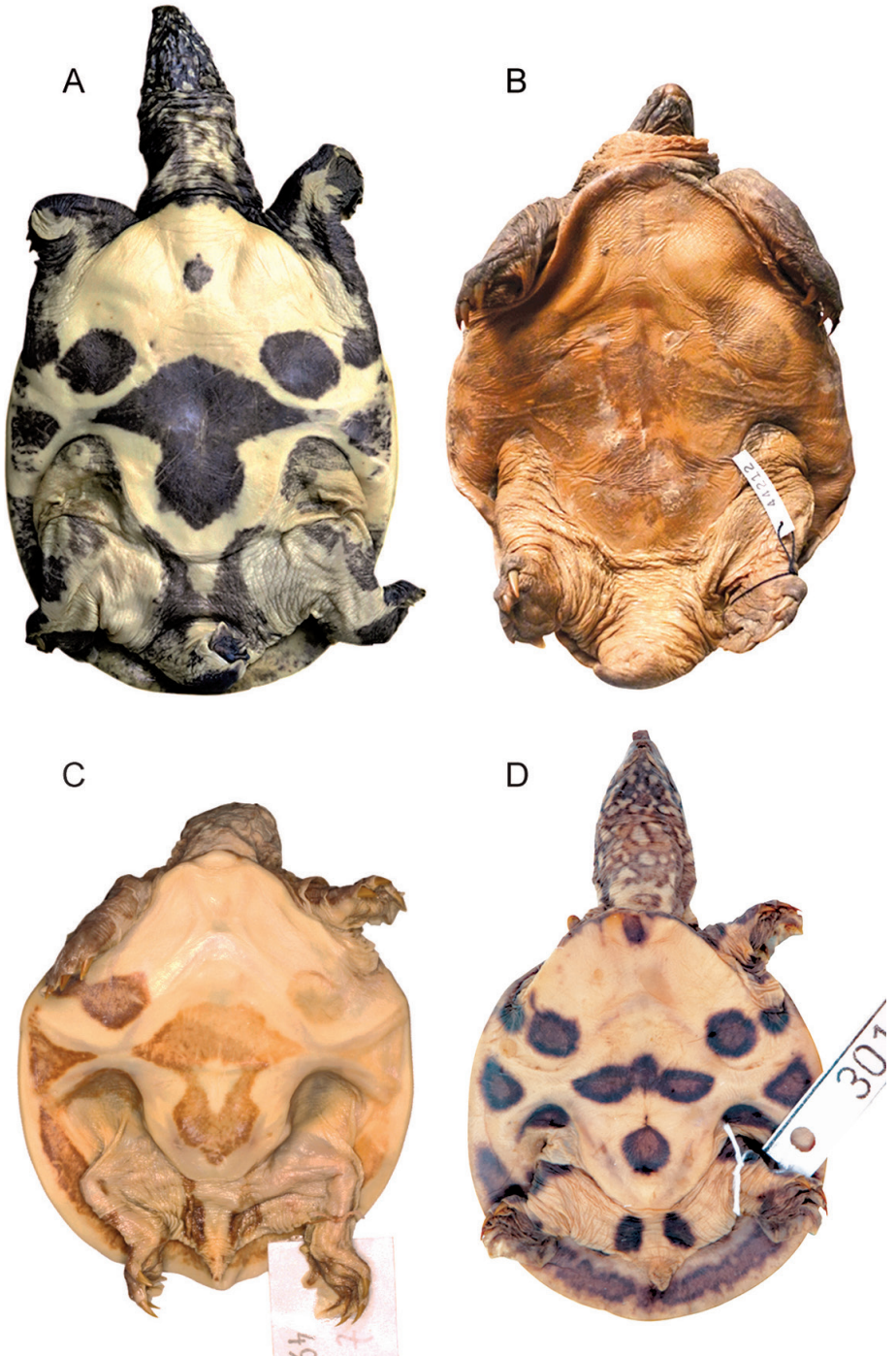


**Figure 4.** Variation in plastral ornamentation of *Pelodiscus variegatus* sp. n. **A** HNHM 2018.111.1, adult male, 109.7 mm PL **B** ZFMK 44212, adult male, 114.4 mm PL **C** juvenile, ZMB 49776, 50.0 mm PL **D** hatchling, AMNH 30125, 37.2 mm PL. Not to scale. Photographs Balázs Buzás (**A**), Balázs Farkas (**B**), Frank Tillack (**C**), Lauren Vonnahme (**D**).



**Figure 5.** Habitat of *Pelodiscus variegatus* sp. n.: Song Rac Lake, Cam Xuyen District, Ha Tinh Province, Vietnam. Photograph An Vinh Ong.

and Wanquan rivers in Hainan Province, China (own data; Fig. 6). In northeastern Vietnam the distribution area of *Pelodiscus variegatus* overlaps with that of *Palea steindachneri* (Bac Giang Province, NMW 23395, NMW 23480:2, Siebenrock 1906; Ha Tinh Province, ZFMK 81539, ZFMK 81540, Ziegler 2002; Quang Binh Province, Ziegler et al. 2004) and further south (Gong et al. 2018) with that of *Pelodiscus sinensis*, believed to have been introduced (Nguyen et al. 2009). On Hainan, *Pelodiscus variegatus* seems to be sympatric with *Pelodiscus parviformis* (vouchers NMW 30232:1–2, NMW 30232:4–8; see Remarks) and *Palea steindachneri* (NMW 20373; Siebenrock 1906). In Vietnam, most records fall within the “Northeast Lowlands Subregion” of Bain and Hurley (2011; encompassing the “Red River System” of Kottelat 1989). The zoogeographical affinities of Hainan lie also with this area (as well as mainland southwestern China), while the southern portion of the purported range forms part of the “Central–South Vietnam Lowlands Subregion” of Bain and Hurley (2011) or the “Annam River System” of Kottelat (1989).

**Etymology.** The specific epithet *variegatus* (spotted) is a Latin adjective in masculine gender alluding to the highly contrasting markings, especially the large plastral blotches, of the new species.

**Remarks.** In addition to the characters used here for diagnosing *P. variegatus*, Gong et al. (2018) described some further genetic differences to other *Pelodiscus* species.

Fritz et al. (2010) suggested that the taxon now named *Pelodiscus variegatus* resembles *P. parviformis*, prompting the TTWG (2011, 2012, 2014, 2017) to identify the *Pelodis-*

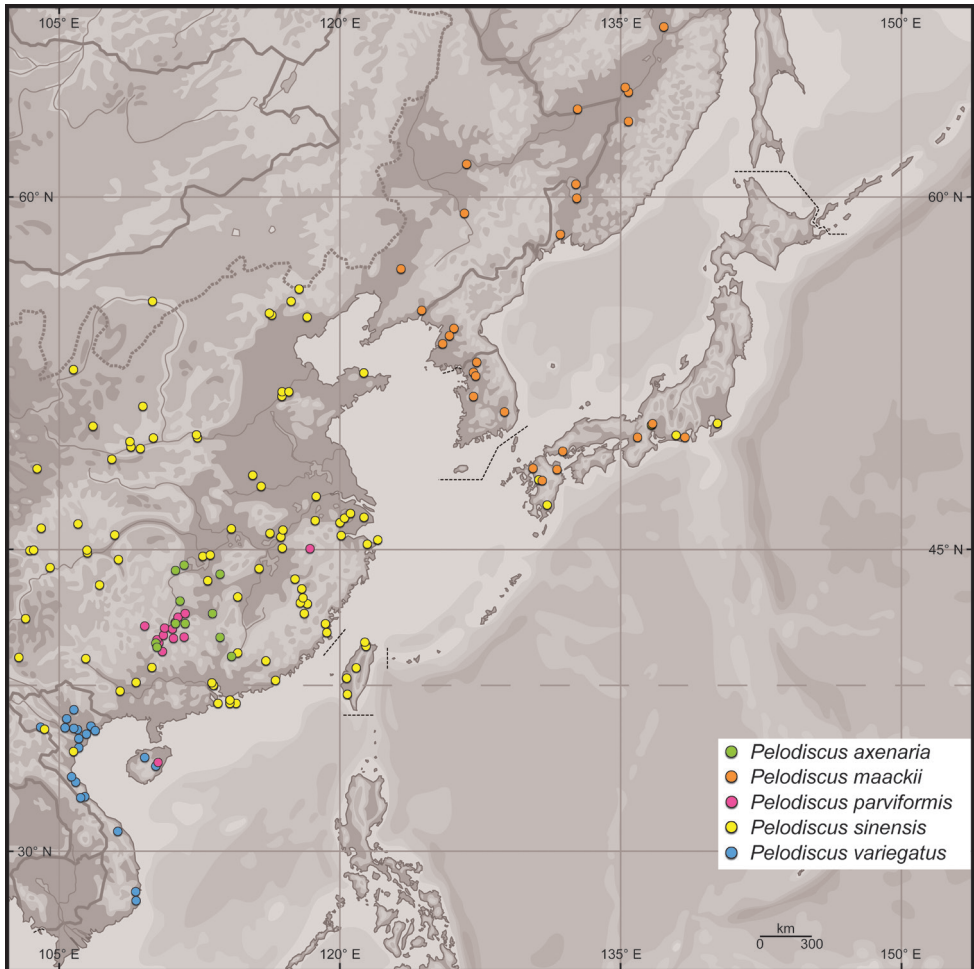


**Figure 6.** Currently known presence points of *Pelodiscus* species based on our own data as well as distribution maps published by the TTWG (2017) and Gong et al. (2018). Earlier records of *P. sinensis* from Hainan Island are referable to *P. parviformis* or *P. variegatus* sp. n. (see Remarks).

*cus* records from Vietnam with the latter species. However, as explained in Gong et al. (2018), this is no longer tenable in the face of the genetic distinctness of the two species.

Traditionally, Chinese softshell turtles from Hainan were identified as *P. sinensis* (e.g., Pope 1935; Ernst and Barbour 1989; Ernst et al. 2000; TTWG 2011, 2012, 2014, 2017). However, the few old (early 20<sup>th</sup> century) museum specimens serving as record sources represent either *P. variegatus* (AMNH 28345, AMNH 30125, FMNH 6626, FMNH 6627, MVZ 23946, NMW 30219:1, NMW 30232:3) or *P. parviformis* (NMW 30232:1–2, NMW 30232:4–8). Thus, the native occurrence of *P. sinensis* sensu stricto on Hainan seems questionable, even though this species is now most likely bred there in local farms. We cannot exclude that also some of the presence points of

*P. sinensis* from southwestern mainland China mapped by the TTWG (2017) refer to *P. parviformis* or *P. variegatus* (and in part perhaps to *P. axenaria*).

**Conservation implications.** While *Pelodiscus sinensis* is listed as “Vulnerable (VU)” by the IUCN Red List of Threatened Species (Asian Turtle Trade Working Group 2000), the conservation status of *P. axenaria*, *P. maackii*, *P. parviformis*, and now *P. variegatus*, remains unassessed, in spite of their proven genetic distinctness (Fritz et al. 2010; Yang et al. 2011; Gong et al. 2018). Given their restricted distributional ranges and the intense exploitation to which they are subjected, all these species would certainly classify for a higher category rating. In this vein, the most recent red list of Chinese vertebrates compiled by Jiang et al. (2016) proposed the conservation status of *P. axenaria*, *P. parviformis* and *P. sinensis* be upgraded to “Endangered (EN)” and indicated *P. maackii* to be “Data Deficient (DD).” Rhodin et al. (2018) suggested for *P. parviformis* “Critically Endangered (CR)” and for *P. sinensis* “Endangered (EN),” whereas *P. axenaria* and *P. maackii* were identified as “Data Deficient (DD).” Consequently, also *P. variegatus*, which was included in *P. parviformis* by Rhodin et al. (2018), should be classified as “Critically Endangered (CR).”

## Acknowledgments

Cuijuan Niu (Beijing), Marinus Hoogmoed (Belém, formerly Leiden), Carol Spencer, Mikaila Baskin (both Berkeley), Rainer Günther, Frank Tillack (both Berlin), Wolfgang Böhme, Morris Flecks (both Bonn), Judit Vörös, Viktória Szóke, Gábor Csorba (all Budapest), Alan Resetar, Joshua Mata (both Chicago), Markus Auer (Dresden), Gerold Schipper (Frankfurt am Main), Balázs Buzás (Fujairah), Truong Quang Nguyen (Hanoi), David Kizirian, David Dickey, Lauren Vonnahme (all New York), Georg Gassner, Richard Gemel, Franz Tiedemann (all Vienna), and Quang Xuan Hoang (Vinh) are acknowledged for access to collection material, providing photographs, as well as information and/or for various courtesies over the years. Anders Rhodin (Lunenburg) is thanked for his valuable comments on the first draft of this paper. Fieldwork in Vietnam was supported by the Volkswagen Foundation.

## References

- Asian Turtle Trade Working Group (2000) *Pelodiscus sinensis*. The IUCN Red List of Threatened Species 2000: e.T39620A97401140. <https://www.iucnredlist.org/species/39620/97401140>
- Bain RH, Hurley MM (2011) A biogeographic synthesis of the amphibians and reptiles of Indochina. *Bulletin of the American Museum of Natural History* 360: 1–138. <http://digitallibrary.amnh.org/handle/2246/6141>
- Brandt JF (1857) Observaciones quaedam ad generis *Trionychum* species duas novas spectantes auctore J.F. Brandt. *Bulletin de la Classe physico-mathématique de l'Académie impériale des Sciences de Saint Pétersbourg* 16: 110–111.

- Chkhikvadze VM (1987) On systematic position of the USSR Far East soft-shelled turtle. Bulletin of the Academy of Sciences of the Georgian Soviet Socialist Republic 128: 609–611. [In Russian with Georgian and English summary]
- Ernst CH, Barbour RW (1989) Turtles of the World. Smithsonian Institution Press, Washington, DC, xxii + 313 pp.
- Ernst CH, Altenburg RGM, Barbour RW (2000) Turtles of the world. Version 1.2, CD-ROM. ETI BioInformatics, Amsterdam.
- Farkas B, McCormack T (2010) Le Trionyx de Chine *Pelodiscus sinensis* (Wiegmann, 1834) (Ang: Chinese softshell turtle). Chéloniens 18: 56–63.
- Fritz U, Gong S, Auer M, Kuchling G, Schneeweiss N, Hundsdörfer AK (2010) The world's economically most important chelonians represent a diverse species complex (Testudines: Trionychidae: *Pelodiscus*). Organisms, Diversity & Evolution 10: 227–242. <https://doi.org/10.1007/s13127-010-0007-1>
- Gong S, Vamberger M, Auer M, Praschag P, Fritz U (2018) Millennium-old farm breeding of Chinese softshell turtles (*Pelodiscus* spp.) results in massive erosion of biodiversity. Science of Nature 105: 34. <https://doi.org/10.1007/s00114-018-1558-9>
- Jiang Zh, Jiang J, Wang Y, Zhang E, Zhang Y, Li L, Xie F, Cai B, Cao L, Zheng G, Dong L, Zhang Zh, Ding P, Luo Zh, Ding Ch, Ma Zh, Tang S, Cao W, Li Ch, Hu H, Ma Y, Wu Y, Wang Y, Zhou K, Liu Sh, Chen Y, Li J, Feng Z, Wang Y, Wang B, Li Ch, Song X, Cai L, Zhang Ch, Zeng Y, Meng Zh, Fang H, Ping X (2016) Red list of China's vertebrates. Shengwu Duoyangxing (Biodiversity Science) 24: 500–551.
- Kottelat M (1989) Zoogeography of the fishes from Indochinese inland waters with an annotated check-list. Bulletin Zoologisch Museum, Universiteit van Amsterdam 12: 1–53.
- Meylan PA (1987) The phylogenetic relationships of soft-shelled turtles (family Trionychidae). Bulletin of the American Museum of Natural History 186: 1–101. <http://digitallibrary.amnh.org/handle/2246/972>
- Nguyen VS, Ho TC, Nguyen QT (2009) Herpetofauna of Vietnam. Edition Chimaira, Frankfurt am Main, 768 pp.
- Pope CH (1935) The Reptiles of China – Natural History of Central Asia 10. American Museum of Natural History, New York, lii + 604 pp.
- Pritchard PCH (1979) Encyclopedia of turtles. T.F.H. Publications, Neptune, 895 pp.
- Rhodin AGJ, Stanford CB, van Dijk PP, Eiseberg C, Luiselli L, Mittermeier RA, Hudson R, Horne BD, Goode EV, Kuchling G, Walde A, Baard EHW, Berry KH, Bertolero A, Blanck TEG, Bour R, Buhlmann KA, Cayot LJ, Collett S, Currylow A, Das I, Dagne T, Ennen JR, Forero-Medina G, Frankel MG, Fritz U, García G, Gibbons JW, Gibbons PM, Gong S, Guntoro J, Hofmeyr MD, Iverson JB, Kiester AR, Lau M, Lawson DP, Lovich JE, Moll E, Páez VP, Palomo-Ramos R, Platt K, Platt SG, Pritchard PCH, Quinn HR, Rahman SC, Randrianjafizanaka ST, Schaffer J, Selman W, Shaffer HB, Sharma DSK, Shi H, Singh S, Spencer R, Stannard K, Sutcliffe S, Thomson S, Vogt RC (2018) Global conservation status of turtles and tortoises (order Testudines). Chelonian Conservation and Biology 17: 135–161. <https://doi.org/10.2744/CCB-1348.1>
- Rudolphi M, Weser R (1998) Die Weichschildkröten Nordvietnams unter besonderer Berücksichtigung der Nackendornen-Weichschildkröte, *Palea steindachneri* (Siebenrock, 1906). Sauria (Berlin) 20(1): 3–14.

- Siebenrock F (1906) Zur Kenntnis der Schildkrötenfauna der Insel Hainan. Zoologischer Anzeiger 30: 578–586.
- Stuckas H, Fritz U (2011) Identity of *Pelodiscus sinensis* revealed by DNA sequences of an approximately 180-year-old type specimen and a taxonomic reappraisal of *Pelodiscus* species (Testudines: Trionychidae). Journal of Zoological Systematics and Evolutionary Research 49: 335–339. <https://doi.org/10.1111/j.1439-0469.2011.00632.x>
- TTWG [Turtle Taxonomy Working Group] (2007) An annotated list of modern turtle terminal taxa with comments on areas of taxonomic instability and recent change. Chelonian Research Monographs 4: 173–199.
- TTWG [Turtle Taxonomy Working Group] (2011) Turtles of the world, 2011 update: Annotated checklist of taxonomy, synonymy, distribution, and conservation status. Chelonian Research Monographs 5: 165–242. <https://doi.org/10.3854/crm.5.000.checklist.v4.2011>
- TTWG [Turtle Taxonomy Working Group] (2012) Turtles of the world, 2012 update: Annotated checklist of taxonomy, synonymy, distribution, and conservation status. Chelonian Research Monographs 5: 243–328. <https://doi.org/10.3854/crm.5.000.checklist.v5.2012>
- TTWG [Turtle Taxonomy Working Group] (2014) Turtles of the world: Annotated checklist of taxonomy, synonymy, distribution with maps, and conservation status (7<sup>th</sup> edn). Chelonian Research Monographs 5: 329–479. <https://doi.org/10.3854/crm.5.000.checklist.v7.2014>
- TTWG [Turtle Taxonomy Working Group] (2017) Turtles of the world. Annotated checklist and atlas of taxonomy, synonymy, distribution, and conservation status (8<sup>th</sup> edn). Chelonian Research Monographs 7: 1–292. <https://doi.org/10.3854/crm.7.checklist.atlas.v8.2017>
- Wermuth H, Mertens R (1961) Schildkröten, Krokodile, Brückenechsen. VEB Gustav Fischer Verlag, Jena, XXVI + (1) + 422 pp.
- Wermuth H, Mertens R (1977) Liste der rezenten Amphibien und Reptilien. Testudines, Crocodylia, Rhynchocephalia. Das Tierreich 100: I–XXVII + 1–174.
- Yang P, Tang Y, Ding L, Guo X, Wang Y (2011) Validity of *Pelodiscus parviformis* (Testudines: Trionychidae) inferred from molecular and morphological analysis. Asian Herpetological Research 2: 21–29. <https://doi.org/10.3724/SPJ.1245.2011.00021>
- Zhao E, Adler K (1993) Herpetology of China. Society for the Study of Amphibians and Reptiles (Contributions to Herpetology 10), Oxford, Ohio, 521 pp.
- Zhou G, Zhang X, Fang Z (1991) Bulletin of a new species *Trionyx*. Acta Scientiarum Naturalium Universitatis Normalis Hunanensis 14: 379–382. [In Chinese with English abstract]
- Ziegler T (2002) Die Amphibien und Reptilien eines Tieflandfeuchtwald-Schutzgebietes in Vietnam. Natur & Tier Verlag, Münster, 342 pp.
- Ziegler T, Herrmann H-W, Vu NT, Le KQ, Nguyen TH, Cao XC, Luu MT, Dinh HT (2004) The amphibians and reptiles of the Phong Nha–Ke Bang National Park, Quang Binh Province, Vietnam. Hamadryad 28: 19–42.

### Supplementary material 1

#### Reference alignment of 397 bp of the 12S rRNA gene of different *Pelodiscus* species and lineages

Authors: Balázs Farkas, Thomas Ziegler, Cuong The Pham, An Vinh Ong, Uwe Fritz

Data type: molecular data

Copyright notice: This dataset is made available under the Open Database License (<http://opendatacommons.org/licenses/odbl/1.0/>). The Open Database License (ODbL) is a license agreement intended to allow users to freely share, modify, and use this Dataset while maintaining this same freedom for others, provided that the original source and author(s) are credited.

Link: <https://doi.org/10.3897/zookeys.824.31376.suppl1>

### Supplementary material 2

#### Reference alignment of the *cyt b* gene of different *Pelodiscus* species and lineages (1168 bp)

Authors: Balázs Farkas, Thomas Ziegler, Cuong The Pham, An Vinh Ong, Uwe Fritz

Data type: molecular data

Copyright notice: This dataset is made available under the Open Database License (<http://opendatacommons.org/licenses/odbl/1.0/>). The Open Database License (ODbL) is a license agreement intended to allow users to freely share, modify, and use this Dataset while maintaining this same freedom for others, provided that the original source and author(s) are credited.

Link: <https://doi.org/10.3897/zookeys.824.31376.suppl2>

### Supplementary material 3

#### Reference alignment of the partial ND4 gene and adjacent DNA coding for tRNAs (838 bp) of different *Pelodiscus* species and lineages

Authors: Balázs Farkas, Thomas Ziegler, Cuong The Pham, An Vinh Ong, Uwe Fritz

Data type: molecular data

Copyright notice: This dataset is made available under the Open Database License (<http://opendatacommons.org/licenses/odbl/1.0/>). The Open Database License (ODbL) is a license agreement intended to allow users to freely share, modify, and use this Dataset while maintaining this same freedom for others, provided that the original source and author(s) are credited.

Link: <https://doi.org/10.3897/zookeys.824.31376.suppl3>

# Two new enchytraeid species from Jeju Island, Korea (Annelida, Clitellata)

Klára Dózsa-Farkas<sup>1</sup>, Tamás Felföldi<sup>2</sup>, Hajnalka Nagy<sup>2</sup>, Yong Hong<sup>3</sup>

**1** Department of Systematic Zoology and Ecology, ELTE Eötvös Loránd University H-1117 Budapest, Pázmány Péter sétány 1/C, Hungary **2** Department of Microbiology, ELTE Eötvös Loránd University H-1117 Budapest, Pázmány Péter sétány 1/C, Hungary **3** Department of Agricultural Biology, College of Agriculture & Life Science, Chonbuk National University, Jeonju 561-756, South Korea

Corresponding author: Yong Hong ([geoworm@hanmail.net](mailto:geoworm@hanmail.net))

---

Academic editor: F. Govedich | Received 5 April 2018 | Accepted 15 October 2018 | Published 14 February 2019

<http://zoobank.org/549FF675-44A7-42FE-ADF9-74E318EE0AA5>

---

**Citation:** Dózsa-Farkas K, Felföldi T, Nagy H, Hong Y (2019) Two new enchytraeid species from Jeju Island, Korea (Annelida, Clitellata). ZooKeys 824: 87–108. <https://doi.org/10.3897/zookeys.824.25544>

---

## Abstract

The enchytraeid fauna of three areas in Jeju Island (Korea) was studied, and comparative morphological and molecular taxonomic examinations (based on CO1, ITS and H3 sequences) were performed on nine samples collected in 2016. Twenty-two enchytraeid species were recorded and identified. The descriptions of two new species (*Achaeta multisacculata* **sp. n.** and *Fridericia floriformis* **sp. n.**) are presented in this paper. The main diagnostic features of *A. multisacculata* **sp. n.** are: three pairs of pyriform glands per segment, clitellum with two “baguette-like” packages of glands, dorsal blood vessel from VII, secondary pharyngeal glands absent, oesophageal appendages well developed, two pairs of preclitellar nephridia, the reproductive organs (except the spermathecae in V) shifted one segment forward. The main features of *F. floriformis* **sp. n.** are that they are large worms, have up to 2–4 chaetae in bundles, strong body wall, thick cuticle, five pairs of preclitellar nephridia, c-type coelomo-mucocytes sometimes with some refractile vesicles, chylus cells in XII–XV, sperm funnels approximately twice as long than wide, spermathecae with long ectal duct without glands, ampullae surrounded distally by about 9–12 sessile diverticula of varying size. Molecular phylogenetic analyses supported the morphological results and confirmed the status of the two new species.

## Keywords

*Achaeta multisacculata*, Enchytraeidae, *Fridericia floriformis*, molecular analysis, new species

## Introduction

The investigation of the previously unknown enchytraeid fauna of Korea has been continuing since 2007. Results have been published in four previous papers that yielded a total of 19 species new to science (Dózsa-Farkas and Hong 2010; Christensen and Dózsa-Farkas 2012; Dózsa-Farkas et al. 2015; Dózsa-Farkas et al. 2018). For Jeju Island, the fauna of Hallasan National Park (Mount Hallasan) was studied and published separately (Dózsa-Farkas et al. 2018). In this paper, further faunistic results from the lowland areas of Jeju Island, outside the Hallasan National Park, are presented, including two new species. The morphological studies are supplemented with molecular taxonomic analyses targeting the mitochondrial cytochrome c oxidase subunit 1 (CO1) gene, the nuclear ribosomal ITS region and the nuclear histone 3 (H3) gene, as in earlier studies (Dózsa-Farkas et al. 2015, 2018). For this, morphologically similar species and species described previously from Korea have been selected.

## Materials and methods

### Study sites

Jeju Island (Jeju Province) encompasses 1,848 km<sup>2</sup> and is the largest island in South Korea. It was formed by volcanic eruptions approximately 2 million years ago. The center of its area is occupied by Mt. Hallasan. The island has a humid subtropical climate, making it warmer than the rest of South Korea. Winters are cool and dry while summers are hot, humid, and sometimes rainy. One of our study areas, Jocheon-eup, is a wetland and currently a candidate for designation as a Ramsar Wetland City, while the two other areas have relatively stronger human impact, being both popular sites for tourists.

The three study areas and nine sites within these areas are listed below. All samples were collected in 2016 by Yong Hong, similarly as in our parallel study regarding Mt. Hallasan (Dózsa-Farkas et al. 2018).

#### Area I: Dongbaekdongsan, Jocheon-eup

1. Loamy soil and litter layers in *Camellia japonica* forest (33.50925°N; 126.72014°E; 185 m asl.), 18 Aug 2016
2. Loamy soil and leaf litter in *C. japonica* forest (33.50911°N; 126.72086°E; 181 m asl.), 18 Aug 2016.
3. Clayey soil, arboreal, under *C. japonica* (33.51831°N; 126.71492°E; 150 m asl.), 18 Aug 2016.
4. Silty soil and leaf litter in *C. japonica* forest (33.51831°N; 126.71081°E; 137 m asl.), 18 Aug 2016.

## Area II: Seongsan Ilchulbong Tuff Cone, Seongsan-eup, Seogwipo-si

5. Loamy soil under *Euonymus japonicus* (33.45972°N; 126.94056°E; 129 m asl.), 29 Sept 2016.
6. Clayey soil and leaf litter under *E. japonicus* (33.46008°N; 126.93789°E; 66 m asl.), 29 Sept 2016.
7. Loamy soil and litter layers under *E. japonicus* (33.46192°N; 126.93511°E; 16 m asl.), 29 Sept 2016.

## Area III: Yongnuni-orum, Gujwa-eup

8. Clayey soil at the bottom of the dormant crater, meadow (33.45859°N; 126.83192°E; 193 m asl.), 26 Oct 2016.
9. Clayey soil, meadow (33.45895°N; 126.83276°E; 207 m asl.), 26 Oct 2016.

**Methods of morphological examination**

Soil samples were refrigerated until processing. Worms were extracted from the soil by the wet funnel method (O'Connor 1962). Enchytraeids were first observed and measured alive, and subsequently fixed in 70% ethanol. Some of the fixed specimens were stained with borax-carmin, and then passed through an ethanol dehydration series (from 70% to absolute), mounted temporarily in clove oil, then permanently in Euparal between two coverslips. Hence the worms were observable from both sides (Schmelz 2003). All the important morphological characters were recorded in vivo, drawn and photographed [Axio Imager.A2 microscope with DIC (differential interference contrast) illumination, AxioCam MRc 5 (Zeiss) digital camera, Axiovision software]. The whole-mounted specimens were reexamined and photographed as well. In all micrographs presented in this study, the orientation of specimens is the same: the head is either on the left side or at the top of the picture.

The holotypes and two paratypes are deposited in the National Institute of Biological Resources, Korea (NIBRIV). The remaining paratypes ("P", together with slide numbers) and further studied materials are deposited at the Department of Systematic Zoology and Ecology, ELTE Eötvös Loránd University, Hungary.

**Methods of molecular analysis**

Genomic DNA was extracted with the DNeasy Blood & Tissue Kit (Qiagen) according to the instructions given by the manufacturer. CO1, H3 genes and the ITS region were amplified separately by PCR using the primer pairs HCO2198 (5'-TAA ACT TCA GGG TGA CCA AAA AAT CA-3') and LCO1490 (5'-GGT CAA CAA ATC ATA AAG ATA TTG G-3') (Folmer et al. 1994), H3a-F (5'-ATG GCT CGT ACC

AAG CAG ACV GC-3') and H3a-R (5'-ATA TCC TTR GGC ATR ATR GTG AC-3') (Colgan et al. 1998), ETTS1 (5'-TGC TTA AGT TCA GCG GGT-3') and ETTS2 (5'-TAA CAA GGT TTC CGT AGG TGA A-3') (Kane and Rollinson 1994), respectively. PCRs, sequencing and phylogenetic analyses were performed as described in detail previously by Dózsa-Farkas et al. (2015). Briefly, Sanger sequencing was carried out by the LGC Genomics GmbH (Berlin, Germany), while phylogenetic analyses including the search for the best-fit model were performed with the MEGA 7 software (Kumar et al. 2016). The obtained sequences were deposited in GenBank under the following accession codes: MH124584-MH124596 (CO1), MH124597-MH124605 (H3), and MH128727-MH128735 (ITS).

## Results

### Morphological results

In total, 22 enchytraeid species belonging to seven genera were found in the samples (Table 1), among which two are new to science: *Achaeta multisacculata* sp. n. and *Friedericia floriformis* sp. n. With the two new species described here, the Korean fauna consists of 36 recorded terrestrial enchytraeid species to date. Additionally, one terrestrial polychaete, *Hrabeiella periglandulata* Pižl & Chalupský, 1984, was recorded at site 8.

### Description of the new species

#### *Achaeta multisacculata* sp. n.

<http://zoobank.org/BB0641AE-3012-4D55-B23E-455AF235ED33>

Figs 1A–D, 2, 3

**Type locality.** Clayey soil, meadow (site 9), Yongnuni-orum, Gujwa-eup, Jeju Island, South Korea.

**Holotype.** NIBRIV0000813658, slide No. 2329, adult, stained whole mounted specimen, collected on 26 Oct 2016 by Y. Hong. **Paratypes.** In total six stained adult and one subadult specimens on slides, coll. Y. Hong. NIBRIV0000813659, slide No. 2459 and NIBRIV0000813660, slide No. 2462 from type locality. P.120.1–P.120.4, slides No. 2305, 2460, 2478, 2482 from type locality. P.120.5, subadult specimen, slide No. 2464, site 8 (clayey soil at the bottom of the dormant crater, meadow; 33.45859°N; 126.83192°E; 193 m asl.), 26 Oct 2016. **Further material examined.** Two specimens for DNA analysis and four subadults and six juvenile specimens only in vivo.

**Diagnosis.** The new species can be recognized by the following combination of characters: (1) small, slender worms (2.5–4.2 mm long and 160–220 µm wide at clitellum in vivo), segments 25–31; (2) six pyriform glands per segment in general; (3)

**Table 1.** Detected enchytraeid species (and the polychaeta) and their distribution at the study sites. New species described here are highlighted in bold, while new species from Jeju Island described earlier in a previous paper (Dózsa-Farkas et al. 2018) are marked with an asterisk, species new to science from Korea with #.

Species site code	Dongbaekdongsan, Jocheon-eup 18.08.2016				Seongsan Ilchulbong Tuff Cone 29.09.2016			Youngnuni- orum, Jeju 26.10.2016	
	1	2	3	4	5	6	7	8	9
<i>Achaeta macroampullacea</i> Dózsa-Farkas et al., 2018 *,#								+	+
<b><i>Achaeta multisacculata</i> sp. n.</b>								+	+
<i>Enchytraeus buchholzi</i> Vejdovsky, 1878 <i>sensu lato</i>	+				+	+	+	+	+
<i>Enchytraeus christenseni</i> Dózsa-Farkas, 1992						+	+		
<i>E. dichaeus</i> Schmelz & Collado, 2010								+	+
<i>Fridericia cusnicaformis</i> Dózsa-Farkas et al., 2015 *,#									+
<i>Fridericia</i> cf. <i>sphaerica</i> Dózsa-Farkas et al., 2015 *,#						+			
<i>Fridericia seoraksani</i> Christensen & Dózsa-Farkas, 2012 #								+	
<i>Fridericia bulboides</i> Nielsen & Christensen, 1959								+	
<i>Fridericia</i> sp.					+				
<i>Fridericia granulocyta</i> Dózsa-Farkas et al., 2015 *,#					+	+	+		
<i>Fridericia</i> cf. <i>paroniana</i> Issel, 1904								+	
<b><i>Fridericia floriformis</i> sp. n.</b>								+	+
<i>Hemienchytraeus jeonjuensis</i> Dózsa-Farkas & Hong, 2010 #	+	+			+				
<i>Hemienchytraeus quadratus</i> Dózsa-Farkas & Hong, 2010 #	+	+	+	+					
<i>Hemienchytraeus koreanus</i> Dózsa-Farkas & Hong, 2010 #	+								
<i>Hemifridericia parva</i> Nielsen & Christensen, 1959						+			
<i>Henlea</i> cf. <i>ventriculosa</i> (Udekem, 1854)					+	+	+	+	
<i>Henlea perpusilla</i> Friend, 1911									+
<i>Xetadrilus jejuensis</i> Dózsa-Farkas et al., 2018 *,#		+						+	
<i>Xetadrilus aphanoides</i> Dózsa-Farkas et al., 2018 *,#		+							
<i>Xetadrilus aphanus</i> Schmelz et al., 2011		+							
<b>Enchytraeid species number (total: 22)</b>	4	5	1	1	5	6	4	10	7
<i>Hrabeiella periglandulata</i> Pižl & Chalupsky, 1984								1	

clitellum weakly developed, interrupted middorsally and midventrally, with two elongate, “baguette-like” packages of gland cells on each dorso-lateral side; (4) dorsal blood vessel from VII; (5) pharyngeal glands at 4/5–6/7 connected dorsally, with ventral lobes and no secondary glands; (6) two pairs of preclitellar nephridia; (7) pars tumida of midgut from XII–XVI, extending over 2–3 segments, circumferal; (8) sperm funnels small, barrel-shaped, collar well developed about as wide as funnel body; (9) male pores in XI, ventro-lateral, each pore surrounded by small inconspicuous glands; (10) spermathecae free, confined to V with an asymmetrical dilation of ampulla and the ental tube ending in an oval reservoir.

**Description.** Small, slender worm (Fig. 2E). Holotype (fixed) 3.2 mm long, 190 µm wide at VIII and 200 µm wide at clitellum (fixed), 31 segments. Paratypes 2.5–4.2 mm long, 155–200 µm wide at VIII and 160–220 µm wide at clitellum in vivo; 2.4–3.6 mm long, 150–210 µm wide at VIII and 160–210 µm wide at clitel-

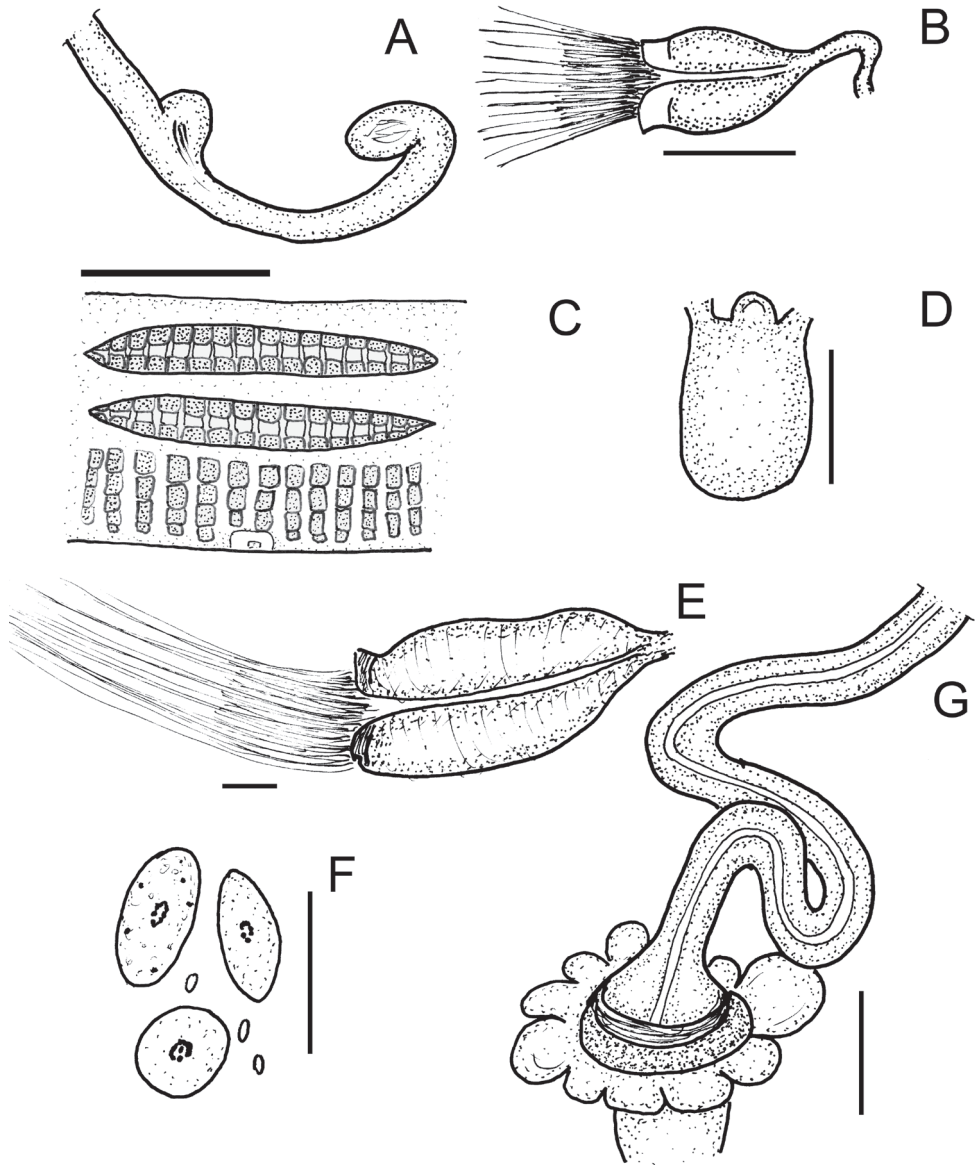


**Figure 1.** **A–D** *Achaeta multisacculata* sp. n.: **A** Spermatheca **B** Sperm funnel **C** Clitellar glands, lateral view (glands middorsally and midventrally absent; two “baguette-like” packages of gland cells dorso-laterally, granular gland cells in transverse rows latero-ventrally) **D** Brain **E–G** *Fridericia floriformis* sp. n.: **E** Sperm funnel **F** Coelomocytes **G** Spermatheca.

lum when fixed; segments 25–31. Head pore on prostomium (Fig. 3A). Clitellum in XI–1/2 XII weakly developed, gland cells absent dorsally and ventrally, laterally cells in transverse rows (Figs 1C, 2G, H). On each side dorso-laterally two elongate, baguette-like packages of swollen gland cells (in the middle hyalocytes, on the two margins granulocytes) narrowing at both ends (Figs 1C, 2G, I), length of baguette

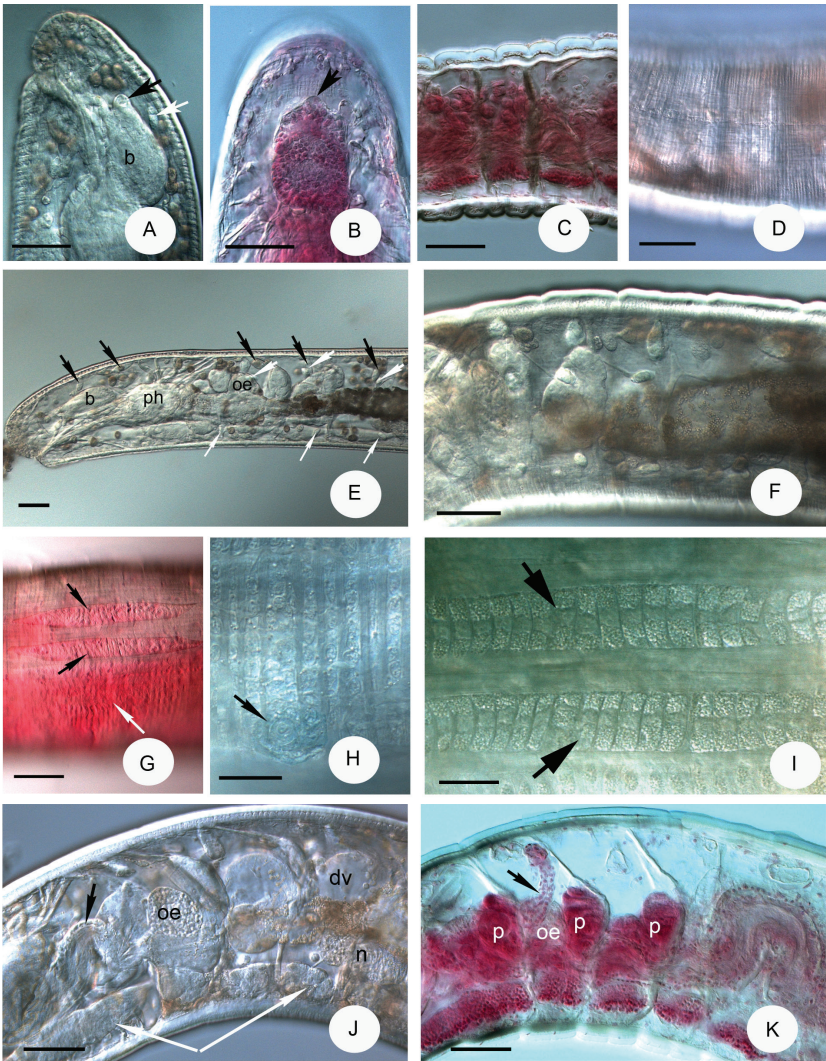


**Figure 2.** Micrograph of *Achaeta multisacculata* sp. n. **A** Head lateral view (b = brain, knob on brain marked with black arrow, first dorsal pyriform glands marked with white arrow) **B** Brain dorsal view (knob on brain marked with arrow) **C** Cuticle thicker dorsally than ventrally, lateral view **D** Transverse body wall striation by strong ring muscles **E** Forepart of body to VII, lateral view (b = brain, ph = pharynx, oe = oesophageal appendages, dorsal pyriform glands marked with black arrows, lateral pyriform glands marked with wider white arrows, ventral pyriform glands marked with narrower white arrows) **F** Pyriform glands in IV–IX lateral view **G** Clitellar glands of holotype, lateral view (dorso-laterally 2 elongate, “baguette-like” packages of hyalocytes marked with black arrows, granulocytes ventro-laterally marked with white arrow) **H** Granular clitellar glands in transverse rows ventrally, lateral view (male openings marked with arrow) **I** Two baguette-like packages of clitellar glands (marked with arrows, in the middle hyalocytes, on the margins granulocytes) **J** Segments III–VIII, lateral view (oe = oesophageal appendages with meandering canal, marked with black arrow, dv = origin of dorsal vessel, n = first nephridium, ganglia of ventral nerve cords marked with white arrows) **K** Segments IV–VIII of paratypes NIBRIV0000813659, No. 2459 lateral view (p = pharyngeal glands, oe = oesophageal glands, spermatheca marked with arrow) **A, D–F, H–J** in vivo, **B–C, G, K** fixed, stained. Scale bars: 50  $\mu$ m, in **H, I**: 20  $\mu$ m.

190–270  $\mu\text{m}$  and width 21–26  $\mu\text{m}$  in the middle in vivo (100–180  $\mu\text{m}$  and 20–25  $\mu\text{m}$  in fixed specimens, respectively). Spermathecal pores at 4/5 in lateral position. Male pores in XI (Fig. 2H).

Body wall in vivo 10–21  $\mu\text{m}$  with cuticle 5–9  $\mu\text{m}$  thick dorsally and 3–5  $\mu\text{m}$  thick ventrally (Fig. 2C). Ring muscles strong, resulting in transverse body wall striation (Fig. 2D). Septa 4/5–7/8 thickened (Fig. 2K). Frontal prostomial epithelium thickened ventrally. Pyriform epidermal glands (Fig. 2E, F) generally 3 pairs in dorsal, lateral and ventral position in each segment (XI also), sometimes difficult to observe or lateral, and ventral pairs absent: size variable, dorsal pairs largest, from II onwards, length 17–18  $\mu\text{m}$  at II, 22–40  $\mu\text{m}$  preclitellarly, 26–54  $\mu\text{m}$  in the middle of body 22–26  $\mu\text{m}$  posteriorly in vivo: lateral and ventral pairs from III onwards, length in vivo 11–25  $\mu\text{m}$  and 11–18  $\mu\text{m}$  preclitellarly, 21–24 and 15–17  $\mu\text{m}$  in the middle of body, 19–25 and 12–20  $\mu\text{m}$  posteriorly, respectively, but size subequal when fixed.

Brain posteriorly rounded, anteriorly convex with a conspicuous knob, 77–90  $\mu\text{m}$  long, 1.6–1.8 times longer than wide in vivo (Figs 1D, 2A) (70–95  $\mu\text{m}$  long and 1.5 times longer than wide, fixed, Fig. 2B). Suboesophageal ganglion of ventral nerve cord in II–IV undivided, posterior ganglia segmental and separate (Fig. 2J). Two small paired post-pharyngeal bulbs present. All pharyngeal glands at 4/5–6/7 united dorsally and with ventral lobes (Fig. 2K): first pair of glands largest, no secondary glands. Two pairs of preclitellar nephridia at 7/8–8/9 slightly constricted by septa: length ratio anteseptale : postseptale 1 : 2–3 preclitellarly, postseptale bent and tapering gradually into efferent duct, with small terminal vesicle (Fig. 3B). About 6 pairs of postclitellar nephridia (Fig. 3C) from 19/20. Dorsal blood vessel from VII (Fig. 2J), often with intensive pulsation in VII and VI, blood colourless. Coelomocytes disc-like, with fine granules, dark brown with clear nucleus, about 15–30  $\mu\text{m}$  long in vivo (Fig. 3E, F) (12–16  $\mu\text{m}$ , fixed). One pair of oesophageal appendages well developed dorso-laterally in V, with meandering canal in IV (Fig. 2E, J, K), clearly visible only in live worms (Fig. 3D). Chloragocytes brown, about 10–13  $\mu\text{m}$  long in vivo. Midgut pars tumida inconspicuous, circumferal (i.e., not confined to ventral region of intestine), in XII–XVI (occupying 2–3 segments). Pygidium short, anal muscles developed (Fig. 3G).

Sperm funnels small, mostly barrel-shaped, 42–65  $\mu\text{m}$  long in vivo (26–42  $\mu\text{m}$ , fixed), about 1.5–2 times longer than wide, collar distinct 8–10  $\mu\text{m}$  high, about as wide as diameter of funnel body (Figs 1B, 3H–J). Sperm ducts about 6  $\mu\text{m}$  thick in vivo (4–5  $\mu\text{m}$ , fixed). Spermatozoa with unusual strong tails (Fig. 3H), 50–70  $\mu\text{m}$  long, heads 15–22  $\mu\text{m}$  long in vivo (26–42  $\mu\text{m}$  and 11–14  $\mu\text{m}$ , fixed). Seminal vesicle absent. Male copulatory organs small oval, widely separated ventro-laterally, pore surrounded by small inconspicuous glands (Fig. 2H). Spermathecae free, confined to V (in one case extending into VI in vivo and in one case bent backwards into IV (slide 2478) (Fig. 3M). Ectal ducts 30–32  $\mu\text{m}$  long and 14–16  $\mu\text{m}$  wide in vivo (31–42  $\mu\text{m}$  long and 9–10  $\mu\text{m}$  wide, fixed), ducts slightly widen out to a dilation of ampullae with a diverticulum-like protrusion (dilation diameter 20–25  $\mu\text{m}$ ). After dilation, ental tubes (about 40–65  $\mu\text{m}$  long and 20  $\mu\text{m}$  wide) end in an elongated reservoir

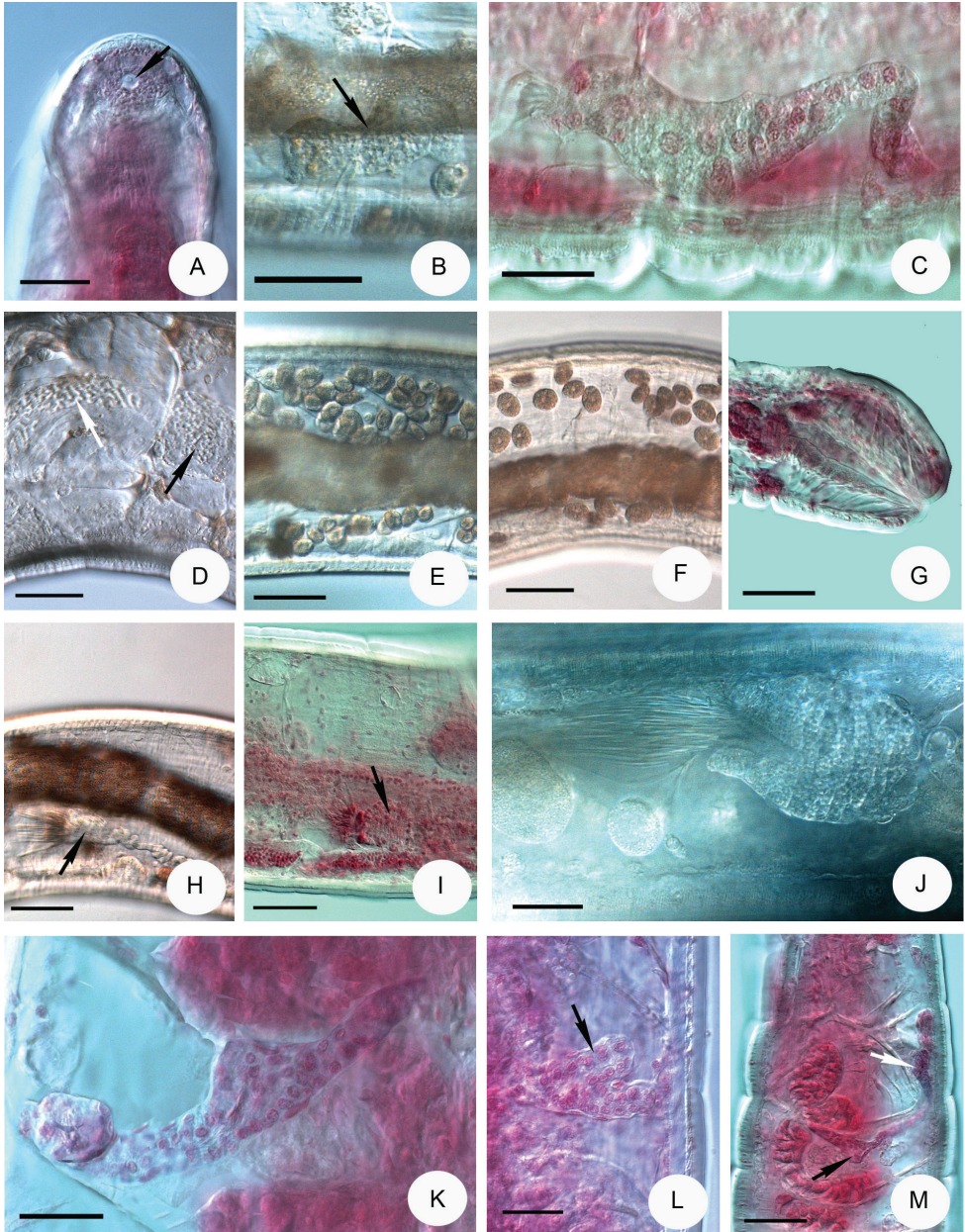


**Figure 3.** Micrograph of *Achaeta multisacculata* sp. n. **A** Head pore dorsal view (marked with arrow) **B** Preclitellar nephridia at 8/9 (marked with arrow) **C** Last nephridia at 26/27 of paratype P.120.2, No. 2460 **D** Oesophageal appendages in V (marked with black arrow), meandering canal in IV (marked with white arrow) **E–F** Coelomocytes **G** Pygidium, the anal muscles well developed **H–J** Sperm funnels **K–L** Spermathecae of paratype NIBRIV0000813659, No. 2459 (the diverticulum-like dilation of ampulla marked with arrow in L) **M** Spermatheca of paratype P.120.3 slide No. 2478 (here the ental reservoir bent back into IV marked with arrow). **B, D–E, G, I, J** in vivo **A, C, F, H, J–L** fixed, stained. Scale bars: 50  $\mu\text{m}$ , in **H, I**: 20  $\mu\text{m}$ .

(24–45 µm long, 15–26 µm wide in vivo) (20–27 µm long and 13–18 µm wide, fixed) (Figs 1A, 3K–M).

Although the specimens are adult, the clitellar glands appear weakly developed. The reason is that this organ is fully developed only just before the release of an egg (as was remarked by Schmelz et al. 2008), and indeed our worms did not have mature eggs.

**Etymology.** Named after the high number of ‘pyriform glands’ (*sacculus* = saccule, Latin).

**Molecular data.** Sequences deposited in GenBank: MH128727–MH128728 (ITS), MH124584–MH124585 (CO1).

**Distribution.** In South Korea, at sites 8–9, Jeju Island, Yongnuni-orums, clayey soil, meadows.

**Morphologically similar species.** Two *Achaeta* species with six pyriform glands per segment have been previously described: the European *Achaeta aberrans* Nielsen & Christensen, 1961 and the South American *Achaeta piti* Bittencourt, 1974, emended Schmelz et al. 2008. The new species can be easily distinguished from *A. aberrans* which has fewer segments, 20–23 (vs. 26–31 in the new species), dorsal vessel originating in VI (vs. in VII), oesophageal appendages small and only in V (vs. well developed in IV–V), male opening in XII (vs. in XI), coelomocytes oval, finely granulated and at one end tapering into a thin process (vs. discoid and brown), the preclitellar nephridia in 6/7 and 7/8 (vs. 7/8 and 8/9), the spermathecae, when present, with laterally symmetrical ampullae. The other species, *A. piti* is very similar to *A. multisacculata* sp. n., because of the reproductive organs (except the spermathecae) shifted one segment forward, the oesophageal appendages well developed with canal in IV–V, two pairs of nephridia in 7/8–8/9, dorsal blood vessel origin in VII and the spermatheca with ectal asymmetry. In addition, in both species two elongate, dorso-lateral „baguette-like” packages of hyalocytes occur in the clitellum. Characters that differentiate *A. multisacculata* sp. n. from *A. piti* are: (1) body size slightly smaller: 2.5–4.2 mm in vivo and 2.2–3.6 mm, fixed, 160–220 µm wide at clitellum [according to Schmelz et al. 2008, live *A. piti* worms are ca. 5 mm long and 150 µm wide in vivo (fixed type specimens are 3.5–5 mm long, 190 µm wide and specimens at Zoological Museum in Hamburg even longer, 4.5–6.5 mm and up to 250 µm wide)]; (2) segment number smaller, 26–31 (vs. 31–36); (3) brain anteriorly with a conspicuous knob (vs. without knob); (4) coelomocytes dark brown, 15–30 µm long (vs. pale, 15–18 µm long, cells somewhat darker than coelom); (5) sperm funnel smaller, mostly barrel-shaped, without vesicles, 42–65 µm long in vivo, 26–42 µm, fixed, only 1.5–2 times longer than wide (vs. cylindrical, with large vesicles, ca. half as long as body diameter, more than 3 times longer than wide); (6) pars tumida of midgut at XII–XVI, 2–3 segments long (vs. XX–XXIV); (7) in pygidium anal muscles clearly visible (vs. not strongly developed); (8) spermatheca similar but except one specimen always confined in V (vs. ampulla extending into VI or VII).

***Fridericia floriformis* sp. n.**

<http://zoobank.org/1A44BB5D-9D8D-49B2-BCAD-E86D27A7B5AA>

Figs 1E–G, 4–5

**Type locality.** Clayey soil, meadow (site 9), Yongnuni-orums, Gujwa-eup, Jeju Island, South Korea.

**Holotype.** NIBRIV0000813661, slide No. 2437, adult, not stained, whole mounted specimen, collected on 26 Oct 2016 by Y. Hong.

**Paratypes.** In total 18 adult stained and not stained specimens on slides and eight specimens in 70% ethanol, coll. Y. Hong. NIBRIV0000813662, slide No. 2293, DNA 1133, adult stained, whole mounted specimen from type locality. NIBRIV0000813663, slide No. 2427, from site 8 (clayey soil at the bottom of the dormant crater, meadow; 33.45859°N; 126.83192°E; 193 m asl.), 26 Oct 2016. P.121.1–P.121.14, slides No. 2291, 2314, 2332–2333, 2389, 2428–2432, 2436, 2438, 2440, 2481 from type locality. P.121.15–121.17, slides No. 2295, 2434, 2439 from site 8 (four specimens: slide 2434, 2436, 2438 and 2481 were not stained). P.121.18, five specimens in 70 % ethanol from type locality; and P.121.19, three specimens in 70 % ethanol from site 8.

**Further material examined.** Four juvenile and five adult specimens only in vivo (one of the whole, adult specimens was processed with molecular analysis, DNA 1136). One additional specimen in vivo and for molecular analysis (DNA 1088) from Mt. Hallasan, Jeju Island (Gwaneumsa trail, 33.41667°N, 126.55000°E, 634 m asl., 26 Oct 2016, coll. Y. Hong), referred as '*Fridericia* sp. 2' in Dózsa-Farkas et al. (2018).

**Diagnosis.** The new species can be recognized by the following combination of characters: (1) large size (body length 14–20.5 mm in vivo), segments 48–65; (2) lateral chaetae often absent, maximum 2 per bundle, ventrally maximum 3–4 chaetae per bundle; (3) clitellum well developed, between bursal slits and before the male apparatus only granulocytes; (4) body wall strong and cuticle thick (3–5 µm); (5) five preclitellar pairs of nephridia; (6) coelomo-mucocytes c-type occasionally with some refractile vesicles, lenticytes scarce and small; (7) dorsal vessel from XV–XVIII; (8) chylus cells in XII–XV, occupying 2–3 segments; (9) bursal slit longitudinal slightly bent, with small transverse extensions; (10) seminal vesicle not brown; (11) subneural glands absent; (12) sperm funnel approximately as long as half body diameter, collar narrower than funnel diameter, spermatozoa 400–580 µm long, heads 100–150 µm in vivo; (13) spermatheca with 9–12 sessile diverticula of varying size mostly without sperm in them, ectal duct long without ectal glands and ampulla entally openings separately into oesophagus.

**Description.** Large, whitish, stiff worms. Holotype 15.3 mm long, 470 µm wide at VIII and 550 µm at the clitellum (fixed), 59 segments. Body length of the paratypes 14–20.5 mm, width 400–530 µm at VIII and 500–640 µm at the clitellum in vivo. Length of fixed specimens 8–17.3 mm, width 470–580 µm at VIII and 500–620 µm at the clitellum. Segments 48–65. Chaetal formula: 1,2,(0) – 2,0,1,2 : 2,3,4 –

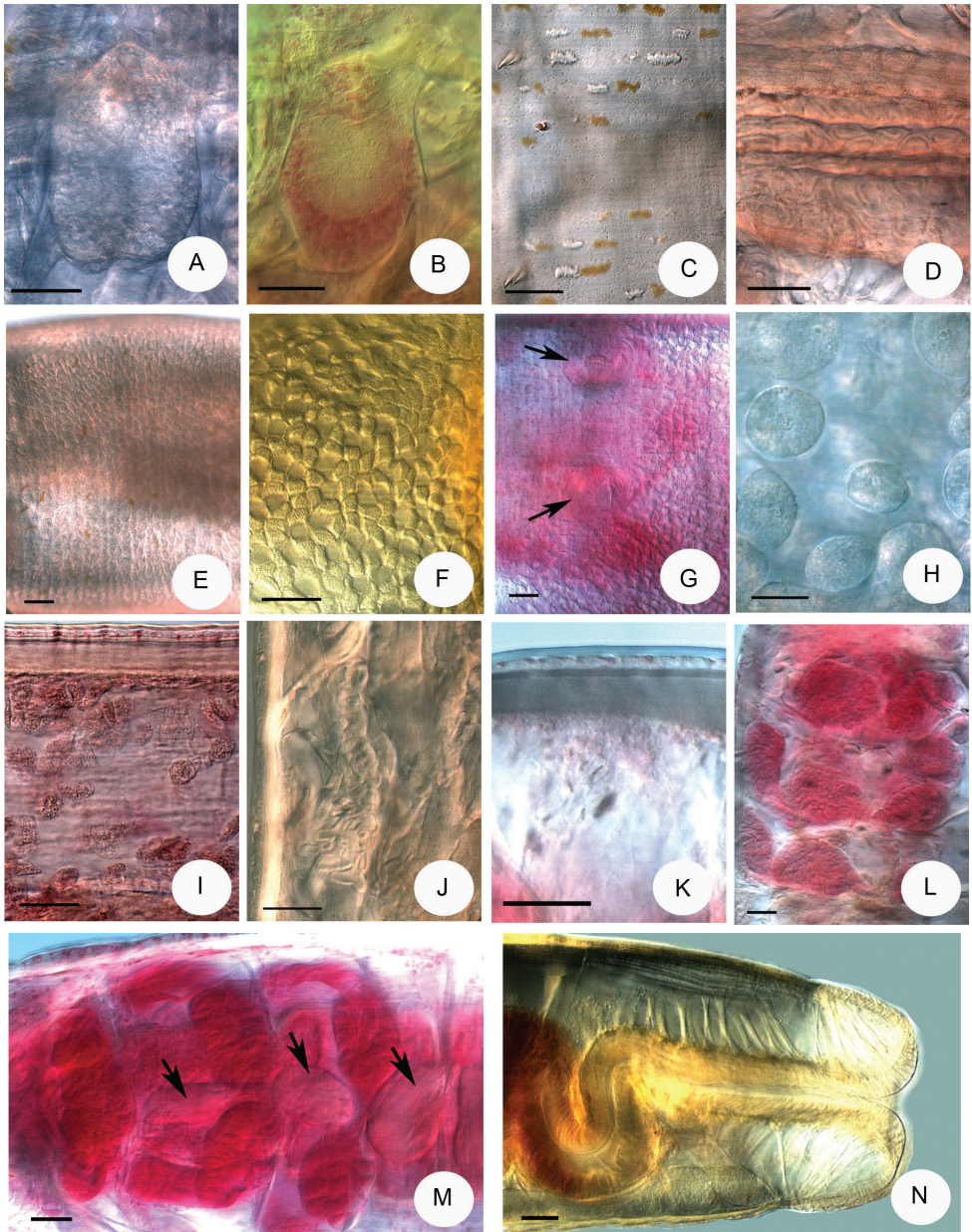


**Figure 4.** Micrograph of *Fridericia floriformis* sp. n. **A–B** Brain (**B** paratype P. 121.4, slide 2389) **C** Epidermal glands **D** Chylus cells in XII **E–F** Clitellar glands dorsal view **G** Clitellar glands ventrally, male copulatory organs of paratype P.121.7 slide No. 2429 (marked with arrows) **H–I** Coelomocytes **J** Oesophageal appendage **K** Body wall with strong longitudinal muscles and cuticle **L–M** Pharyngeal glands (**L** paratype P. 121.15 slide No. 2295 **M** paratype P121.8 slide No. 2430 dorsal vessel marked with arrows) **N** Pygidium with well-developed anal muscle, paratype 121.12 slide No. 2438. **A**, **C–E**, **H**, **J** in vivo **B**, **G**, **I**, **K–M** fixed, stained **F**, **N** fixed, not stained. Scale bars: 50  $\mu$ m, in **H**: 20  $\mu$ m.

(4),3,2,1. The inner chaetae being shorter and thinner than the outers:  $30\text{--}35 \times 2.5\text{--}3 \mu\text{m}$  and  $54\text{--}63 \times 5\text{--}6 \mu\text{m}$  (in preclitellar bundles). In the bundles with 2 chaetae the length of chaetae is different, in those with 3 chaetae one chaeta longer and the other two shorter. After the clitellum in lateral bundles of the middle part of body the chaetae mostly absent but at posterior body-end again occur 1 or 2 chaetae per bundle, length about  $59\text{--}63 \times 4.5\text{--}7 \mu\text{m}$ . Head pore at 0/I. Dorsal pores from VII; 2–3 transverse rows of hyaline epidermal gland cells per segment and in addition more transverse rows of dark yellow glands (visible only in vivo) (Fig. 4C). Clitellum in XII–1/2XIII, well developed, girdle-shaped, hyalocytes and granulocytes arranged in indefinite rows or reticulate pattern (Fig. 4E, F), between bursal slits and before the male apparatus only granulocytes (Fig. 4G). Body wall strong, thickness about  $40\text{--}54 \mu\text{m}$ , cuticle thick about  $3\text{--}5 \mu\text{m}$  in vivo and fixed (Fig. 4I, K), in forepart slightly stronger than at the body end.

Brain egg-shaped, about  $140\text{--}180 \mu\text{m}$  long, about 1.5–2 times longer than wide in vivo (Fig. 4A) and  $120\text{--}150 \mu\text{m}$  long and 1.4–1.7 times longer than wide in the fixed specimens (Fig. 4B). Oesophageal appendages long with many branches at the end in V (Fig. 4J). All pharyngeal glands with ventral lobes, those in 4/5 united dorsally, those in the 5/6 weakly united or unconnected dorsally and those in 6/7 unconnected dorsally but occasionally weakly united (Fig. 4L, M). All septa at 5/6–9/10 thickened. At anal region the radial gut dilator muscles well developed (Fig. 4N). Chloragocytes from V,  $12\text{--}26 \mu\text{m}$  long in vivo. Dorsal vessel from XV–XVIII, (in one case in XIX), blood colourless. Midgut pars tumida in XXVI–XXXII occupying 4–7 segments (only in two specimens were visible). Five pairs of preclitellar nephridia from 6/7 to 10/11, length ratio anteseptale : postseptale 1 : 2–2.5, adseptal origin of the efferent duct. Coelomo-mucocytes c-type, rounded or elliptic, sometimes with some refractile vesicles, length  $28\text{--}44 \mu\text{m}$  in vivo (Figs. 1F, 4H), in the fixed worms with granules and  $15\text{--}28 \mu\text{m}$  long (Fig. 4I). Lenticytes scarce, small  $4\text{--}7 \mu\text{m}$  long. Chylus cells in XII–XV, occupying 2–3 segments (Fig. 4D).

Seminal vesicle in XI, not brown. Sperm funnels cylindrical (Figs 1E, 5A), about  $180\text{--}330 \mu\text{m}$  long and about 2 times longer than wide (in vivo). Funnel length in fixed specimens  $100\text{--}220 \mu\text{m}$ , funnel body 1.2–1.8 times longer than wide (Fig. 5B); collar narrower than funnel body. The length of spermatozoa  $400\text{--}580 \mu\text{m}$ , heads  $100\text{--}150 \mu\text{m}$  in vivo (Fig. 5A), in fixed specimens spermatozoa  $200\text{--}360 \mu\text{m}$  long and sperm heads  $70\text{--}80 \mu\text{m}$ . Diameter of sperm ducts  $9\text{--}10 \mu\text{m}$  in vivo, ( $7.5\text{--}8 \mu\text{m}$ , fixed). Male copulatory organs  $130\text{--}170 \mu\text{m}$  long,  $60\text{--}140 \mu\text{m}$  wide and  $70\text{--}80 \mu\text{m}$  high, fixed (Figs 4G, 5C–D), retractor muscles conspicuous (Fig. 5C). Bursal slits longitudinal, slightly bent, with small additional transverse extensions (Fig. 5E). Subneural glands absent. Spermathecae (Figs 1G, 5F–J): no ectal gland, ectal ducts long, about  $360\text{--}500 \mu\text{m}$  and  $20\text{--}25 \mu\text{m}$  wide, canal  $5\text{--}6 \mu\text{m}$  wide in vivo ( $250\text{--}500 \mu\text{m}$  long,  $20\text{--}25 \mu\text{m}$  wide, canal  $5 \mu\text{m}$ , fixed), not widened entally, projecting into ampulla, ental bulbs about  $40\text{--}55 \mu\text{m}$  wide, fixed. Ampullae are surrounded distally by about 9–12 sessile diverticula of varying size : length  $24\text{--}45 \mu\text{m}$  (fixed). Sperm in a circle in lumen

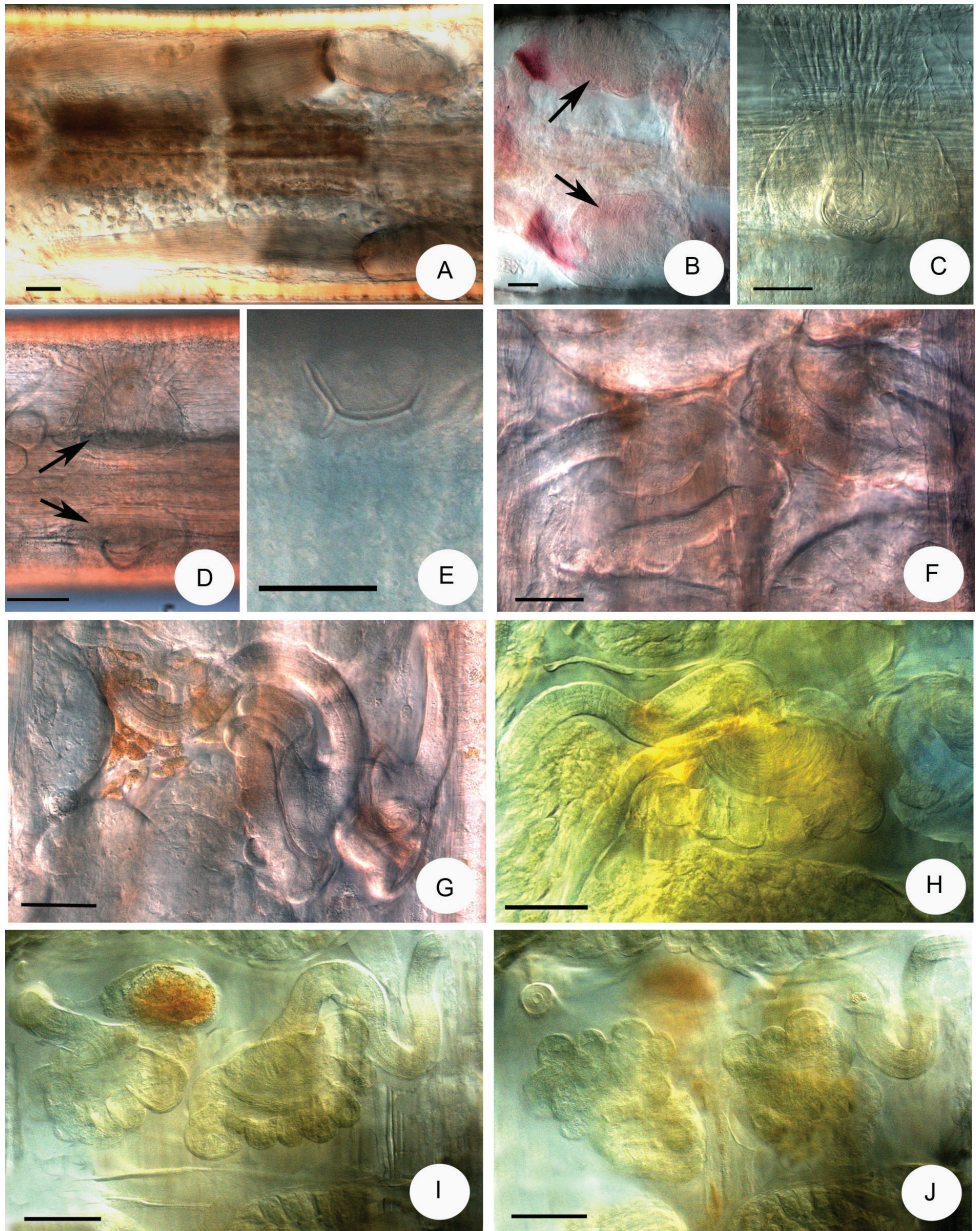


**Figure 5.** Micrograph of *Fridericia floriformis* sp. n. **A** Sperm funnels with very visible long spermatozoa **B** Sperm funnels of paratype 121.15 slide No. 2295 (marked with arrows) **C** Male copulatory apparatus, with well-developed muscle of paratype P.212.16 slide No. 2434 latero-ventral view **D** Male copulatory organs, ventral view (marked with arrows) **E** Bursal slit **F–J** Spermathecae (holotype NI-BRIV0000813661, slide No. 2437, **I–J** Spermathecal ampullae of paratype P. 121.16 slide No. 2434 where the ampullar diverticula are visible on all sides around the ampullae). **A, D–G** in vivo **B** fixed, stained **C, H–J** fixed, not stained. Scale bars: 50  $\mu$ m.

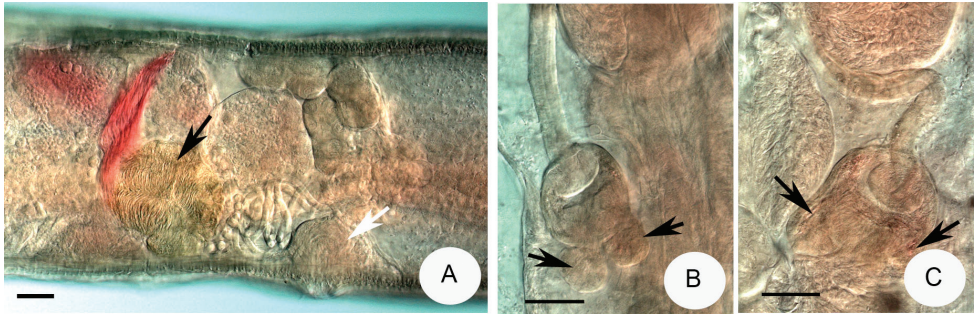


**Figure 6.** Micrograph of a *Fridericia callosa* specimen which has spermathecae with diverticula, collected from Siberia in 1994 (Christensen and Dózsa-Farkas 1999) fixed and stained on slide. **A** X–XII (sperm funnel marked with black arrow, male copulatory apparatus marked with white arrow, lateral view) **B–C** Spermathecae (diverticula marked with arrows lateral view).

of ampullar distal part. Diameter of ampulla and diverticula together 110–150  $\mu\text{m}$ , mostly no sperm in the diverticula. Separate openings into oesophagus dorso-laterally. 1–4 mature eggs at a time.

**Etymology.** Named after the shape of the spermathecal ampulla (more diverticula), which resembles a flower (*flos*, *floris*= flower, and *formis* = shaped as, Latin).

**Molecular data.** Sequences deposited in GenBank: MH128729–MH128733 (ITS), MH124586–MH124589 (CO1), MH124597–MH124598 (H3).

**Distribution.** In South Korea, at sites 8 and 9, Jeju Island, Yongnuni-orums, clayey soil, meadows.

**Morphologically similar species.** There are only three species (*F. paraunistetosa* Xie et al., 2000, *F. ventrochaetosa* Nagy, Dózsa-Farkas & Felföldi, 2018 and *F. callosa* Eisen, 1878) among all *Fridericia* species, which possess more diverticula of spermathecae and the lateral chaetal bundles absent or incomplete, varying with 0, 1 or maximum 2 chaetae. *Fridericia paraunistetosa* can easily be distinguished from *F. floriformis* sp. n. based on the following characters: smaller size (5.0–7.8 mm long vs. 8–17.3 mm, fixed), lateral chaetal bundles absent, ventrally only one chaeta per bundle (vs. 2–4 chaetae ventrally and 0–2 laterally), dorsal pores only from XVIII (vs. from VII), brain incised anteriorly (vs. convex), oesophageal appendages stout and unbranched (vs. with branches at the end) (Xie et al. 2000). *Fridericia ventrochaetosa* could be distinguished from the new species by the total absence of the lateral chaetae and having spermathecal diverticula with stalk (vs. sessile) (Nagy et al. 2018). The new species is similar to *F. callosa* in most traits (e.g., body size, segment number, strong body wall, thick cuticle, chaetal arrangement, number of preclitellar nephridia, position of chylus cells, the length of sperm), but the main differences between the two species are: in *F. callosa* the collar of sperm funnel not narrower than funnel body (Fig. 6A) (vs. narrower, Fig. 5A, B), seminal vesicle 2–3 segment large (vs. only in XI and not conspicuous). The spermathecae very variable in *F. callosa* (probably species complex) with or without diverticula, and the maximum number

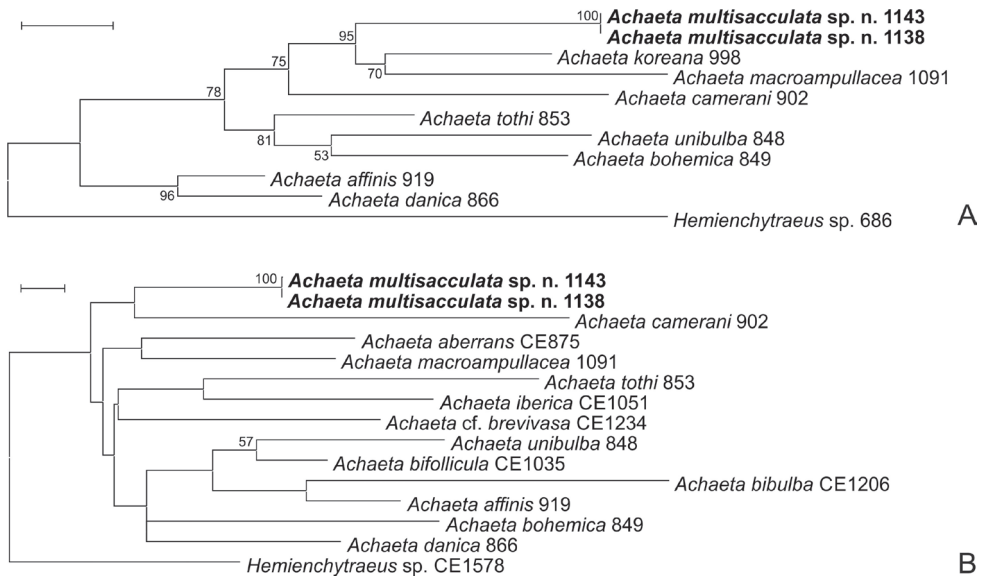


**Figure 7.** Maximum likelihood (ML) trees of studied *Achaeta* species based on the ITS region (**A**) and CO1 (**B**) gene. Bootstrap values greater than 50 are shown at the nodes. Sequences from new species described here appear in bold. **A** ML tree of the ITS region based on 736 nucleotide positions using the K2+G substitution model **B** ML tree of the CO1 gene based on 543 nucleotide positions using the GTR+G+I substitution model. Scale bars: 0.1 substitutions per nucleotide position.

of diverticula is 6 (Eisen 1878, 1879; Christensen and Dózsa-Farkas 1999; Schmelz 2003). From the material collected in Siberia in 1994, some stained slides were prepared now. On these slides, it was visible that the few diverticula are oriented towards the proximal ampullar part (Fig. 6B–C) in contrast to the spermathecae of the new species, which always have many diverticula or diverticula-like protrusions surrounding the ampullae (Fig. 5F–J).

## Results of molecular analysis

In total, 9, 13 and 9 new sequences were determined from various *Achaeta* and *Friedericia* species in the case of ITS, CO1 and H3, respectively. Additional sequences determined in previous studies (Erséus et al. 2010; Dózsa-Farkas et al. 2015, 2018; Dózsa-Farkas and Felföldi 2017, 2018; Nagy et al. 2018) were also used for comparison (Table 2). However, unfortunately, we failed to amplify the H3 gene from specimens of *Achaeta multisacculata* sp. n., which was probably due to the improper hybridization of PCR primer sequences to the extracted genomic DNA. Results of the molecular analyses confirmed that the two new species are genetically separate from morphologically similar species and species described previously from Korea and their sequences form distinct lineages on the phylogenetic trees (Figs 7, 8). This was also supported by interspecific sequence distances, since in the case of the

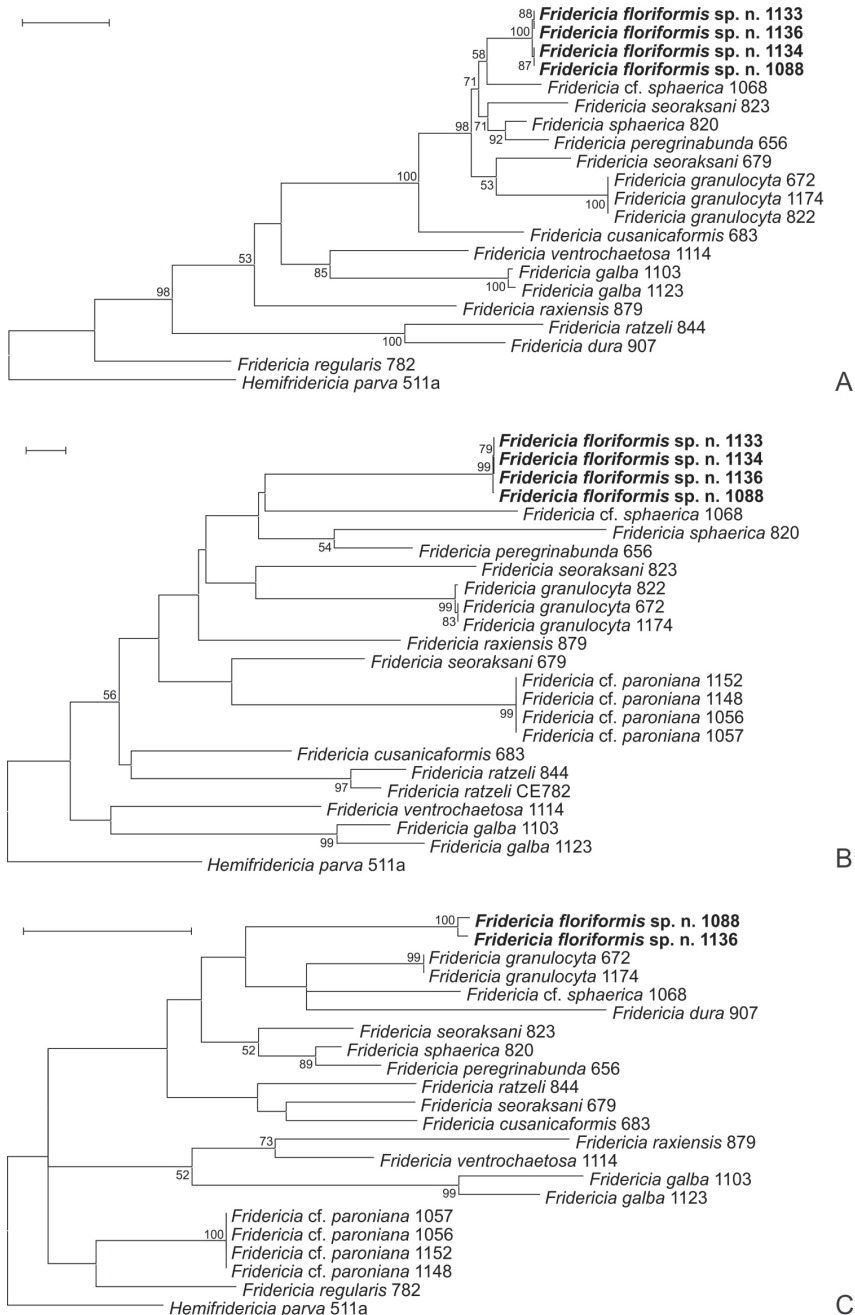


**Figure 8.** Maximum likelihood (ML) trees of studied *Fridericia* species based on the ITS region (A), CO1 (B) and H3 genes (C). Bootstrap values greater than 50 are shown at the nodes. Sequences from new species described here appear in bold. **A** ML tree of the ITS region based on 634 nucleotide positions using the K2+G+I substitution model **B** ML tree of the CO1 gene based on 455 nucleotide positions using the T93+G substitution model **C** ML tree of the H3 gene based on 145 nucleotide positions using the K2+G substitution model. Scale bars: 0.1 substitutions per nucleotide position, except H3 gene 0.05.

**Table 2.** List of specimens used for molecular taxonomic analyses with collection data and GenBank accession numbers. Sequences determined in this study appear in bold. Paratype and holotype of the new species are indicated with P and H in parentheses, respectively.

Species	Collection information	Specimen ID	Genbank accession numbers		
			ITS	CO1	H3
<i>Achaeta multisacculata</i> sp. n.	Korea, site 9, 26.09.2016, coll. Y. Hong	1138	<b>MH128727</b>	<b>MH124584</b>	–
		1143	<b>MH128728</b>	<b>MH124585</b>	–
<i>Achaeta aberrans</i>	(see reference Erséus et al. 2010)	CE875	–	GU902030	–
<i>Achaeta affinis</i>	(see reference Dózsa-Farkas and Felföldi 2017)	919	KY583122	KY583145	–
<i>Achaeta bibulba</i>	(see reference Erséus et al. 2010)	CE1206	–	GU902031	–
<i>Achaeta bifollicula</i>		CE1035	–	GU902032	–
<i>Achaeta bohémica</i>	(see reference Dózsa-Farkas and Felföldi 2017)	849	KY583110	KY583128	–
<i>Achaeta camerani</i>		902	KY583126	KY583143	–
<i>Achaeta</i> cf. <i>brevivasa</i>	(see reference Erséus et al. 2010)	CE1234	–	GU902034	–
<i>Achaeta</i> cf. <i>danica</i>	(see reference Dózsa-Farkas and Felföldi 2017)	866	KY583118	KY583137	–
<i>Achaeta iberica</i>	(see reference Erséus et al. 2010)	CE1051	–	GU902036	–
<i>Achaeta koreana</i>	(see reference Dózsa-Farkas et al. 2018)	998	MG252199	–	–
<i>Achaeta macroampullacea</i>		1091	MG252200	MG252131	–
<i>Achaeta tothi</i>	(see reference Dózsa-Farkas and Felföldi 2017)	853	KY583113	KY583131	–
<i>Achaeta unibulba</i>		848	KY583109	KY583127	–
<i>Hemienchytraeus</i> sp. (outgroup)	(see references Erséus et al. 2010 and Dózsa-Farkas and Felföldi 2017)	CE1578	–	GU902080	–
		686	KY583108	–	–
<i>Fridericia floriformis</i> sp. n.	Korea, Gwaneumsa Trail, Mt. Hallasan, coordinates: 33.41667°N, 126.56000°E, 634 m asl., 27.10.2016, coll. Y. Hong.	1088	<b>MH128733</b>	<b>MH124586</b>	<b>MH124597</b>
		1133 (H)	<b>MH128730</b>	<b>MH124587</b>	–
		1134 (P)	<b>MH128731</b>	<b>MH124588</b>	–
		1136	<b>MH128729</b>	<b>MH124589</b>	<b>MH124598</b>
<i>Fridericia</i> cf. <i>paroniana</i>	Korea, Seongpanak Trail, Mt. Hallasan, coordinates: 33.37111°N, 126.56433°E, 1352 m asl., 17.08.2016, coll. Y. Hong	1056	–	<b>MH124590</b>	<b>MH124599</b>
		1057	–	<b>MH124591</b>	<b>MH124600</b>
		1148	–	<b>MH124592</b>	<b>MH124601</b>
		1152	–	<b>MH124593</b>	<b>MH124602</b>
		1068	<b>MH128732</b>	<b>MH124594</b>	<b>MH124603</b>
<i>Fridericia cusnicaformis</i>	(see reference Dózsa-Farkas et al. 2015)	683	KR872373	KR872339	<b>MH124604</b>
<i>Fridericia duna</i>	(see references Dózsa-Farkas and Felföldi 2018 and Nagy et al. 2018)	907	MF547696	–	KX985894
<i>Fridericia galba</i>	(see reference Nagy et al. 2018)	1103	MF547697	MF547667	MF547688
		1123	MF547698	MF547668	MF547693
<i>Fridericia granulocyta</i>	(see reference Dózsa-Farkas et al. 2015)	672	KR872378	KR872344	KR872354
		822	<b>MH128734</b>	<b>MH124595</b>	–
		1174	<b>MH128735</b>	<b>MH124596</b>	<b>MH124605</b>
<i>Fridericia peregrinabunda</i>	(see reference Dózsa-Farkas et al. 2015)	656	KR872375	KR872338	KR872351
<i>Fridericia rutzeli</i>	(see reference Dózsa-Farkas and Felföldi 2018)	844	KX985875	KX985884	KX985895
<i>Fridericia ruzsanyi</i>	(see reference Erséus et al. 2010)	CE782	–	GU902070	–
		879	KX985868	MG921590	KX985885
<i>Fridericia regularis</i>	(see reference Nagy et al. 2018)	782	MF547703	–	MF547682
<i>Fridericia seonaksani</i>	(see reference Dózsa-Farkas et al. 2015)	679	KR872374	KR872340	KR872356
		823	KR872372	KR872342	KR872353
<i>Fridericia sphaerica</i>	(see reference Dózsa-Farkas et al. 2015)	820	KR872370	KR872334	KR872349
<i>Fridericia ventrochaetosa</i>	(see reference Nagy et al. 2018)	1114	MF547700	MF547676	MF547690
<i>Hemifridericia parva</i> (outgroup)	(see reference Dózsa-Farkas and Felföldi 2015)	511a	KM591939	KM591923	KM591931

two new species these values were similar to the interspecific sequence distances of other species involved in the analysis: 18.3-25.5% and 15.5-33.2% (*Achaeta* CO1), 42.2-66.9% and 22.3-66.6% (*Achaeta* ITS), 18.0-25.0% and 16.4-27.4% (*Fridericia* CO1), 9.1-46.3% and 6.1-56.6% (*Fridericia* ITS), 8.6-17.6% and 2.9-23.3% (*Fridericia* H3).

## Discussion

Earlier we studied and described the enchytraeid fauna of Hallasan National Park (Mt. Hallasan) from Jeju Island (Dózsa-Farkas et al. 2018). In the present study, we investigated nine new samples collected from other areas of Jeju Island. This time 22 enchytraeid species were found, two of which are new to science. According to the studied samples, sites 8 and 9 (Youngnuni-orum) were the most species-rich (with ten and seven detected species), harboring the two new species, *Achaeta multisacculata* sp. n. and *Fridericia floriformis* sp. n. (both new species were found only in this area) (Table 1). This could be explained probably with the meadow habitat, since the other samples were collected from forest habitats. Results of molecular analyses confirmed the status of the two new species.

Four species (*Achaeta macroampullacea*, *Xetadrilus jejuensis*, *X. aphanoides*, *Fridericia* cf. *paroniana*) which were described from Mt. Hallasan previously, were found also in the lowland areas of Jeju Island. *Xetadrilus aphanus* did not occur in the Hallasan National Park, so the present record from Dongbaekdongsan, Jocheon-eup (site 2) is new for the Korean fauna. The comparison of the three *Xetadrilus* species (a genus established by Schmelz et al. 2011) is given in Dózsa-Farkas et al. (2018, Table 2). Six other species (*Fridericia cusanicaformis*, *F. seoraksani*, *F. granulocyta*, *Hemienchytraeus jeonjuensis*, *H. quadratus*, *H. koreanus*) described originally from other parts of Korea (Dózsa-Farkas and Hong 2010; Christensen and Dózsa-Farkas 2012; Dózsa-Farkas et al. 2015) were also found in the present study. It seems that these species are characteristic members of the Korean enchytraeid fauna, and that the genus *Hemienchytraeus* has a wide geographic distribution within the country. *Fridericia* cf. *paroniana* was found in this study and also in Mt. Hallasan, and the differences from *F. paroniana* were discussed in Dózsa-Farkas et al. (2018). At site 6, a species very similar to *F. sphaerica* Dózsa-Farkas et al., 2015 occurred, but according to the results of molecular analysis, it is different from *F. sphaerica*. Unfortunately, we found only two specimens from this putatively new species, and we will try to solve its taxonomic status later (therefore we referred to it now as *F. cf. sphaerica*).

As mentioned above, the specimens of *Achaeta multisacculata* sp. n. did not possess any mature eggs, although the extraction of worms from soil samples was carried out several times from autumn to January. In contrast, *Achaeta macroampullacea* specimens mostly had mature eggs, so it can be assumed that *A. multisacculata* sp. n. belongs to that enchytraeid group where the worms reproduce only in certain seasons, as e.g. most *Mesenchytraeus* species (Dózsa-Farkas 1996).

Before 2007, the Korean enchytraeids were completely unknown. Results of subsequent studies (Dózsa-Farkas and Hong 2010; Christensen and Dózsa-Farkas 2012; Dózsa-Farkas et al. 2015; Dózsa-Farkas et al. 2018) indicated that the fauna is species rich. Including the findings in this paper, we described 23 species new for science and 13 new records for the Korean fauna. Thus, the Korean fauna now consists of 36 recorded terrestrial enchytraeid species. The high species number could be explained by the diverse geographic relief of the area which would result in many different microhabitats with differing microclimates, providing both for subtropical and temperate species (e.g., the typical tropical and subtropical *Hemienchytraeus* species or the widely distributed European *Fridericia bulboides* and *Hemifridericia parva*) suitable conditions to flourish. We think that some worms are introduced species, e.g., the two terrestrial polychaetes, *Parergodrilus heideri* Reisinger, 1925 detected in a previous survey (Dózsa-Farkas and Hong 2010) and *Hrabeiella periglandulata* (a typical European taxon) which was detected in this study for the second time in Korea (only at site 8). Probably *Xetadrilus aphanus*, an enchytraeid species described from Brazil (Schmelz et al. 2011), is also an introduced species. Unfortunately, detailed biogeographical conclusions cannot be drawn yet regarding the Korean enchytraeid fauna, since the fauna of several areas has not been studied yet or is under study; furthermore some morphologically identical material (e.g., *Fridericia seoraksani*, *F. sphaerica*), possibly representing cryptic species, requires further analysis.

## Acknowledgements

This study was supported by the National Research Foundation of Korea (NRF) funded by the Ministry of Education (NRF-2015R1D1A2A01057305), by the National Institute of Biological Resources (NIBR) funded by the Ministry of Environment (MOE) of the Republic of Korea (NIBR201801202), and by the National Research, Development and Innovation Office, Hungary (108582 NKFIH). T. F. was supported by the New National Excellence Program of the Ministry of Human Capacities, Hungary (grant number: ÚNKP-17-4-III-ELTE-111).

## References

- Bittencourt E (1974) Algumas Enchytraeidae (Oligochaeta) de São Paulo. *Revista Brasileira de Biologia*. Rio de Janeiro 34: 369–378.
- Christensen B, Dózsa-Farkas K (1999) The enchytraeid fauna of the Palearctic tundra (Oligochaeta, Enchytraeidae). *Biologiske Skrifter, The Royal Danish Academy of Sciences and Letters* 52: 1–37.
- Christensen B, Dózsa-Farkas K (2012) A new genus *Globulidrilus* and three new enchytraeid species (Oligochaeta: Enchytraeidae) from Seoraksan National Park (Korea). *Journal of Natural History* 46: 2769–2785. <https://doi.org/10.1080/00222933.2012.737038>

- Colgan DJ, McLauchlan AA, Wilson GDF, Livingston SP, Edgecombe GD, Macaranas J, Casis G, Gray MR (1998) Histone H3 and U2 snRNA DNA sequences and arthropod molecular evolution. *Australian Journal of Zoology* 46: 419–437. <https://doi.org/10.1071/ZO98048>
- Dózsa-Farkas K (1996) Theorie zur Vermehrungsstrategie einiger Enchytraeiden Arten (Oligochaeta). *Newsletter on Enchytraeidae* 5: 25–33.
- Dózsa-Farkas K, Hong Y (2010) Three new *Hemienchytraeus* species (Enchytraeidae, Oligochaeta, Annelida) from Korea, with first records of other enchytraeids and terrestrial polychaetes (Annelida). *Zootaxa* 2406: 29–56.
- Dózsa-Farkas K, Felföldi T, Hong Y (2015) New enchytraeid species (Enchytraeidae, Oligochaeta) from Korea. *Zootaxa* 4006: 171–197. <https://doi.org/10.11646/zootaxa.4006.1.9>
- Dózsa-Farkas K, Felföldi T (2017) Comparative morphological and molecular taxonomic study of six *Achaeta* species (Clitellata: Enchytraeidae) with the description of a new *Achaeta* species from Kőszeg Mountains, Hungary. *Zootaxa* 4273: 177–194. <https://doi.org/10.11646/zootaxa.4273.2.2>
- Dózsa-Farkas K, Felföldi T (2018) The enchytraeid fauna (Enchytraeidae, Clitellata) of Rax Mountain (Austria) with the description of two new species and comparison of *Fridericia discifera* Healy, 1975 and *F. alpica* sp. n. *Acta Zoologica Academiae Scientiarum Hungaricae* 64: 1–20. <https://doi.org/10.17109/AZH.64.1.1.2018>
- Dózsa-Farkas K, Felföldi T, Nagy H, Hong Y (2018) New enchytraeid species from Mount Hallasan (Jeju Island, Korea). *Zootaxa* 4496: 337–381. <https://doi.org/10.11646/zootaxa.4496.1.27>
- Eisen G (1878) Redogörelse för oligochaeter samlade under de Svenska expeditionerna till Arktiska trakter. Öfvers. af Kongliga Vetenskaps-Akademiens Förhandlingar Stokholm 3: 63–79.
- Eisen G (1879) On the Oligochaeta collected during the Swedish Expeditions to the Arctic Regions in the years 1870, 1875 and 1876. *Kongliga Svenska Vetenskaps-Akademiens Handlingar* 15(7): 10–49. [16 pl.]
- Erséus C, Rota E, Matamoros L, De Wit P (2010) Molecular phylogeny of Enchytraeidae (Annelida, Clitellata). *Molecular Phylogenetics and Evolution* 57: 849–858. <https://doi.org/10.1016/j.ympev.2010.07.005>
- Folmer O, Black M, Hoeh W, Lutz R, Vrijenhoek R (1994) DNA primers for amplification of mitochondrial cytochrome c oxidase subunit I from diverse metazoan invertebrates. *Molecular Marine Biology and Biotechnology* 3: 294–299.
- Kane RA, Rollinson D (1994) Repetitive sequences in the ribosomal DNA internal transcribed spacer of *Schistosoma haematobium*, *Schistosoma intercalatum* and *Schistosoma mattheii*. *Molecular and Biochemical Parasitology* 63: 153–156. [https://doi.org/10.1016/0166-6851\(94\)90018-3](https://doi.org/10.1016/0166-6851(94)90018-3)
- Kumar S, Stecher G, Tamura K (2016) MEGA7: Molecular Evolutionary Genetics Analysis version 7.0 for bigger datasets. *Molecular Biology and Evolution* 33: 1870–1874. <https://doi.org/10.1093/molbev/msw054>
- Nagy H, Felföldi T, Dózsa-Farkas K (2018) Morphological and molecular distinction of two *Fridericia* species (Clitellata, Enchytraeidae) having same spermatheca-type. *Zootaxa* 4496: 111–123. <https://doi.org/10.11646/zootaxa.4496.1.8>

- Nielsen CO, Christensen B (1961) The Enchytraeidae. Critical revision and taxonomy of European species. Supplement 1. *Natura Jutlandica* 10: 1–23.
- O'Connor FB (1962) The extraction of Enchytraeidae from soil. In: Murphy PW (Ed.) *Progress in Soil Zoology*. Butterworths Publishers, London, 279–285.
- Schmelz RM (2003) Taxonomy of *Fridericia* (Oligochaeta, Enchytraeidae). Revision of species with morphological and biochemical methods. *Abhandlungen des Naturwissenschaftlichen Vereins in Hamburg (Neue Folge)* 38: 1–415.
- Schmelz RM, Collado R, Römbke J (2008) Mata Atlántica enchytraeids (Paraná, Brasil): The genus *Achaeta* (Oligochaeta, Enchytraeidae). *Zootaxa* 1809: 1–35.
- Schmelz RM, Collado R, Römbke J (2011) Mata Atlántica enchytraeids (Paraná, Brazil): A new genus, *Xetadrilus* gen. nov., with three new species, and four new species of *Guaranidrilus* Černosvitov (Enchytraeidae, Oligochaeta). *Zootaxa* 2838: 1–29.
- Xie Z, Liang Y, Wang H (2000) Two new species of *Fridericia* (Enchytraeidae, Oligochaeta) from Changbaishan Mountain, Jili Province, China. *Species Diversity* 5: 53–58. <https://doi.org/10.12782/specdiv.5.53>

# *Hippocampus whitei* Bleeker, 1855, a senior synonym of the southern Queensland seahorse *H. procerus* Kuitert, 2001: molecular and morphological evidence (Teleostei, Syngnathidae)

Graham Short<sup>1</sup>, David Harasti<sup>2</sup>, Healy Hamilton<sup>3</sup>

**1** California Academy of Sciences, San Francisco, USA **2** Fisheries Research, Port Stephens Fisheries Institute, New South Wales, Australia **3** NatureServe, Arlington, Virginia, USA

Corresponding author: *Graham Short* ([gshort@calacademy.org](mailto:gshort@calacademy.org))

---

Academic editor: *David Morgan* | Received 29 October 2018 | Accepted 29 January 2019 | Published 14 February 2019

---

<http://zoobank.org/9D629EC8-38F9-4672-88A4-1D3D632DC543>

---

**Citation:** Short G, Harasti D, Hamilton H (2019) *Hippocampus whitei* Bleeker, 1855, a senior synonym of the southern Queensland seahorse *H. procerus* Kuitert, 2001: molecular and morphological evidence (Teleostei, Syngnathidae). ZooKeys 824: 109–133. <https://doi.org/10.3897/zookeys.824.30921>

---

## Abstract

The taxonomic status of the seahorse *Hippocampus procerus* Kuitert, 2001, type locality Hervey Bay, QLD, Australia, was re-examined based on its strong morphological similarity and geographical proximity to its congener *H. whitei* Bleeker, 1855, a species recorded in ten estuaries of New South Wales, Australia. Kuitert (2001) distinguished *H. procerus* from *H. whitei* by a taller coronet, marginally lower meristics, and spiner physiognomy. Meristic, morphometric, and key diagnostic morphological character comparisons from vouchered specimens of the two purported species collected from Sydney Harbour, Nelson Bay, Port Stephens, NSW and Hervey Bay, Bundaberg, and Moreton Bay, QLD did not show diagnostic differences to support species-level classification of *H. procerus*. Furthermore, partial mitochondrial COI sequence data from specimens sampled from known geographical distributions in NSW and Southport, QLD failed to discriminate between populations as a result of shared haplotypes, and revealed an average intraspecific divergence of 0.002%. *Hippocampus procerus* is hereby placed in the synonymy of *H. whitei*; a redescription is provided, with a revised record of its range across eastern Australia.

## Keywords

Acanthomorpha, Australia, COI, marine fish, morphology, systematics, taxonomy

“Sea-horse, or *Hippocampus*. This animal, like the Flying-fish, being commonly known, a description is not necessary. It is the *Syngnathus Hippocampus* of Linnaeus. See plate 264” (White 1790: 295).

## Introduction

*Hippocampus whitei* Bleeker, 1855, is a geographically restricted species of seahorse recorded in ten coastal estuaries and embayments of central New South Wales (NSW), and also farther north in the Tweed River, Australia. It can be found occurring in a variety of habitats including seagrasses, soft corals, sponge gardens, and artificial structures to depths of 15 m (Vincent et al. 2004; Hellyer et al. 2011; Harasti et al. 2014a). It is listed as ‘Endangered’ under criterion A2bc of the IUCN Red List due its restricted distribution, loss of essential marine habitats, and associated population declines in developed urban estuaries, including Port Stephens and Sydney Harbour (Harasti 2016; Harasti and Pollom 2017). Therefore, the conservation of *H. whitei* populations through the implementation of species monitoring and various management options, such as habitat protection and no-take policies are important for their protection and recovery, as well as for scientific, ecological, and economic purposes (Harasti et al. 2010, 2012, 2014b; Hellyer et al. 2011; Vincent et al. 2011).

Efforts to advance the conservation of seahorse populations are highly dependent on being able to confidently identify individual species in and beyond their known geographic distributions. The most recent and comprehensive taxonomic review of the genus *Hippocampus* (Lourie et al. 2016) places the number of recognized seahorse taxa occurring in Australia at sixteen species. However, the validity of several putative species remains uncertain. Seahorses are challenging to identify: multiple species have been synonymized based on recent genetic data, and there are many previous descriptions now recognized as spurious misidentifications attributed to the use of unreliable or non-diagnostic morphological characters (Lourie et al. 2016).

The taxonomic identity of *Hippocampus procerus* Kuitert, 2001, originally described from Hervey Bay, Queensland (QLD), with a known distribution in Gold Coast Seaway and Moreton Bay, QLD, has been in question due to its strong morphological similarity and geographic proximity to *H. whitei* (Lourie et al. 2016). It was distinguished from *H. whitei* primarily by a taller coronet, subtle differences in meristic characters, and a spinier physiognomy (Kuitert 2001). These indistinct morphological differences between the two species prompted a re-examination of the holotype and non-type specimens of *H. procerus* from Hervey Bay, paratypes of *H. procerus* from Bundaberg and Moreton Bay, QLD, non-type specimens of *H. procerus* from Mackay, Elliot Heads, and Gold Coast Seaway, QLD, and non-type specimens of *H. whitei* from Sydney Harbour and Nelson Bay, Port Stephens, NSW, employing meristic, morphometric, and key diagnostic morphological character comparisons. The diagnostic characters comprise in part the absence or presence of principal spines, including snout, cleithral ring, neck, and subdorsal spines, with respect to their spatial position on the head and body. We demonstrated that the morphological characters in the non-

type specimens of *H. whitei* corresponded closely with the examined non-type specimens, paratypes, and the holotype specimen of *H. procerus*, including: coronet height, absence of neck spines, indiscernible or small parietal spine, the numbers and positions of cleithral ring and subdorsal ridge spines, and overall spine physiognomy. Partial mitochondrial COI sequence data generated from specimens sampled from known geographical distributions in NSW and from Southport, QLD failed to discriminate between populations as a result of shared haplotypes, and revealed an average intraspecific divergence of 0.002%. *Hippocampus whitei* Bleeker, 1855, is herein formally re-described as a senior synonym of *H. procerus*. This estuarine species is apparently endemic to estuaries of central NSW, the Tweed River, and southern QLD.

## Materials and methods

Four individuals referred to as *H. procerus*, based on known locality of this species (Kuitert 2001), were collected from Southport, Gold Coast Harbour, QLD in 2014 by seine in seagrass beds in 1–2 m depth or by hand nets while scuba diving in less than 8 m depth (Figure 1), from which tissue was sampled from the caudal tip of the tails and preserved in a NaCl-saturated DMSO solution for genetic analyses. Similarly, thirty-one individuals of *H. whitei* were tissue sampled from the caudal tip of the tail at seven localities along the species' known geographic range in New South Wales, Australia (Table 1, Figure 1) from 2007–2009. DNA extraction, PCR amplification, alignment,



**Figure 1.** Collection locations for *H. procerus* in QLD and *H. whitei* in NSW, Australia.

**Table 1.** List of *H. whitei* specimens, and those referred to as *H. procerus*, including collection locality, voucher or field number, and COI GenBank accession numbers.

	Species	Locality	Voucher / Field	COI GenBank accession no.
1	<i>Hippocampus procerus</i>	Southport, QLD, Australia	CAS 241511	MH745371
2	<i>Hippocampus procerus</i>	Southport, QLD, Australia	CAS 241512	MH745372
3	<i>Hippocampus procerus</i>	Southport, QLD, Australia	CAS 241513	MH745373
4	<i>Hippocampus procerus</i>	Southport, QLD, Australia	CAS 241514	MH745374
5	<i>Hippocampus whitei</i>	Sydney, NSW, Australia	HH-0418	MH745375
6	<i>Hippocampus whitei</i>	Sydney, NSW, Australia	HH-0419	MH745376
7	<i>Hippocampus whitei</i>	Sydney, NSW, Australia	HH-0469	MH745377
8	<i>Hippocampus whitei</i>	Sydney, NSW, Australia	HH-0470	MH745378
9	<i>Hippocampus whitei</i>	Sydney, NSW, Australia	HH-0667	MH745379
10	<i>Hippocampus whitei</i>	Empire Bay, NSW, Australia	HH-1276	MH745380
11	<i>Hippocampus whitei</i>	Empire Bay, NSW, Australia	HH-1277	MH745381
12	<i>Hippocampus whitei</i>	Nelson Bay, NSW, Australia	HH-1287	MH745382
13	<i>Hippocampus whitei</i>	Tuggerah Lake, NSW, Australia	HH-1290	MH745383
14	<i>Hippocampus whitei</i>	Tuggerah Lake, NSW, Australia	HH-1291	MH745384
15	<i>Hippocampus whitei</i>	Tuggerah Lake, NSW, Australia	HH-1292	MH745385
16	<i>Hippocampus whitei</i>	Nelson Bay, NSW, Australia	HH-1295	MH745386
17	<i>Hippocampus whitei</i>	Nelson Bay, NSW, Australia	HH-1299	MH745387
18	<i>Hippocampus whitei</i>	Nelson Bay, NSW, Australia	HH-1300	MH745388
19	<i>Hippocampus whitei</i>	Nelson Bay, NSW, Australia	HH-1305	MH745389
20	<i>Hippocampus whitei</i>	Port Hacking, NSW, Australia	HH-1321	MH745390
21	<i>Hippocampus whitei</i>	Port Hacking, NSW, Australia	HH-1322	MH745391
22	<i>Hippocampus whitei</i>	Port Hacking, NSW, Australia	HH-1329	MH745392
23	<i>Hippocampus whitei</i>	Port Hacking, NSW, Australia	HH-1330	MH745393
24	<i>Hippocampus whitei</i>	Port Hacking, NSW, Australia	HH-1340	MH745394
25	<i>Hippocampus whitei</i>	Port Hacking, NSW, Australia	HH-1341	MH745395
26	<i>Hippocampus whitei</i>	Nelson Bay, NSW, Australia	HH-1352	MH745396
27	<i>Hippocampus whitei</i>	Nelson Bay, NSW, Australia	HH-1353	MH745397
28	<i>Hippocampus whitei</i>	Nelson Bay, NSW, Australia	HH-1354	MH745398
28	<i>Hippocampus whitei</i>	Nelson Bay, NSW, Australia	HH-1357	MH745399
30	<i>Hippocampus whitei</i>	Nelson Bay, NSW, Australia	HH-1359	MH745400
31	<i>Hippocampus whitei</i>	Forster, NSW, Australia	HH-1363	MH745401
32	<i>Hippocampus whitei</i>	Nelson Bay, NSW, Australia	HH-1364	MH745402
33	<i>Hippocampus whitei</i>	Nelson Bay, NSW, Australia	HH-1365	MH745403
34	<i>Hippocampus whitei</i>	Forster, NSW, Australia	HH-1366	MH745404
35	<i>Hippocampus whitei</i>	Forster, NSW, Australia	HH-1367	MH745405
36	<i>Hippocampus whitei</i>	Forster, NSW, Australia	HH-1368	MH745406

and analysis of partial mitochondrial cytochrome c oxidase subunit I (COI) sequences was performed following standard protocols described in Hamilton et al. (2017). Genetic distances (uncorrected  $p$ -distances) were calculated and neighbour-joining (NJ) trees constructed with confidence levels assessed using 1000 bootstrap replications based on partial COI using MEGA v. 7.0.26 (Kumar et al. 2017).

Proportional measurements and counts based on eight morphometric and six meristic variables (Tables 2, 3), including 17 diagnostic morphological characters, were per-

**Table 2.** Counts and morphometric measurements of specimens of *H. whitei* from Nelson Bay, NSW and those referred to as *H. procerus* from Southport, Moreton Bay, and Hervey Bay, QLD. Abbreviations: SnD (snout depth), SnL (snout length), CH (coronet height), HL (head length), HD (head depth), PO (post-orbital length), TrL (trunk length), TaL (tail length), SL (standard length). Numbers separated by a colon represent proportions (%). Lines present, from top to bottom, counts for trunk rings, tail rings, subdorsal rings, dorsal and pectoral fin rays.

	<i>H. whitei</i>	<i>H. whitei</i>	<i>H. procerus</i>						
Voucher or field number	PSFC-DH-1	PSFC-DH-2	CAS 241511	CAS 241512	QM I.30772	AMS I.12554	AMS E2914	CAS-SU 36420-3	CAS-ICH 13406
Type status	non-type	non-type	non-type	non-type	Paratype	Paratype	Holotype	non-type	non-type
Sex	adult male	subadult female	adult female	juvenile female	subadult female	adult male	adult female	subadult female	adult male
Location	Nelson Bay, NSW	Nelson Bay, NSW	Southport, QLD	Southport, QLD	Moreton Bay, QLD	Moreton Bay, QLD	Hervey Bay, QLD	Bundaberg, QLD	Mackay, QLD
Trunk rings	11	11	11	11	11	11	11	11	11
Tail rings	34	34	35	35	34	35	35	35	35
Subdorsal rings	3	3	3	3	3	3	3	3	3
Dorsal fin rays	17	17	18	18	18	18	18	18	18
Pectoral fin rays	16	16	16	16	16	16	18	17	18
SL (mm)	142.7	47.7	122.1	58.5	95.0	105.0	123.3	124.7	113.4
SnD:SnL	23.9	24.9	24.2	27.6	28.7	23.9	31.2	21.9	23.5
CH:HL	45.5	46.5	45.1	47.8	52.9	48.9	44.8	50.8	46.7
HD:HL	57.0	60.6	55.6	60.4	48.4	52.4	47.8	47.0	49.5
SnL:HL	46.2	45.5	43.6	46.2	49.3	44.3	43.6	48.9	46.1
PO:HL	33.8	37.0	40.6	38.1	38.9	36.7	36.8	34.9	33.8
HL:SL	22.9	20.3	21.5	24.2	27.3	25.7	25.2	22.6	21.9
TrL:SL	41.4	29.3	33.8	39.1	45.7	37.6	39.3	31.8	38.7
TaL:SL	58.6	50.5	66.2	60.9	63.8	62.5	60.7	65.26	54.8

formed on dried or ethanol-preserved specimens and high-resolution digital images of specimens using ImageJ (Rasband et al. 1997) to the nearest 0.1 mm following Lourie and Randall (2003) and Lourie and Kuitert (2008). External morphological characters were documented using a dissecting microscope or on high-resolution digital images of specimens. The holotype specimen of *H. whitei* is unknown. The original description of *H. whitei* Bleeker, 1855 is based on an artistic and non-informative rendering (White 1790: 264, plate 50) from Sydney Harbour, NSW. Morphometric measurements were recorded for two non-type specimens of *H. whitei* from Nelson Bay, NSW, two non-type specimens of *H. procerus* from Southport, Gold Coast Harbour, QLD, two non-type specimens of *H. procerus* from Moreton Bay, QLD, and one non-type specimen of *H. procerus* from Bundaberg and Mackay, QLD, respectively (Table 2). These data were compared to morphometric data from the holotype specimen of *H. procerus* from Hervey Bay, QLD (Table 2). Meristic counts and diagnostic morphological characters were recorded for 12 non-type specimens of *H. whitei*, including two from Sydney Harbour, six from Pittwater, and four from Nelson Bay, NSW, and 13 type and non-type specimens of *H. procerus*, including four from Southport, Gold Coast Harbour, QLD, two from Moreton Bay, one from Hervey Bay, QLD, one from Elliot Bay, four from Bundaberg, and one from Mackay, QLD (Table 3). These data were compared with similar morphological data (Table 3) for the holotype specimen of *H. procerus* from Hervey Bay, QLD.

**Table 3.** Comparison of diagnostic morphological characters in non-types specimens of *H. whitei* from NSW and non-type and type specimens of *H. procerus* from QLD.

	<i>H. whitei</i>	<i>H. whitei</i>	<i>H. whitei</i>	<i>H. procerus</i>	<i>H. procerus</i>					
Voucher number	CAS-SU 36407	CAS-SU 36417	PSFC-DH	CAS 24151-14	QM1.30772	AMS 1.12554	AMS E2914	QM1.39230	CAS-SU 36420-2,3,4	CAS-ICH 13406-1
Type status	non-type	non-type	non-type	non-type	Paratype	Paratype	Holotype	non-type	Paratype	non-type
Location	Port Jackson, NSW	Port Hacking, NSW	Nelson Bay, NSW	Southport, QLD	Moreton Bay, QLD	Moreton Bay, QLD	Hervey Bay, QLD	Ellitor Heads, QLD	Bundaberg, QLD	Mackay, QLD
Number of specimens	2	6	4	4	1	1	1	1	4	1
Coronet					distinct and tall					
Neck spines					absent	present			absent/present	absent
Upper cleithral spine						present				
Mid cleithral spine						present				
Ventral cleithral spine								present (single)		
Upper cleithral spine position										
Mid cleithral spine position										
Ventral cleithral spine position										
Subdorsal rings spines	3/0,1,0	3/0,1,0	3/0,1,0	3/0,1,0	3/0,1,0	3/0,1,0	3/0,1,0	3/0,1,0	3/0,1,0	3/0,1,0
Parietal spine	absent or blunt	absent or blunt	absent or blunt	absent or blunt	absent or blunt	absent or blunt	absent or blunt	absent or blunt	absent/blunt/present	present
Lateral head spine						present				
Snout spine						present				
Dorsal eye spine										present (single)
Small posterior eye spine										
Superior trunk ridge spines enlarged	1,8	1,8	1,8	1,8	1,8	1,7,8,9	1,7,8,9	1,8	1,8 - 1,7,8,9	1,4,6,7,8,9
Lateral trunk ridge spines enlarged	8-11	8-11	8-11	8-11	8-11	8-11	2-11	6-11	2-11	4-11
Inferior trunk ridge spines enlarged	4-11	4-11	4-11	4-11	4-11	4-11	4-11	5-11	5-11	5-11
Superior tail ridge spines enlarged	1-12	1-12	1-12	1-12	1-12	1-12	1-13	1-10	1-10	1-12
Inferior tail ridge spines enlarged	1-8	1-8	1-8	1-8	1-8	1-9	1-7	1-10	1-10	1-5

## Taxonomy

### *Hippocampus whitei* Bleeker, 1855

Figures 2–12, Tables 1–6

Common names: White's seahorse; New Holland seahorse; Sydney seahorse (Australia)

*Hippocampus novaehollandiae* Steindachner, 1866: 474 (Sydney Harbour, Australia).

*Hippocampus procerus* Kuitert, 2001: 328–329, figs. 4, 40 (Hervey Bay, Queensland, Australia).

**Material examined.** CAS 241511, adult female, Wave Island, Southport, QLD, Australia, 27°55'56.2"S 153°25'08.4"E, 5 m depth, in seagrass bed, November 27, 2014; CAS 241512, juvenile female, South West Wall, Southport, QLD, Australia, 27°56'32.7"S 153°25'14.7"E, 5 m depth, rocks and sand, November 26, 2014; CAS 241513, adult male, South West Wall, Southport, QLD, Australia, 27°56'32.7"S 153°25'14.7"E, 5 m depth, rocks and sand, November 26, 2014; CAS 241514, subadult male, Broadwater, QLD, Australia, 27°57'09.3"S 153°24'37.0"E, in seagrass bed, November 27, 2014; PSFC-DH (Port Stephens Fisheries Centre NSW field designation), 4 specimens in lot, PSFC-DH-1 adult male, PSFC-DH-2, subadult female, Nelson Bay, NSW, Australia, 32°42'59.9"S 152°08'57.2"E, 7 m depth, sandy rubble and seagrass, 2007–2016; SU 36407, 2 specimens in lot, adult males, Port Jackson, NSW, Australia, 33°50'42.6"S 151°14'50.5"E; SU 36417, 6 specimens in lot, Port Hacking, Gunnamatta Bay, NSW, Australia, 34°03'50.0"S 151°08'39.0"E, October 30, 1939; QM I.30772, subadult female, Chain Banks, Moreton Bay, QLD Australia, J Johnson, dredge, depth 3–7 m, January 24, 1997; AMS I.12554, adult male, Moreton Bay, QLD Australia, Amateur Fishermans Association of Qld, 1912; CAS 13406, 2 in lot, 13406-1 adult male, 13406-2 juvenile female, Mackay, QLD, Australia, 21°09'48.1"S 149°12'58.2"E, 11 m depth, July 12, 1939; SU 36420, 4 in lot, 36420-1 adult female, 36420-2, adult male, 36420-3 adult female, 36420-4 adult female, 4 miles east of Burnett R, Queensland, Australia, 25°20'21.0"S 151°52'41.7"E, 18 m depth, September 14, 1938; QM I.39230, subadult male, 2 miles NE of Elliot Heads, QLD, 24°55'00.0"S 152°31'00.0"E, March 4, 1982, trawl; QM I. 39656, adult female, east of Waddy Point, 24°58'36.0"S 153°24'08.4"E, March 26, 2005, trawl; CAS-SU 35442, 2 specimens in lot, F43-A adult female, F43-C adult male, Corny Point, South Australia, 34°54'38.7"S 137°03'35.7"E, October 31, 1912; AMS E2914, female holotype, 120 mm, 5–11 km east of Hervey Bay, Fairway Buoy, QLD, Australia, 25°8'59.64"S 152°50'26.94"E, FIS Endeavour, July 7, 1910; AMS IA4205, juvenile female, height 57 mm, Port Curtis, QLD, Australia, 23°55'S 151°23'E, dredged, M Ward & W Boardman, December 14, 1929.

**Diagnosis.** *Hippocampus whitei* differs from its congeners by the following combination of characters: trunk rings 11; tail rings 34–35; dorsal fin rays 17–18; pectoral fin rays 16; subdorsal rings three; subdorsal spines four, superior trunk ridge ending with three enlarged spines, superior tail ridge commencing with one enlarged spine

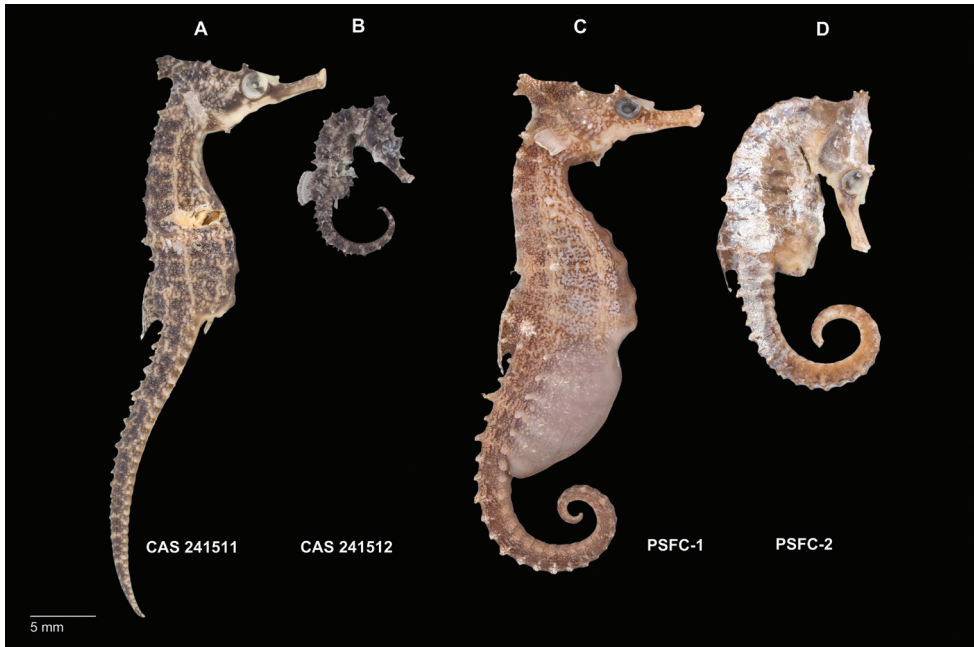


**Figure 2.** Comparison of non-type specimens of **A** *Hippocampus procerus* CAS 241511, preserved adult female, 142.7 mm SL, Southport, QLD **B** *Hippocampus procerus* CAS 241512, preserved juvenile, 112.7 mm SL, Southport, QLD **C** *Hippocampus whitei* PSFC-DH-1, preserved adult male, 122.1 mm SL, Nelson Bay, NSW **D** *Hippocampus whitei* CAS PSFC-DH-2, preserved subadult female, 47.7 mm SL, Nelson Bay NSW. Note the differences in coronet profile between juvenile/subadult and adult: projecting anteriad in juvenile/subadult versus lower or projecting posteriorly in adults.

(3/0,1,0); cleithral ring spines three, one small spine at each end of pectoral-fin base but none at gill-opening, large single or double spine at ventral extent of head; small lateral head spines, two, one directly posterior of eye, one anterodorsally of operculum and ventral of coronet; distinct snout spine; parietal spine, diminutive or absent; single eye spine, large, protruding dorsally; small single or double spine, rugose, posterovertrally of eye; coronet, distinct and tall, protruding anteriorly in juveniles, angled dorsoposteriorly in adults, five small spines present on apex in a star-like arrangement; superior trunk with enlarged spines on 1<sup>st</sup> and 8<sup>th</sup> tail ridges.

**Redescription.** General body shape as in Figs 2–11. Morphometric and meristic characters are listed in Table 2. Coronet distinct and tall, coronet height 44.8–47.89% in HL, protruding anteriad in juveniles, angled dorsoposteriorly in adults; bilateral gill-openings ventral of coronet; dorsal fin rays 17–18; pectoral fin rays 16; subdorsal rings three; dorsal fin base starting immediately posterior to ninth trunk ring and ending immediately posterior to first tail ring; trunk rings 11; tail rings 34–35. Body spines: coronet with five small spines present on apex in a star-like arrangement; neck spines absent; prominent spine dorsally of eye, small single or double spine, rugose, ventroposteriorly of eye; small lateral head spines, two, one directly posterior of eye,

**Table 4.** Comparison of morphological characters in *H. whitei* from NSW and other *Hippocampus* spp. occurring in Australia.

	<i>H. whitei</i>	<i>H. abdominalis</i>	<i>H. angustus</i>	<i>H. breviceps</i>	<i>H. dabli</i>	<i>H. histrix</i>	<i>H. jugannus</i>	<i>H. kelloggi</i>	<i>H. plamifrons</i>	<i>H. spinosissimus</i>	<i>H. zebra</i>
Trunk rings	11	12-13	11	11	11	11	12	11	11	11	11
Tail rings	33-35	44-48	39-41	38-42	37-40	33-34	37	39-41	37-38	35-36	37-39
Snout stripe or striation pattern	absent										
Coronet	distinct, tall	low	distinct, tall	distinct, tall	low	distinct, tall	distinct, tall	distinct, tall	low	distinct, tall	distinct, tall
Subdorsal rings	2+1	3-5+1-2	2+1	3+1	2-3+1-2	2+1	3+2	2+1	3-4+1	2+1	2-3+1
Subdorsal ring spines	3/0,1,0	5/0,0,1,1,1	3/0,1,0	3-4/0,0,1,0	3/0,1,1	3/0,1,0	4/0,1,1,1,1	3/0,1,0	4/0,0,1,1	3/0,1,0	3-4/0,1,0
Cleithral ring	discontinuous										
Upper cleithral spine	dorsal level of pectoral fin base absent	ventral of gill opening absent	dorsal level of pectoral fin base present	ventral of gill opening absent	ventral of gill opening absent	ventral of gill opening present	dorsal level of pectoral fin base present	ventral of gill opening absent	ventral of gill opening absent	ventral of gill opening present	dorsal level of pectoral fin base absent
Neck spine	absent	absent	present	absent	absent	present	present	absent	absent	present	absent
Eye spine	single										
Lateral head spine	single and small										
	double and large										
	single and small										
	single and small										



**Figure 3.** *Hippocampus whitei* in situ, adult female, Nelson Bay, NSW, Australia at 5 m depth (photograph David Harasti).

one anterodorsally of operculum and ventral of coronet; cleithral ring spines three, one small spine at each end of pectoral-fin base but none at gill-opening, large single or double spine at ventral extent of head; distinct snout spine on midline between eyes; parietal spine, diminutive or absent in adults, present in juveniles and subadults;



**Figure 4.** *Hippocampus whitei* in situ, adult female, Gold Coast, QLD, Australia at 5 m depth (photograph David Harasti).

subdorsal spines four, superior trunk ridge ending with three enlarged spines, superior tail ridge commencing with one enlarged spine (3/0,1,0); superior trunk with enlarged spines on 1<sup>st</sup> and 8<sup>th</sup> tail ridges observed in adults, on 1<sup>st</sup>, 7<sup>th</sup>, 8<sup>th</sup>, and 9<sup>th</sup> tail ridges observed in subadults; lateral trunk ridge with small spines on 2<sup>nd</sup>–11<sup>th</sup> trunk



**Figure 5.** *Hippocampus procerus*, AMS E2914, adult female, holotype, 120 mm SL, Hervey Bay, Queensland, Australia (photograph Mark Allen).

rings; inferior trunk ridge with small spines beginning on 5<sup>th</sup> trunk ring and ending on 11<sup>th</sup> trunk ring; superior tail ridge spines well developed anteriorly, becoming smaller posteriorly, with enlarged spines on 1<sup>st</sup>–12<sup>th</sup> tail rings; inferior tail ridge spines well developed anteriorly, becoming smaller posteriorly, with enlarged spines on 1<sup>st</sup>–8<sup>th</sup> tail rings; caudal fin absent in juveniles and adults.

**Morphological remarks.** In his original description, Kuitert (2001:328–329) erected *H. procerus* based on several observations on its distinguishing characters: “Previously confused with *Hippocampus tristis* and *H. whitei*, *H. procerus* is more similar to the latter, differing from it in having a taller and spinier coronet, higher fin-ray

**Table 5.** Distribution of haplotypes based on partial mtDNA COI sequence data (655 bp) tabulated across sampled *H. whitei* and localities in central NSW and southern QLD.

Species designation	Collection locality	Nucleotide position	Haplotype
Hippocampus whitei_1300a_CO1_Nelson	Nelson	81	A
Hippocampus whitei_1767_CO1_GoldCoast	Gold Coast	174	T
Hippocampus whitei_1783_CO1_GoldCoast	Gold Coast	174	T
Hippocampus whitei_1364_CO1_Forster	Forster	174	T
Hippocampus whitei_1365_CO1_Forster	Forster	174	T
Hippocampus whitei_1295_CO1_Nelson	Nelson	259	C
Hippocampus whitei_1364_CO1_Forster	Forster	342	G
Hippocampus whitei_1365_CO1_Forster	Forster	342	G
Hippocampus whitei_1767_CO1_GoldCoast	Gold Coast	378	A
Hippocampus whitei_1783_CO1_GoldCoast	Gold Coast	378	A
Hippocampus whitei_1364_CO1_Forste	Forster	378	A
Hippocampus whitei_1365_CO1_Forster	Forster	378	A
Hippocampus whitei_1305_CO1_Nelson	Nelson	412	A
Hippocampus whitei_1353_CO1_Nelson	Nelson	412	A
Hippocampus whitei_0418_CO1_Sydney	Sydney	429	G
Hippocampus whitei_0470_CO1_Sydney	Sydney	429	G
Hippocampus whitei_1767_CO1_GoldCoast	Gold Coast	489	G
Hippocampus whitei_1783_CO1_GoldCoast	Gold Coast	489	G
Hippocampus whitei_1364_CO1_Forster	Forster	489	G
Hippocampus whitei_1365_CO1_Forster	Forster	489	G
Hippocampus whitei_1295_CO1_Nelson	Nelson	495	G
Hippocampus whitei_1783_CO1_GoldCoast	Gold Coast	504	T
Hippocampus whitei_1364_CO1_Forster	Forster	513	T

**Table 6.** List of seahorse specimens originally identified as *H. whitei*, including voucher number, collection date, collection location, and status.

Original identification	Voucher number	Collection date	Collection location	Species
<i>H. whitei</i>	AMS I.6637	1885	Port Moresby, Papua New Guinea	<i>Hippocampus</i> sp.
	SU 35442	1912	Corny Point, South Australia	<i>H. breviceps</i>
	AMS IA4205	1929	Port Curtis, Qld, Australia	<i>H. spinosissimus</i>
	CAS-SU 31443	1934	Durban Bay, KwaZulu-Natal, South Africa	<i>H. camelopardalis</i>
	MNHN-IC-2008-1326	2006	Espiritu Santo, Vanuatu	<i>H. kelloggi</i>
	MNHN-IC-2008-1441	2006	Espiritu Santo, Vanuatu	<i>H. kelloggi</i>
	MNHN-IC-2008-1662	2006	Malekula, Vanuatu	<i>H. kelloggi</i>
	MCZ 168083	unknown	Western Port, Victoria, Australia	<i>H. breviceps</i>

counts, and generally a spinier physiogamy.” We show that morphometric, meristic, and diagnostic morphological characters reported herein (Tables 2, 3) correspond closely among the non-type specimens of *H. whitei* from NSW, type and non-type specimens referred to as *H. procerus* from Gold Coast Seaway, Moreton Bay, Elliot Heads, Bundaberg, and Mackay, QLD, and the holotype specimen of *H. procerus* from Hervey Bay, QLD.



**Figure 6.** *Hippocampus procerus*, QM I.30772, subadult female, paratype, 95.0 mm SL, Moreton Bay, Queensland, Australia (photograph Jeff Johnson).



**Figure 7.** *Hippocampus procerus*, AMS I.12554, adult male, paratype, 105 mm SL, Moreton Bay, Queensland, Australia (photograph Kerry Parkinson).

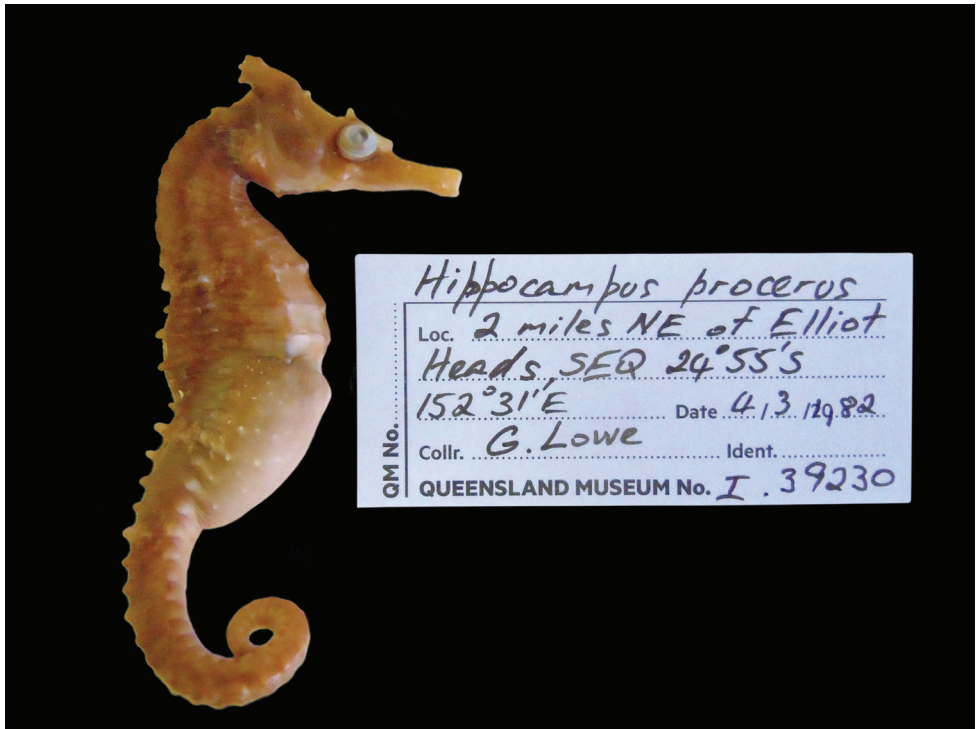


**Figure 8.** *Hippocampus procerus*, QM I.39230, adult male, non-type, Elliot Heads, Queensland, Australia (photograph Jeff Johnson).



**Figure 9.** *Hippocampus procerus*, CAS-SU 36420, 4 specimens in lot, paratypes, Burnett River, Queensland, Australia (photograph Jon Fong).



**Figure 10.** *Hippocampus procerus*, CAS-ICH 13406, adult male, non-type, 113.4 mm SL, Mackay, Queensland, Australia (photograph Jon Fong).

Based on the material examined, we found minor variation in coronet height in proportion to the head (45.5–46.6% in *H. whitei* from Nelson Bay, NSW vs. 45.1–47.8% in *H. procerus* from Gold Coast Harbour, QLD, 48.9–52.9% in the paratypes from Moreton Bay, QLD, 44.8% in the holotype from Hervey Bay, QLD, 50.8% in the paratype from Bundaberg, QLD and 46.7% from Mackay, QLD). The non-type specimens are comprised of juveniles, subadults, and adults, all of which exhibit distinct and tall coronets. However, we noted that in juveniles the coronet protrudes anteriorly whereas in subadults and adults it is strongly angled dorsoposteriorly. Similarly, dorsal fin ray counts exhibited marginal differences (17 in non-type specimens of *H. whitei* vs. 18 in all the specimens of *H. procerus* from Queensland), which may



**Figure 11.** *Hippocampus procerus*, AMS IA4205, juvenile female, non-type, Point Curtis, Queensland, Australia (photograph Jeff Johnson).

reflect north-south clinal variation. We did not observe an overall spinier physiognomy in the majority of adult specimens of *H. procerus* relative to *H. whitei*. However, a spinier physiognomy was present in one juvenile specimen from Mackay, and Port

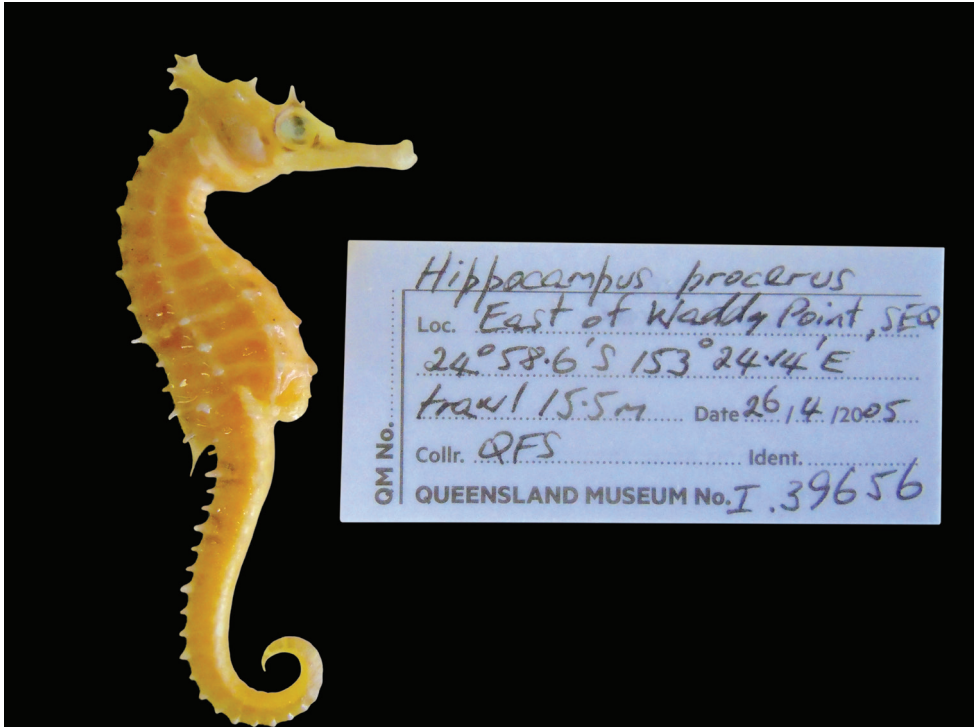


**Figure 12.** *Hippocampus procerus*, QM I.39656, adult female, non-type, Waddy Point Queensland, Australia (photograph Jeff Johnson).

Curtis, QLD (Figs 10, 11), respectively, and one adult specimen from Burnett River (Fig. 9) and Waddy Point, QLD (Fig. 12), respectively, on all principal trunk and tail ridges and head. It has been observed that in juvenile and subadult *H. whitei* from NSW (<8 cm Total Length) that spines are more pronounced, but as they increase in size the spines disappear, with specimens > 12 cm TL being much smoother and spines not obvious. The adult specimens from Burnett River and Waddy Point, QLD, are an exception to these observations and appear to reflect variation in spine morphology similarly observed in juvenile *H. whitei*.

We also observed across the majority of examined adult specimens the following key diagnostic morphological characters (Table 3): the absence of true neck spines between the coronet and the 1<sup>st</sup> superior trunk ring spines (small neck spines were detected in juvenile specimens; variation in neck ridge topology is often mistaken for true neck spines in adult specimens), indiscernible or small parietal spine, three cleithral ring spines with the uppermost spine at the dorsal level of the pectoral fin base, presence of a distinct snout spine, four subdorsal ridge spines (3/0,1,0), and superior trunk ridge with enlarged spines on 1<sup>st</sup> and 8<sup>th</sup> tail ridges. Based on these findings, we find that spine physiognomy, neck spines present or absent in juveniles and adults, respectively, and subtle differences in meristics, are unreliable diagnostic characters, and

that key and informative morphological characters are congruent across all specimens, which conform to the diagnosis of *H. whitei*. Therefore, it can be concluded that the species-level classification of *H. procerus* is unsupported, and that *H. procerus* may be treated as a junior synonym of *H. whitei*.

Several seahorse species endemic to Australia, including Indo-Pacific seahorses with overlapping latitudinal distributions in Queensland, Australia, are superficially similar to and often misidentified as juvenile and adult *H. whitei* (Kuitert 2001; Table 5). These species include *H. abdominalis* Lesson, 1827, *H. angustus* Günther, 1870, *H. breviceps* Peters, 1869, *H. dahli* Ogilby 1908, *H. histrix* Kaup, 1856, *H. jugumus* Kuitert, 2001, *H. kelloggi* Jordan & Snyder, 1901, *H. planifrons* Peters, 1877, *H. spinosissimus* Weber, 1913, and *H. zebra* Whitley, 1964. Despite the morphological similarities, meristic and diagnostic morphological characters support the distinctions among these species (Table 4).

**Genetic remarks.** Meristic, morphometric, and key diagnostic morphological characters in our study did not support the separation of *H. procerus* from *H. whitei* into two distinct species. Here we further confirm the synonymization of *H. procerus* with *H. whitei* based on partial mitochondrial COI (655 bp) data. This analysis is based on sequences generated from 31 *H. whitei* individuals sampled from Empire Bay, Forster (Wallis Lake), Port Hacking, Nelson Bay, Sydney Harbour, and Tuggerah Lake, NSW, and from 4 specimens referred to as *H. procerus* from Southport, Gold Coast Seaway, QLD. Alignment of sequence data detected 23 variable sites without any indels, resulting in 14 haplotypes: one in Sydney, four in Nelson Bay, five in Forster, and four in Gold Coast Seaway (Suppl. material 1, 2). Three haplotypes are shared between Forster and Gold Coast Seaway whereas no other haplotypes are shared between collection localities. One unique haplotype was obtained in Sydney, four in Nelson Bay, two in Forster, and one in Gold Coast Seaway (Suppl. material 1, 2). Fig. 12 shows a neighbour-joining tree based on the same mtDNA COI data, which recovered *H. procerus* as paraphyletic with respect to *H. whitei*. *Hippocampus procerus* clustered among individuals of *H. whitei* from Forster, NSW in one subclade and with individuals from several localities in NSW in another subclade. Additionally, genetic distance analysis (uncorrected p distances) of the same data failed to discriminate *H. procerus* from *H. whitei* (Suppl. material 3), which revealed an average intraspecific divergence of 0.002%, further confirming lack of support of species status for *H. procerus*.

**Distribution and habitat.** *Hippocampus whitei* is known to occur in coastal estuaries and embayments of central NSW and southern QLD, Australia. In central NSW it has been recorded, from south to north, in St. Georges Basin, Port Hacking, Botany Bay, Sydney Harbour, Hawkesbury River, Tuggerah Lake, Lake Macquarie, Port Stephens, Wallis Lake – Forster, and Tweed River. The record from St Georges Basin was based on a recent sighting and photograph of a small juvenile in January 2018 that was logged through REDMAP (<http://www.redmap.org.au/sightings/3379/>) and therefore extends the range reported by Harasti et al. (2012) southwards by 70 km. A previous 1903 Australian Museum record from Lake Illawarra cannot be confirmed as the local-

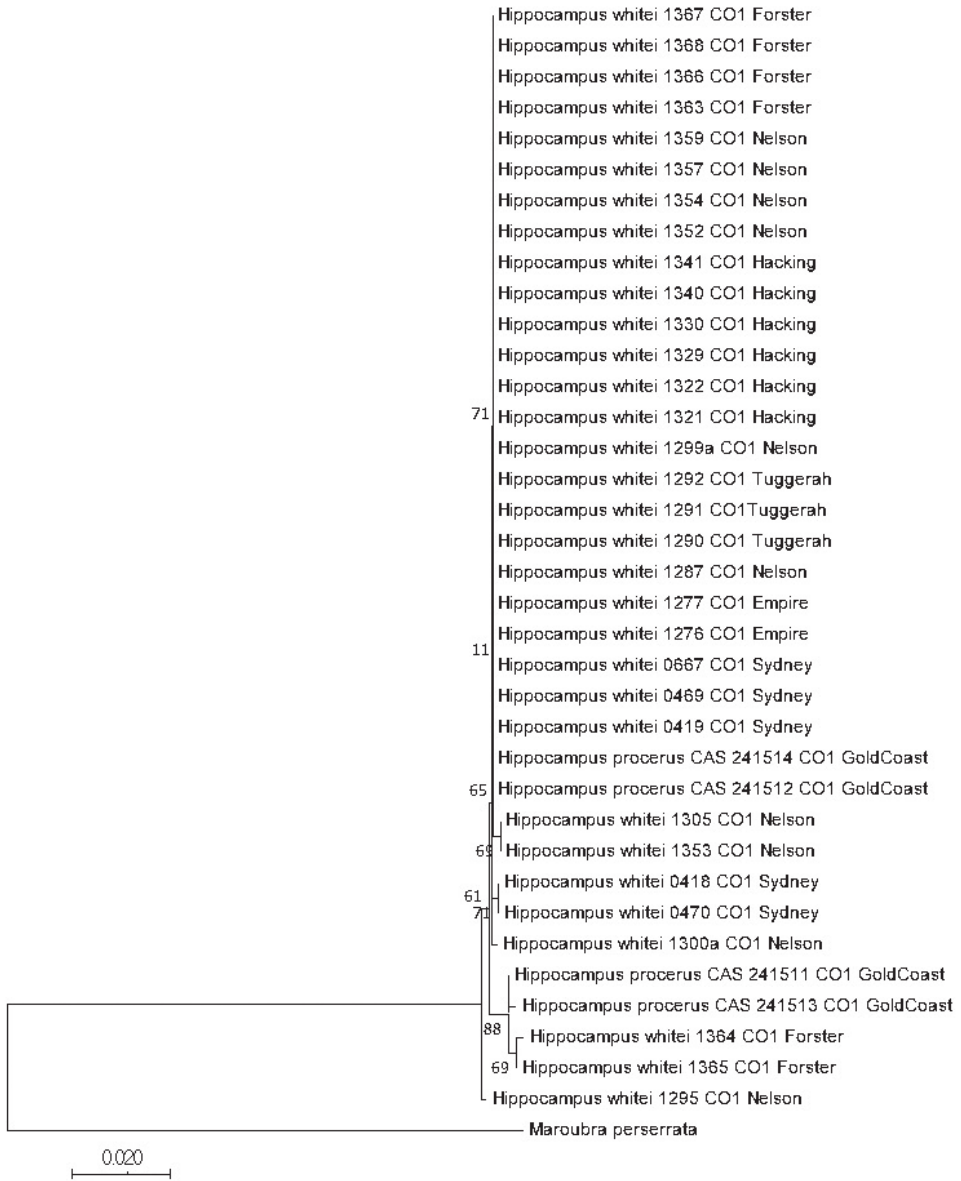


**Figure 13.** Neighbor-joining tree based on mtDNA COI sequences showing the relationships among specimens of *H. whitei* collected from various sites in NSW and *H. procerus* from Southport, Gold Coast Harbour, QLD. Numbers in branches indicate bootstrap probabilities obtained from 1000 bootstrap replications. Scale bar = genetic distance of 0.02.

ity information is likely erroneous (Mark McGrouther, pers. comm.) and whilst it is possible that *H. whitei* could occur in Lake Illawarra, at this stage there is no definitive evidence. Museum records indicate the species has been recorded in QLD within the



**Video 1.** *Hippocampus whitei*, in situ, Seahorse Gardens, Nelson Bay, NSW, Australia (video by David Harasti 2011).

Gold Coast Seaway, at various locations around Moreton Bay estuary, Hervey Bay, Waddy Point, Elliot Heads, Bundaberg, Port Curtis, and Mackay. The synonymization of *H. procerus* extends the northward range significantly by approximately 1,000 kilometres for *H. whitei* to Mackay QLD; as of now, this is the most northern location with confirmed *H. whitei* specimens. However, its current occurrence in the Mackay region, Port Curtis, Burnett River, and Bundaberg, is unknown as it has not been recorded in those locales since 1939, 1929, and 1938, respectively. The most recent northern records are from Elliot Heads in 1982 and Waddy Point in 2005.

Additionally, museum records claim species occurrences of *H. whitei* outside its geographic range, in South Australia, Victoria Australia, Papua New Guinea, South Africa, Solomon Islands, and Vanuatu (Kuitert 2009; Lourie et al. 2016). However, these specimens have subsequently been re-identified by the authors as *H. breviceps*, *H. camelopardalis*, *H. kelloggi*, or *H. spinosissimus* (see Table 6). The specimens originally identified as *H. whitei* from Port Moresby, Papua New Guinea and the Solomon Islands are no longer accessible and therefore cannot be re-identified; however, we consider them highly unlikely to be *H. whitei* since it is markedly outside the range for this species. We now consider that the species is constrained to estuaries and embayments along the east coast of Australia from Hervey Bay, QLD, in the north to St Georges Basin, NSW, in the south.

*Hippocampus whitei* occurs in a variety of habitats including seagrasses, soft corals, sponge gardens and artificial structures to depths of 12 m (Hellyer et al. 2011; Harasti et al. 2014a; Manning et al. 2018), and is known to display strong site fidelity and monogamous behaviour (Vincent and Sadler 1995; Vincent et al. 2005; Harasti and

Gladstone 2013). The locations with the largest recorded populations are found within Sydney Harbour and Port Stephens (Harasti et al. 2012; Harasti et al. 2014b), beyond which there is very little information about the occurrence, habitat use, and population numbers in QLD as the species is not known to be regularly found in any QLD locations and is seldom seen or collected.

We introduced this paper with a quote from John White (1736–1832) who was under the assumption that the Mediterranean and North Atlantic seahorse *H. hippocampus* and *H. whitei* from Australia were conspecific due to highly similar morphology. Seahorse taxonomy has been in a state of confusion since its inception. While comprehensive revisions of the genus have greatly advanced our understanding of how many species of seahorses exist (Lourie et al. 2016), much further work remains to answer this most fundamental question about one of the world's most extraordinary fish.

## Acknowledgements

We are grateful to: Jeff Leis, Senior Fellow, Ichthyology Collection, Australian Museum, for discussions on *H. whitei*; Jeff Johnson, Collection Manager, Ichthyology, Biodiversity Program, Queensland Museum, for discussions on and providing an image of a paratype of *H. whitei* from Queensland; Amanda Hay, Mark McGrouther, and Matthew Lockett, Department of Ichthyology, Australian Museum, for curatorial assistance; Jon Fong and David Catania, Ichthyology, California Academy of Sciences, for curatorial assistance and images of paratypes and non-type specimens of *H. procerus*; Kerryn Parkinson, Technical Officer, Ichthyology and Institute Data and DigiVol Coordinator, Digital Collections and Citizen Science, Australian Museum Research Institute, for an image of the holotype of *H. procerus*; and Beth Tate and Brian Simison of the Center for Comparative Genomics at the California Academy of Sciences for support with generating genetic data. This work was partially funded by a grant to DH from the Sydney Aquarium Conservation Fund.

## References

- Bleeker P (1855) Over eenige visschen van Van Diemensland. Verhandelingen van het Koninklijke Akademie van Wetenschappen te Amsterdam 2: 17, 28–31.
- Bruckner, AW, Field, JD, Daves N (2005) Proceedings of the International Workshop on CITES Implementation for Seahorse Conservation and Trade, February 3–5, 2004, Mazatlan, Sinaloa, Mexico.
- Froese R, Pauly D (2018) FishBase. <http://www.fishbase.org>
- Hamilton H, Saarman N, Short G, Sellas AB, Moore B, Hoang T, Grace CL, Gomon M, Crow K, Simison, WB (2017) Molecular phylogeny and patterns of diversification in Syngnathid fishes. *Molecular phylogenetics and Evolution* 107: 388–403. <https://doi.org/10.1016/j.ympev.2016.10.003>

- Han S, Kim JK, Kai Y, Seno H (2017) Seahorses of the *Hippocampus coronatus* complex: taxonomic revision, and description of *Hippocampus haema*, a new species from Korea and Japan (Teleostei, Syngnathidae). *ZooKeys* 712: 113–139. <https://doi.org/10.3897/zookeys.712.14955>
- Harasti D, Martin-Smith K, Gladstone W (2012) Population dynamics and life history of a geographically restricted seahorse, *Hippocampus whitei*. *Journal of Fish Biology* 81(4): 1297–1314. <https://doi.org/10.1111/j.1095-8649.2012.03406.x>
- Harasti D, Glasby TM, Martin-Smith KM (2010) Striking a balance between retaining populations of protected seahorses and maintaining swimming nets. *Aquatic Conservation: Marine and Freshwater Ecosystems* 20(2): 159–166. <https://doi.org/10.1002/aqc.1066>
- Harasti, D, Gladstone W (2013) Does underwater flash photography affect the behaviour, movement and site persistence of seahorses? *Journal of Fish Biology* 83: 1344–1353. <https://doi.org/10.1111/jfb.12237>
- Harasti D, Martin-Smith K, Gladstone W (2014a) Ontogenetic and sex-based differences in habitat preferences and site fidelity of the White's seahorse *Hippocampus whitei*. *Journal of Fish Biology* 85: 1413–1428. <https://doi.org/10.1111/jfb.12237>
- Harasti D, Martin-Smith K, Gladstone W (2014b) Does a no-take marine protected area benefit seahorses? *PLoS One* 9(8): e105462. <https://doi.org/10.1371/journal.pone.0105462>
- Harasti D (2016) Declining seahorse populations linked to loss of essential marine habitats. *Marine Ecology Progress Series* 546: 173–181. <https://doi.org/10.3354/meps11619>
- Harasti D, Pollom R (2017) *Hippocampus whitei*. The IUCN Red List of Threatened Species 2017: e.T10088A46721312. <https://doi.org/10.3354/meps11619>
- Hellyer CB, Harasti D, Poore AG (2011) Manipulating artificial habitats to benefit seahorses in Sydney Harbour, Australia. *Aquatic Conservation: Marine and Freshwater Ecosystems* 21(6): 582–589. <https://doi.org/10.1002/aqc.1217>
- Kuiter RH (2001) Revision of the Australian seahorses of the genus *Hippocampus* (Syngnathiformes: Syngnathidae) with descriptions of nine new species. *Records-Australian Museum* 53(3): 293–340. <https://doi.org/10.3853/j.0067-1975.53.2001.1350>
- Lourie SA, Pollom RA, Foster SJ (2016) A global revision of the Seahorses *Hippocampus* Rafinesque 1810 (Actinopterygii: Syngnathiformes): Taxonomy and biogeography with recommendations for further research. *Zootaxa* 4146(1): 1–66. <https://doi.org/10.11646/zootaxa.4146.1.1>
- Short G, Smith, R, Motomura H, Harasti D, Hamilton H (2018) *Hippocampus japapigu*, a new species of pygmy seahorse from Japan, with a redescription of *H. pontohi* (Teleostei, Syngnathidae). *ZooKeys* 779: 27–49. <https://doi.org/10.3897/zookeys.779.24799>
- Steindachner F (1866) Zur Fischfauna von Port Jackson of Australien. *Sitzungsberichte Akademie Wissenschaften, Wien* 53: 424–480.
- Vincent AC, Sadler LM (1995) Faithful pair bonds in wild seahorses, *Hippocampus whitei*. *Animal Behaviour* 50(6): 1557–1569. [https://doi.org/10.1016/0003-3472\(95\)80011-5](https://doi.org/10.1016/0003-3472(95)80011-5)
- Vincent AC, Evans KL, Marsden AD (2005) Home range behaviour of the monogamous Australian seahorse, *Hippocampus whitei*. *Environmental Biology of Fishes* 72(1): 1–12. <https://doi.org/10.1007/s10641-004-4192-7>
- Vincent AC, Foster SJ, Koldewey HJ (2011) Conservation and management of seahorses and other Syngnathidae. *Journal of Fish Biology* 78(6): 1681–1724. <https://doi.org/10.1111/j.1095-8649.2011.03003.x>

## Supplementary material 1

### COI alignment haplotypes *Hippocampus whitei* NSW QLD

Authors: Graham Short, David Harasti, Healy Hamilton

Data type: molecular data

Copyright notice: This dataset is made available under the Open Database License (<http://opendatacommons.org/licenses/odbl/1.0/>). The Open Database License (ODbL) is a license agreement intended to allow users to freely share, modify, and use this Dataset while maintaining this same freedom for others, provided that the original source and author(s) are credited.

Link: <https://doi.org/10.3897/zookeys.824.30921.suppl1>

## Supplementary material 2

### Distribution haplotypes *H. procerus whitei*

Authors: Graham Short, David Harasti, Healy Hamilton

Data type: molecular data

Explanation note: Distribution of haplotypes based on partial mtDNA COI sequence data (655 bp) tabulated across sampled *H. procerus* and *H. whitei* from localities in central NSW and southern QLD.

Copyright notice: This dataset is made available under the Open Database License (<http://opendatacommons.org/licenses/odbl/1.0/>). The Open Database License (ODbL) is a license agreement intended to allow users to freely share, modify, and use this Dataset while maintaining this same freedom for others, provided that the original source and author(s) are credited.

Link: <https://doi.org/10.3897/zookeys.824.30921.suppl2>

## Supplementary material 3

### Genetic analysis uncorrected p distances COI *H. procerus whitei*

Authors: Graham Short, David Harasti, Healy Hamilton

Data type: molecular data

Explanation note: This document was exported from Numbers. Each table was converted to an Excel worksheet. All other objects on each Numbers sheet were placed on separate worksheets. Please be aware that formula calculations may differ in Excel.

Copyright notice: This dataset is made available under the Open Database License (<http://opendatacommons.org/licenses/odbl/1.0/>). The Open Database License (ODbL) is a license agreement intended to allow users to freely share, modify, and use this Dataset while maintaining this same freedom for others, provided that the original source and author(s) are credited.

Link: <https://doi.org/10.3897/zookeys.824.30921.suppl3>



# First description of the immature stages of *Dasyhelea alula* and a redescription of adults from China (Diptera, Ceratopogonidae)

Chen Duan<sup>1</sup>, Xiao Hong Jiang<sup>1</sup>, Qiong Qiong Chang<sup>1</sup>, Xiao Hui Hou<sup>1</sup>

<sup>1</sup> Zunyi Medical University, Zunyi 563000, Guizhou Province, China

Corresponding author: *Xiao Hui Hou* ([hxh19801122@163.com](mailto:hxh19801122@163.com))

---

Academic editor: *Art Borkent* | Received 17 November 2018 | Accepted 7 January 2019 | Published 14 February 2019

---

<http://zoobank.org/8B12D0BB-E777-41A3-BCAB-8A1197ADD888>

---

**Citation:** Duan C, Jiang XH, Chang QQ, Hou XH (2019) First description of the immature stages of *Dasyhelea alula* and a redescription of adults from China (Diptera, Ceratopogonidae). ZooKeys 824: 135–145. <https://doi.org/10.3897/zookeys.824.31722>

---

## Abstract

The fourth instar larva and pupa of *Dasyhelea alula* Yu, 2005 are described and illustrated using a Scanning Electron Microscope. The adult male and female of this species are redescribed. Immatures were collected from flooded soil near a pond in Xiaojiawan village, Guizhou province, China and reared in the laboratory. The studied material is deposited in the Insect Collection of Zunyi Medical University.

## Keywords

Adult, aquatic, biting midge, China, description, fourth instar larva, pupa

## Introduction

Biting midges of the genus *Dasyhelea* Kieffer, 1911 (Diptera: Ceratopogonidae) are common and widespread, and are found in all regions of the world in a wide variety of habitats (Wirth and Linley 1990). At present there are 191 species of the genus in China (Yu et al. 2005, 2006, 2015; Lai et al. 2006, 2015, 2016, 2018; Yan and Yu 2008;

Sun et al. 2010; Nie et al. 2016; Yang et al. 2017; Mahe et al. 2018), but only seven of these species are known as their immature stages (Yu et al. 2005, 2013). *Dasyhelea alula* Yu, 2005 belongs to the subgenus *Dasyhelea* (*Pseudoculicoides* Malloch), 1915 and *johannseni* group as defined by Dominiak (2012) and Szadziewski (1985). The purpose of this paper is to provide a complete description, with illustrations, of the fourth instar larva and pupa of *Dasyhelea alula* and a redescription of the adult male and female using a compound microscope and Scanning Electron Microscope.

## Materials and methods

The specimens were collected with the aid of a scoop from flooded soil in Xiaojiawan village, Guizhou province, China and carried to the laboratory in summer of 2018. They were placed in separate Petri dishes (larvae) and glass vials (pupae) with a small amount of water and reared in an environmental chamber (LZX-300L-III, Shanghai Xinlang Electronic Technology Ltd, Shanghai, China) maintaining  $28 \pm 2$  °C temperature, RH  $75 \pm 2\%$  and photoperiod of 12 h: 12 h (6W LED tube-light). The pupae were observed daily until adult emergence. The emergent adults and whole larvae and pupae were preserved in ethanol. The specimens were mounted in Canada balsam following Yu et al. (2005). For the Scanning Electron Microscope (SEM) study, one larva of *D. alula* was prepared following the technique of Ronderos et al. (2000, 2008). Ink illustrations were made using an attached camera lucida. Photographs of specimens were taken with a digital system adapted to an Olympus BX43 with a digital camera DP26. Studied material was deposited in the Insect Collection, Zunyi Medical University, Guizhou province, China (ICZU). The morphological terms and identification methods used in the study follow Yu et al. (2005), Díaz et al. (2013) and Borkent (2014). The following abbreviations are used:

<b>HL</b>	head length;
<b>HW</b>	head width;
<b>HR</b>	head ratio;
<b>SGR</b>	ratio of subgenal and head width;
<b>SGW</b>	subgenal width;
<b>MDL</b>	mandible length;
<b>MDW</b>	mandible width;
<b>LAW</b>	width across the lateral arms of epipharynx;
<b>DCW</b>	width across each of the paired dorsal comb sclerites of the epipharynx;
<b>ROL</b>	respiratory organ length;
<b>ROW</b>	respiratory organ width;
<b>ROP/ROL</b>	respiratory organ pedicel length / respiratory organ length;
<b>DAL</b>	dorsal apotome length;
<b>DAW</b>	dorsal apotome width;
<b>DAW/DAL</b>	dorsal apotome width / dorsal apotome length.

## Results

### *Dasyhelea alula* Yu, 2005

*Dasyhelea (Pseudoculicoides) alula* Yu, 2005: 259 (male and female, China)

**Material examined.** 2 males, 3 females, 3 larvae, 3 larval exuviae, 2 male pupal exuviae, 3 female pupal exuviae. Xiaojiawan village, Xinpu new district, Zunyi city, Guizhou province, China, 27°43'22.83"N; 107°04'27.62"E, 7.VII.2018, alt. 866 m, Chen Duan leg.

**Descriptions. Fourth instar larva (Figs 1a–c; 2a–f).** Head capsule yellowish, short, wide (Fig. 1a); HL 0.20–0.21 (0.20, n = 2) mm; HW 0.15–0.16 (0.15, n = 2) mm; HR 1.31–1.33 (1.32, n = 2); SGW 0.07–0.08 (0.08, n = 2) mm; SGR 0.47–0.50 (0.49, n = 2). Antenna short, cylindrical. Anterior portion of palatum (Figs 1a, 2a, b) with four pairs of campaniformia sensilla, posterior portion with three pairs of coeloconica sensilla, two simple, one serrate (Fig. 2a, c); messors well developed; scopae (Fig. 2a, c, d) well developed with more than 67 elongate, strong pointed teeth; maxilla (Fig. 2a) well sclerotized; mandible (Fig. 1a) stout, with three similar teeth, MDL 0.06 mm, MDW 0.02 mm; galeolacinia (Fig. 2a) with concentrated flap-like papillae, one seta; maxillary palpus (Fig. 2a, c) cylindrical, with 5–6 apical papillae; lacinial sclerite I with one short seta, dorsal view of lacinial sclerite I with three pairs of lobes; lacinial sclerite II without seta. Hypostoma (Fig. 2a) with mesal portion smooth, flanked with four strong, lanceolate lateral teeth on each side. Epipharynx (Fig. 1b) massive, strongly sclerotized, dorsal comb moderately wide, round, with 12 teeth, subequal elongate, lateral arms stout, elongate, with two auxiliary sclerites. LAW 0.08–0.13 (0.11, n = 3), DCW 0.03–0.04 (0.04, n = 3). Hypopharynx (Fig. 1c) stout, heavily sclerotized, posterior comb straight with fringe, with labium sclerotized. Thoracic pigmentation diffused, pale brown. Abdominal segments whitish, with diffused pale brown pigmentation. Caudal segment (Fig. 2e, f) with single comb, which has dense elongate and subequal teeth, with three long and stout crooked hooks.

**Pupa (Figs 1d–g; 3f–k). Male.** Total length 1.97 mm. General coloration of exuviae pale brown. Dorsal apotome (Fig. 1d) 2.7 × broader than long, triangular, with apex rounded, surface covered with brown rounded tubercles, anterior margin straight, lateral margin smooth, with three anterior wrinkles; apotome sensilla (Fig. 1d): DA-1-H elongate, thin seta, insert on well-developed tubercle, DA-2-H campaniform sensillum at base; disc surface covered by stout, rounded spinules; DAL 0.07 mm, DAW 0.19 mm, DAW/DAL 2.71. Respiratory organ, apex medium dark brown, 7.5 × longer than broad, with circular fold, 7–8 apical, three lateral pores; ROL 0.15 mm, ROW 0.02 mm; pedicel pale brown, short, length 0.01 mm, ROP/ROL 0.07. Mouthparts with mandible, lacinia absent; two clypeal/labral (Fig. 3f), CL-1-H and CL-2-H both medium-sized and thin setae; two ocular sensilla, O-1-H long, thin seta, O-2-H campaniform sensillum (Fig. 3f); cephalothorax surface with small rounded tubercles, length 0.63 mm, width 0.45 mm; cephalothoracic sensilla as follows: three dorsolateral cephalic sclerite sensilla (Fig. 3g), DL-1-H and DL-2-H both medium-

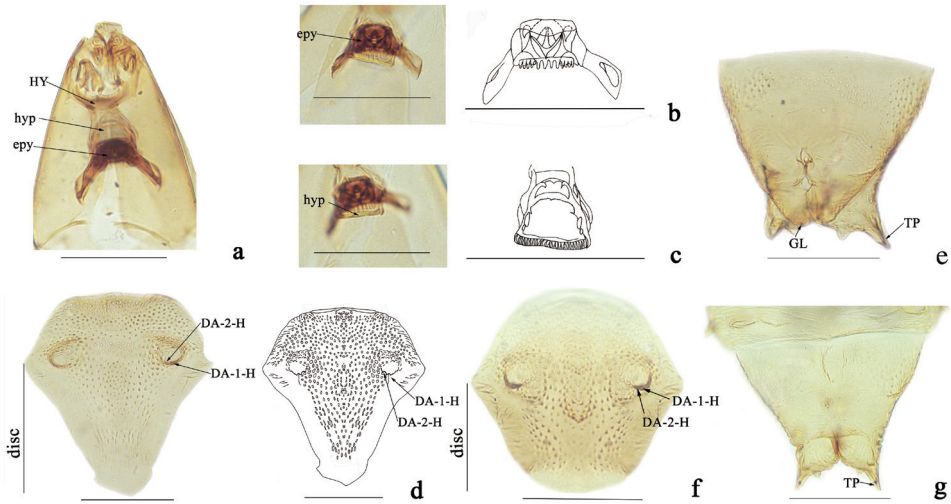


**Figure 1.** *Dasyhelea alula* Yu. Larva (a–c), male pupa (d–e), female pupa (f–g). **a** head, dorsal view **b** epipharynx, dorsal view **c** hypopharynx, dorsal view **d** dorsal apotome (male) **e** segment IX (male) **f** dorsal apotome (female) **g** segment IX (female). Scale bars: 0.1 mm. Abbreviations: hypostoma (HY); hypopharynx (hyp); epipharynx (epy); genital lobe (GL); terminal process (TP).

sized, thin setae, DL-3-H campaniform sensillum; three anterolateral sensilla (Fig. 3h), AL-1-T, AL-2-T both medium-sized, thin setae, AL-3-T short, stout seta; two anteromedial sensilla (Fig. 3h), AM-1-T medium-sized, thin seta, AM-2-T short, thin seta. Cephalothorax length 0.63 mm, width 0.45 mm. Cephalothoracic sensilla as follows (Fig. 3j): three dorsal setae (D-1-T, D-2-T, and D-3-T), D-1-T and D-2-T short, thin setae, D-3-T campaniform sensillum, SA-2-T supraalar campaniform sensillum. Metathoracic sensilla (Fig. 3i): M-2-T and M-3-T both campaniform sensilla. Abdomen: covered with short, stout spinules on anterior, posterior margin. Tergite I (Fig. 3i) with two depressions in the middle, setae as follows: D-2-I medium-sized, thin seta; D-4-I, D-7-I both campaniform sensilla; L-1-I long, thin seta. Segment IV (Fig. 3k) with sensillar pattern, as follows: D-2-IV short, stout seta; D-4-IV, D-7-IV both campaniform sensilla, D-8-IV short, stout seta, all located on flattened tubercles; L-1-IV long and stout setae, L-2-IV short, thin seta, L-3-IV short, thin seta, L-4-IV short, stout seta, all located on triangular tubercles; V-6-IV long, thin seta, V-7-IV short, stout seta, also located on flattened tubercles. Segment IX (Fig. 1e) 0.95 × longer than wide, length 0.19 mm, width 0.20 mm; ventral and dorsal surface with many spinules; terminal process triangular, elongated, acute, length 0.07 mm.

**Female.** Similar to male with usual sexual differences. Total length 1.64–1.75 (1.70,  $n = 2$ ) mm. General coloration of exuviae pale brown, except dorsolateral cephalic sclerite brown. Dorsal apotome (Fig. 1f), DAL 0.08 mm, DAW 0.18 mm, DAW/DAL 2.25. Cephalothorax length 0.71 mm, width 0.42 mm. ROL 0.16–0.18 (0.17,  $n = 3$ ) mm, ROW 0.02 ( $n = 3$ ) mm; pedicel length 0.01 ( $n = 3$ ) mm, ROP/ROL

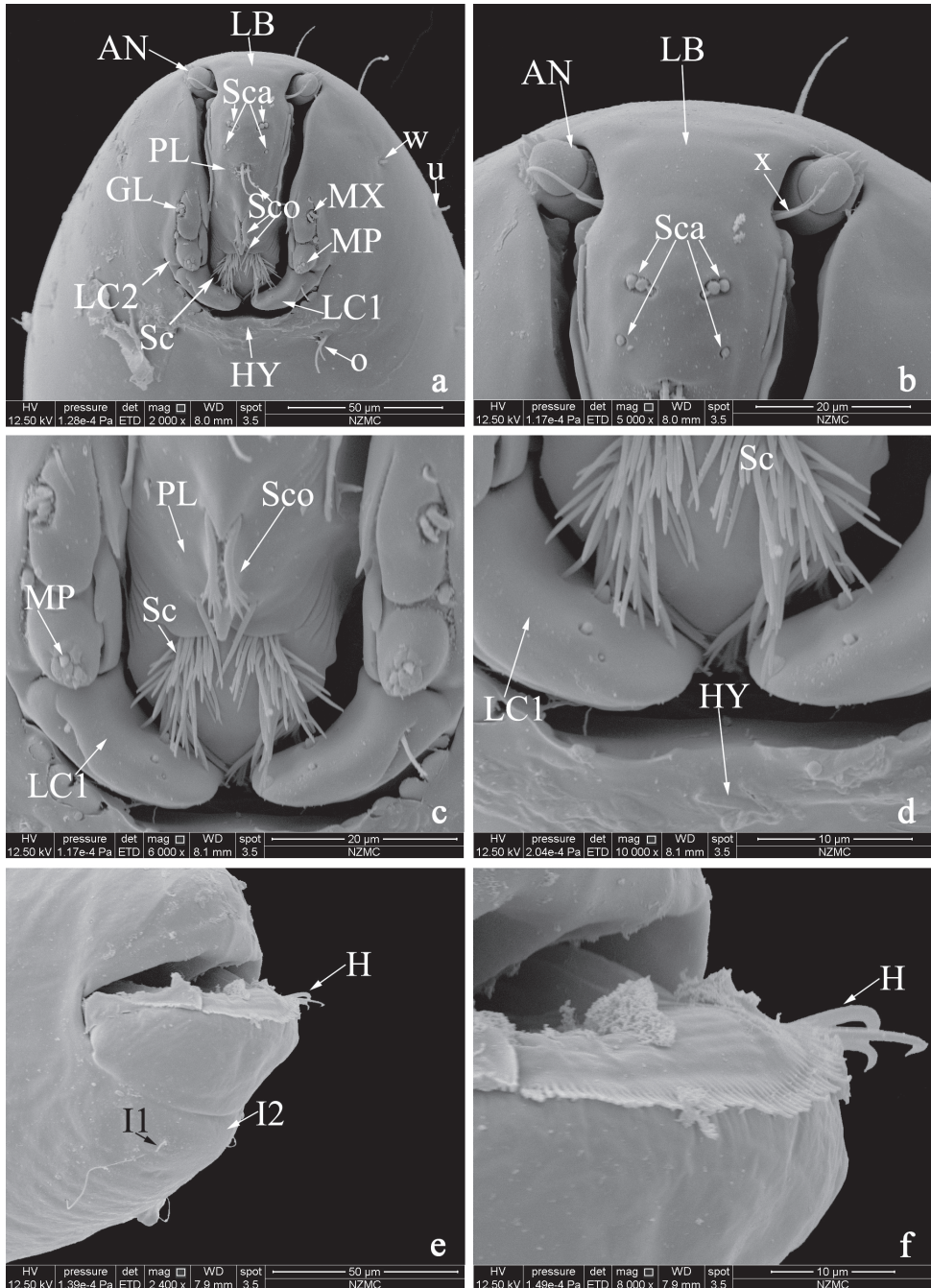


**Figure 2.** *Dasyhelea alula* Yu, larva. **a** head capsule (palatum, frontal view) **b** detail of labrum **c** detail of scopae **d** detail of lacinial sclerite **e** caudal segment **f** detail of caudal segment. Abbreviations: antenna (AN); galeolacinia (GL); hypostoma (HY); hooks (H); labrum (LB); lacinial sclerite I (LC1); lacinial sclerite II (LC2); maxilla (MX); maxillary palpus (MP); palatum (PL); sensilla coeloconica (Sco); sensilla campaniformia (Sca); scopae (Sc).

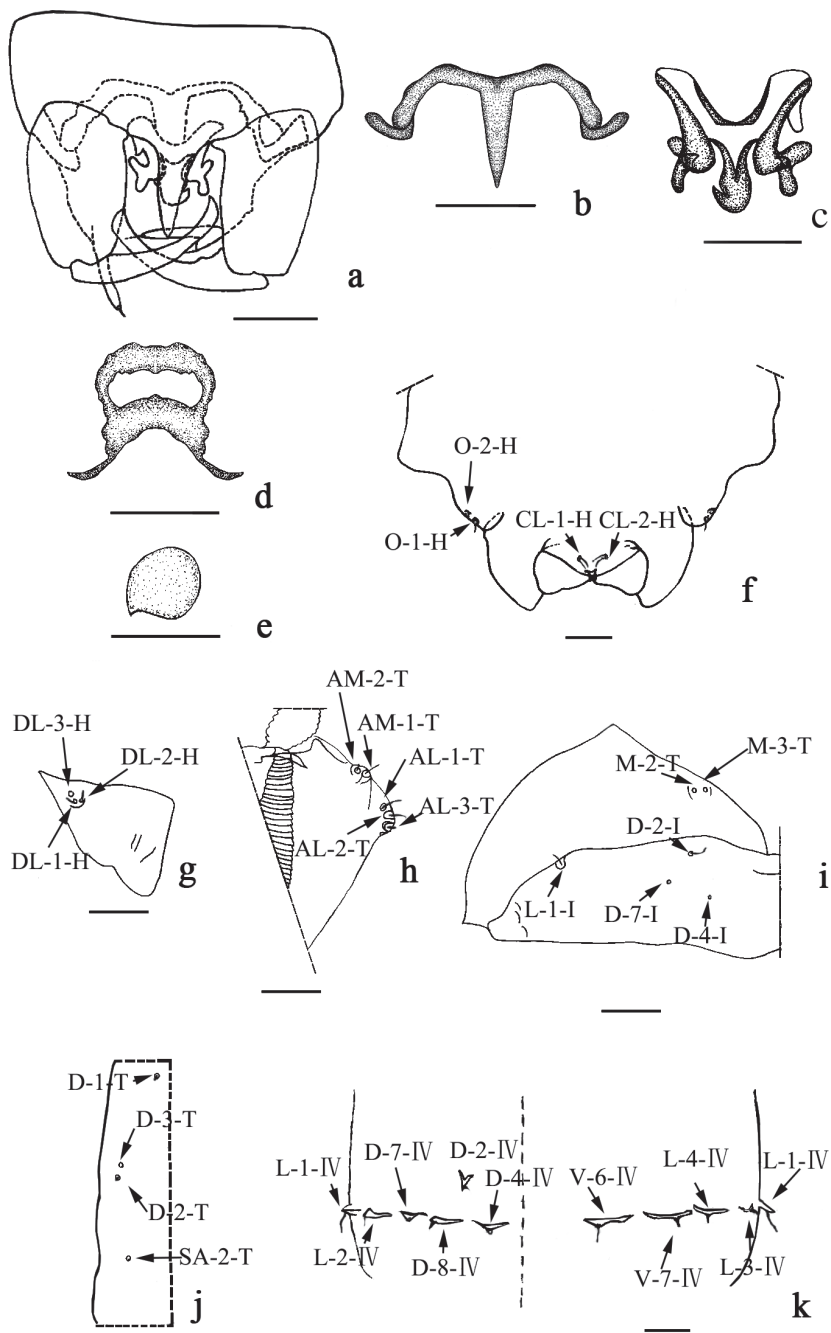


**Figure 3.** *Dasybelea alula* Yu. Male adult (**a–c**), female adult (**d–e**), male pupa (**f–k**). **a** genitalia **b** paramer **c** aedeagus **d** subgenital plate **e** spermatheca **f** clypeal/labral sensilla and ocular sensilla **g** dorsolateral cephalic sclerite sensilla **h** anterolateral and anteromedial sensilla **i** metathoracic sensilla, lateral and dorsal sensilla of first abdominal segment **j** dorsal and supraalar sensilla **k** dorsal, lateral and ventral sensilla of segment IV. Scale bars: 0.1 mm.

0.11–0.13 (0.12, n = 3). Segment IX (Fig. 1g) length 0.17–0.20 (0.19, n = 2) mm, width 0.20 (0.15, n = 2) mm; ventral surface with many spicules, single funnel-like structure medially. Terminal process (Fig. 1g) triangular, elongated, pointed, length 0.02–0.03 (0.02, n = 2) mm.

**Redescription of adults (Figs 3a–e; 4a–k). Male (Figs 3a–c; 4a–e).**

**Head.** Eyes (Fig. 4a) contiguous, abutting medially for length of 1.0 ommatidia, with interfacetal hairs. Antennal flagellum (Fig. 4b) brown, with distinct sculpture, sparsely plumose, flagellomere 13 without apical projection; AR 1.28. Frontal sclerite nearly round, with long, slender ventral projection (Fig. 4a). Clypeus (Fig. 4c) with four pairs of setae. Palpus (Fig. 4d) brown; third segment slender, the length almost the sum of the fourth and fifth segment. Lengths of palpus segments in ratio of 5: 8: 27: 12: 14.

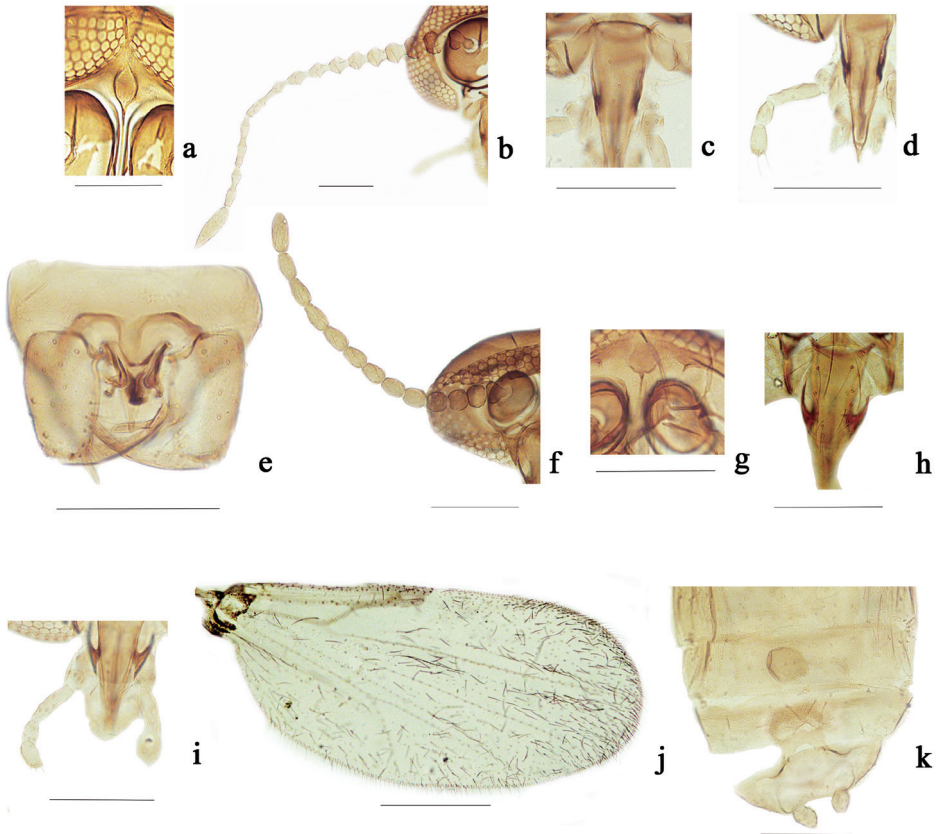


**Figure 4.** *Dasyhelea alula* Yu. Male adult (a–e), female adult (f–k). a frontal sclerites, anterior view b flagellomeres, anterior view c clypeus, anterior view d palpus, anterior view e genitalia, ventral view f flagellomeres, anterior view g frontal sclerites, anterior view h clypeus, anterior view i palpus, anterior view j wing k subgenital plate and spermatheca, ventral view. Scale bars: 0.1 mm.

**Thorax.** Scutum dark brown, scutellum yellow, with six stout setae. Legs brown; hind tibial comb with eight spines; foreleg TR 2.18, midleg TR 2.21, hind leg TR 2.33. Wing length 1.12 mm, width 0.33 mm, CR 0.40; wing membrane hyaline, densely covered with microtrichia, cubital fork at same level of distal portion of second radial cell.

**Abdomen.** Brown. Tergite IX nearly trapezoidal with prominent apicolateral processes. Posteromedial margin of sternite IX with elongate, slender projection, gonostylus slender (Figs 3a, 4e). Parameres fused, with median lobe short, thick, lateral lobe directly ventrolaterally (Figs 3b, 4e). Aedeagus complex, median process thick, long, its lateral processes each with curved apex (Figs 3c, 4e).

**Female (Figs 3d–e; 4f–k).**

**Head.** Eyes contiguous. Antennal flagellum (Fig. 4f) brown, without sculpture, flagellomere 13 without apical projection; AR 0.93. Frontal sclerite oval, with long, slender ventral projection (Fig. 4g). Clypeus (Fig. 4h) with seven pairs of setae. Palpus (Fig. 4i) brown; third segment slender, without capitate sensillae, lengths of palpus segments in ratio of 4: 7: 17: 7: 12.

**Thorax.** Hind tibial comb with seven spines; foreleg TR 2.00, midleg TR 2.14, hind leg TR 2.16. Wing length 0.82 mm, width 0.34 mm, CR 0.50 (Fig. 4j).

**Abdomen.** Similar to male. Subgenital plate (Figs 3d, 4k) flat, ring-shaped, posterolateral arms sclerotized into darker bands. Spermatheca round (Figs 3e, 4k), strongly pigmented, diameter 53.60  $\mu\text{m}$ , neck short, stout, oblique, length 6.20  $\mu\text{m}$ .

**Distribution.** China (Guizhou province Fig.5).

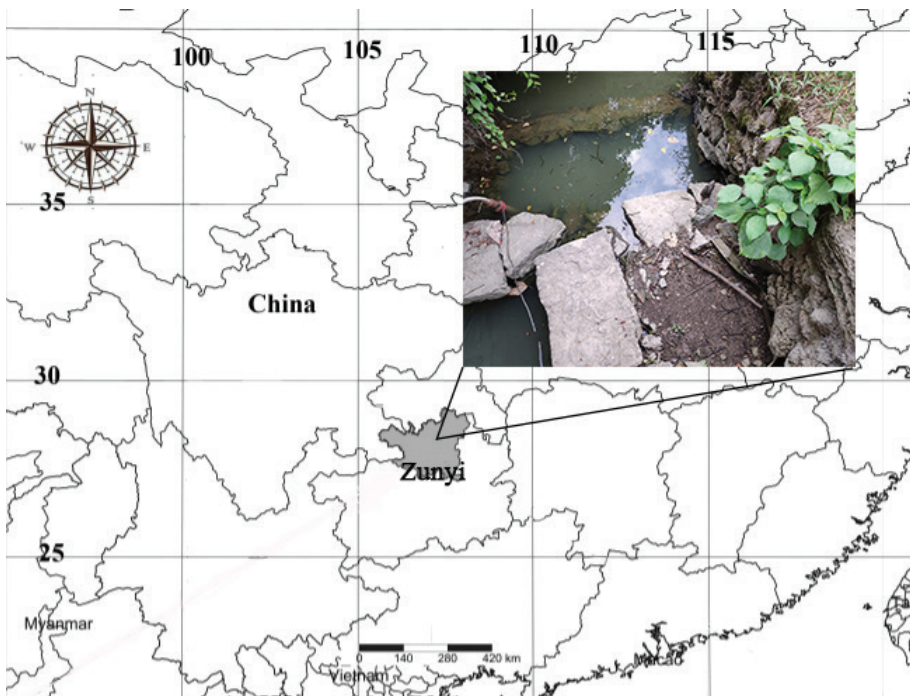


**Figure 5.** Geographical location of collecting site (inset) of *Dasyhelea alula* in Guizhou province, China.

## Discussion

*Dasyhelea alula* belongs to the subgenus *Pseudoculicoides* and the *johannseni* group, of which are there 12 species in China: *D. arciforceps* Tokunaga, *D. alula* Yu, *D. curtus* Yu & Yan, *D. communis* Kieffer, *D. ermeri* Remm, *D. excellentis* Borkent, *D. microsporea* Hao & Yu, *D. navai* Xue & Yu, *D. subcommunis* Yu, *D. turficola* Kieffer, *D. turanicola* Remm, and *D. tessicola* Remm. Other than *D. alula*, the larvae and pupae of *D. communis* are the only described immatures of any species within this group. The larva of *D. alula* is similar to *D. communis* by virtue of the mandible with three same-sized teeth, but the dorsal comb of epipharynx has small and dense teeth. In addition, the larva of *D. alula* is also similar to that of *D. mediomunda*, the shared features as follows: head capsule is short, the medial portion of the hypostoma smooth, the lateral arms of the epipharynx stout and lacking teeth, but the larva of *D. mediomunda* differs by having inconspicuous scopae, the mandible with two teeth and the anterior portion of palatum with three pairs of campaniformia. The pupa of *D. alula* is similar to that of *D. eloyi* with scale-like spines on the respiratory organ, but the latter differs by having 16–18 apical and 5–6 lateral pores. The pupa of *D. alula* otherwise matches the generic features of *Dasyhelea* as described by Borkent (2014). The larva and pupa of *D. caeruleus* and an unidentified species of *Dasyhelea* also breed in the small wetland, and the larva and pupa of two species of *Forcipomyia* Meigen were also found in the same place. The small wetland was near a fishpond surrounded by an orchard containing *Prunus cerasifera* Ehrh, *Pyrus sorotina* Will, and *Prunus persica* (L.) Batsch.

## Acknowledgements

We are grateful to Pr Run Zhi Zhang for help in the laboratory platform, to Dr Kui Yan Zhang for technical assistance, and to Dr Art Borkent for critical reading of the manuscript. This research was financially supported by the grant from the National Natural Science Foundation of China (No. 81802040) and the Western Light Project.

## References

- Borkent A (2014) The pupae of the biting midges of the world (Diptera: Ceratopogonidae), with a generic key and analysis of the phylogenetic relationships between genera. *Zootaxa* 3879(1): 1–327. <https://doi.org/10.11646/zootaxa.3879.1.1>
- Dominiak P (2012) Biting midges of the genus *Dasyhelea* Kieffer (Diptera: Ceratopogonidae) in Poland. *Polskie Pismo Entomologiczne* 81: 211–304. <https://doi.org/10.2478/v10200-012-0009-8>
- Díaz F, Ronderos MM, Spinelli GR, Ferreira-Kepler RL, Torreiras SRS (2013) A new species of *Dasyhelea* Kieffer (Diptera: Ceratopogonidae) from Brazilian Amazonia. *Zootaxa* 3686(1): 85–93. <https://doi.org/10.11646/zootaxa.3686.1.5>

- Kieffer JJ (1911) Nouvelles descriptions de chironomides obtenus d'éclosion. Bulletin de la Société d'Histoire Naturelle de Metz 27: 1–60.
- Lai CC, Liu ZH, Fang JM, Yu YX (2018) A new species of *Dasyhelea* from Conghua District in Guangdong Province. Chinese Journal of Hygienic Insecticides and Equipments 24(3): 278–279. <http://www.cnki.com.cn/Article/CJFDTotal-WSSC201803019.htm>
- Li JC, Li DX, Nie WZ (2006) The composition of biting midges in Beijing and Hebei Areas. Chinese Journal of Frontier Health and Quarantine 29(5): 282–287. <https://doi.org/10.3969/j.issn.1004-9770.2006.05.008>
- Li XC, Long C, Ren YL, Yang L, Wang FP, Yu YX (2015) Two new species of *Dasyhelea* from Emei Mountain. Chinese Journal of Hygienic Insecticides & Equipments 21(2): 169–170. <https://www.ixueshu.com/document/367b5269fae49d17318947a18e7f9386.html>
- Liu YQ, Chen HY, Yu YX (2016) Genus *Dasyhelea* Kieffer and two new species (Diptera: Ceratopogonidae) in Jiangxi Province, China. Chinese Journal of Vector Biology and Control 27(5): 498–500. <https://doi.org/10.11853/j.issn.1003.8280.2016.05.021>
- Mahe MT, Zhang J, Gao ZG, Zhang XB, Zhang S, Yu YX (2018) One new species and one new record of *Dasyhelea* from China (Diptera: Ceratopogonidae). Chinese Journal of Vector Biology and Control 29(1): 76–77. <https://doi.org/10.11853/j.issn.1003.8280.2018.01.019>
- Nie WZ, Bo JX, Yu XY (2016) A new species of genus *Dasyhelea* (Diptera: Ceratopogonidae) collected on an entry ship. Chinese Journal of Vector Biology and Control 27(1): 44–45. <https://doi.org/10.11853/j.issn.1003.4692.2016.01.013>
- Ronderos MM, Díaz F, Sarmiento P (2008) A new method using acid to clean and a technique for preparation of eggs of biting midges (Diptera: Ceratopogonidae) for scanning electron microscope. Transactions of the American Entomological Society 134(3/4): 471–476. <https://doi.org/10.3157/0002-8320-134.3.471>
- Ronderos MM, Spinelli GR, Sarmiento P (2000) Preparation and Mounting of Biting Midges of the Genus *Culicoides* Latreille (Diptera: Ceratopogonidae) to be observed with a scanning electron microscope. Transactions of the American Entomological Society 126(1): 125–132. <https://doi.org/10.1016/j.virusres.2005.02.011>
- Sun H, Gong B, Ke MJ, Wu ZX, Guo QL, Yu YX (2010) Two new species of the *Dasyhelea* (Diptera: Ceratopogonidae) from Macao, China. Acta Parasitologica et Medica Entomologica Sinica 17(4): 246–248. <https://doi.org/10.3969/j.issn.1005-0507.2010.04.012>
- Szadziewski R (1985) A review of the Palaearctic *Dasyhelea* (Pseudoculicoides) species of the Johannseni group, with a description of new two species (Diptera: Ceratopogonidae). Polskie Pismo Entomologiczne 55: 79–98.
- Wirth WW, Linley JR (1990) Description of *Dasyhelea chani* new species (Diptera: Ceratopogonidae) from leaves of the water lettuce (*Pistia stratiotes*) in Florida. Florida Entomologist 73(2): 273–279. <http://journals.fcla.edu/flaent/article/download/58615/56294> <https://doi.org/10.2307/3494811>
- Yan HH, Yu YX (2008) A new species of *Dasyhelea* Kieffer from Shanxi, China (Diptera: Ceratopogonidae). Sichuan Journal of Zoology 27(4): 481–482. <https://www.ixueshu.com/document/3294a06769504e4a.html>
- Yang QG, He DY, Zhang L, Qiu WY, Yu YX (2017) Two new species of *Dasyhelea* from Changzhou City, Jiangsu Province, China. Acta Parasitologica et Medica Entomologica Sinica 24(1): 52–55. <https://doi.org/10.3969/j.issn.1005-0507.2017.01.008>

- Yu YX, Liu JH, Liu GP, Liu ZJ, Hao BS, Yan G, Zhao TS (2005) Ceratopogonidae of China, Insecta, Diptera, Military Medical Science Press, Beijing. Vol 1–2, 1699 pp.
- Yu YX, Yan G (2015) New species of genus *Dasyhelea* (Diptera: Ceratopogonidae). *Acta Parasitologica et Medica Entomologica Sinica* 22(3): 198–204. <https://doi.org/10.3969/j.issn.1005-0507.2015.03.009>
- Yu YX, Yan G, Liu GP, Liu ZJ (2013) A new species and three new record species of biting midge from China (Diptera, Ceratopogonidae). *Acta Zootaxonomica Sinica* 38(2): 372–376. <https://doi.org/10.3969/j.issn.1000-7083.2007.03.001>
- Yu YX, Yuan MZ, Chen ML, Zeng ZX, Yan SM (2006) New species and new record of *Dasyhelea* from Hong Kong (Diptera: Ceratopogonidae). *Sichuan Journal of Zoology* 25(4): 687–689. <https://doi.org/10.3969/j.issn.1000-7083.2006.04.003>

